

This full text version, available on TeesRep, is the final version of this PhD Thesis:

Rasoul, A.A. (2014) Modelling of vapour-liquid-liquid equilibria for multicomponent heterogeneous systems, Unpublished PhD Thesis. Teesside University

This document was downloaded from <http://tees.openrepository.com/tees/handle/10149/337883>

All items in TeesRep are protected by copyright, with all rights reserved, unless otherwise indicated.

**MODELLING OF VAPOUR-
LIQUID-LIQUID EQUILIBRIA
FOR MULTICOMPONENT
HETEROGENEOUS SYSTEMS**

ANWAR ALI RASOUL

A thesis submitted in partial fulfilment of the
requirements of Teesside University for the
degree of Doctor of Philosophy

17 October 2014

Acknowledgment

I would like to express my gratitude to my supervisory team Dr. C. Peel, Dr. D.W. Pritchard and Dr. P. Russell for their support and academic expertise. In particular my thanks go to Dr. Pritchard who has given friendship and constant encouragement throughout all my academic studies at Teesside University. His involvement over this time has been invaluable.

I would like to thank members of staff from the School of Science and Engineering and also the school of computing for their support and advice throughout my academic studies at Teesside University.

I also acknowledge the support and encouragement given by constant friends without whose help this work would not have been completed.

Abstract

This work is focused on thermodynamic modelling of isobaric vapour-liquid-liquid equilibrium (VLLE) (homogeneous) and (heterogeneous) for binary, ternary and quaternary systems. This work uses data for organic/aqueous systems; historically these mixtures were used in the production of penicillin and were required to be separated by continuous fractional distillation. Modelling of the separation required phase equilibrium data to be available so that predictions could be made for equilibrium stage temperatures, vapour compositions, liquid compositions and any phase splitting occurring in the liquid phase. Relevant data became available in the literature and work has been carried out to use relevant theories in correlating and predicting as was originally required in the distillation equilibrium stage modelling. All the modelling carried out was at atmospheric pressure.

The modelling has been done using an Equation of State, specifically Peng Robinson Styrjek Vera (PRSV), combined with the activity coefficient model UNiversal QUAsi Chemical (UNIQUAC) through Wong Sandler mixing rules (WSMR). The success of all correlations and predictions was justified by minimizing the value of the Absolute Average Deviation (AAD) as defined within the thesis. Initially the integral Area Method and a method called Tangent Plane Intersection (TPI) were used in the prediction of liquid-liquid equilibrium (LLE) binary systems. This work used a modified 2-point search, suggested a 3-point search and has successfully applied both of these methods to predict VLLE for binary systems. It was discovered through the application of the TPI on ternary VLLE systems that the method was strongly sensitive to initial values. This work suggested and tested a Systematic Initial Generator (SIG) to provide the TPI method with realistic initial values close to the real solution and has demonstrated the viability of the SIG on improving the accuracy of the TPI results for the ternary systems investigated.

In parallel with the TPI another method the Tangent Plane Distance Function (TPDF) was also investigated. This method is based on the minimisation of Gibbs free energy function related to the Gibbs energy surface. This method consistently showed it was capable of predicting VLLE for both ternary and quaternary systems as demonstrated throughout this work. The TPDF method was found to be

computationally faster and less sensitive to the initial values. Some of the methods investigated in this work were also found to be applicable as phase predictors and it was discovered that the TPDF and the SIG methods were successful in predicting the phase regions; however the TPI method failed in identifying the 2 phase region.

Applying the techniques described to newly available quaternary data has identified the strengths and weaknesses of the methods. This work has expanded the existing knowledge and developed a reliable model for design, operation and optimisation of the phase equilibria required for prediction in many separation processes. Currently available modelling simulation packages are variable in their predictions and sometimes yield unsatisfactory predictions.

Many of the current uses of VLLE models are particularly focused on Hydrocarbon/Water systems at high pressure. The work described in this thesis has demonstrated that an EOS with suitable mixing rules can model and predict data for polar organic liquids at atmospheric and below atmospheric pressure and offers the advantage of using the same modelling equations for both phases.

Contents

1. Introduction.....	1
2. Literature Survey.....	5
2.1 General survey of Phase Equilibrium.....	5
2.2 Phase Equilibrium	6
2.2.1 Background Theory.....	6
2.2.2 Phase Equilibrium Models	8
2.2.3 Activity Coefficient Models	8
2.2.4 UNIQUAC.....	10
2.2.5 Equation of State (EOS).....	10
2.3 Mixing Rules.....	16
2.3.1 van der Waals Mixing Rules.....	16
2.3.2 Huron and Vidal Mixing Rules.....	17
2.3.3 Wong Sandler Mixing Rules.....	18
2.4 Optimisation methods for phase equilibrium modelling.....	21
2.4.1 Equation solving method.....	21
2.4.2 Direct minimisation techniques.....	22
2.4.2.1 Deterministic methods.....	23
2.4.2.2 Stochastic method.....	24
2.4.2.3 Nelder Mead.....	26
2.4.3 Other method of phase equilibrium calculations (Reduced Variables).....	27
2.5 The problem of initialisation in Phase Equilibria Calculations	27
2.5.1 Initialisation method for VLE calculations.....	29
2.5.2 Initialisation method for LLE calculations.....	30
2.5.3 Initialisation method For VLLE calculations.....	31
2.6 Experimental measurement of phase equilibrium data.....	32
2.7 Comments on the reviewed literature.....	35
3. Theory	41
3.1 Introduction.....	41
3.2 Background.....	42
3.3 Thermodynamic of Phase Equilibrium.....	47
3.4 Equation of State.....	49
3.5 Activity Coefficients.....	50
3.6 Mixing Rules.....	51
3.7 Thermodynamic Model Description.....	53
3.8 Estimation of Parameters.....	56
3.9 VLLE three Phase Flash Calculation.....	58
3.10 Gibbs Optimisation Methods.....	60
3.10.1 Area Method in Integral Form.....	61
3.10.2 Tangent Plane Intersection Method.....	62

3.10.3	Equal Area Rule.....	64
3.10.4	Tangent Plane Distance Function.....	65
3.11	Methods of Initialisation.....	68
3.11.1	Initialisation Techniques used in Stability Test.....	68
3.11.2	Direct Initialisation of Three Phase Multi component Systems.....	69
3.12	Nelder-Mead simplex.....	70
4.	Results and Discussions.....	74
4.1	Binary System results.....	74
4.1.1	VLE Homogeneous systems.....	75
4.1.2	VLE Heterogeneous systems.....	81
4.1.3	LLE binary systems.....	86
4.1.4	VLLE binary systems.....	87
4.2	Discussion.....	88
4.2.1	VLE binary homogeneous mixtures.....	89
4.2.2	VLE binary heterogeneous mixtures.....	91
4.2.3	Conclusion on PRSV EOS + WSMR.....	101
4.3	Prediction methods for modelling binary LLE & VLLE systems	102
4.3.1	Modified 2-Point and direct 3-Point search for TPI for binary VLLE phase equilibrium calculation	105
4.3.2	Conclusion on prediction methods for LLE and VLLE binary systems.....	114
4.4	VLLE Ternary System Results.....	115
4.4.1	VLLE system: water (1)-acetone (2)-MEK (3) at pressure 760 mmHg.....	121
4.4.2	VLLE system: Water (1)-Ethanol (2)-Methyl Ethyl Ketone (3) at pressure 760 mmHg.....	125
4.4.3	VLLE system: Water (1)-Acetone (2)-n Butyl Acetate (3)..	128
4.4.4	VLLE system: Water (1)-Ethanol (2)-n Butyl Acetate (3)...	138
4.5	Equilibrium Phase prediction at a fixed T & P.....	144
4.5.1	Water (1) –acetone (2)-MEK (3).....	145
4.5.2	Water (1) –ethanol (2)-MEK (3).....	146
4.5.3	Water (1) –acetone (2)-n-butyl acetate (3)	147
4.5.4	Water (1) –ethanol (2)-n-butyl acetate (3).....	150
4.6	Discussion on VLLE ternary systems.....	153
4.6.1	Application of the TPI and TPDF method on artificial ternary systems.....	154
4.6.2	The sensitivity of TPI method to initial values.....	160
4.6.3	Systematic Initial Generator (SIG).....	166

4.6.4	Application of the Tangent Plane Distance Function for prediction of 3 phase equilibrium.....	168
4.6.5	The SIG, TPI and TPDF as Phase predictors.....	170
4.6.6	The Flash, TPI and TPDF Phase Equilibrium results..	171
4.7	Conclusions on phase equilibrium for ternary VLLE	189
4.8	Quaternary systems.....	192
4.8.1	VLLE water (1) ethanol (2) acetone (3) MEK (4).....	195
4.8.2	VLLE water (1) ethanol (2) acetone (3) n-butyl acetate (4) at 760 mmHg.....	198
4.8.3	VLLE water (1) ethanol (2) acetone (3) n-butyl acetate (4) at 600 mmHg.....	202
4.8.4	VLLE water (1) ethanol (2) acetone (3) n-butyl acetate (4) at 360 mmHg.....	206
4.9	Discussion.....	209
5.	Conclusion and Future work.....	215
6.	References.....	219
7.	Appendix.....	232
A.	VLLE Flash Calculation Algorithm.....	232
B.	Systematic Initial Generator	233
C.	Nelder-Mead Simplex.....	234
D.	Selected VBa program code.....	235
D.1	Binary system calculations.....	235
D.1.1	VLE Calculations.....	235
D.1.1.1	Main program for bubble point calculation...	235
D.1.1.2	Sub program of Peng Robinson Styjrek Vera EOS with Wong Sandler Mixing Rule through UNIQUAC...	236
D.1.2	Area Method main program for binary LLE.....	245
D.1.2.1	Area Method main program for binary LLE.....	245
D.1.2.2	Sub program to calculate roots of PRSV EOS.....	246
D.1.2.2.1	The compressibility factor for liquid phase...	246
D.1.2.2.2	The compressibility factor for vapour phase	247
D.1.2.3	Calculation of pure component Gibbs free energy...	248
D.1.2.4	Calculation of Gibbs free energy for the mixture.....	250
D.1.2.5	Integration of Gibbs free energy curve using Simpson's rule.....	253
D.1.3	TPI for VLLE binary systems.....	254
D.1.3.1	Main program	254
D.1.3.2	Sub procedure to calculate pure component Gibbs free energy.....	255
D.1.3.3	Tau Objective Function.....	257
D.1.3.4	Sub program of Gibbs free energy calculation for vapour phase.....	258

D.2	Ternary systems.....	263
D.2.1	VLE Flash calculation main program.....	263
D.2.2	VLE Tangent Plane Intersection TPI.....	265
D.2.2.1	The main program.....	265
D.2.2.2	Liquid phase fugacity coefficient.....	266
D.2.2.3	Estimation of Angles and length of the Arms of the search from initial values.....	269
D.2.2.4	Calculation of the Area of intersection of the tangent plane with Gibbs energy surface	270
D.2.2.5	Writing the results to the spread Sheet and storing them.....	275
D.2.3	VLE Tangent Plane Distance Function TPDF.....	276
D.2.3.1	TPDF Main program.....	276
D.2.3.2	Search in Organic Phase	277
D.2.3.3	Sub program calculation of organic phase fugacity coefficients.....	278
D.2.4	Initial generator.....	285
D.2.4.1	Main program.....	285
D.2.4.2	The organic and aqueous ratio.....	287
D.2.5	Nelder Mead Simplex	288
D.2.5.1	Declaration and sub procedures.....	288
D.2.5.2	Main minimisation function.....	288
D.2.5.3	Getting the initial, storing and sorting the Matrix.....	291
E.	Computer programs on a Compact Disc.....	293

Nomenclature

a	equation of state parameter corresponding molecular attraction, liquid phase activity, and adjustable parameter in liquid phase excess Gibbs energy equations
A_{∞}^E	molar excess Helmholtz energy at infinite pressure
A	net area
b	equation of state mixing parameter representing repulsion
C	equation of state dependent constant
g	molar Gibbs energy of a mixture
g^E	molar excess Gibbs energy
G	Gibbs energy
k	cubic equation of state adjustable parameter
K	ratio of liquid and vapour fugacity coefficients
n	number of components
P	pressure
P_c	critical pressure
P^{θ}	pure component vapour pressure
q	pure component area parameter in UNIQUAC
\bar{q}	modified pure component area parameter for water and alcohols in UNIQUAC
r	UNIQUAC pure component volume parameter
R	universal gas constant
T	temperature
T_R	reduced temperature
T_c	critical temperature
x	liquid mole fraction
y	vapour mole fraction
Z	co-ordination number in UNIQUAC equation, compressibility factor
z	overall mixture composition

Greek symbols

α	non-randomness parameter in NRTL equation
τ	interaction parameter in NRTL equation and TPI method function
φ	segment fraction in modified UNIQUAC
ϕ	reduced Gibbs energy of mixing, and fugacity coefficient
θ	area fraction in modified UNIQUAC
$\bar{\theta}$	modified area fraction in modified UNIQUAC
U_{ij}	average interaction energy for species i - species j
γ	activity coefficient
ω	acentric factor
μ	chemical potential

Subscripts

exp experimental value

<i>cal</i>	calculated value
<i>org</i>	organic phase
<i>aq</i>	aqueous phase
<i>comb</i>	combinatorial
<i>res</i>	residual
<i>max</i>	maximum
<i>min</i>	minimum

Abbreviations

PRSV	Peng Robinson Stryjek Vera
TPI	Tangent Plane Intersection
AM	Area Method
EAR	Equal Area Rule
TPDF	Tangent Plane Distance Function
SIG	Systematic Initial Generator
RMSD	Root Mean Square Deviation
AAD	Absolute Average Deviation
MPNA	Maximum Positive Net Area
WSMR	Wong Sandler Mixing Rules

List of tables

Table 4.1: VLE bubble point calculation for methanol (1)-water (2) isothermal binary system at 25, 50, 65 and 100 ^o C using PRSV with WSMR through UNIQUAC	.76
Table 4.2: VLE bubble point calculation for methanol (1)-water (2) isobaric binary system at 760 mmHg	77
Table 4.3: VLE bubble point calculation for ethanol (1)-water (2) isothermal binary system at 20, 30, 40, 50, 60 and 70 ^o C, pressures in mmHg	78
Table 4.4: VLE bubble point calculation for ethanol (1)-water (2) isobaric binary system at 760 mmHg	79
Table 4.5: VLE bubble point calculation for 1-propanol (1)-water (2) isothermal binary system at 79.80 ^o C	80
Table 4.6: VLE bubble point calculation for 1-propanol (1)-water (2) isobaric binary system at 760 mmHg	80
Table 4.7: VLE bubble point calculation for water (1)-n-butanol (2) isothermal binary system at 35 ^o C	81
Table 4.8: VLE bubble point calculation for water (1)-n-butanol (2) isobaric binary system at 760 mmHg	82
Table 4.9: VLE bubble point calculation for MEK (1)-water (2) isothermal binary system at 73.8 ^o C	82
Table 4.10: VLE bubble point calculation for MEK (1)-water (2) isobaric binary system at 760 mmHg	83
Table 4.11: VLE bubble point calculation for water (1)-hexanol (2) isothermal binary system at 21 ^o C	84
Table 4.12: VLE bubble point calculation for water (1)-hexanol (2) isobaric binary system at 760 mmHg	84
Table 4.13: UNIQUAC parameters and PRSV interaction parameters and AAD for vapour phase, temperature and pressure for VLE binary homogeneous and heterogeneous systems (isothermal and isobaric)	85
Table 4.14: Area Method and TPI predictions for LLE 1-butanol (1)-water (2) system with the parameters obtained from data correlation	86
Table 4-15: Area Method and TPI predictions for LLE ethyl acetate (1)-water (2) system with the parameters obtained from data correlation. The results are obtained using Pentium(R) 4 CPU 3.00GHz. Simpson's rule is used as numerical integration	86
Table 4.16A: The experimental and correlated values for VLLE binary systems with UNIQUAC and PRSV interaction parameter and the AAD	87
Table 4.16B: The predicted values for VLLE binary systems using the TPI method: Modified 2Point and Direct 3Point search with AAD values and the computational duration for both methods. The results are obtained using Pentium(R)4 CPU 3.00GHz	87
Table 4.17: The AAD values using the TPI method with initial random generator, the test was carried out 10 times on four VLLE systems, at a fixed feed composition 0.5 and grid number 1000	108
Table 4.18: Results for the TPI method for system 1 of Shyu et al. at various feed composition(inside and outside heterogeneous regions) , a set of initial values and fixed grid number	117

Table 4.19: Results for the TPI method for system 1 of Shyu et al. at various feed composition (inside and outside heterogeneous regions), a set of initial values and fixed grid number	118
Table 4.20: The summary table for the VLLE ternary systems: Absolute Average Deviation (AAD) for the Flash calculations, the TPDF and TPI predictions.....	119
Table 4.21: UNIQUAC parameters and PRSV EOS interaction parameters for four VLLE ternary systems using flash calculations	120
Table 4.22: VLLE ternary system water (1)-acetone (2)-methyl ethyl ketone (3) at 760 mmHg, flash calculation, TPDF & TPI predictions	121
Table 4.23: VLLE water (1)-acetone (2)-MEK (3) sensitivity of TPI and TPDF methods to different initial values at various temperatures and 760 mmHg...	122
Table 4.24: The SIG, TPI and TPDF results on VLLE ternary system of water (1)-acetone (2)MEK (3) at 760 mm Hg, different sets of feed composition were chosen outside heterogeneous region with various temperatures	124
Table 4.25: VLLE ternary system (water-ethanol-methyl ethyl ketone) at 760 mmHg flash calculation, TPDF & TPI predictions.....	125
Table 4.26: VLLE water (1)-ethanol (2)-MEK (3) sensitivity of TPI and TPDF methods to different initial values at temperatures; 73.2, 72.8 & 72.1 ⁰ C, pressure 760 mmHg	126
Table 4.27: Results for SIG, TPI and TPDF methods on VLLE ternary system of water (1)-ethanol (2)MEK (3) at 760 mm Hg. different sets of fixed values of feed composition were chosen outside heterogeneous region with various temperatures	127
Table 4.28: VLLE ternary system (water-acetone-n-butyl acetate) at 360 mmHg, flash calculation, TPDF and TPI predictions.....	128
Table 4.29: VLLE water (1)-acetone (2)-n-butyl acetate (3) sensitivity of TPI and TPDF methods to different initial values at various temperatures and 360 mmHg	129
Table 4.30: SIG, TPI and TPDF results on VLLE ternary system of water (1) acetone (2) n-butyl acetate (3) at 360 mm Hg. Different sets of fixed values of feed composition were chosen outside heterogeneous region with various temperatures	131
Table 4.31: VLLE ternary system (water-acetone-n-butyl acetate) at 600 mmHg, flash calculation, TPDF and TPI predictions.....	132
Table 4.32: SIG, TPI and TPDF results on VLLE ternary system of water (1)-acetone (2)n-butyl acetate (3) at 600 mm Hg. Different sets of fixed values of feed composition were chosen outside heterogeneous region with various temperatures	133
Table 4.33: VLLE ternary system (water-acetone-n-butyl acetate) at 760 mmHg, flash calculation, TPDF and TPI predictions.....	134
Table 4.34: Results for the SIG, TPI and TPDF methods on VLLE ternary system of water (1)-acetone (2)n-butyl acetate (3) at 760 mm Hg. Different sets of fixed values of feed composition were chosen outside heterogeneous region with various temperatures	136
Table 4.35: VLLE ternary system (water-ethanol-n-butyl acetate) at 360 mmHg, flash calculation, TPDF and TPI predictions.....	138

Table 4.36: SIG, TPI and TPDF results on VLLE ternary system of water (1)-ethanol (2)n-butyl acetate (3) at 360 mm Hg. Different sets of fixed values of feed composition were chosen outside heterogeneous region with various temperatures	139
Table 4.37: VLLE ternary system (water-ethanol-n-butyl acetate) at 600 mmHg, flash calculation, TPDF and TPI predictions.....	140
Table 4.38: SIG, TPI and TPDF results on VLLE ternary system of water (1) ethanol (2)n-butyl acetate (3) at 600 mm Hg. Different sets of fixed values of feed composition were chosen outside heterogeneous region with various temperatures	141
Table 4.39: VLLE ternary system (water-ethanol-n-butyl acetate) at 760 mmHg, flash calculation, TPDF and TPI predictions.....	142
Table 4.40: Results for SIG, TPI and TPDF methods on VLLE ternary system of water (1)-ethanol (2) n-butyl acetate (3) at 760 mm Hg. Different sets of fixed values of feed composition were chosen outside heterogeneous region with various temperatures	143
Table 4.41: Summary table for VLLE ternary systems shows Absolute Average Deviation (AAD) for SIG, TPDF and TPI predictions. These predictions are based on temperature and pressure	144
Table 4.42: VLLE prediction values for VLLE water (1)-acetone (2) MEK (3) system at 760 mmHg using SIG, TPI and TPDF methods	145
Table 4.43: VLLE prediction values for VLLE water (1)-ethanol (2) MEK (3) system at 760 mmHg using SIG, TPI and TPDF methods	146
Table 4.44: VLLE prediction values for VLLE water (1)-acetone (2)-n-butyl acetate (3) system at 360 mmHg using SIG, TPI and TPDF methods	147
Table 4.45: VLLE prediction values for VLLE water (1)-acetone (2)-n-butyl acetate (3) system at 600 mmHg using SIG, TPI and TPDF methods	148
Table 4.46: VLLE prediction values for VLLE water (1)-acetone (2)-n-butyl acetate (3) system at 760 mmHg using SIG, TPI and TPDF methods	149
Table 4.47: VLLE prediction values for VLLE water (1)-ethanol (2)-n-butyl acetate (3) system at 360 mmHg using SIG, TPI and TPDF methods	150
Table 4.48: VLLE prediction values for VLLE water (1)-ethanol (2)-n-butyl acetate (3) system at 600 mmHg using SIG, TPI and TPDF methods	151
Table 4.49: VLLE prediction values for VLLE water (1)-ethanol (2)-n-butyl acetate (3) system at 760 mmHg using SIG, TPI and TPDF methods	152
Table 4.50: Summary table for VLLE quaternary systems, over all Absolute Average Deviation (AAD) for the flash calculations, the TPDF and SIG predictions	193
Table 4.51: Shows UNIQUAC and PRSV EOS interaction parameters for two VLLE quaternary systems using flash calculations	194
Table 4.52: VLLE quaternary system water (1)-ethanol (2)-acetone (3)-MEK (4) at 760 mmHg, experimental Flash, TPDF and SIG predictions	195
Table 4.53: VLLE quaternary system water (1)-ethanol (2)-acetone (3)-n butyl acetate (4) at 760 mmHg, experimental, Flash, TPDF and SIG predictions	198
Table 4.54: VLLE quaternary system water (1)-ethanol (2)-acetone (3)-n butyl acetate (4) at 600 mmHg, experimental, Flash, TPDF and SIG predictions	202
Table 4.55: VLLE quaternary system water (1)-ethanol (2)-acetone (3)-n butyl acetate (4) at 360 mmHg, experimental, Flash, TPDF and SIG predictions	206

List of figures

Figure 2.1: Schematic diagram of circulating stills.....	33
Figure 3.1: Types of binary systems showing T-x-y & P-x-y phase diagram.....	43
Figure 3.2: T-x-y spatial representation of the VLLE data for a ternary system; (b) Projection of the VLLE region	44
Figure 3.3: The Gibbs energy of mixing ϕ curve for a two phase binary system	62
Figure 3.4: Representation of the search procedure for 3 phase binary system using TPI method	64
Figure 3.5: VLLE prediction for water(1)-n butyl acetate(2) system at 364 K and 1.013 bar , shows the equal areas (A,B) and (C,D) confined between the line and the first derivative of Gibbs energy curve in Equal Area Rule	65
Figure 4.1: A&B: isobaric VLE at 760 mmHg and isothermal at 65 ⁰ C for the system methanol (1)-water (2) respectively. C&E: comparison of experimental (solid symbols) and estimated (hollowed symbols) equilibrium temperature and composition for isobaric condition. C&E: comparison of experimental (solid symbols) and estimated (hollowed symbols) equilibrium temperature and composition for isobaric condition.....	93
Figure 4.2: A&B: isobaric VLE at 760 mmHg and isothermal at 50 ⁰ C for the system ethanol (1)-water (2) respectively. C&E: comparison of experimental (solid symbols) and estimated (hollowed symbols) equilibrium temperature and composition for isobaric condition. D&F: comparison of experimental and correlated equilibrium pressure (mmHg) and composition for isothermal condition.	94
Figure 4.3: A&B: isobaric VLE at 760 mmHg and isothermal at 79.80 ⁰ C for the system 1-propanol (1)-water (2) respectively. C&E: comparison of experimental (solid symbols) and estimated (hollowed symbols) equilibrium temperature and composition for isobaric condition. D&F: comparison of experimental and correlated equilibrium pressure (mmHg) and composition for isothermal condition.....	95
Figure 4.4: A&B: isobaric VLE at 760 mmHg and isothermal at 35.0 ⁰ C for the system water (1)-n-butanol (2) respectively. C&E: comparison of experimental (solid symbols) and estimated (hollowed symbols) equilibrium temperature and composition for isobaric condition. D&F: comparison of experimental and correlated equilibrium pressure (mmHg) and composition for isothermal condition.	96
Figure 4.5: A&B: isobaric VLE at 760 mmHg and isothermal at 73.80 ⁰ C for the system MEK (1)-water (2) respectively. C&E: comparison of experimental (solid symbols) and estimated (hollowed symbols) equilibrium temperature and composition for isobaric condition. D&F: comparison of experimental and correlated equilibrium pressure (mmHg) and composition for isothermal condition.....	97
Figure 4.6: A&B: isobaric VLE at 760 mmHg and isothermal at 21.0 ⁰ C for the system water (1)-1-hexanol (2) respectively. C&E: comparison of experimental (solid symbols) and estimated (hollowed symbols) equilibrium temperature and composition for isobaric condition. D&F: comparison of experimental	

and correlated equilibrium pressure (mmHg) and composition for isothermal condition.....	98
Figure 4.7: Experimental versus calculated values for vapour phase composition for binary VLE systems, the solid icon represents the value when the Sandler's programme was used and the hollowed icon represents the value obtained by this work (PRSV+WSMR model). A. VLE isothermal data at 35.0 ^o C for the system water(1)-n-butanol(2) B. Binary VLE isothermal data at 73.80 ^o C for the system MEK(1)-water(2), C. Binary VLE isothermal data at 21.0 ^o C for the system water(1)-1-hexanol(2).	99
Figure 4.8: Experimental versus calculated values for pressure (mmHg) for binary VLE systems, the solid icon represents the AD value when the Sandler's programme was used and the hollowed icon represents the AD value obtained by this work (PRSV+WSMR model). A. VLE isothermal data at 35.0 ^o C for the system water(1)-n-butanol(2) B. Binary VLE isothermal data at 73.80 ^o C for the system MEK(1)-water(2), C. Binary VLE isothermal data at 21.0 ^o C for the system water(1)-1-hexanol(2).	100
Figure 4.9: Gibbs energy curve of liquid-liquid equilibrium for 1-butanol (1)-water (2) system at temperature range (0-120) ^o C.....	103
Figure 4.10: Gibbs free energy curve of liquid-liquid equilibrium for ethyl acetate (1)-water (2) system at temperature range (0-70) ^o C	103
Figure 4.11: Schematic representation of a 3-phase binary at fixed T and P, showing the solution tangent line.....	106
Figure 4.12: The fluctuations in the results for the TPI method using random initial generator in prediction of VLLE for four binary systems.....	108
Figure 4.13: Organic part of Gibbs energy curve (ϕ) for VLLE water(1)-n-butyl acetate(2) system at 91.85 ^o C & 1.013 bar, the circled area is expected for the tangent line to intersect with the energy curve (ϕ)	110
Figure 4.14: VLLE water (1)-n butyl acetate (2) system at 91.85 ^o C and 1.013 bar, showing the tangent line and Gibbs free energy curve.....	112
Figure 4.15: VLLE ethyl acetate (1)-water (2) system at 72.05 ^o C and 1.013 bar, showing the tangent line and Gibbs free energy curve.....	112
Figure 4.16: VLLE n-butanol (1)-water (2) system at 36 ^o C and 0.068 bar, showing the tangent line and Gibbs free energy curve.....	113
Figure 4.17: VLLE Water (1)-n-butanol (2) system at 93.77 ^o C and 1.013 bar, showing the tangent line and Gibbs free energy curve.....	113
Figure 4.18: A plot of the grid number against the Absolute Average Deviation for composition for the artificial systems of Shyu et al. (1995).....	154
Figure 4.19: A plot showing Gibbs energy surface and the tangent plane under the surface for two ternary 3-phase systems of Shyu et al. (System 1 & System 2)	158
Figure 4.20: TPI method predictions for 10 sets of initial values of VLLE water (1)-acetone (2)-MEK (3) at temperature 73.10 & 72.60 ^o C and pressure of 760 mmHg. The solid line represents TPI values and the dotted line the initial values.....	161
Figure 4.21: TPI method predictions for 10 sets of initial values of VLLE water (1)-ethanol (2)-MEK (3) at temperature 73.20 & 72.80 ^o C and pressure of 760 mmHg. The solid line represents TPI values and the dotted line the initial values.....	162

Figure 4.22: Gibbs energy surface (ϕ) with the tangent plane under the ϕ surface is intersecting in three stationary points for the VLLE water(1)-acetone(2)-MEK system at 760 mmHg and temperature of 73.10°C.....	163
Figure 4.23: Gibbs energy surface (ϕ) with the tangent plane under the ϕ surface is intersecting in three stationary points, for the VLLE water(1)-ethanol(2)-MEK system at 760 mmHg and temperature of 73.20°C.....	164
Figure 4.24: Gibbs energy surface (ϕ) with the tangent plane under the ϕ surface is intersecting in three stationary points for the VLLE water(1)-acetone(2)-n-butyl acetate system at 360 mmHg and temperature of 59.00°C	165
Figure 4.25: Gibbs energy of mixing for a hypothetical binary system showing the tangent line at feed composition (z) and tangent distance F at trial composition (y) and the parallel tangent at the stationary point.....	168
Figure 4.26: VLLE (mole fraction) representation for ternary system (water (1)-acetone (2)-MEK (3) at 760 mmHg. The diagram shows the comparison of experimental data, correlated using flash calculation and predicted values using TPDF and TPI	173
Figure 4.27: VLLE (mole fraction) representation for ternary system (water (1)-ethanol (2)-MEK (3) at 760 mmHg. The diagram shows the comparison of experimental data, correlated using flash calculation and predicted values using TPDF and TPI	174
Figure 4.28: VLLE (mole fraction) representation for ternary system (water (1)-acetone (2)-n-butyl acetate (3) at 360 mmHg. The diagram shows the comparison of experimental data, correlated using flash calculation	175
Figure 4.29: VLLE (mole fraction) representation for ternary system (water (1)-acetone (2)-n-butyl acetate (3) at 360 mmHg. The diagram shows the comparison of experimental data, correlated using flash calculation and predicted values using TPDF	176
Figure 4.30: VLLE (mole fraction) representation for ternary system (water (1)-acetone (2)-n-butyl acetate (3) at 360 mmHg. The diagram shows the comparison of experimental data, correlated using flash calculation and predicted values using TPI	177
Figure 4.31: VLLE (mole fraction) representation for ternary system (water (1)-acetone (2)-n-butyl acetate (3) at 600 mmHg. The diagram shows the comparison of experimental data, correlated using flash calculation.....	178
Figure 4.32: VLLE (mole fraction) representation for ternary system (water (1)-acetone (2)-n-butyl acetate (3) at 600 mmHg. The diagram shows the comparison of experimental data, correlated using flash calculation and predicted values using TPDF	179
Figure 4.33: VLLE (mole fraction) representation for ternary system (water (1)-acetone (2)-n-butyl acetate (3) at 600 mmHg. The diagram shows the comparison of experimental data, correlated using flash calculation and predicted values using TPI	180
Figure 4.34: VLLE (mole fraction) representation for ternary system (water (1)-acetone (2)-n-butyl acetate (3) at 760 mmHg. The diagram shows the comparison of experimental data, correlated using flash calculation.....	181
Figure 4.35: VLLE (mole fraction) representation for ternary system (water (1)-acetone (2)-n-butyl acetate (3) at 760 mmHg. The diagram shows the	

comparison of experimental data , correlated using flash calculation and predicted values using TPDF	182
Figure 4.36: VLLE (mole fraction) representation for ternary system (water (1) -acetone (2)-n-butyl acetate (3) at 760 mmHg. The diagram shows the comparison of experimental data, correlated using flash calculation and predicted values using TPI	183
Figure 4.37: VLLE (mole fraction) representation for ternary system (water (1) -ethanol (2)-n-butyl acetate (3) at 360 mmHg. The diagram shows the comparison of experimental data, correlated using flash calculation and predicted values using TPDF and TPI	184
Figure 4.38: VLLE (mole fraction) representation for ternary system (water (1) -ethanol (2)-n-butyl acetate (3) at 600 mmHg. The diagram shows the comparison of experimental data, correlated using flash calculation and predicted values using TPDF and TPI	185
Figure 4.39: VLLE (mole fraction) representation for ternary system (water (1) -ethanol (2)-n-butyl acetate (3) at 760 mmHg. The diagram shows the comparison of experimental data, correlated using flash calculation and predicted values using TPDF and TPI	186
Figure 4.40: AAD for VLLE predictions for ternary systems showing the TPI and TPDF methods where TPI-1 and TPDF-1 indicates that the predicted values obtained at known temperature , pressure and feed compositions , TPI-2 and TPDF-2 indicates that the prediction values are obtained from knowing temperature and pressure of the system.....	188
Figure 4.41: VLLE quaternary system water (1)-ethanol (2)-acetone (3)-MEK (4) at 760 mmHg, TPDF prediction versus experimental of water and MEK in the organic, aqueous and vapour phases.....	211
Figure 4.42: VLLE quaternary system water(1)-ethanol(2)-acetone(3)-n-butyl acetate (4) at 760 mmHg , TPDF prediction versus experimental of water and n-butyl acetate in the organic ,aqueous and vapour phases	212
Figure 4.43: VLLE quaternary system water(1)-ethanol(2)-acetone(3)-n-butyl acetate (4) at 600 mmHg , TPDF prediction versus experimental of water and n-butyl acetate in the organic ,aqueous and vapour phases	213
Figure 4.44: VLLE quaternary system water(1)-ethanol(2)-acetone(3)-n-butyl acetate (4) at 360 mmHg , TPDF prediction versus experimental of water and n-butyl acetate in the organic ,aqueous and vapour phases	214
Figure A: The simplex for three Phase Flash calculations.....	232
Figure B: Systematic Initial Generator for TPI method	233
Figure C: Diagram of Nelder-Mead Simplex minimisation procedure	234

1. Introduction

In the 1970s the company then known as GLAXOCHEM operated a penicillin manufacturing site in Ulverston, Cumbria. As part of this process there was an extraction of the penicillin using butyl acetate as the extracting solvent. Other solvents, acetone, methanol and ethanol were also used at other points in the process. A distillation column was built to separate the acetone, methanol and ethanol in the presence of water. When the system was operated it was found that a 5th component, butyl acetate, was contaminating the mixture.

In the bottom section of the column it was found that the higher boiling components, butyl acetate and water, were present in such proportions that a heterogeneous azeotrope formed and this had a significant effect on the column operation and the solvent recovery efficiency.

GLAXOCHEM made significant efforts to model the operation of the five-component system in the column. It was found that the NRTL and UNIQUAC equations could be used by building up the required multicomponent data from the 10 constituent binaries. Such a method should be possible based on the theoretical background of these equations however it was found that the method proved to be inadequate because of the unreliability of the data for the butyl acetate/water system. There were no reliable published data and methods such as UNIFAC did not appear to give useable results. A commercial simulator, HYSYS, uses UNIFAC predictions but was also found to give doubtful results. Subsequently work by Desai (1986), Hodges et al. (1998) and Younis et al. (2007) has attempted to make measurements on heterogeneous 3 phase systems (VLLE) and to model using both activity coefficients based models and Equations of State (EOS) based models.

The work which evolved from the original penicillin based problem has produced a suggested equilibrium still for measurement of 3-phase equilibrium at constant pressure and the extension of activity coefficient based models to model such data. One of the problems in using such models is the difficulty of predicting the phase splitting point based on the overall liquid composition. It was essential that this prediction could be done for the distillation column modelling. In theory this prediction is easier using an EOS model and the original attempts by Hodges et al.

(1998) to demonstrate that EOS can be applied to complex, multicomponent, heterogeneous systems is extended in this work and attempts are made to demonstrate the possibility of predicting phase splitting in the liquid phase. The same organic/aqueous systems used in the penicillin production are considered.

In the modelling of distillation columns, it is necessary to have VLLE data on a quinary system (acetone-methanol-ethanol-butyl acetate-water), this quinary system is made up of 10 constituent binary systems: acetone-water, methanol-water, ethanol-water, butyl acetate-water, methanol-butyl acetate, ethanol-butyl acetate, acetone-butyl acetate, methanol-ethanol, acetone-methanol, acetone-ethanol. Each of these constituent binaries show varying positive deviation from Raoult's law, some of these deviations are large enough to produce minimum boiling azeotrope; for example: acetone-methanol, ethanol-water and ethanol-butyl acetate, the positive deviation in the case of butyl acetate-water is so large that a heterogeneous azeotrope is formed. It would appear any quinary built up of these constituent binaries is going to exhibit complex behaviours and any attempt to predict the quinary behaviour from non-ideal constituent binaries may be problematic.

In the column which was to be modelled the pressure would be fixed and it would be necessary for example, to predict a vapour phase composition from a known liquid composition, This would require the calculation to also fix the phase temperature at equilibrium with the added complication that the liquid phase would also have to be checked for the presence of two liquid phases. To be able to handle this type of modelling it would be useful to set objectives:

1. Obtain reliable data for the quinary system.
2. Correlate these data using known models.
3. Use the correlation obtained to predict phase compositions at given T, P and test whether calculated liquid phase compositions lie within a heterogeneous region.

It was considered that objective 1 was met by the work of Younis et al. (2007) and this current work was designed to deal with objectives 2 and 3 by progressive modelling of binary, ternary and quaternary systems.

When the Gibbs free energy for a mixture at a fixed temperature, pressure and known overall composition exhibits the minimum level, the mixture is thermodynamically stable and splits to a number of phases at equilibrium. A reliable thermodynamic method is crucial to determine the composition of the equilibrium phases and number of phases present. This is a stepping stone to find an efficient thermodynamic model to be used in separation processes as many simulation packages might fail in the prediction of the thermodynamic behaviour of such complex mixtures.

This work includes a literature survey of phase equilibrium and covers the common models available to represent the fugacity of a component in a mixture, for instance Equations of State (EOS) and Activity Coefficients Models (ACM). This chapter also critically analyses the combining Mixing Rules (MR) and assesses the work of other researchers in the field in order to select the correct type of MR for the modelling process of multicomponent multiphase heterogeneous mixtures. Another part of the literature survey covers the methods used in Gibbs free energy minimisations and the initialisation schemes used in VLE, LLE and VLLE phase equilibrium calculations. In this chapter, the available thermodynamic equilibrium methods of correlation and prediction are identified together with the downside and advantages of these approaches such as equation solving methods and Gibbs free minimisation methods.

The theory chapter consists of the thermodynamic development of modelling phase equilibria in particular the use of Equation of State (EOS) and Activity Coefficient Models used in representation of liquid and vapour phase fugacities. This chapter also elaborates the theoretical details of the thermodynamic model (PRSV+WSMR) and the mathematical explanations for the methods of Gibbs free energy minimisation (Area Method (AM), Equal Area Rule (EAR), TPI and TPDF). An important section of the theory includes the algorithm for suggested Systematic Initial Generator (SIG) to be used with the TPI method for the prediction of VLLE

ternary systems. The final section covers the Nelder Mead simplex used in the Gibbs free energy minimisation and the flash correlations.

The final chapter, dedicated to the results and discussion, is basically divided into three sections: binary (DECHEMA Chemistry Data Series (1977, 1979, 1981, 1982 and 1991)), ternary and quaternary phase equilibrium systems of Younis et al. (2007). In each section the modelling results are displayed followed by discussion. The selected modelling package (PRSV+WSMR) was tested on six VLE binary systems ranging from the homogeneous to heterogeneous region at isothermal and isobaric conditions. The model was tested to investigate the applicability and reliability of this model in representing non-ideal behaviour. The prediction methods of Gibbs free minimisation (Area Method developed by Eubank et al. (1992) and the Tangent Plane Intersection (TPI) method developed by Hodges et al. (1998)) have been applied on LLE and VLLE for four binary systems. The reliability and efficiency of both methods were studied in respect of the applicability to extend to multicomponent multi-phase equilibrium calculation. The subsequent section includes results on the VLLE ternary calculation and prediction methods (Flash calculation, TPI, Tangent Plane Distance Function (TPDF)) and the Systematic Initial Generator (SIG) suggested to improve the reliability of the TPI method. Further investigation highlights the possibility of using the prediction methods as a phase predictor in homogeneous and heterogeneous regions for these systems. The final section is dedicated to the modelling results (Flash, TPDF and SIG) for VLLE quaternary systems of Younis et al. (2007).

2. Literature Survey

2.1 General survey of Phase Equilibrium

The study of phase equilibrium of systems is a vital element in design, operation and optimisation of all separation processes. In processes such as the oil recovery industry, solvent recovery in the pharmaceutical industry, bio-ethanol production and most petrochemical industries proper and reliable phase behaviour modelling is required. Consequently thermodynamic modelling of phase equilibrium is a core concern in chemical process design.

A literature survey indicates that a large volume of work has been published for a range of approaches to vapour-liquid-equilibrium (VLE). Many methods rely on the flash calculation which uses material balances and equality of a component fugacity in both phases. Much of basic thermodynamics then requires a consideration of the basic energy driving forces involved in transfer between phases and calculation based on equality of energies between phases. The modelling problem then involves the representation of these energies related to the nature of the phases being considered. In practice the models require as accurate a representation as possible of gas (vapour) and liquid phases. An added complication arises when more than two phases are present in the equilibrium situation. Although most of the systems that require modelling are homogenous there are a number of situations where 3 phases in equilibrium (vapour-liquid-liquid) need to be modelled. In practice considerably less interest has been shown towards thermodynamic modelling of vapour-liquid-liquid Equilibria (VLLE) for heterogeneous systems.

A common element in the calculation of Phase Equilibria is the expression of a component energy through the Component Chemical Potential which can be related to the Thermodynamic Concentration, the Activity, and then to the Component Fugacity, f_i . As pointed out previously, a main approach to Phase Equilibrium Calculations (PEC) is flash calculation which relies on mass balances and equality of fugacity. As described by Prausnitz et al. (1999), three steps are required preceding the PEC: modelling the system according to thermodynamic laws, converting that to a mathematical problem and finally solving the problem.

Thermodynamic modelling of various phase equilibrium systems often employs Equations of State (EOS) and Activity Coefficient Models (ACM). EOS are mainly used for gas or vapour phases and ACM for liquid phases although these can be used in various combinations. Search for the thermodynamic model to describe the equilibrium relationship of heterogeneous systems continues.

A reliable method is required to determine the mixture stability and the accurate number of phases at a given overall composition. As the Flash calculations fail for complex mixtures the tangent plane approach has been developed and used by Michelsen (1982, a, b) in conjunction with multi-phase flash calculations. Since Michelsen's findings, many techniques have been published on global optimisation methods to assist the tangent plane criterion.

2.2 Phase Equilibrium

2.2.1 Background Theory

The classical and fundamental approach of phase equilibrium was developed in the early work of Gibbs, the criteria used to define equilibrium in a closed system is equality of thermal (Temperature), mechanical (Pressure) and chemical potentials (Fugacity) or partial molar Gibbs energy in all phases. This is expressed mathematically as :(Orbey and Sandler, 1998)

$$\bar{G}_i^I(x_i^I, T, P) = \bar{G}_i^{II}(x_i^{II}, T, P) = \bar{G}_i^{III}(x_i^{III}, T, P) = \dots \quad (2.1)$$

If the derivative of \bar{G}_i^J is taken with respect to the number of moles of species i in phase J with all other mole numbers held constant then the partial molar Gibbs free energy of species is equal to chemical potential μ_i as shown in this equation:

$$\bar{G}_i^J(x_i^J, T, P) = \left[\frac{\partial(N^J \bar{G}_i^J)}{\partial N_i^J} \right]_{N_{k \neq i}^J, T, P} = \mu_i^J(x_i^J, T, P) \quad (2.2)$$

Considerable effort in thermodynamics is dedicated to converting the above relationship into interrelations between compositions of the equilibrium phases, consequently in the ideal homogenous system the equation is:

$$\bar{G}_i^{IM}(T, P, x_i) = \underline{G}_i(T, P) + RT \ln x_i \quad (2.3)$$

Where \underline{G}_i is pure component molar Gibbs free energy of species i , IM indicates the ideal mixture and \bar{G}_i is the partial molar Gibbs free energy of the species. A real mixture is described in terms of a departure from the ideal behaviour by introducing an activity coefficient (γ_i); for an ideal mixture the value of γ_i is equal to unity:

$$\bar{G}_i(T, P, x_i) = \bar{G}_i^{IM} + RT \ln \gamma_i = \underline{G}_i(T, P) + RT \ln x_i + RT \ln \gamma_i \quad (2.4)$$

In the Equation of State approach a phase concentration for a component in a mixture is described in terms of the fugacity f_i :

$$\bar{f}_i(T, P, x_i) = x_i f_i(T, P) \exp \left[\frac{\bar{G}_i(T, P, x_i) - \bar{G}_i^{IM}(T, P, x_i)}{RT} \right] \quad (2.5)$$

where $f_i(T, P)$ is pure component fugacity of the species at the temperature and pressure of the system. According to the equations developed the fugacity coefficient for component i in a phase can be defined as:

$$\bar{\phi}_i(T, P, x_i) = \frac{\bar{f}_i(T, P, x_i)}{x_i P} \quad (2.6)$$

It is more convenient to use equality of fugacities:

$$\bar{f}_i^I(x_i^I, P, T) = \bar{f}_i^{II}(x_i^{II}, P, T) = \bar{f}_i^{III}(x_i^{III}, P, T) \quad (2.7)$$

The above equation is impractical unless the fugacities can be related to experimentally available physical properties (T, P, x, y). The fugacity coefficient of a component in a vapour phase can be written as:

$$RT \ln \bar{\phi}_i(T, P, y_i) = \ln \left[\frac{\bar{f}_i(T, P, y_i)}{y_i P} \right] \quad (2.8)$$

This equation can be used to represent component phase fugacities in the mixture using various models.

2.2.2 Phase Equilibrium models

The design of separation, purification processes require the use of accurate phase equilibrium data and correlating models. The phase behaviour of, for instance, vapour-liquid and vapour-liquid-liquid equilibrium is important in this respect and has an effective impact on reducing the operation and design cost within the process industry.

For the representation of any liquid phase, especially at low pressures, activity coefficient models are often used because these models are a function of temperature and composition only and the activity coefficient can be measured and correlated. At low pressures, the vapour phase is usually considered to be ideal and Raoult's law applies. At constant temperature, a P-x diagram for the behaviour of real mixtures can show positive and negative deviations from Raoult's law. There are various models that attempt to predict and correlate non-ideal behaviour for components in liquid phase (γ). Many of these models depend on local compositions in the solution and range of intermolecular forces estimated from few molecular diameters. Whilst the concept of local composition has many theoretical weaknesses, many excess Gibbs energy models have been proposed based on this concept such as Wilson(1964), the Non Random Two Liquid(NRTL) model of Renon and Prausnitz (1968) and the UNIQUAC model of Abrams and Prausnitz (1975).

2.2.3 Activity Coefficient Models

These models usually use excess functions to represent the non-ideal behaviour of a component in a liquid mixture. The two-suffix Margules equation is the

simplest function to represent the excess Gibbs energy for a binary mixture (Prausnitz et al, 1999):

$$\frac{g^E}{RT} = a_{12}x_1x_2 \quad (2.9)$$

where a_{12} is a temperature dependent adjustable parameter. The Margules equation is applicable to mixtures with the same molecular size and shape. For binary mixtures of molecules of different size, Wilson presented an equation for the excess Gibbs energy as:

$$\frac{g^E}{RT} = -x_1 \ln(x_1 + \Lambda_{12}x_2) - x_2 \ln(x_2 + \Lambda_{21}x_1) \quad (2.10)$$

This equation obeys the boundary conditions, that g^E tends to zero as either x_1 or x_2 tend to zero. The Wilson equation was extended by Wang and Chao (1983) in order to increase the capability of representing partially and completely miscible systems in calculation of VLE.

The Wilson and extended equations are not applicable to model liquid –liquid phase equilibrium, however the Non-Random Two Liquid equation (NRTL) was proposed by Renon(1968) which depends on a local composition concept with three adjustable parameters(τ_{ji}, τ_{ij}) and ($\alpha_{ji} = \alpha_{ij}$). Equation 2.11 represents the NRTL equation for multi-component systems:

$$\frac{g^E}{RT} = \sum_{i=1}^m x_i \frac{\sum_{j=1}^m \tau_{ji} G_{ji} x_j}{\sum_{i=1}^m G_{ji} x_i} \quad (2.11)$$

Where:

$$\tau_{ji} = \frac{g_{ji} - g_{ii}}{RT} \quad (2.12)$$

$$G_{ji} = \exp(-\alpha_{ji}\tau_{ji}) \quad (2.13)$$

The value of non-randomness parameter α_{ji} varies between 0.20 and 0.47; it is proven that the value 0.3 can be practically used when there is a scarcity of experimental data.

Abrams and Prausnitz (1975) proposed the UNiversal QUAsi Chemical (UNIQUAC) activity coefficient model to improve the representation of excess Gibbs energy of NRTL equation.

2.2.4 UNIQUAC

The UNIQUAC activity model is derived from the local composition theory preserving the two parameter concept in the Wilson equation. UNIQUAC is capable of representing partially miscible mixtures. The UNIQUAC equation structure consists of two parts: combinatorial (the pure molecular size and shape effects) and residual (energy interaction effects), these terms have a major impact on the estimation of activity of the component in the mixture.

The UNIQUAC equation has been successful in correlating vapour-liquid and liquid –liquid equilibria and it shows some superiority over Wilson, NRTL and Margules equations for asymmetric mixtures (Thomsen et al., 2004; Rilvia et al., 2010).

The UNIQUAC equation is used in this work to represent the Excess Gibbs Energy of Mixing as required by the Wong Sandler Mixing Rules. More details can be found in the theory chapter section (3.5).

2.2.5 Equation of State (EOS)

The thermodynamic properties of a substance are defined by knowing the behaviour of the molecules in that substance. Many theories have been suggested to describe the properties of substances; a major development in these theories was proposed by van der Waals in 1880 arising from the corresponding-state theory. This works on the principle that, in general, the intensive and some extensive properties depend on intermolecular forces that are related to critical properties in a universally applicable way. Developments from the corresponding-states principle were initially based on a consideration of spherical molecules.

The ideal gas law fails to represent real gases under high pressure and low temperatures. Van der Waals proposed two corrections: the parameter b provides a correction for the finite molecular size of gas molecules and atoms; the parameter a corrects for intermolecular forces. The assumptions in the ideal gas

law are that molecules occupy no volume and there are no interaction forces between molecules. (Xiang, 2005)

EOS represent an important foundation stone in thermodynamic modelling of phase equilibrium; they can be used over wide ranges of temperatures and pressures. Since the introduction of van der Waals EOS, hundreds of these equations have been published with varying degrees of success for non-ideal and polar mixtures.

According to van der Waals's hypothesis molecules have a finite diameter, therefore the actual volume available to molecular motion is $-b$, where b is constant for each fluid. As a consequence this increases the number of collisions with the wall of the container subsequently the pressure decreases due to intermolecular attraction forces and the correction for this becomes $(-a/v^2)$. The new terms $-a$ an attraction parameter and b a repulsion parameter often improve the accuracy of prediction compared to the ideal gas law.

$$P = \frac{RT}{V - b} - \frac{a}{V^2} \quad (2.14)$$

By applying the critical point conditions to the above equation a and b can be calculated from pure critical properties with simple algebraic manipulations for the equation (2.15):

$$\frac{\partial P}{\partial V} = \frac{\partial^2 P}{\partial V^2} = 0 \quad (2.15)$$

$$a = \frac{27(RT_c)^2}{64 P_c} \quad (2.16)$$

$$b = \frac{RT_c}{8 P_c} \quad (2.17)$$

Although van der Waals stated that the corresponding state is theoretically valid for all pure substances whose PVT properties may be expressed by two parameters equation of state however the van der Waals EOS cannot adequately represent the behaviour of the other substances with non-spherical molecules

(polar). The deviations of these molecules are large enough to necessitate a third parameter. The acentric factor ω suggested by Pitzer et al. (1955) obtains the deviation of the vapour pressure-temperature relation from that expected for substances consisting of spherically symmetric molecules (Poling et al., 2001). The acentric factor is defined as:

$$\omega = -1.0 - \log_{10} \left[\frac{P^{vap}(T_r = 0.7)}{P_c} \right] \quad (2.18)$$

Here $P^{vap}(T_r = 0.7)$ is the vapour pressure of the fluid at $T_r = 0.7$ and P_c is the critical pressure.

Redlich and Kwong (RK) (1949) introduced a temperature-dependence for the attractive term a which improved the accuracy of van der Waals equation of state. The RK EOS was the first equation to be productively applied to the calculation of thermodynamic properties in the vapour phase, however it is not considered adequate for modelling of both liquid and vapour phases.

$$b = \frac{RT}{v - b} - \frac{a}{T^{0.5}v(v + b)} \quad (2.19)$$

As in the van der Waals equation, the parameters a and b can be calculated from critical point conditions:

$$a = \Omega_a \frac{R^2 T_c^{2.5}}{P_c} \quad (2.20)$$

$$b = \Omega_b \frac{R T_c}{P_c} \quad (2.21)$$

the values of Ω_a and Ω_b are fixed as 0.42747 and 0.0867 respectively.

The success of the RK equation motivated many researchers to focus on modification of the alpha function and predictions of volumetric properties. (Soave, 1972; Peng and Robinson, 1976; Twu et al., 1992). Wilson (1964, 1966) introduced a general form of the a parameter and expressed the $\alpha(T)$ as a function of the temperature and the acentric factor:

$$a(T) = \alpha(T)a(T_c) \quad (2.22)$$

$$\alpha = [T_r + (1.57 + 1.62\omega)(1 - T_r)] \quad (2.23)$$

The Wilson equation never became popular because it is not appropriate for reproducing vapour pressure. A function that has been widely used was proposed by Soave (1972) and has a form:

$$\alpha = [1 + m(1 - T_r^{0.5})]^2 \quad (2.24)$$

$$m = 0.480 + 1.574\omega - 0.175\omega^2 \quad (2.25)$$

Twu et al. (1995) have indicated that the prediction of pure component properties is controlled mainly by temperature-dependent form of alpha. As a result of introducing $\alpha(T)$ as a function of reduced temperature and acentric factor, the SRK correlates the vapour pressures of pure hydrocarbons adequately at high reduced temperatures (0.6 to 1.0) and acentric factor up to 0.6, but at lower reduced temperatures the prediction diverges from experimental data for heavy hydrocarbons. Soave (1993) proposed modifications to his original equation but this attempt failed to improve the performance as indicated by Twu et al. (1994). In contrast, the Soave original modification of the Redlich and Kwong equation proved to be more accurate than his later one. However Soave's equation played a fundamental role in the development of Equations of State and contributed towards their development as tools for vapour-liquid equilibrium for mixtures.

Elliott and Daubert (1985, 1987) and Han et al. (1988) reported accurate results for vapour-liquid equilibria modelling prediction and correlation with the SRK EOS. The most widely used EOS is the PR-EOS (Peng and Robinson, 1976) the thermodynamic relation for the pressure of a pure fluid to the temperature and molar volume is expressed as:

$$P = \frac{RT}{v - b} - \frac{a}{v(v + b) + b(v - b)} \quad (2.26)$$

In equation (2.26) the co-volume parameter b is considered independent of temperature while a depends on temperature to reproduce vapour pressure, for pure component a is specified by:

$$a = \alpha(T)a(T_c) \quad (2.27)$$

Peng and Robinson calculated the first and second isothermal derivatives of pure substance pressure with respect to volume by van der Waals and solved equation (2.26) for parameters $a(T_c)$ and b :

$$a(T_c) = 0.45724 \frac{(RT_c)^2}{P_c} \quad (2.28)$$

$$b = 0.07780 \frac{RT_c}{P_c} \quad (2.29)$$

Where:

$$\alpha(T) = \left\{ 1 + m \left[1 - \sqrt{\frac{T}{T_c}} \right] \right\}^2 \quad (2.30)$$

$$m = 0.37464 + 1.5432\omega - 0.26992\omega^2 \quad (2.31)$$

Stryjek and Vera (1986) modified the attraction term of PR-EOS by introducing the adjustable pure component parameter k_1 and changing the k_0 polynomial fit to power 3 of the acentric factor:

$$k = k_0 + k_1(1 + \sqrt{T_r})(0.7 - T_r) \quad (2.32)$$

$$k_0 = 0.378893 + 1.4897153\omega - 0.17131848\omega^2 + 0.0196554\omega^3 \quad (2.33)$$

The parameter k_1 is obtained by fitting the saturation pressure versus temperature data for a pure component. In their subsequent modification Stryjek and Vera (1986) added two additional pure parameters in an attempt to improve PR-EOS for polar molecules. The last modified version of PR-EOS is PRSV2; this differs from the previous modification in that the expression used for k in equation (2.32) and the k proposed for PRSV2 takes the following form:

$$k = k_0 + [k_1 + k_2(k_3 - T_R)(1 - T_R^{0.5})](1 + T_R^{0.5})(0.7 - T_R) \quad (2.34)$$

The k_1 , k_2 and k_3 are pure component adjustable parameters and their values for some components can be found in Stryjek and Vera (1986). The use of additional parameters does not have significant impact on improving the pure component vapour pressure calculation; however the main emphasis is on the type of mixing rules used in VLE correlation for non-ideal mixtures.

Hinojosa-Gomez et al. (2010) presented two modifications of the Peng Robinson EOS. The first method enhanced the EOS pure component property predictions whilst the second alteration proposed a temperature dependency for b the repulsive parameter. A test was carried out by Hinojosa-Gomez et al. (2010) for 72 pure substances including highly polar compounds and the results were in significant agreement with experimental data. Many researchers have conducted comparative studies in an attempt to identify the best EOS for predicting thermodynamic properties for pure components. Nasrifar (2010) examined eleven equations of state for predicting hydrogen properties at temperatures greater than 200 K and almost all the results are comparable in accuracy.

Different approaches have been proposed by many researchers in an attempt to improve the α function in equation 2.27 for heavy hydrocarbons and polar substances. Carrier et al. (1988) and Rogalski et al. (1990) developed a method in conjunction with the Peng-Robinson EOS. In contrast to the α function, the repulsive parameter b is generally kept independent of temperature. However the main purpose in using an Equation of State (EOS) is a representation of mixture properties and the basic quadratic mixing rules can be assumed from the composition dependence of the two main parameters (a, b) of EOS. The common assumption that the same EOS used for pure fluid can be applied for mixtures is expanding the EOS in virial form, for Peng Robinson EOS one obtains:

$$\frac{PV}{RT} = \sum_{n=0}^{\infty} \left(\frac{b}{V}\right)^n - \frac{a}{RTV} + \frac{2ab}{RTV^2} + \dots \quad (2.35)$$

2.3 Mixing Rules

2.3.1 Van der Waals Mixing Rules

Cubic equations of state (EOS) have been used in the process industries for calculation of phase equilibrium. In order to extend the use of the EOS from pure components to mixtures, the a, b functions must be adjusted for mixtures. Equation (2.35) provides a limit that mixing rules parameters should obey; this is known as the one fluid van der Waals mixing rules 1PVDW:

$$a = \sum_i \sum_j x_i x_j a_{ij} \quad (2.36)$$

$$b = \sum_i \sum_j x_i x_j b_{ij} \quad (2.37)$$

$$a_{ij} = (a_{ii} a_{jj})^{\frac{1}{2}} (1 - k_{ij}) \quad (2.38)$$

$$b_{ij} = \frac{1}{2} (b_{ii} + b_{jj}) (1 - l_{ij}) \quad (2.39)$$

where k_{ij} and l_{ij} are the binary interaction parameters obtained by fitting the model to experimental data. Generally l_{ij} is set to zero, in this case equation (2.37) is simplified to:

$$b = \sum_i \sum_j \frac{1}{2} x_i x_j (b_{ii} + b_{jj}) \quad (2.40)$$

The classical quadratic mixing rules are, in general, appropriate for the representation of VLE phase equilibrium in multicomponent systems containing nonpolar and weakly polar components. Testing the performance of different EOS and obtaining similar results indicates that the mixing rules are more important than the actual mathematical relationship of ($P, V, and T$) embodied in an EOS. An empirical attempt to overcome the weaknesses of the 1PVDW additional composition dependence has been introduced to the a parameter of EOS (2PVDW). The extra parameter considered has improved the capabilities of van

der Waals mixing rules for representing VLE data of non-ideal systems that could not be correlated with 1PVDW.

Orbey and Sandler (1998) tested 1PVDW and 2PVDW predictions for VLE calculations on several binary systems; they concluded that the 1PVDW fluid model is not accurate for the description of the phase equilibria of some simple hydrocarbon/water (i.e. acetone/water) mixtures. However the accuracy of the results using 2PVDW is in contrast with the 1PVDW mixing rules.

Several researchers have proposed new mixing rules by combining the EOS and the activity coefficient models.

2.3.2 Huron and Vidal Mixing Rules (HVMR)

Huron and Vidal (1979) verified that the van der Waals mixing rules are reliable in representing a mixture of hydrocarbons but incapable for polar components. They developed a technique that matches the excess Gibbs energy G^E derived from an equation of state with that from an activity coefficient model at infinite pressure. Their combination produced a mixing rule with the parameter a expressed as in following equation:

$$a = b \left[\sum x_i \left(\frac{a_i}{b_i} \right) + \frac{G^E}{C^*} \right] \quad (2.41)$$

b is as expressed in equation (2.40), C^* is a parameter for EOS, for PRSV EOS is -0.62323. The novelty of Vidal and Huron's innovation has motivated a number of authors to develop several EOS/ G^E models. To further develop these models to be totally predictive, the UNIFAC activity coefficient was introduced instead of empirical models.

In order to improve the HVMR model for low pressure systems using the UNIFAC predictive model, the excess free energies should be matched at zero pressure. In this procedure the molar volume of liquid species must be found from EOS and to solve this problem Michelsen (1990) developed an extrapolation method to approximate the molar volume at zero pressure. This modification evolved into a series of HVMRs so called MHV1, MHV2 and a linear combination of Huron-Vidal and Michelsen (LCHVM).

For some non-ideal mixtures Huron and Vidal mixing rules HVMR are shown to be superior to both 1PVDW and 2PVDW MRs, but not satisfactory for VLE correlation over a wide range of temperatures as observed by Orbey and Sandler (1998). One of the major shortcomings of HVMRs is that the excess Gibbs free energy is independent of pressure and does not satisfy the requirement that the second virial coefficient is a quadratic function of composition (Ghosh and Taraphdar, 1998) consequently this mixing rule cannot be used for the calculation of VLE for highly asymmetric systems.

2.3.3 Wong Sandler Mixing Rules

Wong and Sandler (1992) proposed a Mixing Rule (WSMR) by combining the excess Gibbs free energy models and equation of state. WSMR provides an alternative approach for developing mixing rules as proposed by Huron and Vidal (1979). Wong and Sandler assumed the Helmholtz free energy A^E is relatively insensitive to pressure and this could be used in their mixing rules [as $G^E(x)$ expression at low pressure]. They considered equating the excess Helmholtz free energy at infinite pressure from an EOS to that of an activity coefficient model; the assumption is:

$$\frac{A_{\infty}^E}{RT} = \frac{G^E(x)}{RT} \quad (2.42)$$

The parameter a from any EOS is related to the attractive term b through the relation:

$$B(T) = b - \frac{a}{RT} \quad (2.43)$$

From statistical mechanics the term $(b - \frac{a}{RT})$ for the mixture is written as:

$$\left(b - \frac{a}{RT}\right) = \sum \sum x_i x_j \left(b - \frac{a}{RT}\right)_{ij} \quad (2.44)$$

The x is composition and the term $(b - a/RT)_{ij}$ is composition-independent from EOS is given by:

$$\left(b - \frac{a}{RT}\right)_{ij} = \frac{\left(b - \frac{a}{RT}\right)_{ii} + \left(b - \frac{a}{RT}\right)_{jj}}{2} (1 - k_{ij}) \quad (2.45)$$

k_{ij} is binary interaction parameter and $k_{ii} = k_{jj} = 0$

Coutsikos et al.(1995) indicated that the k_{ij} can be determined either by equating the G^E from an equation of state (at P=1 bar , system temperature, $x = 0.5$) to that from an activity coefficient models or by fitting the VLE data using minimisation function (Average Absolute relative Deviation AAD in bubble point pressure plus the AAD in the vapour phase mole fraction). However they preferred the VLE predictions for symmetric and asymmetric systems using WSMR with the k_{ij} value obtained from the correlation of VLE data, as they identified the inability of a composition-independent k_{ij} for asymmetric mixtures. Orbey and Sandler (1995 a) proposed a slightly reformulated version of the original WS mixing rule in which they retained the main concept but changed the combining rule of equation (2.45) to the following equation:

$$\left(b - \frac{a}{RT}\right)_{ij} = \frac{1}{2}(b_i + b_j) - \frac{\sqrt{a_i a_j}}{RT} (1 - k_{ij}) \quad (2.46)$$

This mixing rule has been successful and widely used in the way that an activity coefficient model can be combined with any EOS to represent vapour pressure. The good correlations of vapour-liquid, liquid-liquid and vapour-liquid-liquid equilibria for WSMR as shown by Orbey and Sandler (1998) led them to a conclusion that this mixing rule can be expanded to a wide range of applications which previously could only be correlated with activity coefficient models. When there is an absence of VLE data, this model can be completely predictive with infinite dilution activity coefficients obtained from the UNIFAC model. (Orbey Sandler, 1995a).

Ghosh and Taraphdar (1998) have used PRSV combined with Wong Sandler mixing rules through NRTL activity model for the VLE prediction of forty-three binary mixtures from various ranges of organic, esters, ketones. Their results are comparable to those reported in the DECHEMA data series.

In a comparative study of several mixing rules for EOS in the prediction of multi-component VLE, several mixtures consisting of a polar component (Ethanol), moderately polar (Chloroform), Hexane which represents non-polar component and Acetone which is a highly polar component, were selected in their work. Bazua et al. (1996) showed that in most cases Wong Sandler mixing is the most effective among 22 mixing rules.

There have been several attempts to combine an EOS with a predictive activity coefficient model using an indirect approach. Lee and Lin (2007) reported successful VLE and LLE predictions for highly non ideal mixtures in a wide range of temperature and pressure using PR-EOS combined with a predictive liquid model the Conductor-like Screening Model - Segment Activity Coefficient (COSMO-SAC) through WS mixing rules. They also recommended the WSMR among the best of three different mixing rules. Khodakarami et al. (2005) indicated that the PRSV +WSMR is suitable for the calculation of VLE for strongly non-ideal mixtures, they reached this conclusion by examining the WSMR on several binary and ternary systems. However in the following paper, Lotfollahi et al. (2007) have shown in their proposed predictive method, that the value of the interaction parameter k_{12} can be evaluated directly without the availability of VLE experimental data.

Some researchers have taken the problem a step further by correlating a VLLE model for reactive distillation. Hsieh et al. (2011) conducted a study of multiphase equilibria for mixture and measured experimental VLLE data for a ternary system (water, isopropanol, and isopropyl propionate). They utilised Soave-Redlich-Kwong EOS with Wong-Sandler mixing rule. They agreed on the improvement of the accuracy of the VLLE flash calculation when the parameters of the activity models were determined from the ternary rather than the parameters obtained from binaries VLLE.

Mario and Mauricio (2011) have shown that the PRSV2+UNIQUAC+WS model is capable of correlating the experimental VLE data at 200°C for ethylene-water, ethylene-ethanol and ethanol-water and predicting the VLE of ethylene-water-ethanol ternary system at the same temperature and various pressures.

2.4 Optimisation methods for phase equilibrium modelling

Reliable phase equilibrium modelling is essential for design, simulation and operation of the separation processes. The precise description of phase behaviour of a mixture has a substantial impact on the design plan and the energy costs of operation of any chemical industry process. According to thermodynamic prediction a mixture at specific Temperature (T) and Pressure (P) with overall composition (z) will split to a n number of stable phases at equilibrium.

The optimisation problem for non-reactive systems can be expressed as follows: minimise $F(y)$ subject to material balance constraints. At equilibrium the fugacities of each component are equal in all the phases. The classical approach is equality of fugacities (K-values) and mass balance. These conditions are not sufficient to calculate phase equilibrium particularly in multi-phase multi-component polar systems. It is essential that the Gibbs free energy of mixing will be at the minimum level possible. A global minimisation is required for solving the mathematical problem of phase equilibrium modelling as many optimisation methods fail to converge to the real solution due to a highly non-linear objective function with many local optima and many decision variables.

Generally there are two approaches to solve phase equilibrium problems as pointed out by Iglesias-Silva et al. (2003):

1. solving simultaneously the material balance and thermodynamic equations (K-value method).
2. Gibbs free energy minimisation methods. The traditional optimisation methods may fail to converge to the correct solution when the initial values are not close to the real solution, in the area of phase boundaries and in the critical region.

2.4.1 Equation solving method

The equation solving approach is a classical method of searching for solutions for phase equilibrium calculations. This method requires a good initial estimate if an

iterative calculation is used (Newton method). Michelsen (1993) indicated that in the absence of a good initial estimate, the iterations may converge to trivial solutions especially in the phase boundaries and critical regions.

This method usually consists of solving a system of non-linear and non-convex equations simultaneously which are obtained from the Gibbs free energy optimisation and the mass balances. Some computational difficulties are expected, such as convergence and initial estimates which may produce multiple solutions; in order to guarantee obtaining global solutions a convexity analysis is required. (Teh & Rangaiah, 2002; Lin & Stadtherr, 2004; Rossi & et al., 2011)

2.4.2 Direct minimisation techniques

A reliable and accurate method for global optimisation is desired for thermodynamic phase calculations; due to the non-linearity and complexity of the Gibbs free energy function. The development of global optimisation methods played a significant role in modelling phase equilibria of multi-component multi-phase systems. Since the Michelsen's Tangent Plane Criterion for Gibbs free energy minimisation, many deterministic and stochastic global methods have been used in phase equilibrium computations. The global optimisation problems are a challenging task because the objective functions are highly non-linear and non-convex, the complexity increases when an EOS is used for modelling thermodynamic properties for all the phases at equilibrium. Many researchers have indicated the same problem with the objective function for parameter estimation specifically for VLE and VLLE modelling for multi-component systems as the non-differentiable objective function may converge to a local minimum. This will have significant impact on phase equilibrium calculations and predictions. This will cause uncertainties in design processes. Several studies have emphasized the need for reliable global optimisation techniques. (Bollas et al., 2009; Bonilla-Petriciolet et al., 2010). Global optimisations can be classified into deterministic and stochastic methods.

2.4.2.1 Deterministic methods

Deterministic approaches take advantage of the analytical properties of the mathematical problem to generate a deterministic sequence of points where each point of the sequence does not depend on the value of the objective function at previous points. This method relies on a grid search to converge to a global solution. In their conclusions Lin et al. (2012) have found that stochastic approaches are more flexible and efficient than deterministic approaches.

The different deterministic global optimisation approaches applied to phase equilibrium calculations and modelling are mainly:

1. Branch and Bound Global Optimisation

This method adapts partition strategies, sampling and lower and upper bounding procedures in finding global solutions.

2. Homotopy Continuation Methods

This method is described by continuously constructing a simpler problem from the given one, and then gradually deforming into the original one while solving the constructed simpler problem.

3. Interval analysis

This is a computational method to solve nonlinear equations using interval vectors and matrices starting with an initial interval value and searching all the roots by solving a linear interval equation system for a new interval value.

These methods in general are often slow and require significant numerical calculations that increase proportionally with the problem size; a reasonable and wide initial interval should be provided to converge to a global solution rather than a local minimum. (Zhang et al., 2011)

Deterministic approaches have been used to solve the global stability problem. Sun & Seider (1995) used the Newton homotopy-continuation method to determine phase equilibria for some hydrocarbon mixtures by minimising global Gibbs free energy. McDonald & Floudas (1997) successfully applied the branch and bound method calculating Gibbs free energy for a number of hydrocarbon

systems. The Newton-interval method is used by Burgos-Solorzano et al. (2004) in the calculation of phase equilibria for high pressure multi-phase systems.

The Area Method was developed by Eubank et al. (1992) and later tested by Hodges et al. (1997) on VLE, LLE VLLE binary systems. It is an example of a deterministic optimisation method and utilises a grid search to find a maximum positive net area confined by the Gibbs energy surface (ϕ) and the tangent plane to the surface. Hodges et al. (1998) attempted to extend the area method for ternary multi-phase calculations; this was in fact, a volume method which was not successful. As an alternative approach they developed a Tangent Plane Intersection method. More explanation of this method is given in the theory chapter, section (3.10.2).

2.4.2.2 Stochastic method

Stochastic optimisation uses probabilistic elements and random sequences in the search for global optimum (Rangaiah et al., 2011). In this method new techniques are used such as diversification (explore regions that have not been searched), intensification (provides a simple method to focus the search around the current best solution) and learning strategies to find solutions. In the last two decades, there has been a significant interest in developing reliable optimisation techniques for Phase Equilibrium Calculations (PEC).

Henderson et al. (2001) indicated that emphases were focused on methods which used less computational effort in comparison with deterministic approaches. The main advantages of using stochastic optimisation are: they are applicable to any structures of the problem; require only calculations of objective function and can be used with all thermodynamic models. To date a number of stochastic optimisations have been studied for example:

1. Pure Random Search (PRS) used by Lee et al. (1999) and Adaptive Random Search (ARS) uses random search points and a systematic region reduction strategy to locate the global optimum value for the objective function. (Luus & Rangaiah, 2010).

2. Harmony Search (HS): this algorithm was devised by Geem et al. (2001) using the analogy of the music performance process. The advantageous features of this search are ; makes new vectors by considering all existing vectors, the HS does not require the initial values decision variables, can solve continuous-variables as well as combinatorial problems and can be applied to various fields.
3. Simulated Annealing (SA): was developed by Kirkpatrick et al. (1983). SA is an attempt to mimic the physical phenomenon of annealing in which a solid is first melted and then allowed to cool by decreasing the temperature. During the cooling process the particles form a structure of minimum energy. From a mathematical point of view the SA search process for optimum is through the adaptive acceptance/rejection criterion of the lowest energy points. Various forms of SA have been proposed and applied for phase equilibrium calculations.(Rangaiah, 2001; Zhu et al., 2000 ; Bonilla-Petriciolet et al., 2007)
4. Genetic Algorithm (GA): The main concepts of this algorithm are; survival of the fittest, crossover and mutation operations for generating new individuals. The search starts with initializing of a population which are generated randomly. The objective function is evaluated for the population in the first iteration then the individuals undergo reproduction, crossover and mutation. In the reproduction process more copies of the fittest will meet. The crossover allows the algorithm to escape from local minima. In this procedure new individuals are formed and after mutation the new population is created. This process is repeated until the stopping criteria are satisfied. The GA is widely used in chemical engineering and phase equilibria. (Alvarez et al., 2008; Babu et al., 2009)
5. Tabu Search (TS): This method was developed by Glover (1989) The Tabu means that the algorithm should not re-visit the points which have been searched previously. For creating new points, this algorithm compares the current values with the previous search, lists the worst points in the taboo list and creates a strategy to search in new regions. (Teh & Rangaiah, 2003; Lin & Miller, 2004)

6. Particle Swarm Optimisation (PSO): this algorithm exploits the behaviour of a biological social system of a flock of birds or a school of fish in search for global optimum. PSO consists of a number of particles; each particle has a potential impact on the global solution in the search space. The particles do not recombine directly between each other; they behave socially according to the personal best and the global best positions in the swarm instead. The search strategy allows the particles to stochastically move to the best region in the search space. PSO has been applied successfully in phase stability and phase equilibrium calculations. (Rahman et al., 2009; Zhang et al., 2011)

2.4.2.3 Nelder-Mead

Nelder–Mead is a direct search method widely used in the field of chemical engineering and phase equilibrium calculations. This method optimises non-linear, multi-variable and unconstrained function by using only the function value. The main advantages for using this simplex are; implicitly, no derivatives of function are required. For each of the iterations the search starts with a set of new variables which are generated depending on the coefficient factor values (reflection, expansion, contraction and shrinkage). The search for new variables terminates when the function is at optimum value.

The Nelder-Mead simplex is used through this research to minimise constrained functions (for VLE, LLE, VLLE and Gibbs free energy). The simplex is restricted to search in a required range and this is achieved by giving the function a penalty when the variable values generated are outside the desired range.

Hodges et al. (1998) have demonstrated the applicability of the Tangent Plane Intersection (TPI) for calculations of binary and ternary multiphase equilibrium. The Nelder Mead simplex was used as a minimisation method and in their search procedure local optimum values were found by grouping the variables into two different groups they called this (hybrid1 and hybrid2). The process then conducted an extra plus and cross search near the located values in case these methods failed to find the zero solution for the objection function.

2.4.3 Other method of phase equilibrium calculations (reduced variables)

The reduced variables method was presented by Michelsen (1986); he proved that the phase equilibrium model could be expressed mathematically in terms of three independent variables. The number of variables does not depend on the number of components in the mixture. Michelsen's approach was limited to zero Binary Interaction Coefficients (BIC) parameters in the Peng Robinson EOS. Several researchers developed Michelsen's method for selecting independent variables without restricting the number of non-zero BICs (Hendriks & van Bergen, 1992; Nichita & Minescu, 2004).

The theoretical concept of the reduction method is to express the fugacity coefficients as a function of a reduced number of variables, instead of expressing them as a function of composition. This method is particularly efficient for mixtures with many components and few non-zero BICs such as hydrocarbon systems in oil reservoirs where most BICs are between hydrocarbon molecules in the homogeneous phase and are set to zero (Nichita and Graciaa, 2011).

Nichita et al. (2006) used the reduction method in a combined phase stability analysis and phase splitting procedure to model the phase equilibrium of asphaltene precipitation from oil and also on a sour gas system. They used two cubic EOS; SRK and PR-EOS and claimed their method was robust and efficient.

2.5 The Problem of Initialisation in Phase Equilibria Calculations

In phase equilibrium calculations for heterogeneous multi-phase mixtures regardless of the method used, good initial estimate values are required. Three phase split calculation starts by the mathematically formulating of two sets of equations. The first set describes the equilibrium conditions through the fugacity coefficient ratios so called K_i factors. The second set is the material balance description known as Rachford-Rice (RR) equation. The most efficient approaches in solving the two sets of equations are: equations solving method using deterministic algorithm such as Newton method, and Gibbs free minimisation method.

It has been proven that in the presence of a poor initial estimate it is possible that the optimisation converges to a trivial solution. Many researchers have indicated that this problem is due to non-convex non-linear properties of the objective function with several local minima. (Michelsen, 1982 a; Green et al., 1993; McDonald and Floudas, 1995; Nichita et al., 2002; Teh & Rangaiah, 2002; Leibovici, 2006; Li and Firoozabadi, 2012).

Michelsen (1982 a) observed the effect of initial estimates on flash calculations and in an attempt to improve the reliability of locating the stationary points, he used multiple initial points. Michelsen used the Wilson correlation for low pressure calculations in VLE of hydrocarbon systems and he suggested that the results of a stability test can be used as an initial estimate in flash calculation procedures especially when the Newton-Raphson method is utilised.

Teh and Rangaiah (2002) have applied a Simultaneous Equation Solving (SES) approach in modelling phase equilibria for a series of VLE, LLE and VLLE binary and multicomponent systems. They clearly indicated the issue of convergence to a trivial solution in absence of a good initial estimate especially in the phase boundaries and critical regions.

In their proposal, Haugen and Firoozabadi (2011) used a two-dimensional bisection method in the first iteration of a Successive Substitution Iteration (SSI) loop to obtain a good initial estimate for the Newton algorithm used to solve the three phase split calculations using the Rachford-Rice equations. They pointed out that this problem is due to the lack of an initial estimate for the phase fraction for the first iteration of the successive substitution, particularly when these estimates come from a correlation or from stability analysis. Their method of initialisation based on the two-phase stability analysis test results can be used as a good initial estimate for three- phase equilibria computation.

The contributing factors used in selecting the type of initialisation approach are: the system conditions, complexity of the system (polarity or the level of non-ideality) to be modelled and the type of algorithms used in the minimisation of Gibbs free energy. In general there are two types of initialisation methods found in the literature. The methods are independent of compositions that use Wilson's proposed approximation (eq. 2.48) and methods are depending on composition.

2.5.1 Initialisation method for VLE calculations

Phase stability analysis was first set by Gibbs and subsequently formulated by Michelsen (1982 a) in the term of the Tangent Plane Distance Function TPDF, the function to be minimised globally is: (more details on TPDF can be found in Theory chapter section (3.10.4))

$$TPDF(Y) = \sum_i^{nc} Y_i [(\ln Y_i + \ln \phi_i(Y) - h_i)] \quad (2.47)$$

where : $h_i = \ln z_i + \ln \phi_i(z)$

Where Y_i is trial phase composition for component i and subject to: $\sum Y_i = 1$ and $0 \leq Y_i \leq 1$. At low pressure the K -factor is expressed approximately by Wilson correlation:

$$K_i = \frac{P_{C_i}}{P} \exp \left\{ 5.3727(1 + \omega_i) \left(1 - \frac{T_{C_i}}{T} \right) \right\} \quad (2.48)$$

Michelsen used two sets of initial estimates: $(Y_i = K_i z_i)$ & $(Y_i = K_i / z_i)$ in the minimisation of the TPDF objective function for VLE flash calculation of low pressure hydrocarbon systems.

Michelsen also used a different initialisation approach for high pressure systems which is based on the decreasing monotonic function $F(V)$ which provides assumptions for initial estimates of liquid mole fraction in VLE phase calculations. However the high pressure systems are not in the scope of this research.

A simple initialisation method is proposed by Leibovici (2006) for VLE flash calculation on hydrocarbon mixtures in oil and gas reservoir simulation. The initial values of equilibrium constants (K_i) are estimated from: $K_i = P_i^{sat} / P$ where the saturation pressure of pure component is calculated using an equation of state at the system temperature. The next step computes the infinite dilution fugacity coefficients for all the components in the vapour and liquid phases. The new values of equilibrium constants are generated $K_i^0 = \phi_i^L / \phi_i^V$, the final step is correcting the (K_i) value according to $K_i = K_i^0 \left(\frac{P_i^{sat}}{P} \right)$.

2.5.2 Initialisation method For LLE calculations

Treble (1989) suggested an initialisation scheme similar to that used in the VLE initiation, by assuming the first liquid phase compositions x_i^{L1} equal to overall feed composition. The second liquid phase compositions generated by an equation similar to that described by Michelsen (1982 b) for stability analysis:

$$\ln x_i^{L2} = \ln x_i^{L1} + \ln \phi_i(x^{L1}) - \ln \phi_i^o \quad (2.49)$$

The author indicated the possibility of the trivial solution in LLE iterations due to small differences between the fugacity of the component in the mixture and pure liquid fugacity (ϕ_i^o). In order to solve this issue he suggested resetting the equilibrium ratio K_i values in the range (1.0 - 2.0) to a value of 2.0 and to a value 0.5 in the range of (0.5-1.0) (Treble 1989).

Bonilla-Petriciolet (2007) introduced an initialisation strategy for the Equal Area Rule (EAR) in flash calculations on LLE ternary systems. EAR is Gibbs free energy minimisation method suggested by Eubank and Hall (1995) which uses an integrative approach in the search for equilibrium composition. Bonilla-Petriciolet uses the results obtained from the global optimisation of TPDF as a good initial estimate to calculate the tie-line vector in an attempt to improve the numerical behaviour of the EAR algorithm and produce easy convergence. The author applied this initialisation technique on modelling liquid-liquid equilibrium for three ternary and one hypothetical ternary system using Soave-Redlich-Kwong EOS with classical mixing rules and the Margules equation.

Teh and Rangaiah (2002) have used the procedure of Ohanomah and Thompson (1984) in estimating the initial values for the LLE calculation on six systems (3 binaries, 3 ternaries) using three Activity Coefficient Models (UNIQUAC, NRTL and UNIFAC). Their procedure is based on replacing the multi-component mixture by a hypothetical binary system, then identifying the extract solvent (lowest K_i) and the raffinate solvent (highest K_i). The steps are listed below:

1. Set $x_i^{L1} = z_i$, calculate γ_i^{L1} and then $x_i^{L2} = z_i \gamma_i^{L1}$.
2. Normalise x_i^{L2} , calculate γ_i^{L2} and then $K_i = \gamma_i^{L1} / \gamma_i^{L2}$.

3. Identify the component with the lowest and highest K_i value and their feed compositions are then denoted as z_R and z_E , where R and E raffinate and extracted respectively.
4. Set $x_R^{L1} = x_E^{L2} = 0.98$ and $x_E^{L1} = x_R^{L2} = 0.02$, reevaluate $K_E = x_E^{L2}/x_E^{L1}$ and $K_R = x_R^{L2}/x_R^{L1}$.
5. Finally, calculate the initial estimate for the second liquid phase split :

$$\theta^{L2} = \left[z_E \left(1 - \frac{1}{K_E} \right) + z_R K_R \right] (z_E + z_R).$$

2.5.3 Initialisation method for VLE calculations

The main focus in the literature on the prediction of multiphase equilibrium flash calculations is the reliability of the algorithms. Convergences of these algorithms depend on the initial values of compositions of each component between different phases. The methods of generation of initial estimates for VLE of polar systems in the literature are given uneven treatment. A few researchers have implemented the Wilson approximation (K_i) for non-polar hydrocarbon mixtures. Pan and Firoozabadi (2003) used both the Wilson equation and stability test in VLE calculations. They observed that the Wilson approximation increases the number of iterations and at high pressure often lead to a single phase in comparison with using the stability test method in initial estimation methods.

In a comparison study by between the equation solving method and Gibbs free energy minimisation for phase equilibrium calculation, Teh and Rangalah,(2002) applied the Trebble VLE initialisation scheme (Treble, 1989). Their procedure depends on the assumption that the first liquid composition set is the known feed composition. The second liquid phase compositions are evaluated by comparing the mixture phase coefficient fugacity to the pure liquid fugacity coefficients in a way similar to that described by Michelsen (1982 a, b). For initiation of vapour phase compositions the same scheme was adopted. The next step was to find the estimated values of equilibrium ratios K_i and use these values to solve the

Rachford –Rice equation by the Newton method to find the initial values for phase ratios.

Other researchers used the results from a two-phase flash and stability analysis to provide initial values for multi-phase equilibrium. Nichita et al. (2002) efficiently utilised Tunnelling Optimisation in direct minimization of Gibbs free energy in equilibrium calculations on multi-phase hydrocarbon mixtures. They applied this initialisation strategy to the calculation of a VLLE ternary system (carbon dioxide, methane and normal-hexadecane), this system exhibits three phases at $T=294.3$ K and over the pressure range (64.07- 69.45) bar. A Simulated Annealing (SA) algorithm was used by Pan and Firoozabadi (1998) on the same system. This method is outlined in section (2.4.2.2) and it relies on a prior stability test (based on Gibbs free energy minimisation) and phase split calculations on two phase mixtures in applying three phase flash calculations. Li and Firoozabadi (2012) used this initialization technique to find phase fractions in Rachford–Rice equations. These authors concluded that the direct Newton method of minimisation combined with the initial guesses from the stability analysis test for two-phases is simple and efficient for three phases PEC of a mixture of CO₂, acid gas and oil in oil recovery processes.

2.6 Experimental measurement of phase equilibrium data

The measurement of partially miscible (heterogeneous) vapour-liquid-liquid equilibrium systems is very scarce in the literature, due to the fact that it is very expensive in terms of time and cost. Over the years many authors have called attention to the shortage of data for VLLE compared to existing data on VLE (Norman 1945, Pham and Doherty 1990, Younis et al 2007 and Gomis et al 2010). The techniques available in the literature is summarised in five generic groups: distillation, circulation, dew and bubble, flow and static. (Younis et al. 2007, Gomis et al. 2010). Each of these methods has their relative advantages and disadvantages and the decision as to which method is chosen for a particular study is likely to depend on the type of measurements to be made, e.g. either isobaric or isothermal, the type of system being studied, and the required conditions, e.g. low or high pressure. For isobaric VLE and VLLE measurements

the circulation method is appropriate providing sufficient mixing in the equilibrium chamber is maintained.

In their article, Gomis et al. (2010) represented an overview of the experimental VLLE data for multicomponent systems under isobaric conditions published so far and the methods used in their determinations(36 ternary and three quaternary systems), they confirm the existing lack of data and provide a picture of difficulties measuring equilibrium data in the heterogeneous liquid region.

The principle operation of a general circulation still is quite simple, even though the various equilibrium stills can differ significantly one from another in their construction details. As shown in figure (2.1) , the operation starts with vapour evolved from distilling flask **A** through a vapour conduit (1) and after complete condensation passes to flask **B** then the condensate in flask **B** returns to flask **A** by means of conduit (2). This process repeats until the steady state is reached. In practice, the quantity of vapour produced in the boiling flask is generally small relative to the quantity of liquid that remains in the boiling flask. The size of the boiling flask to be used in the design of a circulation still will have a critical role in the sensitivity of the system to internal fluctuations of pressure and temperature. Thus it is essential to charge a suitable quantity of liquid to the boiling flask to ensure that internal fluctuations are eliminated.

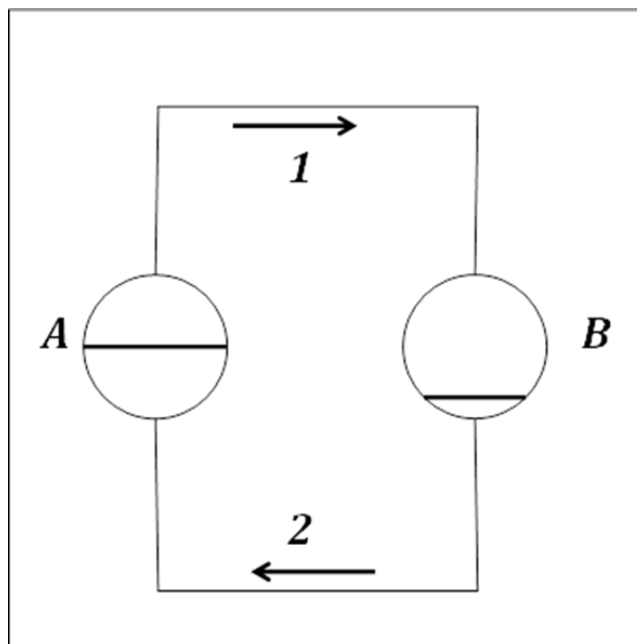


Figure 2.1: Schematic diagram of circulating stills

The main concept of the Othmer's still (1928) was that if the vapour condensate was returned continuously to the boiling flask, the composition of the streams 1 and 2 would reach a true equilibrium. The Othmer still was originally designed to measure isobaric VLE data; however the application of the circulation method to partially miscible systems exhibiting two liquid phases is more difficult when using Othmer's still and its modifications.

The experimental apparatus' applying the circulation method are based on two principles; in Othmer's principle only the vapour phase circulates, whereas in Gillespie's principle both the vapour and liquid phases circulate simultaneously.

One of the main problems concerns the condensation of the vapour phase and phase splitting of the liquid in the condensate flask, as observed by Lee and Lin (2008). This phase splitting influences the ratio of the returning condensate, consequently making a steady state difficult to obtain. Another source of error is the improper mixing of two liquid phases in the boiling flask to achieve intimate contacting of two liquid phases. The magnetic mixing used is insufficient for the complete mixing of two liquid phases in the boiling chamber. Younis et al. (2007) employed a mechanical mixing in the boiling flask to measure the isobaric VLLE data used in this research. The authors indicated that the accuracy of the thermocouple used in monitoring temperature of the system was within 0.1°C and they also applied the Wisniak method (1993) for testing the thermodynamic consistency and declared that the data are consistent.

The literature surveyed up to this point has all dealt with theoretical correlation and predictions with various equilibrium data. This section gives a brief over view of the experimental methods available to measure VLE and VLLE. There are also details supplied of the experimental method used by Younis et al. (2007) to generate the data used in this thesis. In a private communication, Younis has indicated that a cumulative error was calculated for the data measured, this error was to be included in a yet unpublished paper and he quoted the overall error to be not greater than 2%.

2.7 Comments on the reviewed literature

The literature survey has been split into five sections. Each section deals with separate aspects of the overall modelling of heterogeneous phase equilibrium.

In the modelling, the basic requirement is a set of thermodynamic equations that represent the establishment of equilibrium between phases. The equations set out are fundamental and are quoted so that the basic model is clearly established. The issue then is how some of the required parameters in these equations can be represented and then calculated. These representations become complex as phase splitting appears in systems to be modelled; it was therefore important that the available models were presented in this survey.

In representing the required parameters, the literature survey reviews what are essentially two different approaches: Equation of State (EOS) and Activity Coefficient Models (ACM). Both approaches are based on the representation of phases as component molecules that can interact. The two different approaches adopt different bases for modelling these interactions.

The survey on EOS lists a number of different equations that basically attempt to model a phase by: a) representing molecules occupying a finite volume and b) interaction between molecules. The EOS attempts to model phase behaviour by proposing the use of various constants to represent phase effects in determining the value of these constants. They are usually based on pure component properties.

The survey indicates that a number of ACM have been proposed to describe the energy interactions between molecules based on temperature and compositions. These models attempt to measure the molecular distributions in the liquid; hence the models based on this assumption are essentially applicable to the liquid phase. The survey shows that these models can be applied to VLE and LLE usually assuming the vapour phase is ideal. It is desirable to apply the same model to both liquid and vapour phases.

In the EOS there are constants introduced which account for size and volume of the molecules. These constants are an attempt to correct for the fact that the molecules occupy different finite spaces. The approach to modelling the

interaction in EOS is such that it is not completely capable of modelling relatively strong interactions. Consequently the problem is the need to be able to adequately model the strong interactions between unlike molecules, especially polar molecules. Introducing mixing rules to the EOS will improve models for polar mixtures.

In the representation of a liquid phase using EOS the theory of Free-Volume has to be considered. Free-Volume is the difference between the volume of the liquid and the minimum volume occupied by molecules as they are close packed spheres ($V_f = V - b$). In using this concept the thermodynamic properties depend on the Free-Volume calculated from an EOS. The complexity arises when the strong interaction appears in the mixtures with highly polar molecules and asymmetric shapes. The literature shows that a number of classical mixing rules have been developed for VLE modelling for hydrocarbon systems, for instance 1 parameter van der Waals (1PVDW) and (2PVDW). These mixing rules are dependent on composition and are not applicable to polar and highly non-ideal mixtures. The interaction parameter tendency in EOS depends not only on mixing rules but on the theory of combining rules of intermolecular forces.

This literature review has included a survey of all existing EOS and also the attempt to introduce their different approaches to the Free-Volume. The EOS reviewed were: van der Waals, Redlich Kwong (RK), Soave Redlich Kwong (SRK), Peng Robinson (PR), and Peng Robinson Stryjek Vera (PRSV). Section 2.2.5 outlines the reason for selecting PRSV to model the selected systems.

The possibility of the description of the energy parameter in EOS leads to developing a new mixing rule, which incorporates the excess Helmholtz free energy from an activity coefficient model A^E into EOS at a reference pressure (infinite or zero). The literature contains several mixing rules, for example: Huron and Vidal (HVMR) and Wong and Sandler (WSMR). According to the observations made, these mixing rules (EOS/ G^E) are capable of representing phase equilibrium for different systems (including heterogeneous and polar) over a wide range of temperatures and low or moderate pressures. In spite of many advantages for using these models, poor performance was noticed for the size-asymmetric systems (the molecules differ significantly in size). However, according to reported

literature this model, (EOS/ G^E) is more than adequate when applied to the phase calculations of VLE, LLE and VLLE heterogeneous systems.

Published work on modelling and prediction of VLLE for multi-component heterogeneous systems using EOS is scarce. The evaluation of the applicability of the various thermodynamic models for such systems remains a critical issue.

The PRSV EOS combined with UNIQUAC activity coefficient model through Wong and Sandler Mixing Rule (WSMR), is recommended in the literature as successful in modelling PEC for heterogeneous systems. This work has utilised this model for selected systems.

In correlation and prediction using the thermodynamic equations the literature indicates that the classical approach of equality of fugacity and mass balance as a main criterion in phase equilibrium calculations are not sufficient due to the failure of this method in multi-phase multicomponent polar systems. New approaches have been adopted which require the minimisation of the Gibbs free energy of mixing incorporating the classical method. There are two main approaches to solve the phase equilibrium problems:

- a) equation solving methods : solving a system of non-linear and non-convex equations simultaneously , the downside of these methods is convergence to trivial solutions in the absence of a good initial estimate.
- b) Gibbs free energy minimisation methods: it is direct global minimisation techniques (deterministic and stochastic) for the non-differentiable objective function. The deterministic methods are slow; require significant numerical computations and a reasonable initial value needs to be provided to prevent the convergence to local minima. Conversely the stochastic methods adopt new techniques such as: diversification, intensification and learning strategies to find solutions. Currently the main focus in the literature is on the stochastic methods.

In the comprehensive review on global optimisation methods for phase equilibrium calculations, Zhang et al. (2011) summarised that, despite many researchers declaring the reliability of usage of both deterministic and stochastic methods for PEC on different systems, these methods require some improvement in reliability

of initial estimates and computational efficiency. They indicate clearly the major difficulties of Gibbs free energy minimisation using both methods for modelling highly non-ideal mixtures particularly in the critical region and phase boundaries. To date the need for a developed, effective and reliable method for PEC remains a critical issue.

Another aspect is the mathematical formulation of the Gibbs free energy objective function and the search method for Global solutions. The literature survey indicates that there are various methods available; some rely on integration of the Gibbs energy curve (Area Method, Equal Area Rule), others rely on the first or second differentiation of the objective function (Phase Stability analysis and Interval Newton method). Other methods conduct the direct search techniques (Tangent Plane Intersection, Tangent Plane Distance Function) which have a problem of sensitivity to the initial values; consequently this increases the complexity of the minimisation methods.

It has been clearly observed in phase equilibrium calculations that in the presence of poor initial values the method may converge to trivial rather than global solutions and consequently fails in prediction of the correct number of phases or produces negative values of the compositions. The initialisation methods published are based on Wilson's approximation for equilibrium ratios (K_i) for hydrocarbon systems and there are different methods based on estimates/assumptions for unknown phases from the feed composition. It was found in the literature that the initialisation of VLLE for heterogeneous systems lacks thorough investigation as previously indicated due to the scarcity of data for such systems.

This research attempts to model multi-component multi-phase heterogeneous systems using PRSV EOS combined with UNIQUAC, testing the TPI method on newly available VLLE ternary data, as well as the sensitivity of this method to the initial values and the approaches used in solving this problem. Investigation will be carried out on the possibility of extending the TPI method for the prediction of VLLE for multi-component systems.

This literature survey has shown that there is a lack of experimental measured data for heterogeneous multi-component systems containing polar molecules particularly vapour-liquid-liquid equilibrium (VLLE). The work that follows uses the

appropriate EOS and mixing rule as outlined in the review and applies them to multicomponent VLLE data particularly that of Younis et al. (2007). The literature survey indicates that any results obtained will add to the body of knowledge in the area of multi-component VLLE.

Cubic Equations of State are broadly used in the chemical process industry due to their applicability over wide ranges of temperature and pressure. These equations were originally developed to estimate vapour pressure for pure components and have subsequently been extended to the modelling of VLE binary and multi-component systems through mixing rules. The van der Waals mixing rules are adequate to model ideal mixtures, but totally inadequate for the description of phase equilibrium of highly non-ideal mixtures. Recently new mixing rules have been developed which combine the EOS with excess Gibbs energy models (EOS/ G^E) for example Wong Sandler mixing rule (WSMR) is widely used for the modelling of polar and non-ideal complex mixtures. In a capability and limitations test of WSMR in correlation of some VLE binary asymmetric systems, Coutsikos et al. (1995) indicated that WSMR provides a successful correlation for such systems in spite of the different molecular size of the components in the mixture. In a correlation study of VLE for supercritical methanol glycerol system, Liu et al. (2012) showed the results improved using PR-EOS combined with WSMR when compared with PR-conventional mixing rules. As recorded by Wyczesany (2010, 2012) the available models (ACM) can correlate VLE precisely and LLE with less accuracy. The correlation of VLLE for heterogeneous systems (using EOS) has not been thoroughly investigated yet. The flash calculation fails in some cases of multi-component multi-phase equilibrium calculation and Michelsen suggested testing phase stability using Tangent Plane Distance Function (TPDF) criterion. As the literature suggested the TPDF for phase stability test, this research will be applying this method on VLLE ternary and quaternary data and will compare the results with the TPI method.

Briefly the theorem of reduction of variables is proposed to decrease the number of dimensions in the phase equilibrium calculations. The number of variables does not depend on the number of components in the mixture, however the number of BICs control the reduced variable numbers. This method can be applied on

various types of phase calculations such as; multi-phase flash, phase stability analysis and phase envelope construction for hydrocarbon mixtures.

3. Theory

3.1 Introduction

In the phase equilibrium calculations carried out in this work, one of the main goals is to determine the number and the type of phases present and the composition of each phase. As previously pointed out the reliable modelling of multi-component equilibria for a heterogeneous system is an important issue in design, optimisation and simulation in industrial processes, especially distillation and extraction. In vapour-liquid-liquid-equilibrium (VLLE) calculations, at constant temperature and pressure, the total Gibbs energy of the system has to be minimised. The Tangent Plane Intersection (TPI) method has been developed and used by Hodges et al. (1998) for ternary heterogeneous systems. This research attempts to test this method on new published data by Younis et al. (2007) and extend it to quaternary systems. Further tests were carried out by applying the Area Method in integral form and the Equal Area Rule on binary (LLE) and (VLLE) systems. Finally it was discovered that the direct minimisation of the Tangent Plane Distance Function (TPDF) was the most efficient and reliable method which can be utilised in phase equilibrium for all heterogeneous systems.

The theory section explains the background of modelling phase equilibria and also the thermodynamic development of representation of liquid and vapour phase behaviours using Equation of State (EOS) and Activity Coefficient Models (ACM) through Mixing Rules. The flash calculation method based on the Rachford Rice equation is explored with the Peng Robinson Styrjek Vera EOS/ Wong Sandler Mixing Rules. The various mathematical approaches of minimisation of the Gibbs free energy are presented with graphical explanations and the limitations and applicability of these techniques. An important part of the theory is the Systematic Initial Generator (SIG) algorithm and the search procedures for the Nelder Mead simplex optimisation.

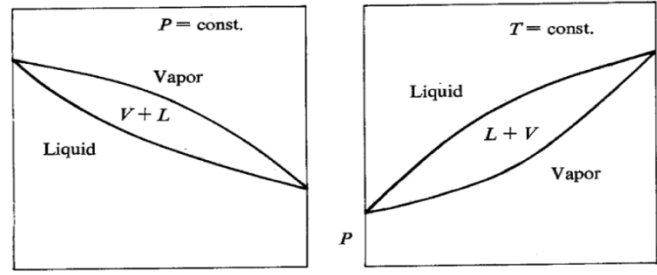
3.2 Background

The design of any separation process requires accurate vapour-liquid, liquid-liquid or vapour-liquid-liquid data and there is a need for modelling the phase behaviour of the system. Equations of state (EOS) have played a central role in the thermodynamic modelling of phase equilibrium and the most recent phase equilibrium modelling utilises EOS and the same Excess Gibbs Energy expressions as those used in activity coefficient models, these are combined by using appropriate mixing rules.

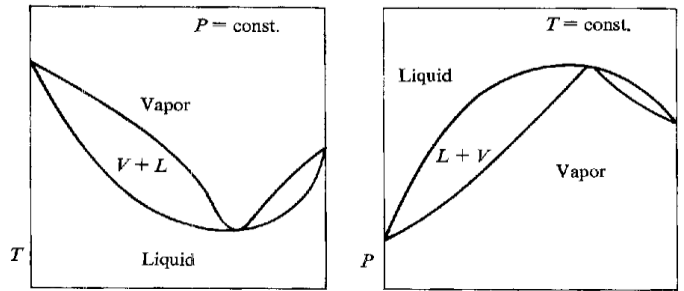
In considering VLE and VLLE for binary and multicomponent systems a consideration must always be given to the system parameters Temperature (T), Pressure (P) and composition usually in terms of Mole Fractions (x_i). With one of these parameters fixed (Usually T or P) the variation of the other parameters can be explored. This variation can reasonably be represented graphically for binary systems but as the number of components increase it becomes more difficult to graphically represent the variations.

In representing binary VLE and VLLE it has to be appreciated that the nature of the plots differs according to the type and extent of variations from Raoult's Law. Thus if pressure is held constant for a binary system a typical plot of VLE for a system close to obeying Raoult's law is shown in figure 3.1-A.

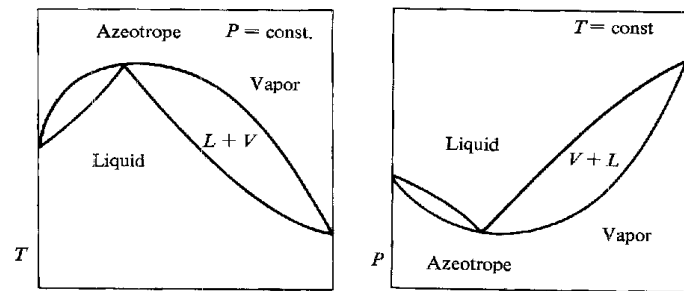
The non-ideal polar systems start to show positive deviations and as the deviations increase it is possible to get the formation of a minimum boiling azeotrope, a typical plot will have a phase diagram as shown in figure 3.1-B. If the binary system exhibits negative deviations from Raoult's law it is possible to get a maximum boiling azeotrope (figure 3.1-C). If the positive deviations from Raoult's law are very large it is possible to get a heterogeneous azeotrope e.g. systems having immiscible liquid phases (figure 3.1-D) and systems having partially miscible liquid phases (figure 3.1-E).



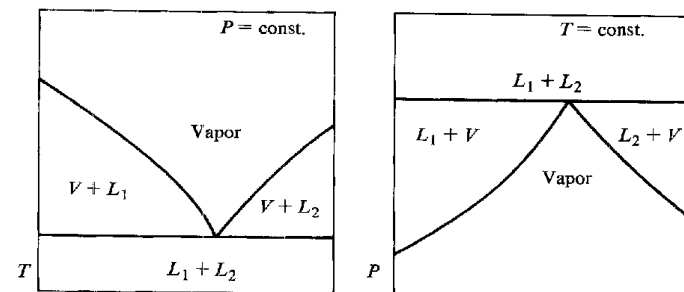
A. system close to Raoult's law



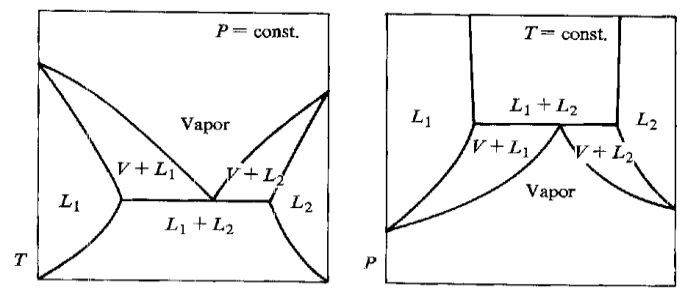
B. minimum boiling azeotrope



C. maximum boiling azeotrope



D. immiscible liquid phases



E. partially miscible liquid phases

Figure 3.1: Types of binary systems showing T-x-y & P-x-y phase diagram

Typically a three component (ternary) system, showing deviations from Raoult's law can be represented on triangular diagrams. These diagrams are usually composition diagrams where the liquid and vapour phase compositions can be represented. This is graphically illustrated by reference to the paper of Younis et al. (2007).

If it is necessary to also illustrate for example a phase diagram where pressure is constant and temperature varies then it is usually necessary to use a 3D diagram.

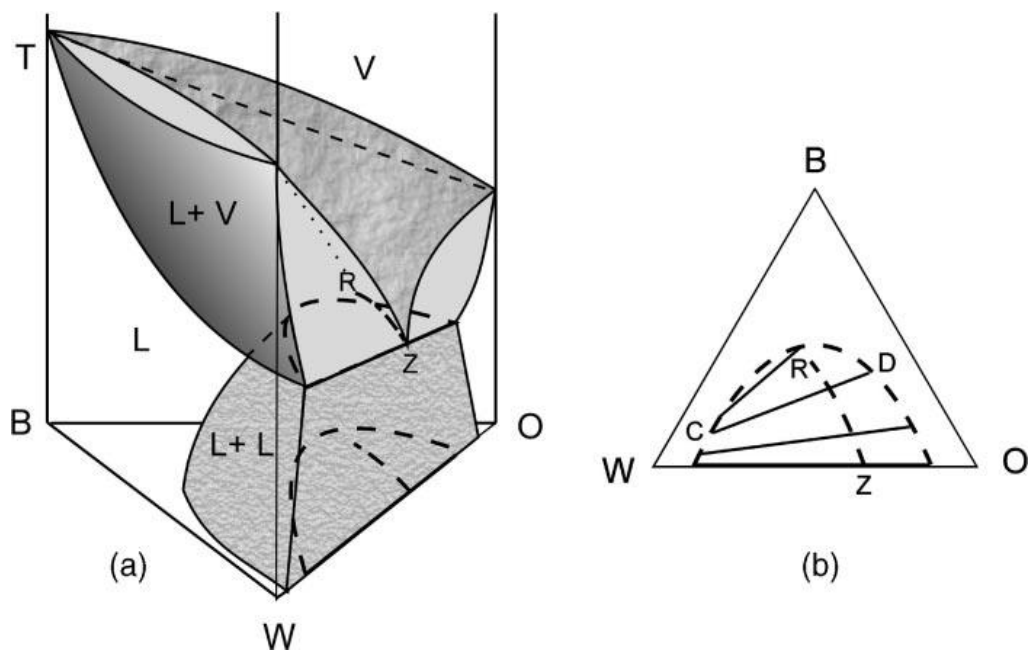


Figure 3.2: T-x-y spatial representation of the VLLE data for a ternary system; (b) Projection of the VLLE region

This diagram represents the liquid and vapour for a ternary system. The region below Z represents a typical liquid-liquid phase region at temperatures below the saturation azeotropic temperature. Point Z represents the binary heterogeneous azeotrope at the appropriate temperature and pressure composition within the ternary system; as can be seen from the accompanying ternary composition diagram (b) the heterogeneous azeotrope occurs when the composition of component B is zero. The line ZR represents vapour phase composition and corresponding liquid phase compositions can be found using appropriate tie lines such as CD.

For such a ternary system Gibbs phase rule could be applied and writing the rule for a non-reactive system gives:

$$F = C - \pi + 2 \quad (3.1)$$

where F is degree of freedom, C is number of components and π is number of phases.

For the ternary system described the degree of freedom is 2, thus for a given conditions there are 2 degrees of freedom appropriately for this system and these would be designated as temperature and pressure. Gibbs phase rule has been used throughout this work.

Phase equilibrium calculations are classified into two main categories; flash calculation and the Gibbs energy minimization (Eubank 1992). The first method is used in solving the material balance equations and the equality of chemical potentials. The weakness in this method is the failure to predict the correct number of phases. The second method utilises global optimisation techniques for the accurate and reliable prediction of phase Equilibria. (Stadtherr et al., 2007).

Since van der Waals produced the first viable cubic equation of State (EOS) in 1873. Many equations of state have been developed by researchers over the intervening years e.g. Redlich-Kwong, Soave- Redlich-Kwong (SRK), Peng-Robinson (PR) and Patel & Teja (Kontogeorgis & Gani, 2004; Sandler 1994).

The Stryjek-Vera modification of Peng-Robinson EOS and Wong Sandler mixing rule (WSMR) incorporated with modified UNiversal QUAsi Chemical (UNIQUAC) activity model is used in this research.

In phase Equilibria calculations several mixing rules have been developed to extend the applicability of the EOS in predicting VLE & VLLE for highly non-ideal polar systems. Wong and Sandler (1992) suggested mixing rules utilising excess Gibbs free energy models in which they combined the attractive term a and co-volume b through a mathematical relationship.

A fundamental concept in phase equilibria calculations is minimising the total Gibbs energy of the system. This method as outlined by Michelsen (1982 a, b) is done in two stages: phase stability (using tangent plane analysis) and phase split.

The major failure with his method is that a good initial phase estimate is required and there is no guarantee that all the stationary points of the tangent plane distance have been found. To overcome this problem the area method was adopted by Eubank et al. (1992) for binary systems and although this produces more reliable predictions than the Michelsen method it is a computationally time consuming process. Hodges et al. (1996) suggested that it was mathematically possible to extend the area method to ternary systems (volume method). The volume method was tested and ultimately failed due to the incorrect bounding of the reduced Gibbs energy of the mixing surface (ϕ) by the 3-phase prism during the integration of the surface. Although the results for some binary systems agree with the experimental data some were poor, particularly the systems with very small mutual solubility.

Hodges et al.(1998) successfully used an alternative approach to the integral area method namely the tangent plane intersection method (TPI) applied to a range of binary and ternary 2 and 3-phase mixtures. They announced that the TPI method could be extended to quaternary 3-phase systems. This work is continuing to develop the TPI method for multi-phase multi-component heterogeneous systems.

In studying the phase equilibrium of a mixture at constant temperature and pressure the most important criteria is to predict the composition of each component in different phases and also the number of phases. It is crucial to know the behaviour of the system at the design stage of the separation process.

As stated previously the thermodynamic calculation for phase equilibrium is classified into two main categories; flash calculation and the Gibbs energy minimization .The first method solves a number of equations relating to material balance and the equality of chemical potentials; this is a classical solution which is unable to predict the correct number of phases. The second method is based on the Michelson tangent plane stability analysis (Michelsen, 1982a, b) this does not guarantee the global equilibrium solution due to a failure in finding the stationary points of the tangent plane distance. An alternative for phase stability analysis is the use of an interval-Newton approach (Schnepper and Stadtherr, 1996) which is defined as an equation solving method. Stadtherr and his colleagues concluded that in the computation of phase equilibrium there is a challenging problem and

although many solutions have been proposed these methods may still fail to solve the problem correctly in some cases. (Stadtherr et al., 2007)

In phase equilibrium prediction the requirement is to model the Gibbs energy of the system according to temperature, pressure and composition of the system. In general there are two types to represent vapour and liquid; the Excess Gibbs energy model (activity coefficient models) and Equation of State (EOS) models.

3.3 Thermodynamic of Phase Equilibrium

The basic requirement for phases to be at equilibrium for pure component or multi component systems is that the state variables (temperature, pressure, chemical potential) must be equal for all the phases. Equilibrium between phases ($\alpha, \beta, \gamma \dots$) in a multi-component system means that:

$$T^\alpha = T^\beta = T^\gamma \dots \quad (3.2)$$

$$P^\alpha = P^\beta = P^\gamma \dots \quad (3.3)$$

$$\mu_i^\alpha = \mu_i^\beta = \mu_i^\gamma \dots \quad (3.4)$$

The chemical potential μ can be expressed in term of fugacities:

$$f_i^\alpha = f_i^\beta = f_i^\gamma \dots \quad (i = 1,2,3, \dots n) \quad (3.5)$$

If the case is vapour-liquid equilibrium:

$$f_i^G = f_i^L \quad (3.6)$$

The vapour phase fugacity can be expressed:

$$f_i^G = y_i \phi_i P \quad (3.7)$$

ϕ_i is the fugacity coefficient which approaches unity for low pressure.

$$\phi_i = \exp\left(\frac{1}{RT} \int_0^P \left(V_i^G - \frac{RT}{P}\right) dP\right) \quad (3.8)$$

Using Peng Robinson ϕ_i can be written in the term:

$$\ln \phi_i = (Z^V - 1) - \ln \left(Z^V - \frac{bP}{RT} \right) - \frac{a}{2\sqrt{2}bRT} \ln \left[\frac{Z^V + \frac{(1 + \sqrt{2})bP}{RT}}{Z^V + \frac{(1 - \sqrt{2})bP}{RT}} \right] \quad (3.9)$$

$$a = 0.45724 \frac{(RT_c)^2 \alpha(T)}{P_c} \quad (3.10)$$

$$\alpha(T) = \left(1 + k(1 - \sqrt{T/T_c}) \right)^2 \quad (3.11)$$

$$k = 0.37464 + 1.54226\omega - 0.26992\omega^2 \quad (3.12)$$

$$b = 0.07780 \frac{RT_c}{P_c} \quad (3.13)$$

The liquid phase fugacity f_i^L is related to mole fraction x_i :

$$f_i^L = x_i \gamma_i f_i^{OL} \quad (3.14)$$

γ_i is the liquid phase activity coefficient of component i , it is function of temperature , pressure and composition.

f_i^{OL} is the fugacity of liquid i at system temperature and pressure

For $x_i = 1$ pure liquid $f_i^L = f_i^{OL}$ and $\gamma_i = 1$

$$f_i^{OL} = P_i^o \phi_i^o \exp \left(\frac{1}{RT} \int_{P_i^o}^P V_i^L dP \right) \quad (3.15)$$

P_i^o is vapour pressure , $\left(\frac{1}{RT} \int_{P_i^o}^P V_i^L dP \right)$ is pointing correction

$$\phi_i^o = \frac{1}{RT} \int_0^{P_i^o} \left(V_i^G - \frac{RT}{P} \right) dP \quad (3.16)$$

ϕ_i^o is fugacity coefficient for pure component at the pressure P_i^o

The Poynting pressure correction is only important at high pressure (an exception to this is for cryogenic systems where T is very low).

3.4 Equations of State

Since van der Waals found the thermodynamic relationship between T, V and P for a system many EOS have been developed. Most of these equations have two specific parameters (a, b) , a is related to molecular energy and the energetic interaction b called co-volume, to the molecular volume. The pure fluid parameters are estimated from the critical properties and acentric factor. In modelling phase equilibrium for mixtures these parameters are extended to mixtures by applying the appropriate mixing rules. Historically the most used mixing rules have been van der Waals one fluid mixing rules 1VDWMR and 2VDWMR (Kontogeorgis et al., 2004). In a later section there is an explanation of the mixing rules. The advantage of EOS is that they can be used over a wide range of temperatures and pressures. The modified PR EOS by Stryjek-Vera is shown below (equation 3.16):

$$P = \frac{RT}{v - b} - \frac{a}{v^2 + 2bv - b^2} \quad (3.17)$$

In the phase equilibrium criteria the starting point for VLE calculation is the thermodynamic requirement that the temperature (T), pressure (P), partial molar Gibbs energy and fugacity of each species be same in all phases:

$$\bar{G}_i^I(x_i^I, T, P) = \bar{G}_i^{II}(x_i^{II}, T, P) = \bar{G}_i^{III}(x_i^{III}, T, P) = \dots$$

The equality of fugacity for VLE:

$$\bar{f}_i^L(x_i, T, P) = \bar{f}_i^V(y_i, T, P) \quad \text{for } i = 1, 2, 3, \dots, n$$

The Peng- Robinson EOS to calculate the fugacity of a component in a liquid mixture is:

$$\frac{\ln(\bar{f}_i^L(T, P, x_i))}{x_i P} = \frac{B_i}{B} (Z^L - 1) - \ln(Z^L - B) - \frac{A}{2\sqrt{2}B} \left[\frac{2 \sum_i^n x_i A_{ij}}{A} - \frac{B_i}{B} \right] \ln \left[\frac{Z^L + (\sqrt{2} + 1)B}{Z^L - (\sqrt{2} + 1)B} \right] \quad (3.18)$$

where $A = \frac{aP}{(RT)^2}$, $B = \frac{bP}{RT}$ the subscript L refers to liquid phase (Sandler 1989).

In applying the above equation to vapour phase subscript L must be changed to V .

3.5 Activity Coefficients

Liquid phase models were developed to determine the departure of a real mixture from the ideal behaviour of low pressure VLE and LLE systems. Renon and Prausnitz (1968) proposed the Non Random Two Liquid (NRTL) equation and later it was extended for multicomponent systems. These models are capable of representing adequately the excess Gibbs energy for a mixture through calculation of the activity coefficient γ_i of each component.

There are two different methods for the description of VLE. The Gamma-Phi ($\gamma - \phi$) method in which the liquid phase is represented with an activity coefficient model e.g UNIQUAC and EOS used for vapour phase. Phi-Phi ($\phi - \phi$) is the second method in which EOS represents both phases. The Phi-Phi method is used in this work and both phases have been represented by Peng Robinson Stryjek Vera (PRSV)(1986) combined with Wong Sandler Mixing Rules (WSMR) through the UNIQUAC model which represents the excess Gibbs energy part in the mixing rule.

The modified UNIQUAC equation for excess Gibbs energy g^E consists of two parts: combinatorial and residual. The combinatorial part represents the size and shape of the molecules and the residual part represents interaction energies between molecules:

$$\frac{g^E(\text{combinatorial})}{RT} = \sum_i x_i \ln \frac{\phi_i}{x_i} + \frac{z}{2} \sum_i q_i x_i \ln \frac{\theta_i}{\phi_i} \quad (3.19)$$

$$\frac{g^E(\text{residual})}{RT} = - \sum_i \bar{q}_i x_i \ln \left(\sum_i \bar{\theta}_i \tau_{ji} \right) \quad (3.20)$$

Where segment fraction for ϕ and $\bar{\theta}$ are given by

$$\phi_i = \frac{r_i x_i}{\sum_j r_j x_j} \quad \theta_i = \frac{q_i x_i}{\sum_j q_j x_j} \quad \bar{\theta}_i = \frac{\bar{q}_i x_i}{\sum_j \bar{q}_j x_j}$$

For any component i the activity coefficient is given by

$$\ln \gamma_i = \ln \frac{\varphi_i}{x_i} + \frac{z}{2} q_i \ln \frac{\theta_i}{\varphi_i} + l_i - \frac{\varphi_i}{x_i} \sum_j x_j l_j - \bar{q}_i \ln \left(\sum_j \bar{\theta}_j \tau_{ji} \right) + \bar{q}_i - \bar{q}_i \sum_j \frac{\bar{\theta}_j \tau_{ij}}{\sum_k \bar{\theta}_k \tau_{kj}} \quad (3.21)$$

Where

$$\tau_{ij} = \exp \left(- \frac{(U_{ij} - U_{ji})}{RT} \right) \quad l_j = \frac{z}{2} (r_j - q_j) - (r_j - 1)$$

r_i is volume parameter of species i

q_i is surface area parameter for species i

θ_i is area fraction of species i

U_{ij} is the average interaction energy for species i - species j

Z is the average coordination number usually equals 10 .

3.6 Mixing Rules

The conventional van der Waals mixing rules have been applied successfully to ideal gas mixtures such as hydrocarbons. Subsequently Orbey and Sandler (1998) encountered failure when these mixing rules were tested on polar and non-ideal mixtures.

In vapour liquid equilibria (VLE) calculations using Equations Of State (EOS) several mixing rules have been developed to extend the applicability of the EOS in predicting VLE for highly non ideal polar systems. Essentially the pure component fugacities have to be systematically rendered into an expression for the

component mixture in the liquid phase. Wong and Sandler (1992) suggested mixing rules that need a value of Helmholtz Free Energies. It is not usually possible to calculate these energies in the situations where a calculation is required; therefore the expressions used employ an approximation by utilising excess Gibbs free energy models. Thus in expressing the mixing rules they combined the attractive term a and co-volume b through a following relationship:

$$B(T) = \left(b - \frac{a}{RT}\right) = \sum \sum x_i x_j \left(b - \frac{a}{RT}\right)_{ij} \quad (3.22)$$

x is composition and $\left(b - \frac{a}{RT}\right)_{ij}$ is the composition independent cross second virial coefficient from the EOS given by :

$$\left(b - \frac{a}{RT}\right)_{ij} = \frac{\left(b - \frac{a}{RT}\right)_{ii} + \left(b - \frac{a}{RT}\right)_{jj}}{2} (1 - k_{ij}) \quad (3.23)$$

k_{ij} is the binary interaction parameter between unlike molecules. Wong and Sandler calculated k_{ij} by equating the Helmholtz free energy at infinite pressure from EOS to that of activity coefficient model for binary systems at composition 0.5 and ambient temperature .

Many workers have been able to demonstrate that an EOS (usually PRSV) can be applied to moderately polar systems using WSMR that display homogeneous behaviour in the liquid phase and produce results in close agreement with experimental data. However there are always problems in systems where the nature of the polar interactions and molecule size is such that there can be a phase split within the liquid phase i.e. the formation of two liquid phases. There are advantages in applying an EOS with appropriate mixing rules in this situation. It is possible to demonstrate the existence of the 2 liquid phases using the mixture Gibbs Energy expressed through the EOS. The test is then whether the EOS can be used to predict the component compositions of the two-phase liquid.

In this work, systems were chosen to check certain predictions that had already been made and then produce a working algorithm that could be tested by applying it to other experimentally measured systems. Thus a range of systems were chosen that would test the EOS with mixing rules within homogeneous and heterogeneous regions.

Six binary VLE mixtures were modelled using PRSV combined with UNIQUAC activity coefficient. The systems selected are homogenous from slightly non-ideal to heterogeneous highly non-ideal polar systems: (methanol-water, ethanol-water, 1-propanol-water, water-n butanol, MEK-water and water-hexanol).

The section below sets out the specific form of the PRSV EOS used with the WSMR. These equations have been used to produce a working model for homogeneous and heterogeneous vapour liquid equilibria initially for binary systems.

3.7 Thermodynamic model description

The equation of state used in this work is Peng Robinson EOS modified by Stryjek Vera (1986a) combined with Wong Sandler Mixing Rules which utilises modified UNIQUAC as an activity coefficient model in the calculation of excess Gibbs energy (1992). The equations needed to estimate the pure component parameters a_i and b_i are:

$$a_i = \frac{0.457235R^2 T_{c_i}^2 \alpha_i}{P_{c_i}} \quad (3.24)$$

$$b_i = \frac{0.077796 R T_{c_i}}{P_{c_i}} \quad (3.25)$$

where:

$$\alpha_i = \left[1 + K_i \left(1 - \sqrt{T_{Ri}} \right) \right]^2 \quad (3.26)$$

$$K_i = K_{0i} + K_{1i} (1 + \sqrt{T_{Ri}}) (0.7 - T_{Ri}) \quad (3.27)$$

$$K_{0i} = 0.378893 + 1.4897153 \omega_i - 0.17131848 \omega_i^2 + 0.0196554 \omega_i^3 \quad (3.28)$$

$$T_{Ri} = \frac{T}{T_{ci}} \quad (3.29)$$

Wong and Sandler (1992) demonstrated in their work the applicability of their Mixing Rules which they developed by testing experimental vapour – liquid, vapour – liquid- liquid and liquid – liquid equilibrium data for several binary systems (cyclohexane- water , propane – methanol and benzene-ethanol) and ternary systems (Carbon dioxide –propane – methanol) at low and high pressure. The systems are in a range of ideal to highly non ideal mixtures. They have shown that their mixing rules can be used for a wide variety of mixtures and phase behaviour and also for the systems that could not be described with EOS. The modified PRSV EOS is:

$$P = \frac{RT}{(v - b)} - \frac{a}{(v^2 + 2bv - b^2)} \quad (3.30)$$

where:

$$A = \frac{aP}{(RT)^2} \quad B = \frac{bP}{RT}$$

the relationship between the mixture parameters a and b is defined as:

$$a = RT \frac{QD}{(1 - D)} \quad b = \frac{Q}{(1 - D)}$$

with

$$Q = \sum_i \sum_j x_i x_j \left(b - \frac{a}{RT} \right)_{ij} \quad (3.31)$$

$$D = \sum_i x_i \left(\frac{a_i}{b_i RT} \right) + \left(\frac{\bar{G}^{ex}}{CRT} \right) \quad (3.32)$$

then the term $\left(b - \frac{a}{RT} \right)_{ij}$ is determined with the following combining rules:

$$\left(b - \frac{a}{RT}\right)_{ij} = \frac{1}{2} \left[\left(b_i - \frac{a_i}{RT}\right) + \left(b_j - \frac{a_j}{RT}\right) \right] (1 - k_{ij}) \quad (3.33)$$

PRSV EOS with WS mixing rules equation in the form of fugacity coefficient is:

$$\begin{aligned} \ln \phi_i = & -\ln \left[\frac{P(v-b)}{RT} \right] + \frac{1}{b} \left(\frac{\partial nb}{\partial n_i} \right) \left(\frac{Pv}{RT} - 1 \right) \\ & + \frac{1}{2\sqrt{2}} \left(\frac{a}{bRT} \right) \left[\frac{1}{a} \left(\frac{1}{n} \frac{\partial n^2 a}{\partial n_i} \right) - \frac{1}{b} \left(\frac{\partial nb}{\partial n_i} \right) \right] \ln \left[\frac{v+b(1-\sqrt{2})}{v+b(1+\sqrt{2})} \right] \end{aligned} \quad (3.34)$$

$$\left(\frac{\partial nb}{\partial n_i} \right) = \frac{1}{(1-D)} \left(\frac{1}{n} \frac{\partial n^2 Q}{\partial n_i} \right) - \frac{Q}{(1-D)^2} \left(1 - \frac{\partial D}{\partial n_i} \right) \quad (3.35)$$

$$\frac{1}{RT} \left(\frac{1}{n} \frac{\partial n^2 a}{\partial n_i} \right) = D \frac{\partial b}{\partial n_i} + b \frac{\partial D}{\partial n_i} \quad (3.36)$$

$$\left(\frac{1}{n} \frac{\partial n^2 Q}{\partial n_i} \right) = 2 \sum_j x_j \left(b - \frac{a}{RT} \right)_{ij} \quad (3.37)$$

and

$$\frac{\partial D}{\partial n_i} = \frac{a_i}{b_i RT} + \frac{\ln \gamma_{i\infty}}{C} \quad (3.38)$$

with

$$\ln \gamma_{i\infty} = \frac{1}{RT} \frac{\partial n A_\infty^E}{\partial n_i} \quad (3.39)$$

C is a constant dependent on the equation of state being used and for PRSV EOS is defined as:

$$C = \frac{1}{\sqrt{2}} \ln(\sqrt{2} - 1) \quad (3.40)$$

Equation (3.34) has been used through this work to calculate the component fugacity coefficients in the mixture in both liquid and vapour phases. The PRSV EOS can be written in this form:

$$Z^3 + \alpha Z^2 + \beta Z + \gamma = 0 \quad (3.41)$$

The parameters for the above equation are:

$$\alpha = -1 + B$$

$$\beta = A - 3B^2 - 2B$$

$$\gamma = -AB + B^2 + B^3$$

A and B are defined earlier in this section .

The solution for the cubic equation of state (equation 3.40) for compressibility factor produces three roots. The large value of the root is used for vapour phase and the small value is used for liquid phase fugacity calculation. (Sandler, 2006)

The minimization function used by Orbey (Orbey et al., 1993) is based on equality for excess Gibbs energy from the Activity Coefficient Model UNIQUAC and PRSV EOS to estimate binary interaction parameters. This estimation was based on the assumption that the system is at ambient condition and the composition is 0.5.

$$\left(\frac{G^{ex}}{RT}\right)^{EOS} = \left(\frac{G^{ex}}{RT}\right)^{Ac} \quad (3.42)$$

This work relies on the experimental data for the systems investigated to obtain the binary interaction parameters values for PRSV EOS.

3.8 Estimation of parameters

In thermodynamic phase equilibrium modelling, an important requirement is the estimation of parameters by determining the value of model parameters that provide the 'best fit' to the set of the experimental data. The VLE, LLE and VLLE data reduction is generally based on least squares or maximum likelihood approach. The most popular approach according to literature is the least square objective function (Lopez et al., 2006). In the VLE data correlation for isothermal and isobaric condition the objective functions used are:

$$F = \sum_j^n \sum_i^{nc} \left[\frac{y_{ij}^{exp} - y_{ij}^{cal}}{\sigma_y} \right]^2 + \sum_j^n \left[\frac{P_j^{exp} - P_j^{cal}}{\sigma_p} \right]^2 + \sum_j^n \left[\frac{T_j^{exp} - T_j^{cal}}{\sigma_T} \right]^2 \quad (3.43)$$

Where n, n_c are the number of data points and the number of components in the mixture respectively, and $\sigma_y, \sigma_p, \sigma_T$ are the standard deviation in vapour mole fraction, pressure and temperature respectively. Equation (3.43) is minimised using the Nelder-Mead simplex to obtain the UNIQUAC energy parameters τ_{ij} and k_{ij} the binary interaction parameter used in PRSV EOS.

$$F = \sum_j^n \sum_i^{nc} \left[\frac{y_{ij}^{exp} - y_{ij}^{cal}}{y_{ij}^{exp}} \right]^2 + \left[\frac{P_j^{exp} - P_j^{cal}}{P_j^{exp}} \right]^2 + \left[\frac{T_j^{exp} - T_j^{cal}}{T_j^{exp}} \right]^2 \quad (3.44)$$

In modelling LLE the objective function used can be written as:

$$F = \sum_j^n \sum_i^{nc} \left| \frac{x_{ijorg}^{exp} - x_{ijorg}^{cal}}{x_{ijorg}^{exp}} \right| + \left| \frac{x_{ijaq}^{exp} - x_{ijaq}^{cal}}{x_{ijaq}^{exp}} \right| \quad (3.45)$$

The objective function used in VLLE calculation is based on minimisation of the average absolute deviation for composition in organic, aqueous and vapour phases and also pressure and temperature for each data point of the calculation.

$$F = \sum_j^n \sum_i^{nc} \left| \frac{x_{ijorg}^{exp} - x_{ijorg}^{cal}}{x_{ijorg}^{exp}} \right| + \left| \frac{x_{ijaq}^{exp} - x_{ijaq}^{cal}}{x_{ijaq}^{exp}} \right| + \left| \frac{y_{ij}^{exp} - y_{ijorg}^{cal}}{y_{ij}^{exp}} \right| + \left| \frac{y_{ij}^{exp} - y_{ijaq}^{cal}}{y_{ij}^{exp}} \right| \quad (3.46)$$

$$F = \sum_j^n \sum_i^{nc} \left| \frac{P_j^{exp} - P_j^{cal}}{P_j^{exp}} \right| + \left| \frac{T_j^{exp} - T_j^{cal}}{T_j^{exp}} \right| \quad (3.47)$$

In modelling VLLE flash calculation, equation (3.46) reduces to three parts and can be expressed as:

$$F = \sum_j^n \sum_i^{nc} \left| \frac{x_{ijorg}^{exp} - x_{ijorg}^{cal}}{x_{ijorg}^{exp}} \right| + \left| \frac{x_{ijaq}^{exp} - x_{ijaq}^{cal}}{x_{ijaq}^{exp}} \right| + \left| \frac{y_{ij}^{exp} - y_{ij}^{cal}}{y_{ij}^{exp}} \right| \quad (3.48)$$

were n is the number of data points and n_c is the number of components in the mixture.

3.9 VLLLE three phase Flash calculation

The Modified Peng Robinson equation of state as proposed by Styrjek and Vera has been used successfully to describe the multiphase multi-component heterogeneous systems of Younis et al. (2007). In the flash calculation formulation for VLLLE of multi-component the mass balances and summations are:

$$F = V + L_{org} + L_{aq} \quad (3.49)$$

$$z_i F = y_i V + x_i^{org} L_{org} + x_i^{aq} L_{aq} ; \quad i = 1, 2, \dots, n_c \quad (3.50)$$

$$\sum_{i=1}^{n_c} x_i^{org} = \sum_{i=1}^{n_c} x_i^{aq} = \sum_{i=1}^{n_c} y_i = 1 \quad (3.51)$$

The superscripts *aq* and *org* refer to aqueous and organic phases respectively. The iso-activity criterion gives:

$$y_i = K_{i,org} x_i^{org} \quad i = 1, 2, \dots, n_c \quad (3.52a)$$

$$y_i = K_{i,aq} x_i^{aq} \quad i = 1, 2, \dots, n_c \quad (3.52b)$$

In the above equations (3.52a & b) the K_i can be expressed in form of thermodynamic models, using EOS to estimate the equilibrium constants:

$$K_{i,org} = \frac{\phi_i^{org}}{\phi_i^v}; \quad K_{i,aq} = \frac{\phi_i^{aq}}{\phi_i^v} \quad (3.53)$$

Substituting equation (3.52) into equation (3.50), and rearranging yields:

$$y_i = \frac{z_i K_{i,org} K_{i,aq}}{K_{i,org} K_{i,aq} + \theta^{org} K_{i,aq} (1 - K_{i,org}) + \theta^{aq} K_{i,org} (1 - K_{i,aq})} \quad (3.54)$$

$$x_i^{org} = \frac{z_i K_{i,aq}}{K_{i,org} K_{i,aq} + \theta^{org} K_{i,aq} (1 - K_{i,org}) + \theta^{aq} K_{i,org} (1 - K_{i,aq})} \quad (3.55)$$

$$x_i^{aq} = \frac{z_i K_{i,org}}{K_{i,org} K_{i,aq} + \theta^{org} K_{i,aq} (1 - K_{i,org}) + \theta^{aq} K_{i,org} (1 - K_{i,aq})} \quad (3.56)$$

where $i = 1, 2, \dots, nc$, θ^{org} and θ^{aq} are the fractions of molar flow rate of organic and aqueous liquid phase with respect to the overall feed F .

The combination of the equations (3.54, 3.55, and 3.56) can be used to determine the thermodynamic properties of the three phases. Peng and Robinson recommended the following equation for VLE flash calculations:

$$\sum_{i=1}^{nc} x_{i,org} - \sum_{i=1}^{nc} y_i = 0, \left[\sum_{i=1}^{nc} x_{i,aq} \right] - 1 = 0 \quad (3.57)$$

Equation (3.57) is known as the Rachford Rice equation, it can be solved simultaneously using any iterative method and the initial values of equilibrium ratios must be provided to enable the flash equilibrium calculation to proceed reliably. Peng and Robinson adopted Wilson's equilibrium ratio correlation to provide initial values for $K_{i,org}$ in the following equation:

$$K_{i,org} = \frac{P_{c_i}}{P} \exp \left[5.3727(1 + \omega_i) \left(1 - \frac{T_{c_i}}{T} \right) \right] \quad (3.58a)$$

Where P is total pressure in psia; T is system temperature in Fahrenheit; P_{c_i} is critical pressure of component i , and T_{c_i} is critical temperature of component i and ω_i is acentric factor of component i . Peng and Robinson proposed the following expression to estimate the initial values for $K_{i,aq}$ (Mokhatab, 2003):

$$K_{i,aq} = 10^6 \left[\frac{P_{c_i} \cdot T}{P \cdot T_{c_i}} \right] \quad (3.58b)$$

Michelsen (1982 a) uses the stability test results based on the tangent plane criterion of Gibbs energy to provide the flash calculation with initial values. A simplex diagram on flash calculation of three-phase multicomponent system can be found in appendix A.

3.10 Gibbs optimisation methods

At a given temperature and pressure (T, P) with overall composition z , a mixture with M –component and np phase achieves equilibrium when the Gibbs free energy is at the global minimum. The Gibbs free energy is expressed as:

$$G_0 = \sum_i n_i \mu_i^0 \quad (3.59)$$

Where μ_i^0 is chemical potential of component i in the mixture and n_i is a vector containing the component mole fraction. The above equation for G_0 can be expressed in a different form:

$$F(y) = \sum_i y_i (\mu_i(y) - \mu_i^0) \geq 0 \quad (3.60)$$

Michelsen formulated a method (the tangent plane criterion) to overcome the failure of flash calculation in predicting the correct number of phases and also to provide realistic initial estimates for flash calculation (Michelsen, 1982 a, b). The tangent plane distance function is defined as the vertical distance from the tangent hyper-plane to the Molar Gibbs energy surface at composition z to the energy surface at trial composition. The majority of the methods used for phase equilibria modelling are based on direct minimisation of Tangent Plane Distance function (TPDF) subject to the material balance constraints. However many methods may fail in finding the global solution for the TPDF for non-ideal and complex mixtures, because these functions are multivariable, non-convex and highly non-linear. In these methods, the optimisation converges to local minima rather than global. In general global optimisation methods can be categorised into two types: deterministic and stochastic. In the first type, a sequence of points will be

generated and converge to a global optimum (e.g. homotopy continuous, interval analysis). The stochastic method uses random sequences in the search for global optimum value (e.g. pure random search, simulated annealing, genetic algorithm, Tabu search, particle swarm, hybrid methods, ant colony, and harmony search). More details on both methods can be found in Zhang et al. (2011). In their study on parameter estimation of several VLE binary systems, Bonilla et al. (2010) showed weakness and strength of several stochastic global optimisations.

Eubank et al (1992) developed an Area Method which searches for the positive maximum area bounded by the Gibbs free energy curve and the tangent plane, to implement their criterion the Gibbs free energy curve must be integrated. This work tests the Area Method (AM) of Eubank et al. (1992) and the Tangent Plane Intersection (TPI) of Hodges (1998) on LLE binary data taken from the DECHEMA series and compares the results with the experimental values. In modelling phase equilibria this work also tests the TPI method on four VLLE binary heterogeneous systems and demonstrates graphically the applicability of the Equal Area Rule by Eubank and Hall (1995) on such systems. A brief description of these methods appears in the following sub-sections.

3.10.1 Area Method in integral form

The method was defined by Eubank et al. (1992) for accurate determination of binary heterogeneous systems phase equilibrium. This is achieved by searching the entire composition (grid size) and finding the maximum net positive area as shown in figure 3.3. The basis of the area method is dependent on calculations of the net area between a trapezium and the area under the Gibbs energy curve at two fixed points (composition). The net area is defined in the following equation:

$$A(x_a, x_b) = \left| \left[\frac{\phi(x_a) + \phi(x_b)}{2} \right] (x_b - x_a) - \int_{x_a}^{x_b} \phi(x) dx \right| \quad (3.61)$$

The reduced Gibbs energy of mixing (ϕ) equation is formulated by PRSV EOS and WSMR (modified UNIQUAC activity model) as shown in equation (3.62):

$$\phi = \frac{\Delta g}{RT} = \frac{g}{RT} - \sum_{i=1}^n x_i \left(\frac{g_i}{RT} \right) \quad (3.62)$$

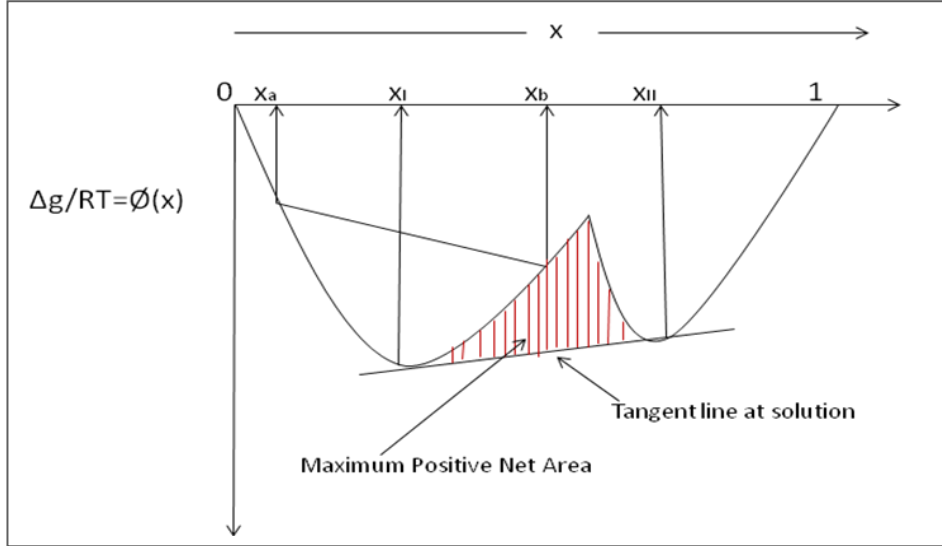


Figure 3.3: The Gibbs energy of mixing ϕ curve for a two phase binary system

Where ϕ is the reduced Gibbs energy of mixing, g is the molar Gibbs energy of mixture at a specific T and P and g_i is corresponding pure component molar Gibbs energy at the same conditions.

$$\frac{g}{RT} = \frac{Pv}{RT} + \ln \left[\frac{v}{v-b} \right] + \frac{a}{2\sqrt{2}RTb} \ln \left[\frac{v + (1 - \sqrt{2})b}{v + (1 + \sqrt{2})b} \right] - \sum_{i=1}^n x_i \ln \left[\frac{v}{x_i RT} \right] \quad (3.63)$$

$$\frac{g_i}{RT} = \frac{Pv_i}{RT} + \ln \left[\frac{v_i}{v_i - b_i} \right] + \frac{a}{2\sqrt{2}RTb_i} \ln \left[\frac{v_i + (1 - \sqrt{2})b_i}{v_i + (1 + \sqrt{2})b_i} \right] - \ln \left[\frac{v_i}{RT} \right] \quad (3.64)$$

The above equations (3.63 & 3.64) are used throughout this work in prediction methods for phase equilibrium calculations (Area Method, Tangent Plane Intersection and Tangent Plane Distance Function).

3.10.2 Tangent plane intersection method

The Tangent Plane Intersection was developed to overcome the problems found within the Volume method in determination of minimum Gibbs energy equilibrium (ϕ). The obvious extension to an area method for binary mixtures is to attempt to construct a corresponding volume method for ternary systems. Hodges et al. (1998) attempted to do this but found it was impossible to account for 'vestigial' parts of the curves constructed. They adapted a 'Tangent Plane' concept and attempted to apply it to selected systems. This method determines the tangent plane at the global minimum ϕ curve. The central idea for this approach is the calculation and optimisation of the ϕ - tangent plane intersection quantity (τ) by applying an appropriate optimisation procedure (Nelder-Mead simplex). The value of (τ) will be zero when the solution is reached. The starting point of the TPI method is the division of the composition space into a search grid and then finding the tangent plane slope (m_{iTP}). The next step is the repeated test of the tangent plane distance function $F(x)$ at each grid point $F(x) = L(x) - \phi(x)$. $L(x)$ is the value of ϕ calculated using the tangent plane equation alternatively it is the vertical distance from a grid point to the tangent plane. $\phi(x)$ is the value of ϕ calculated using equation (3.61) at the same grid point. Optimising (τ) to zero depends on the value of $F(x)$: if $F(x) > 0$ then the tangent plane is above the ϕ curve and one adds to ($\tau = \tau + \Delta\tau$) on the other hand if $F(x) < 0$ the τ is left without change. The $\Delta\tau$ for multi-component form is shown in the following equation (Hodges et al., 1998):

$$\Delta\tau = \prod_{i=1}^{n-1} h_i \sqrt{1 + (m_{iTP})^2} \quad (3.65)$$

This equation changes from line to plane depending on the number of components for example if equation (3.65) is applied for ternary 3-phase system the slopes of the tangent plane will be (m_{1TP} and m_{2TP}) and h_i is the grid size. τ represents the intersection of this area with ϕ surface.

Figure (3.4) shows the TPI method applied to a 3-phase binary mixture in which the τ function is minimised. The tangent line which is bounded by ϕ surface

(indicated by a thick line) is minimised to zero by adjusting the independent variables(α).

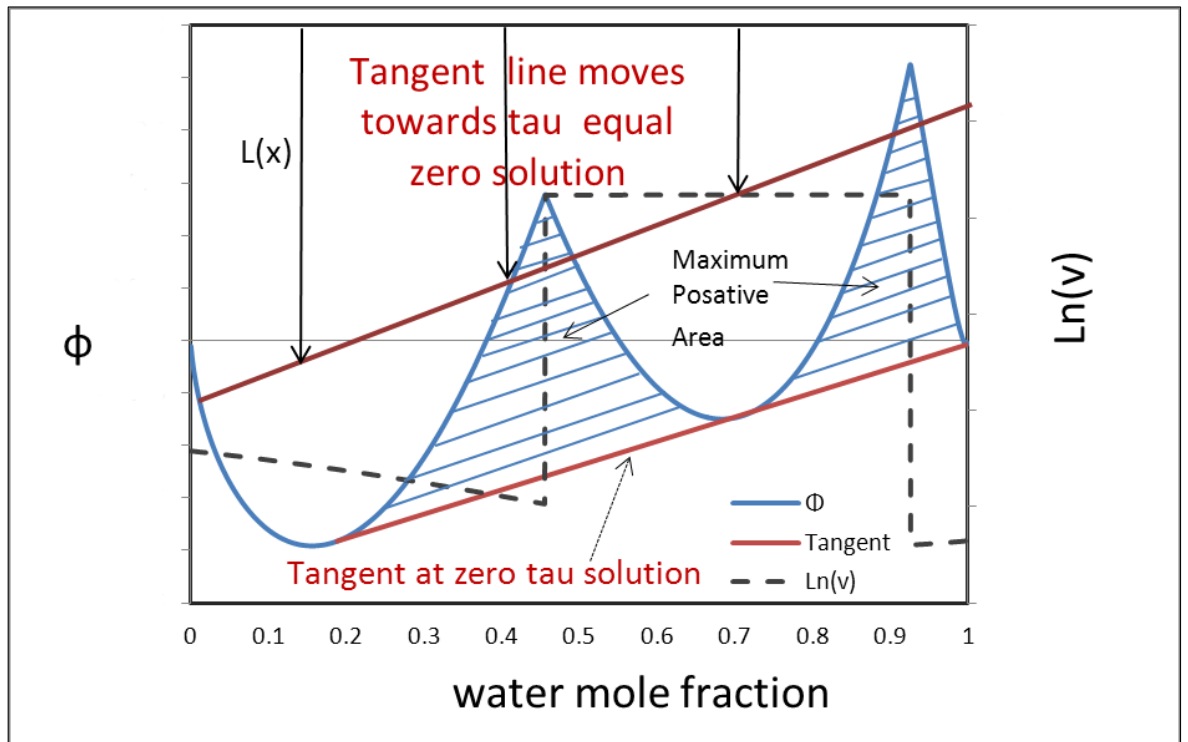


Figure 3.4: Representation of the search procedure for 3 phase binary system using TPI method

3.10.3 Equal Area Rules

Eubank and Hall (1995) have shown that the tangent plane criterion can be reduced to an Equal Area Rule (EAR) by plotting the derivative of the total Gibbs energy against composition and searching for phase loops similar to those of Maxwell. At equilibrium the positive and negative areas are equal above and below a specific value of the derivative. In their work, Nishwan et al. (1996) implemented the EAR on binary LLE and VLLE and claimed that this can be extended to multi-component multi-phase systems. Since the publication of their paper, no attempt has been made to extend and test their theory.

The EAR method can be used for LLE and VLLE predictions in binary systems. The top section of figure 3.5 shows the Gibbs energy curve ϕ for VLLE water (1)-n butyl acetate (2) system at 364 K and 1.013 bar and below this section the first derivative of the ϕ can be seen with the positive and negative equal areas which are bounded by the derivative curve. The intersect points between this curve and a

line at specific values are the stationary points (the VLLE equilibrium compositions for this system).

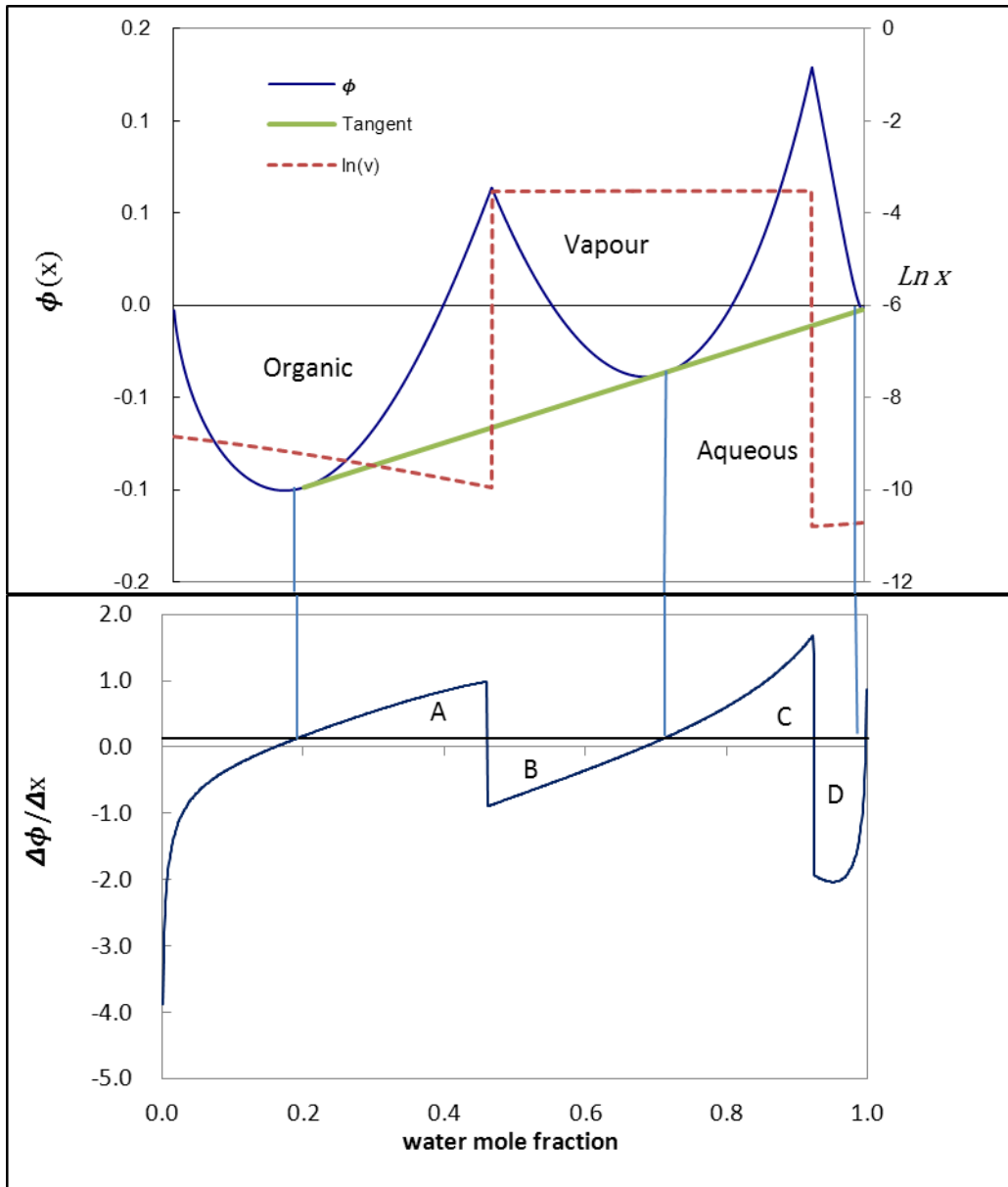


Figure 3.5: VLLE prediction for water(1)-n butyl acetate(2) system at 364 K and 1.013 bar , shows the equal areas (A,B) and (C,D) confined between the line and the first derivative of Gibbs energy curve in Equal Area Rule

3.10.4 Tangent Plane Distance Function

In multiphase equilibrium calculations a phase stability test can be achieved by direct minimisation of Gibbs free energy or minimisation of the tangent plane distance function. The difficulty of such calculation lies in the non-linear and non-convex shape of the objective function which makes the minimisation converge to

local rather than global minima, particularly in the vicinity of phase boundaries or near critical points. Since Michelsen's valuable achievement in finding the stationary points of the TPDF, several attempts have been made to find these stationary points such as: interval Newton methods (e.g., Gecegormez and Demirel, 2005, Xu et al. ,2005), the homotopy continuation method (Kangas et al.,2011; Sun and Seider,1995), branch and bound methods(McDonald and Floudas,1995) and the tunnelling method (Nichita et al.,2002 ; Nichita and Gomez, 2009), in general all these global methods have shortcomings in finding all the roots of the TPDF as the final solutions obtained rely on the initial values. The stability test results can be used for initialising the phase split calculation or validating the results obtained from flash calculations.

Malinen, et al. (2012) recently used the modified Newton homotopy based method in finding the stationary points of TPDF for binary and ternary LLE systems utilising NRTL and UNIQUAC excess Gibbs energy models in describing those systems. They claimed that the starting value does not have any effect on finding all the real roots of the TPDF function. However they have not indicated the applicability of this method on the VLLE ternary and quaternary systems using EOS.

Assuming a mixture at constant temperature and pressure with an overall composition z splits to a number of phases at equilibrium, thermodynamically the Gibbs free energy will be at the minimum level. In order to perform stability test analysis on this mixture, the Tangent Plane Distance function as defined by equation (3.60) in the form of chemical potential (Michelsen 1982 a) must be globally optimised with respect to composition y_i subject to equality constraint in each phase:

$$\sum_i^{nc} y_i = 1 \tag{3.66}$$

$$0 \leq y_i \leq 1 \quad (i = 1,2, \dots nc)$$

The mole fraction y_i is the decision variable in the phase stability test, if the global minimum of TPDF < 0 the mixture is unstable, else the system is stable. It is more

convenient to express the TPDF in term of fugacity coefficients, therefore equation (3.60) can be written as:

$$\frac{F(y)}{RT} = \sum_i y_i (\ln y_i + \ln \phi_i(y) - \ln z_i - \ln \phi_i(z)) \quad (3.67)$$

The stationary criterion is:

$$(\ln y_i + \ln \phi_i(y) - \ln z_i - \ln \phi_i(z)) = k \quad (3.68)$$

Introducing a new variable $Y_i = \exp(-k)y_i$, Y_i can be interpreted as mole numbers of component i , Michelsen showed that equation (3.67) can be written as:

$$TPDF(Y) = 1 + \sum_i^{nc} Y_i [(\ln Y_i + \ln \phi_i(Y) - \ln z_i - \ln \phi_i(z)) - 1] \quad (3.69)$$

Where $y_i = Y_i / \sum_i^{nc} Y_i$

The optimisation problem is minimising the TPDF function for constrained mole fraction as independent variable $0 \leq y_i \leq 1$, when the objective function (TPDF) is at minimum value, $y = y^*$ are the stationary points and the equation (3.67) takes the following form:

$$(\ln y_i^* + \ln \phi_i(y^*) - \ln z_i - \ln \phi_i(z)) = k_i^* \quad (3.70)$$

Geometrically, k_i^* is the distance between two hyper-planes tangent to the Gibbs energy surface and to the tangent at feed composition. A system at a constant temperature, pressure and feed composition is stable if $k_i^* \geq 0$, if it is a negative value, the phase is unstable and splits into two or more stable phases. As shown by Michelsen (1982 a) the direct iteration scheme or any minimisation technique for k^* objective function can be used.

Initialisation is required for all the minimisation techniques for multi-phase equilibria; some methods split the calculation into two main steps; performing two phases stability test and using the results to initialise the three phase flash computation.

It is acknowledged that a distinction exists between correlating the experimental data to produce the model constants and using these values to predict data for

other conditions. In the field of VLE, there is sufficient published data available for correlation of measured data to be carried out and the correlated theoretical parameters to be used to predict and compare to other measured data. However with reference to VLLE the basic problem in this work was that, for the relatively complex systems measured, the amount of data available was limited to the results of one laboratory. Thus the correlated data have been used to produce methods for each system whereby at a given temperature and pressure the phase equilibria can be predicted. This is demonstrated in this work using the measured data that are available. As will be stated in the suggestions for future work, more physical measurement is required to fully establish the predictive abilities of the work on which this thesis is based.

3.11 Methods of initialisation

3.11.1 Initialisation techniques used in stability test

The initialisation procedure for any phase equilibrium calculations (stability test, VLE, and VLLE flash calculation) depend on the selected minimisation method, for instance with Nichita and Gomez (2009) their tunnelling method is based on random multi-starting points. Michelsen and Sun and Seider (1995) suggested the following equations:

$$Y_i = z_i K_i \quad (3.71 a)$$

$$Y_i = z_i / K_i \quad (3.71 b)$$

The equilibrium constants K_i are obtained from the Wilson empirical relation:

$$K_i = \frac{P_{c_i}}{P} \exp \left[5.3727(1 + \omega_i) \left(1 - \frac{T_{c_i}}{T} \right) \right] \quad (3.72)$$

The above equations can be used for initialisation when the mutual solubility of one component in the mixture is not very small. If the solubility value is close to the phase boundaries surface, a different procedure is performed. Many researchers have taken advantage from step by step phase calculations by starting from the stability test on one phase with overall composition as a first step then using the

results to initialise two phase calculations and so on (Nichita et al., 2002). In the initialisation for three phases split calculations for a number of hydrocarbon mixtures, Li and Firoozabadi (2012) have used direct Newton method and two phase stability test based on the Rachford Rice equations. However many of these methods may fail in the critical region or close to the phase boundaries, especially when applied to complex highly non-ideal heterogeneous mixtures.

3.11.2 Direct initialisation for three phase multi component systems

This research adapted a robust and efficient initialisation method for three phase flash calculation, based on combining the use of activity coefficient model (UNIQUAC) and PRSV EOS with WS mixing rules. The objective function in this work is based on relative volatilities calculations of the component i in the mixture, $|K_{iold} - K_{inew}| \geq \epsilon$, ϵ is the tolerance to terminate the optimisation procedure (Nelder- Mead).

The initialisation scheme used in this work for TPI predictions for ternary and quaternary systems can be summarised in these steps and also the diagram shown in appendix B:

- 1- Set $x_i^{aq} = z_i$, Calculate P_i^{sat} from Antoine equation and γ_i^{aq} from UNIQUAC activity coefficient model
- 2- Estimation of organic and vapour phase compositions using equations (3.73) and (3.74) for vapour and organic phase respectively :

$$y_i = \exp\left[\ln x_i^{aq} + \ln(\gamma_i^{aq} + P_i^{sat}) - \ln \phi_i^{V(0)}\right] \quad (3.73)$$

$$x_i^{org} = \exp\left[\ln x_i^{aq} + \ln(\gamma_i^{aq} + P_i^{sat}) - \ln \phi_i^{L(0)}\right] \quad (3.74)$$

Where $\phi_i^{V(0)}$ is pure vapour fugacity coefficient of component i , equal to 1.0 for the systems with low pressure and $\phi_i^{L(0)}$ is pure liquid fugacity coefficient of component i assumed to be P_i^{sat}/P , P is total pressure .

- 3- Calculating the fugacity coefficients in all phases using the PRSV EOS with WS mixing rules. The equilibrium ratio can be obtained from equation:

$$K_{i,org} = \frac{\phi_i^{org}}{\phi_i^v}; \quad K_{i,aq} = \frac{\phi_i^{aq}}{\phi_i^v} \quad (3.75)$$

- 4- Using the overall and component material balance equations, setting the Rachford Rice equation (3.76) as the objective function to be minimised to obtain θ^{org} and θ^{aq} fractions of molar flow rate of organic and aqueous liquid phase with respect to the overall feed. The Nelder Mead optimisation used with the constrained value of both flow rate $0 \geq \theta^{org}$ and $\theta^{aq} \leq 1$, the compositions of organic, aqueous and vapour phase are calculated.

$$\sum_{i=1}^{nc} x_{i,org} - \sum_{i=1}^{nc} y_i = 0, \quad \left[\sum_{i=1}^{nc} x_{i,aq} \right] - 1 = 0 \quad (3.76)$$

- 5- Calculating the organic, aqueous and vapour phase compositions using VLLE flash equations
- 6- Re-estimating new values for fugacity coefficients (ϕ_i) and relative volatilities (K_i) compare these values with the old values, the criterion to stop is $\varepsilon = 0.00001$ otherwise replace the (K_i) with the new values and go to step 3.

This initialisation method has been used throughout this work in an attempt to overcome the sensitivity of the TPI to initial values.

3.12 The Nelder –Mead simplex

The Nelder-Mead simplex is the most widely used method for non-linear function optimisations in the fields of chemical engineering and chemistry. This simplex minimises function values in a direct search of n variables without need for the derivative of the function. The algorithm evaluates the value of a function $f(x)$ for k number of iterations along with regeneration of the new value of variables by using coefficient factors (reflection, expansion, contraction and shrinkage). The standard values chosen for these coefficients are (1, 2, 0.5 and 0.5) respectively. The largest value of $f(x)$ is rejected and the variables replaced with the new values, this process creates a sequence of variable values for which the value of

$f(x)$ will be at the minimum. Nelder-Mead is unconstrained minimisation which strongly relies on the initial values.

In order to find the Best variables (B) to satisfy the $f(x_1) \leq f(x_2) \leq \dots \leq f(x_{n+1})$, the procedure is to move away from the Worst values (W) to Good values (G) by taking the steps below (appendix C shows a diagram of the Nelder-Mead simplex):

1. Compute the initial simplex from the starting values and their function values; sort the variable and the coordinate in $f(B), f(G), f(W)$ in ascending order from best to worst.
2. Compute the centroid: $M = (B + G)/2$, Reflection; $R = M + (M - W) = 2M - W$ and the function value $f(R)$.
3. If $f(R) < f(G)$ then perform one of these cases :
4. First case: if $f(B) < f(R)$ then replace W with R , else compute Expansion: $E = R + (R - M) = 2R - M$ and $f(E)$, if $f(E) < f(B)$ then replace W with E , else replace W with R .
5. Second case: if $f(R) < f(W)$ then replace W with R , compute Contraction: $C = (W + M)/2$ or $C = (M + R)/2$ and $f(C)$, if $f(C) < f(W)$ then replace W with C , else compute Shrink and $f(S)$; replace W with S , replace G with M .
6. The procedure continuously produces a sequence of $f(x)$ and the criterion to terminate the search is when the simplex size is smaller than the tolerance otherwise return to step 2.

Nelder and Mead published their simplex in 1965 and their method of minimisation continues to be popular and broadly used in several practical fields. The main advantages of this simplex are: it is easy to use and can be applied to optimise multi-dimensional complex problems (multi-variable non-linear function). However the disadvantage in some cases it might not converge to a global minimum like some other methods (Newton's method).

The Nelder-Mead optimisation simplex is widely used in the field of thermodynamic modelling of phase equilibria particularly in the correlation of VLE,

LLE, and VLLE to obtain the model parameters. This simplex can also be used in the minimization of Gibbs free energy. Throughout their work, Hodges et al. (1997 and 1998) used the Nelder-Mead method in a series of correlations and predictions for binary and ternary VLE, LLE and VLLE calculations using Gibbs energy minimisation as suggested by Michelson (1982) in the form of the Tangent Plane Intersection method. In the correlation and prediction of VLE for binary systems of alcohol-alcohol and alcohol-water at atmospheric pressure, Yan et al. (1999) and Li et al. (2000) also used Nelder-Mead successfully. To obtain UNIQUAC and NRTL parameters for the partially miscible ternary mixture of ethanol-water-1-butanol at isobaric pressure, Kosuge and Iwakabe (2005) have utilised Nelder-Mead. In modelling of three-phase vapour-liquid-liquid equilibria for a natural gas system rich in nitrogen using the SRK and PC-SAFT equations of state, Justo-Garcia et al. (2010) have also used the minimisation simplex of Nelder-Mead with convergence accelerated by the Wegstein algorithm. Garcia-Flores et al. (2013) correlated liquid-liquid equilibria for ternary and quaternary systems of representative compounds of gasoline + methanol at atmospheric pressure using NRTL and UNIQUAC activity coefficient models; they also used Nelder-Mead in their method. In optimisation of the biodiesel purification process by Pinheiro et al. (2014) Nelder-Mead was used in the correlation of liquid-liquid equilibrium for a ternary system of methanol (1)-water (2)-biodiesel (3) at temperatures of 293.15 and 313.15 K and atmospheric pressure with UNIQUAC, NRTL and UNIFAC activity coefficient models.

Several studies have recently indicated that whilst the method has its drawbacks e.g. the simplex might be trapped in local minima due to initial starting values, its use is well established in the field and it requires no equation derivatives. Many researchers have developed new ideas in an attempt to improve on the drawbacks or deficiencies in NMS. Gao and Han (2010) implemented a method in which the expansion, contraction and shrink parameters depend on the dimensions of the optimisation problem. Pham and Wilamowski (2011) incorporated a Quasi gradient method with the Nelder Mead simplex which approximates gradients of a function in the vicinity of a simplex by using numerical methods. They have demonstrated an improvement in the Nelder Mead algorithm performance for multi-variable functions in their application. In a further study by Wanga and Shoup (2011) on

parameter sensitivity of the Nelder Mead for unconstrained optimisation, they discovered that the standard values for NMS coefficients are not always the best values. They claimed that the simplex performs more efficiently with the obtained values.

When these modifications became available, this work had already implemented the unmodified established Nelder-Mead simplex in optimisation methods in correlation and predictions calculations and therefore did not investigate the modified version. There was also significant experience available from the work of Hodges et al., (1997, 1998) and Younis et al., (2007).

4. Results and discussion

4.1 Binary Systems Results

A range of binary homogeneous and heterogeneous systems were modelled using PRSV EOS combined with WSMR using the UNIQUAC activity coefficient equation. The VLE isobaric and isothermal data have been used to test the suitability of the PRSV model in representing non-ideality in heterogeneous systems.

The VLE binary homogeneous systems consist of isothermal and isobaric data for:

A- Methanol-water

1. VLE isothermal at temperatures: 25, 50, 65 and 100⁰C.
2. VLE isobaric at pressure: 760 mmHg.

B- Ethanol-water

1. VLE isothermal at temperatures: 20, 30, 40, 50, 60 and 70⁰C.
2. VLE isobaric at atmospheric pressure.

C- 1-Propanol-water

1. VLE isothermal at temperature: 79.80⁰C.
2. VLE isobaric at atmospheric pressure.

The VLE binary heterogeneous systems include isothermal and isobaric data for:

A- Water-n-butanol

1. VLE isothermal at temperature: 35⁰C.
2. VLE isobaric at atmospheric pressure

B- Methyl ethyl ketone- water

1. VLE isothermal at temperature 73.80⁰C.
2. VLE isobaric at atmospheric pressure

C- Water-hexanol

1. VLE isothermal at temperature 21⁰C.
2. VLE isobaric at atmospheric pressure.

The Area Method and Tangent Plane Intersection predicted models were used on binary LLE for the systems (1-butanol-water, ethyl acetate-water) and the TPI for VLLE systems (water-n-butyl acetate, ethyl acetate-water, and n-butanol-water). The parameters obtained from the correlation of the experimental data and these data were acquired from DECHEMA Chemistry Data Series (1977- 1991).

The results for VLE P_{xy} isothermal in this work are compared to the results using the WSMR package and the observation shows the model in our work is superior on Sandler's results.

The bubble point calculation was carried out for some binary P_{xy} and T_{xy} data using the objective function: Absolute Average Deviations (AAD) for vapour composition and bubble point pressure and temperature.

$$AAD = \frac{\sum[|exp - calc|]/exp}{No. data points} \quad (4.1)$$

The results are tabulated below:

4.1.1 VLE Homogeneous systems

A. methanol (1)-water (2)

1- P_{xy} methanol (1)-water (2) at temperatures: 25, 50, 65 and 100⁰C

Table 4.1: VLE bubble point calculation for methanol (1)-water (2) isothermal binary system at 25, 50, 65 and 100°C using PRSV with WSMR through UNIQUAC

Temperature	experimental			calculated	
	x_1	y_1	P mmHg	y_1	P mmHg
25°C	0.1204	0.5170	43.92	0.5344	45.50
	0.2039	0.6530	56.07	0.6512	56.23
	0.2919	0.7295	66.04	0.7248	65.50
	0.3981	0.7895	75.39	0.7862	75.20
	0.4831	0.8260	82.32	0.8252	82.40
	0.5349	0.8440	86.29	0.8465	86.70
	0.5871	0.8645	90.54	0.8666	91.01
	0.6981	0.9040	99.63	0.9063	100.26
	0.8023	0.9390	108.35	0.9407	109.17
0.8522	0.9550	113.11	0.9564	113.54	
50°C	0.0486	0.2741	119.50	0.2730	121.39
	0.1218	0.4741	157.00	0.4767	157.26
	0.1478	0.5220	169.10	0.5232	168.36
	0.2131	0.6294	196.00	0.6106	193.50
	0.2693	0.7106	217.10	0.6655	212.78
	0.3252	0.7580	236.60	0.7092	230.46
	0.5143	0.8203	283.00	0.8166	284.34
	0.6219	0.8654	306.40	0.8640	313.41
	0.7083	0.9007	324.10	0.8984	336.75
	0.8037	0.9406	348.00	0.9337	362.85
0.9007	0.9627	373.50	0.9675	389.93	
0.9461	0.9736	391.10	0.9826	402.82	
65°C	0.0000	0.0000	187.54	0.0000	187.60
	0.0854	0.3926	292.72	0.4057	291.54
	0.0874	0.4018	294.04	0.4107	293.50
	0.1328	0.4963	337.21	0.5020	333.83
	0.1816	0.5718	377.29	0.5688	369.80
	0.2586	0.6512	429.60	0.6412	416.20
	0.4920	0.7842	544.83	0.7799	526.31
	0.5815	0.8242	583.87	0.8245	567.55
	0.7043	0.8747	634.71	0.8836	628.27
	0.8028	0.9180	680.39	0.9275	680.54
0.9030	0.9605	727.27	0.9662	733.47	
1.0000	1.0000	774.95	1.0000	776.40	
100°C	0.0022	0.0192	782.52	0.0162	770.81
	0.0110	0.0860	828.40	0.0753	813.31
	0.0350	0.1910	927.20	0.2002	919.76
	0.0530	0.2450	1003.20	0.2700	991.41
	0.0740	0.3130	1071.60	0.3343	1067.19
	0.1210	0.4340	1238.80	0.4367	1211.29
	0.1630	0.4960	1322.40	0.4995	1316.47
	0.2810	0.6190	1535.20	0.6109	1537.34
	0.3520	0.6620	1624.40	0.6579	1641.43
	0.5220	0.7500	1884.80	0.7558	1870.11
	0.6060	0.7920	2029.20	0.8041	1989.90
	0.6670	0.8240	2112.80	0.8397	2084.23
	0.8260	0.9110	2340.80	0.9286	2367.26
	0.9360	0.9690	2508.00	0.9762	2572.73
0.9460	0.9760	2530.80	0.9795	2588.38	
0.9580	0.9810	2530.80	0.9834	2605.51	

2- T_{xy} methanol (1)-water (2) at atmospheric pressure

Table 4.2: VLE bubble point calculation for methanol (1)-water (2) isobaric binary system at 760 mmHg

experimental			calculated	
x_1	y_1	$T_{in} \text{ } ^\circ\text{C}$	y_1	$T_{in} \text{ } ^\circ\text{C}$
0.000	0.000	100.00	0.000	100.00
0.020	0.134	96.40	0.132	96.59
0.040	0.230	93.50	0.232	93.78
0.060	0.304	91.20	0.309	91.43
0.080	0.365	89.30	0.371	89.43
0.100	0.418	87.70	0.422	87.71
0.150	0.517	84.40	0.515	84.29
0.200	0.579	81.70	0.581	81.74
0.300	0.665	78.00	0.669	78.06
0.400	0.729	75.30	0.732	75.39
0.500	0.779	73.10	0.783	73.19
0.600	0.825	71.20	0.830	71.25
0.700	0.870	69.30	0.874	69.44
0.800	0.915	67.50	0.917	67.71
0.900	0.958	66.00	0.959	66.05
0.950	0.979	65.00	0.980	65.25
1.000	1.000	64.50	1.000	64.45

B. ethanol (1)-water (2)

1. P_{xy} ethanol (1)-water (2) at temperatures: 20, 30, 40, 50, 60 and 70°C

Table 4.3: VLE bubble point calculation for ethanol (1)-water (2) isothermal binary system at 20, 30, 40, 50, 60 and 70°C, pressures in mmHg

T	experimental			calculated		T	Experimental			calculated	
	x_1	y_1	P	y_1	P		x_1	y_1	P	y_1	P
20°C	0.100	0.442	28.50	0.439	28.71	60°C	0.051	0.316	219.00	0.339	215.98
	0.300	0.617	37.13	0.612	36.63		0.086	0.393	249.00	0.429	244.08
	0.500	0.690	40.20	0.692	40.08		0.197	0.517	298.00	0.546	288.75
	0.700	0.775	41.93	0.771	42.18		0.375	0.596	325.00	0.619	316.26
	0.900	0.909	43.50	0.889	42.76		0.509	0.648	342.00	0.671	331.21
30°C	0.100	0.454	53.03	0.451	53.40	0.527	0.660	344.00	0.679	333.11	
	0.300	0.619	68.48	0.612	67.22	0.545	0.671	343.00	0.688	334.98	
	0.500	0.685	73.28	0.687	73.09	0.808	0.826	363.00	0.832	355.46	
	0.700	0.767	76.81	0.767	76.78	0.851	0.862	364.00	0.859	356.64	
	0.900	0.903	77.93	0.887	77.66	0.860	0.867	366.00	0.865	356.76	
40°C	0.062	0.374	75.14	0.376	84.08	0.972	0.972	362.00	0.956	351.36	
	0.077	0.406	89.00	0.414	88.55	0.062	0.374	362.50	0.373	353.46	
	0.098	0.450	94.60	0.455	93.75	0.095	0.439	399.00	0.444	390.01	
	0.128	0.488	101.50	0.496	99.53	0.131	0.482	424.00	0.492	417.37	
	0.181	0.543	109.00	0.542	106.59	0.194	0.524	450.90	0.539	446.64	
	0.319	0.598	116.90	0.607	116.38	0.252	0.552	468.00	0.565	462.66	
	0.399	0.628	121.05	0.634	119.97	0.334	0.583	485.50	0.593	478.20	
	0.511	0.676	125.50	0.673	124.18	0.401	0.611	497.60	0.615	488.87	
	0.683	0.746	130.40	0.749	129.29	0.593	0.691	525.90	0.699	517.38	
	0.774	0.809	132.50	0.802	131.05	0.680	0.739	534.30	0.748	528.54	
	0.810	0.829	132.80	0.826	131.50	0.793	0.816	542.70	0.821	539.38	
0.875	0.879	133.50	0.875	131.82	0.810	0.826	543.10	0.833	540.51		
0.957	0.956	133.80	0.951	131.13	0.943	0.941	544.50	0.933	541.54		
50°C	0.000	0.000	92.51	0.000	92.53	0.947	0.945	544.50	0.937	541.22	
	0.027	0.237	108.66	0.225	116.47	0.000	0.000	92.51	0.000	92.53	
	0.074	0.413	138.34	0.402	145.22	0.027	0.237	108.66	0.225	116.47	
	0.133	0.523	170.22	0.497	166.37	0.074	0.413	138.34	0.402	145.22	
	0.217	0.582	187.71	0.564	183.09	0.133	0.523	170.22	0.497	166.37	
	0.280	0.610	192.64	0.593	190.73	0.217	0.582	187.71	0.564	183.09	
	0.367	0.633	199.98	0.626	198.53	0.280	0.610	192.64	0.593	190.73	
	0.432	0.650	202.48	0.649	203.11	0.367	0.633	199.98	0.626	198.53	
	0.566	0.700	200.72	0.697	211.04	0.432	0.650	202.48	0.649	203.11	
	0.664	0.739	215.49	0.740	215.60	0.566	0.700	200.72	0.697	211.04	
	0.780	0.806	211.44	0.803	219.17	0.664	0.739	215.49	0.740	215.60	
0.831	0.845	222.87	0.837	219.85	0.780	0.806	211.44	0.803	219.17		
0.907	0.907	225.41	0.898	219.44	0.831	0.845	222.87	0.837	219.85		
1.000	1.000	220.60	1.000	220.99	0.907	0.907	225.41	0.898	219.44		
					1.000	1.000	220.60	1.000	220.99		

2. T_{xy} ethanol (1)-water (2) at atmospheric pressure

Table 4.4: VLE bubble point calculation for ethanol (1)-water (2) isobaric binary system at 760 mmHg

experimental			calculated	
x_1	y_1	$T_{in} \text{ } ^\circ\text{C}$	y_1	$T_{in} \text{ } ^\circ\text{C}$
0.0190	0.1700	95.50	0.1729	95.22
0.0721	0.3891	89.00	0.3862	88.32
0.0966	0.4375	86.70	0.4330	86.65
0.1238	0.4704	85.30	0.4694	85.33
0.1661	0.5089	84.10	0.5080	83.94
0.2337	0.5445	82.70	0.5482	82.56
0.2608	0.5580	82.30	0.5606	82.15
0.3273	0.5826	81.50	0.5875	81.35
0.3965	0.6122	80.70	0.6134	80.68
0.5079	0.6564	79.80	0.6567	79.80
0.5198	0.6599	79.70	0.6616	79.72
0.5732	0.6841	79.30	0.6848	79.38
0.6763	0.7385	78.74	0.7359	78.84
0.7472	0.7815	78.41	0.7775	78.58
0.8943	0.8943	78.15	0.8884	78.45

C. 1- propanol (1)-water (2)

In order to test the PRSV+WSMR model on more complex systems, with higher polarity than systems previously tested 1-propanol (1)-water (2) was selected. Further tests were carried out using Sandler's programme (Orbey & Sandler, 1998) (This programme is only available for isothermal conditions). When comparing the results obtained using their programme with those produced by this work it shows that the model can cope with highly non-ideal polar systems and therefore our model is appropriate in representing such complex systems.

1. P_{xy} 1-propanol (1)-water (2) at temperature 79.80°C

Table 4.5: VLE bubble point calculation for 1-propanol (1)-water (2) isothermal binary system at 79.80 °C

T	experimental			Calculated this work		calculated Sandler's programme	
	x_1	y_1	P mmHg	y_1	P mmHg	y_1	P mmHg
79.80°C	0.0000	0.0000	352.60	0.0000	352.37	0.0002	350.28
	0.0856	0.3542	530.00	0.3580	518.87	0.3588	525.90
	0.1558	0.3765	539.60	0.3962	541.83	0.3769	536.49
	0.3012	0.4060	547.00	0.4080	546.98	0.3967	543.45
	0.4114	0.4201	548.10	0.4216	548.49	0.4224	546.33
	0.4202	0.4234	548.50	0.4234	548.52	0.4250	546.38
	0.4287	0.4287	549.70	0.4252	548.52	0.4275	546.39
	0.5556	0.4376	545.70	0.4661	543.67	0.4749	541.66
	0.5782	0.4642	541.70	0.4763	541.52	0.4854	539.66
	0.7390	0.5649	506.60	0.5817	510.50	0.5853	511.71
	0.8201	0.6428	479.20	0.6644	482.41	0.6614	485.65
	1.0000	1.0000	374.60	1.0000	380.96	0.9997	378.60

2. T_{xy} 1-propanol (1)-water (2) at atmospheric pressure

Table 4.6: VLE bubble point calculation for 1-propanol (1)-water (2) isobaric binary system at 760 mmHg

experimental			calculated	
x_1	y_1	T_{in} °C	y_1	T_{in} °C
0.0000	0.0000	100.00	0.0000	100.00
0.0500	0.3481	89.30	0.3187	90.54
0.1000	0.3759	88.38	0.3846	88.38
0.1500	0.3858	88.10	0.4021	87.86
0.2000	0.3922	87.95	0.4062	87.75
0.2500	0.3999	87.81	0.4072	87.73
0.3000	0.4065	87.72	0.4089	87.71
0.3500	0.4139	87.65	0.4130	87.67
0.4000	0.4202	87.62	0.4202	87.64
0.4500	0.4397	87.62	0.4310	87.64
0.5000	0.4490	87.65	0.4455	87.70
0.5500	0.4667	87.77	0.4642	87.84
0.6000	0.4878	87.98	0.4873	88.08
0.6500	0.5239	88.31	0.5156	88.45
0.7000	0.5467	88.79	0.5498	88.97
0.7500	0.5834	89.40	0.5911	89.66
0.8000	0.6300	90.24	0.6411	90.55
0.8500	0.6917	91.40	0.7023	91.69
0.9000	0.7690	92.87	0.7783	93.13
0.9500	0.8689	94.75	0.8746	94.95
1.0000	1.0000	97.12	1.0000	97.26

4.1.2 VLE Heterogeneous systems

After successfully applying PRSV+WSMR model on homogeneous systems, this work investigated the modelling of heterogeneous systems. Three VLE binary systems were tested (shown below) and the results illustrate that the model can represent a wide range of temperatures and pressures e.g. isothermal water-n-butanol at a low pressure of 30 mmHg.

A. water (1)-n-butanol (2)

1. P_{xy} water (1)-n-butanol (2) at temperature 35.00°C

Table 4.7: VLE bubble point calculation for water (1)-n-butanol (2) isothermal binary system at 35 °C

Temperature	experimental			Calculated (this work)		calculated (Sandler's programme)	
	x_1	y_1	P in mmHg	y_1	P in mmHg	y_1	P mmHg
35.00°C	0.1000	0.6110	30.60	0.5923	31.46	0.6110	30.60
	0.1460	0.6550	34.30	0.6605	36.47	0.6720	35.18
	0.2000	0.7130	38.60	0.7103	41.09	0.7170	39.33
	0.2500	0.7600	44.20	0.7420	44.52	0.7460	42.41
	0.3600	0.7970	49.40	0.7871	50.03	0.7890	47.44
	0.5190	0.8180	51.30	0.8202	54.14	0.8220	51.36
	0.9830	0.8180	51.30	0.8162	50.97	0.8810	47.09
	1.0000	1.0000	42.20	1.0000	42.17	0.9990	42.13

2. T_{xy} water (1)-n-butanol(2) at atmospheric pressure

Table 4.8: VLE bubble point calculation for water (1)-n-butanol (2) isobaric binary system at 760 mmHg

experimental			calculated	
x_1	y_1	$T_{in} \text{ } ^\circ\text{C}$	y_1	$T_{in} \text{ } ^\circ\text{C}$
0.0390	0.2670	111.50	0.2303	111.24
0.0470	0.2990	110.60	0.2637	110.21
0.0550	0.3230	109.60	0.2938	109.26
0.0700	0.3520	108.80	0.3430	107.65
0.2570	0.6290	97.90	0.6196	97.34
0.2750	0.6410	97.20	0.6325	96.82
0.2920	0.6550	96.70	0.6437	96.37
0.3050	0.6620	96.30	0.6517	96.05
0.4960	0.7360	93.50	0.7313	93.11
0.5060	0.7400	93.40	0.7340	93.03
0.5520	0.7500	92.90	0.7451	92.71
0.5640	0.7520	92.90	0.7476	92.65
0.5710	0.7480	92.90	0.7489	92.61
0.5770	0.7500	92.80	0.7501	92.59
0.9750	0.7520	92.70	0.7512	92.52
0.9800	0.7560	93.00	0.7651	92.97
0.9820	0.7580	92.80	0.7725	93.21
0.9850	0.7750	93.40	0.7866	93.66
0.9860	0.7840	93.40	0.7922	93.84
0.9880	0.8080	93.70	0.8053	94.25
0.9920	0.8430	95.40	0.8415	95.38
0.9940	0.8840	96.80	0.8668	96.16
0.9970	0.9290	98.30	0.9193	97.72
0.9980	0.9510	98.40	0.9423	98.38
0.9990	0.9810	99.40	0.9689	99.14

B. Methyl Ethyl Ketone (1)-water (2)

1. P_{xy} MEK (1) - water (2) at temperature 73.80°C

Table 4.9: VLE bubble point calculation for MEK (1)-water (2) isothermal binary system at 73.8°C

T	experimental			Calculated (this work)		calculated (Sandler's programme)	
	x_1	y_1	P in mmHg	y_1	P in mmHg	y_1	P mmHg
73.80°C	0.5872	0.6530	758.00	0.6452	739.19	0.6030	620.00
	0.6500	0.6590	760.00	0.6656	741.57	0.6308	720.32
	0.7000	0.6680	760.00	0.6862	741.56	0.6945	731.05
	0.8000	0.7110	748.00	0.7419	733.41	0.7320	701.85
	0.9000	0.7960	714.00	0.8289	706.78	0.8210	672.61
	1.0000	1.0000	619.00	1.0000	637.95	0.9996	631.83

2. T_{xy} MEK (1) - water (2) at atmospheric pressure

Table 4.10: VLE bubble point calculation for MEK (1)-water (2) isobaric binary system at 760 mmHg

experimental			calculated	
x_1	y_1	$T_{in} \text{ } ^\circ\text{C}$	y_1	$T_{in} \text{ } ^\circ\text{C}$
0.0020	0.0850	97.60	0.1123	96.73
0.0040	0.1840	93.20	0.2042	93.79
0.0050	0.2070	92.00	0.2437	92.45
0.0110	0.3940	84.60	0.4156	85.83
0.0170	0.5150	81.20	0.5162	81.17
0.0360	0.6180	75.50	0.6499	73.60
0.1900	0.6450	74.40	0.6656	72.26
0.5500	0.6450	74.40	0.6382	73.88
0.6350	0.6450	73.80	0.6606	73.73
0.6550	0.6550	73.30	0.6672	73.72
0.6650	0.6570	73.60	0.6707	73.71
0.6670	0.6610	73.50	0.6714	73.71
0.7090	0.6710	73.90	0.6877	73.73
0.7210	0.6760	73.80	0.6928	73.75
0.7290	0.6760	73.70	0.6964	73.76
0.7440	0.6830	73.80	0.7033	73.80
0.7750	0.6960	74.00	0.7191	73.91
0.7840	0.6980	73.50	0.7240	73.95
0.8000	0.7070	73.90	0.7333	74.04
0.8030	0.7070	73.90	0.7351	74.06
0.8360	0.7380	74.10	0.7568	74.32
0.8480	0.7360	73.80	0.7656	74.44
0.8800	0.7670	74.50	0.7925	74.85
0.9120	0.8160	75.30	0.8259	75.43
0.9580	0.8980	76.40	0.8939	76.80
0.9770	0.9290	77.00	0.9341	77.68
0.9930	0.9630	78.30	0.9773	78.65

C. water (1)-hexanol (2)

1. P_{xy} water (1)-hexanol(2) at temperature 21°C

Table 4.11: VLE bubble point calculation for water (1)-hexanol (2) isothermal binary system at 21°C

T	experimental			Calculated (this work)		calculated (Sandler's programme)	
	x_1	y_1	P in mmHg	y_1	P in mmHg	y_1	P mmHg
21.00°C	0.0000	0.0000	0.80	0.0019	0.58	0.0020	0.60
	0.0540	0.8690	6.00	0.9076	5.92	0.9083	6.21
	0.1060	0.9290	10.40	0.9489	10.18	0.9478	10.40
	0.1620	0.9510	14.10	0.9645	13.95	0.9633	14.10
	0.1910	0.9580	15.80	0.9690	15.61	0.9681	15.79
	0.2340	0.9650	17.90	0.9738	17.74	0.9731	18.07
	0.9990	0.9860	19.00	0.9859	18.89	0.9905	18.77
	1.0000	1.0000	18.70	0.9998	18.65	0.9990	18.63

2. T_{xy} water (1)-hexanol (2) at atmospheric pressure

Table 4.12: VLE bubble point calculation for water (1)-hexanol (2) isobaric binary system at 760 mmHg

experimental			calculated	
x_1	y_1	T in $^{\circ}\text{C}$	y_1	T in $^{\circ}\text{C}$
0.0000	0.0000	157.00	0.0000	151.95
0.0500	0.5800	134.00	0.5536	129.71
0.1000	0.7700	118.40	0.7387	117.04
0.1500	0.8350	110.60	0.8163	109.57
0.2000	0.8750	105.70	0.8557	104.87
0.2500	0.8950	101.80	0.8786	101.76
0.3000	0.9080	100.20	0.8932	99.61
0.4000	0.9250	98.00	0.9102	96.98
1.0000	1.0000	100.00	1.0000	100.00

Table 4.13: UNIQUAC parameters and PRSV interaction parameters and AAD for vapour phase, temperature and pressure for VLE binary homogeneous and heterogeneous systems (isothermal and isobaric)

System	Status	T in $^{\circ}\text{C}$	UNIQUAC		PRSV EOS	AAD		
			A_{12}	A_{21}	K_{12}	AAD y	$P \& T$	
Homogeneous systems								
methanol- water	Isothermal	25	66.60	-101.97	0.1447	0.0059	0.0078	
		50	59.69	-94.12	0.0952	0.0167	0.0220	
		65	947.49	-453.31	0.2536	0.0100	0.0125	
		100	1805.8	-573.77	0.2989	0.0379	0.0141	
	Isobaric		134.93	-152.59	0.1823	0.0059	0.0015	
	ethanol-water	Isothermal	20	279.4	54.52	0.1713	0.0076	0.0094
			30	336.47	-11.67	0.2381	0.0068	0.0064
			40	152.69	69.04	0.2690	0.0079	0.0200
50			169.75	150.42	0.1988	0.0161	0.0243	
60			799.04	-263.11	0.3852	0.0343	0.0249	
70			760.19	-303.15	0.4177	0.0128	0.0128	
propanol- water	Isobaric		110.37	509.03	0.0581	0.0044	0.0018	
	Isothermal	79.8	149.57	296.39	0.4148	0.0192	0.0053	
	Isobaric		139.60	539.83	0.3498	0.0158	0.002	
Heterogeneous systems								
water-n- butanol	Isothermal	35	752.91	352.05	0.4874	0.0105	0.0298	
	Isobaric		1497.44	184.77	0.3639	0.0190	0.0036	
water-hexanol	Isothermal	21	306.64	364.73	0.2900	0.0126	0.0442	
	Isobaric		503.84	622.33	0.031	0.0202	0.0122	
MEK-water	Isothermal	73.8	427.64	559.19	0.4129	0.0223	0.0223	
	Isobaric		543.70	811.01	0.3665	0.0347	0.0059	

4.1.3 LLE binary systems

1- 1-butanol (1)-water (2)

Table 4.14: Area Method and TPI predictions for LLE 1-butanol (1)-water (2) system with the parameters obtained from data correlation

experimental			Area Method				TPI Method			UNIQUAC		PRSV
T in $^{\circ}\text{C}$	Grid No. 1000		MPNA	Time	Grid No. 1000		Time	A_{12}	A_{21}	k_{12}		
	x_1 org	x_1 aq			x_1 org	x_1 aq					x_1 org	x_1 aq
0	0.504	0.026	0.506	0.026	0.0059	157.6	0.506	0.026	4.7	217.55	676.60	0.447
20	0.492	0.020	0.491	0.020	0.0062	187.4	0.492	0.020	6.3	186.97	877.85	0.435
25	0.488	0.019	0.486	0.019	0.0063	148.3	0.487	0.019	8.6	163.07	917.84	0.438
40	0.473	0.017	0.475	0.017	0.0058	151.3	0.473	0.017	4.9	145.42	1063.58	0.431
60	0.441	0.016	0.440	0.016	0.0046	170.6	0.441	0.016	8.2	81.89	1250.07	0.429
80	0.389	0.017	0.390	0.017	0.0028	222.2	0.389	0.017	7.4	-17.03	1459.78	0.429
100	0.322	0.024	0.320	0.024	0.0010	119.4	0.320	0.020	7.8	-40.98	1638.43	0.401
120	0.213	0.043	0.215	0.043	0.0001	172.1	0.231	0.045	6.1	-183.14	2355.99	0.401

2- Ethyl acetate (1)-water (2)

Table 4.15: Area Method and TPI predictions for LLE ethyl acetate (1)-water (2) system with the parameters obtained from data correlation. The results are obtained using Pentium(R) 4 CPU 3.00GHz. Simpson's rule is used as numerical integration

experimental			Area Method				TPI Method			UNIQUAC		PRSV
T in $^{\circ}\text{C}$	Grid No. 1000		MPNA	Time	Grid No. 1000		Time	A_{12}	A_{21}	k_{12}		
	x_1 org	x_1 aq			x_1 org	x_1 aq					x_1 org	x_1 aq
0	0.897	0.021	0.901	0.019	0.012	94.9	0.897	0.021	4.6	797.70	-95.66	0.602
10	0.884	0.019	0.885	0.017	0.016	81.6	0.884	0.019	4.4	751.28	-85.66	0.602
20	0.870	0.017	0.876	0.015	0.022	89.0	0.870	0.017	3.1	698.51	-72.36	0.602
25	0.862	0.016	0.871	0.015	0.026	75.4	0.864	0.017	6.4	668.16	-64.17	0.602
30	0.853	0.015	0.860	0.014	0.037	65.2	0.853	0.015	6.1	591.07	32.42	0.450
40	0.835	0.014	0.855	0.014	0.051	91.8	0.835	0.014	6.0	565.66	134.49	0.300
50	0.815	0.013	0.815	0.013	0.049	91.4	0.815	0.013	8.3	538.37	156.31	0.300
60	0.793	0.012	0.795	0.012	0.046	87.2	0.793	0.012	3.4	508.04	179.43	0.300
70	0.767	0.012	0.765	0.012	0.042	115.3	0.767	0.012	6.2	474.96	209.87	0.290

4.1.4 VLE binary systems

Table 4.16A: The experimental and correlated values for VLE binary systems with UNIQUAC and PRSV interaction parameter and the AAD

VLE Binary system	T in °C	P in Bar	UNIQUAC parameters		PRSV	Experimental			Correlation PRSV			AAD
			A_{12}	A_{21}		organic	aqueous	vapour	organic	aqueous	vapour	
			x_1	x_1		y_1	x_1	x_1	y_1			
Water(1) - n-butyl acetate(2)	91.85	1.013	-210.48	1647.77	1.000	0.1855	0.9981	0.7086	0.1860	0.9981	0.7110	0.0010
ethyl acetate(1) - Water(2)	72.05	1.013	821.97	85.38	0.408	0.7760	0.0120	0.6870	0.7761	0.0120	0.6867	0.0001
n-butanol(1) - water(2)	36.00	0.068	552.59	353.10	0.020	0.4810	0.0170	0.1829	0.4815	0.0170	0.1837	0.0004
Water (1) – n-butanol(2)	93.77	1.013	1792.44	472.72	0.338	0.6393	0.9781	0.7590	0.6395	0.9781	0.7587	0.0002

Table 4.16B: The predicted values for VLE binary systems using the TPI method: Modified 2Point and Direct 3Point search with AAD values and the computational duration for both methods .The results are obtained using Pentium(R)4 CPU 3.00GHz

VLE Binary system	T in °C	P in Bar	TPI Modified 2Point search			AAD	Duration in sec	TPI Direct 3Point search			AAD	Duration in sec
			organic	aqueous	vapour			organic	aqueous	vapour		
			x_1	x_1	y_1			x_1	x_1	y_1		
Water(1) - n-butyl acetate(2)	91.85	1.013	0.1870	0.9980	0.7084	0.0006	2.63	0.1875	0.9980	0.7084	0.0005	2.89
ethyl acetate(1) - Water(2)	72.05	1.013	0.7766	0.0120	0.6844	0.0010	2.75	0.7746	0.0124	0.6881	0.0009	3.52
n-butanol(1) - water(2)	36.00	0.068	0.5166	0.0147	0.1847	0.0132	2.69	0.4740	0.0146	0.1884	0.0050	2.84
Water (1) – n-butanol(2)	93.77	1.013	0.6365	0.9786	0.7584	0.0013	2.72	0.6403	0.9783	0.7583	0.0007	3.30

4.2 Discussion

This work attempts to model Phase Equilibria for highly non-ideal vapour-liquid-liquid systems. The number of components in each phase determines the complexity of the problem. The modelling includes VLE, LLE & VLLE binaries and VLLE ternary and quaternary systems.

The key to the modelling lies in an ability to represent the basic thermodynamics of the systems considered. Over the last 20 years more emphasis has been placed on representing the thermodynamic property of fugacity through universally applicable Equations of State (EOS). This has the advantage that all the phases present are modelled using the same form of equation (as reviewed in chapter 2.3).

The literature survey demonstrates that systems can show deviations from ideality and this non-ideality often arises from strong polar interactions between molecules. The challenge is to be able to satisfactorily model this non-ideal behaviour using an appropriate thermodynamic model. The literature survey (2.2) shows that a range of thermodynamic models are available and these are usually classified through representing the liquid phase fugacity in terms of an activity coefficient model or an appropriate EOS.

As previously stated, this work investigates the applicability and effectiveness of a particular EOS namely the PRSV + Wong Sandler Mixing Rules. Initially to demonstrate the suitability of the proposed model (PRSV+ Wong-Sandler Mixing Rules) and to confirm the work in this field (Ghosh and Taraphar, 1998; Khodakarami et al., 2005; Mario and Mauricio, 2011) it is sensible to check that the model is applicable to the VLE of binary systems showing a range of non-ideal behaviour.

It is known that organic molecules usually show a range of positive deviations from Raoult's law in the presence of water. Allied to these deviations, if the organic component and water are relatively close when boiling at a fixed pressure, there is the possibility of the formation of minimum boiling azeotrope.

4.2.1 VLE binary homogeneous mixtures

Three systems have been chosen where measured VLE data are available under isothermal and isobaric conditions. These are:

1. Methanol-Water
2. Ethanol-Water
3. 1-propanol-Water

The VLE data have been taken from DECHEMA data collection (1977). At normal pressure the following boiling points are known:

Component	B.Pt ⁰ C
methanol	65.00
ethanol	78.37
1-propanol	97.00
water	100.00

The methanol-water system does show positive deviations. When figure 4.1 (A & B) is examined the xy versus temperature & pressure plot shows “Pinch” at high values of x with the fairly high difference in normal boiling points, an azeotrope has not been formed but the behaviour of the system at high values of x indicates deviations from ideality.

The ethanol-water system also shows positive deviation from ideality, with the component boiling points being closer. The system shows evidence of the formation of a minimum boiling azeotrope at values of > 0.95 . This is noticeable when observing the figure 4.2(A&B) where the xy versus T & P plot shows obvious deviations from ideality.

The positive deviation from ideality for 1-propanol–water system is greater than the methanol-water & ethanol-water systems. When the components have close boiling points and the system clearly forms minimum boiling azeotrope behaviour (at value of 0.41), the increase in deviation is apparently linked to an increased carbon number in the alcohol. This highly non-ideality is visible when the xy is plotted against T & P as shown in figure 4.3 (A&B).

The comparisons of experimental and correlated data obtained by using PRSV EOS with WSMR for bubble point temperature, pressure and vapour composition for all three systems are shown in figure 4.1, 4.2 & 4.3(C, D, E & F).

The VLE of the methanol-water system have been modelled for isothermal and isobaric conditions using PRSV+WSMR. The results obtained show that the Absolute Average Deviation (AAD) for the vapour phase is 0.0059 and for pressure 0.0015 in mmHg. The VLE for the above system has been correlated at isothermal conditions at the following temperatures: 25, 50,100⁰C.The results indicate the AAD values for vapour phase and temperature are 0.0176 and 0.0141 in degree Celsius respectively. The values for each point calculations are shown in tables: (4.1 & 4.2). Table (4.13) also displays the UNIQUAC and PRSV parameters.

The results for the VLE of the ethanol-water system using the PRSV+WSMR model show that the AAD in isothermal conditions for the vapour phase is 0.0044 and for pressure is 0.0018 in mmHg. Meanwhile the bubble point calculation at isobaric conditions for the following temperatures: 20, 30, 40, 50, 60 & 70⁰C were carried out and the AAD for the vapour phase composition for all the data points is: 0.0143 and the AAD in temperature is 0.0163 in degree centigrade. The details for each of the calculation results with the energy parameters for UNIQUAC activity model and PRSV binary interaction parameters for each defined system are presented in tables: (4.3, 4.4 & 4.13).

The performance of PRSV+WSMR remains reliable in spite of the increased polarity, for instance the results for 1-propanol-water prove this consistency with the previous homogenous systems. The AAD in vapour phase and pressure at isothermal condition are 0.0195 and 0.0053 respectively. These results compare well with those using VLE Orbey & Sandler's (1998) programme which are 0.0205 and 0.0071 respectively. In isobaric condition the AAD in vapour phase and temperature are 0.0158 and 0.002. The results for this system with the binary interaction parameters are shown in table (4.5, 4.6 & 4.13).

Pervious researchers recommended the WSMR for non-ideal polar organic systems. Orbey and Sandler (1998) and Lee et al. (2007) have examined WSMR on a wide range of VLE binary systems e.g. 2-propanol-water & acetone-water

and they concluded the WSMR performance to be the best when compared to other mixing rules e. g. Huron-Vidal & van der Waals. Other researchers have come to the same conclusion and in a study by Ghosh et al. (1998) on VLE for forty-three binary systems including various mixtures (organic alcohols, esters, ketones, amines etc.) using WSMR, the results obtained were comparable with DECHEMA data series. When modelling VLE for ethanol mixtures found in alcoholic beverage production, Claudio et al. (2009) recommended the use of WSMR to model low pressure complex mixtures.

It was noticed when fitting the model (PRSV+WSMR) incorporated with UNIQUAC activity coefficient as excess Gibbs energy to the VLE binary data for three homogenous systems, the results prove that the model accurately represents such systems, therefore the WSMR were found to be satisfactory in description of phase behaviour of non-ideal systems.

4.2.2 VLE binary heterogeneous mixtures

The 1-propanol-water is a highly non-ideal polar system when compared to other homogenous systems. In order to be assured that PRSV EOS combined with UNIQUAC activity coefficient through WS mixing rule can model heterogeneous mixtures successfully; three binary systems were selected and tested for this purpose:

- 1- Water-n-butanol
- 2- Methyl Ethyl Ketone (MEK)-water
- 3- Water-1-hexanol

As the interaction between unlike molecules decreases and increases for like molecules the mixture shows a tendency to split into two liquid phases. This behaviour occurs when the number of CH₂ group increases in the alcohol molecule and as a consequence leads to a reduction in the mutual solubility of the alcohol in water. Heterogeneous systems form a minimum azeotrope. The composition value for this azeotrope in water- n-butanol system is 0.74 at temperature of 92.70⁰C, in MEK-water system is 0.65 at temperature 73.60⁰C and for water-hexanol system is 0.91 at temperature 96⁰C.

Observations of the correlation of VLE for highly non ideal polar systems using PRSV EOS show the capability of this model to adequately represent the vapour pressure for these systems. The AAD for isobaric water-n butanol is 0.0107 in vapour mole fraction and 0.35 for the temperature. The estimated values versus the experimental are shown in figure 4.4(C&E) and table (4.8). The AAD results for isothermal data at 35⁰C are 0.0075 for vapour fraction and 0.0016 for pressure (in mmHg), the comparisons between the experimental versus calculated values are plotted and shown in figure 4.4(D&F) and in table 4.7.

Figure 4.4(A & B) show the excellent agreement between the experimental and correlated values for the mixture water-n-butanol VLE system and similar results were found by Sandler et al. (1998). In a comparison study of liquid –liquid equilibrium at low pressure using the optimised parameters for predicting a high pressure system using WSMR and (MHV1, MHV2), the authors indicated the WSMR results were more accurate than MHV mixing rules.

Figure 4.5(A&B) represent isobaric and isothermal binary VLE MEK-water system. The AAD for the isobaric condition are 0.0347 and 0.0059 for vapour mole fraction and temperature in centigrade respectively. In isothermal conditions the AAD are 0.0223 for both vapour and pressure in mmHg. The details and the values for each calculation are tabulated in table (4.9 & 4.10). The VLE results for isobaric MEK-water prove that the PRSV+WSMR can represent the polar and asymmetric systems. In spite of the fact that the water –hexanol system is highly asymmetric the results for VLE correlation using PRSV+WSMR model were in agreement with other researchers findings (Coutsikos et al., 1995). Table 4.11 and 4.12 show the values for the calculations with experimental data. The AAD for isobaric data are: 0.0202 and 0.0122 for vapour mole fraction and temperature in centigrade and for isothermal data are 0.0126 and 0.442 for vapour and pressure in mmHg respectively. Figures 4.6(A&B) show the temperature and pressure versus water mole fraction for water-1-hexanol system, the calculated values are comparable with experimental values. Figure 4.6(C, D, E & F) illustrate the visual comparison between the estimated and experimental values. The graphical observation of calculated values of vapour compositions & pressure versus experimental values demonstrates that our model (PRSV+WSMR) produced better results than those

obtained from Sandler's programme; this could be due to the modified UNIQUAC effect on the classical one (Figure 4.7&4.8).

Binary VLE methanol-water

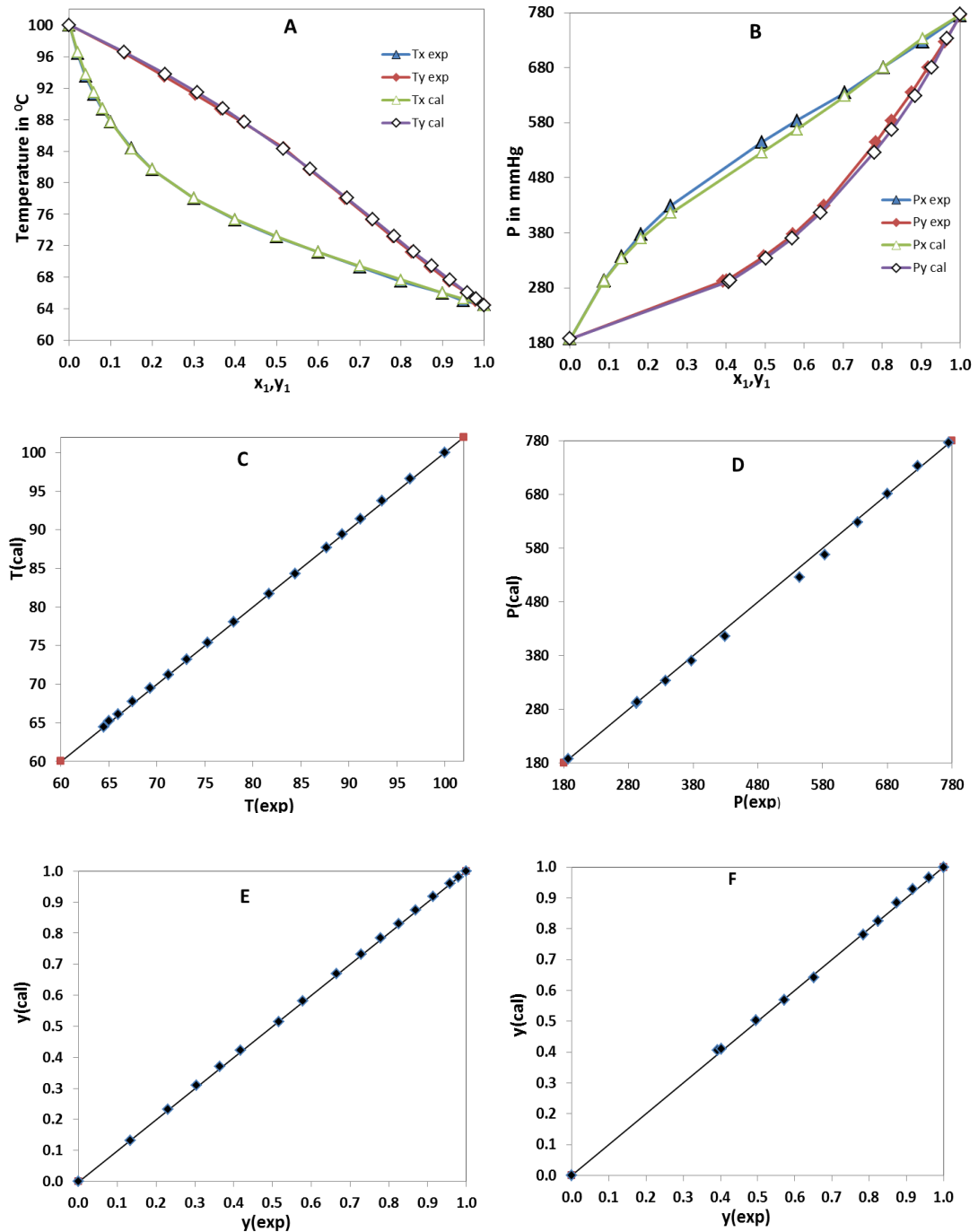


Figure 4.1: A&B: isobaric VLE at 760 mmHg and isothermal at 65°C for the system methanol (1)-water (2) respectively. C&E: comparison of experimental (solid symbols) and estimated (hollowed symbols) equilibrium temperature and composition for isobaric condition. D&F: comparison of experimental (solid symbols) and estimated (hollowed symbols) equilibrium pressure and composition for isothermal condition

Binary VLE ethanol-water

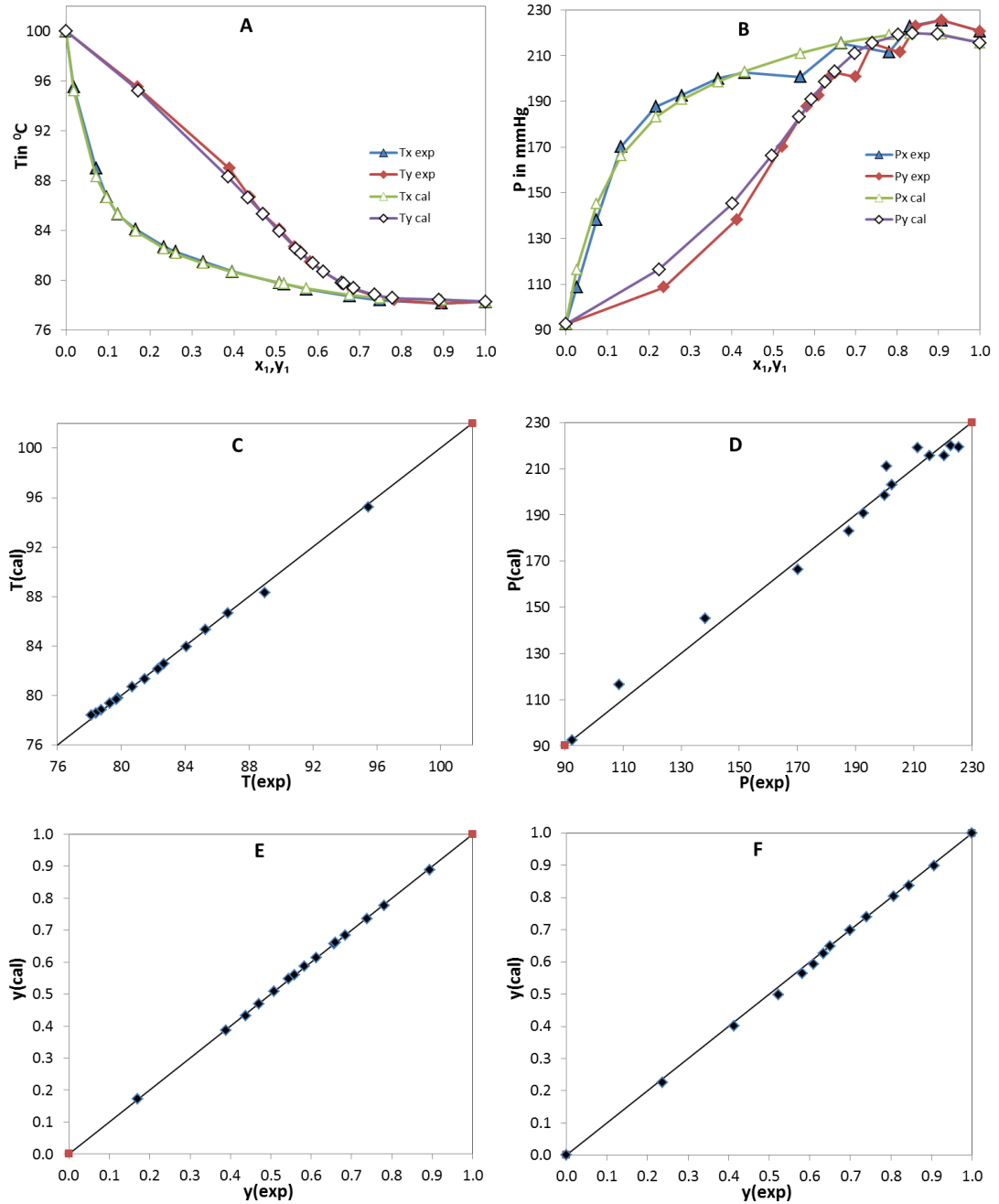


Figure 4.2: A&B: isobaric VLE at 760 mmHg and isothermal at 50°C for the system ethanol (1)-water (2) respectively. C&E: comparison of experimental (solid symbols) and estimated (hollowed symbols) equilibrium temperature and composition for isobaric condition. D&F: comparison of experimental and correlated equilibrium pressure (mmHg) and composition for isothermal condition.

Binary VLE 1-propanol-water

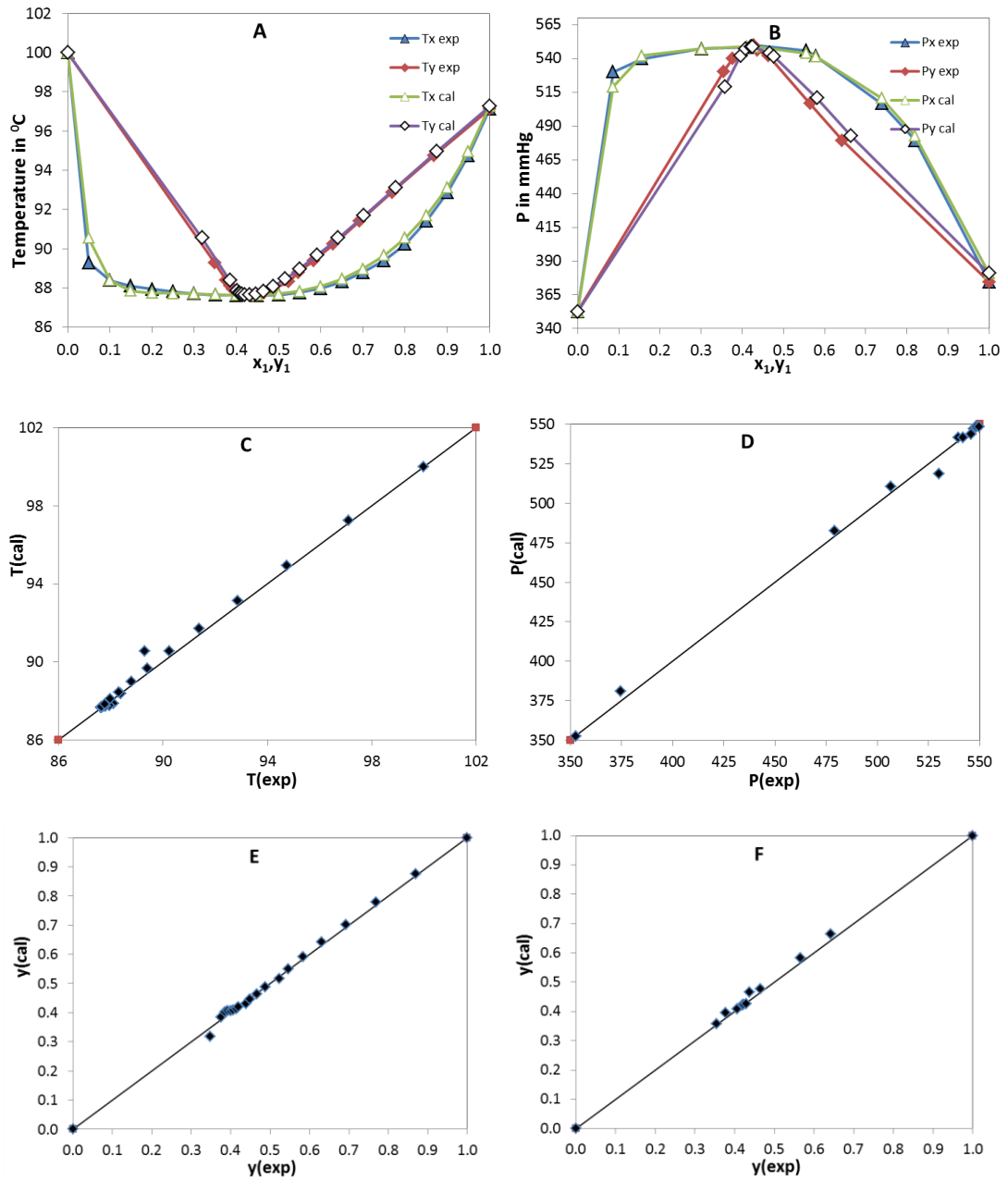


Figure 4.3: A&B: isobaric VLE at 760 mmHg and isothermal at 79.80⁰C for the system 1-propanol (1)-water (2) respectively. C&E: comparison of experimental (solid symbols) and estimated (hollowed symbols) equilibrium temperature and composition for isobaric condition. D&F: comparison of experimental and correlated equilibrium pressure (mmHg) and composition for isothermal condition.

Binary VLE water-n-butanol

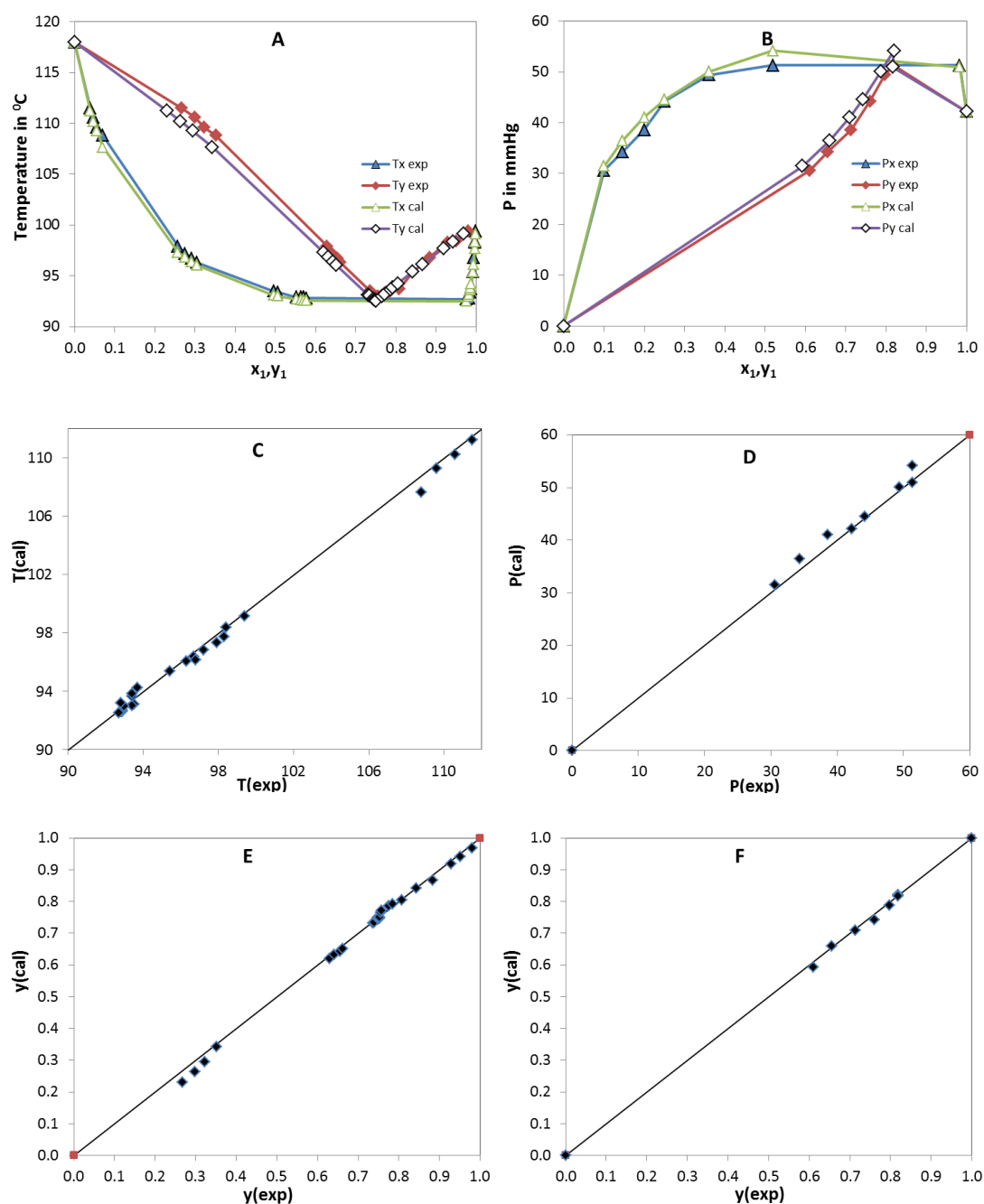


Figure 4.4: A&B: isobaric VLE at 760 mmHg and isothermal at 35.0 $^{\circ}\text{C}$ for the system water (1)-n-butanol (2) respectively. C&E: comparison of experimental (solid symbols) and estimated (hollowed symbols) equilibrium temperature and composition for isobaric condition. D&F: comparison of experimental and correlated equilibrium pressure (mmHg) and composition for isothermal condition.

Binary VLE MEK-water

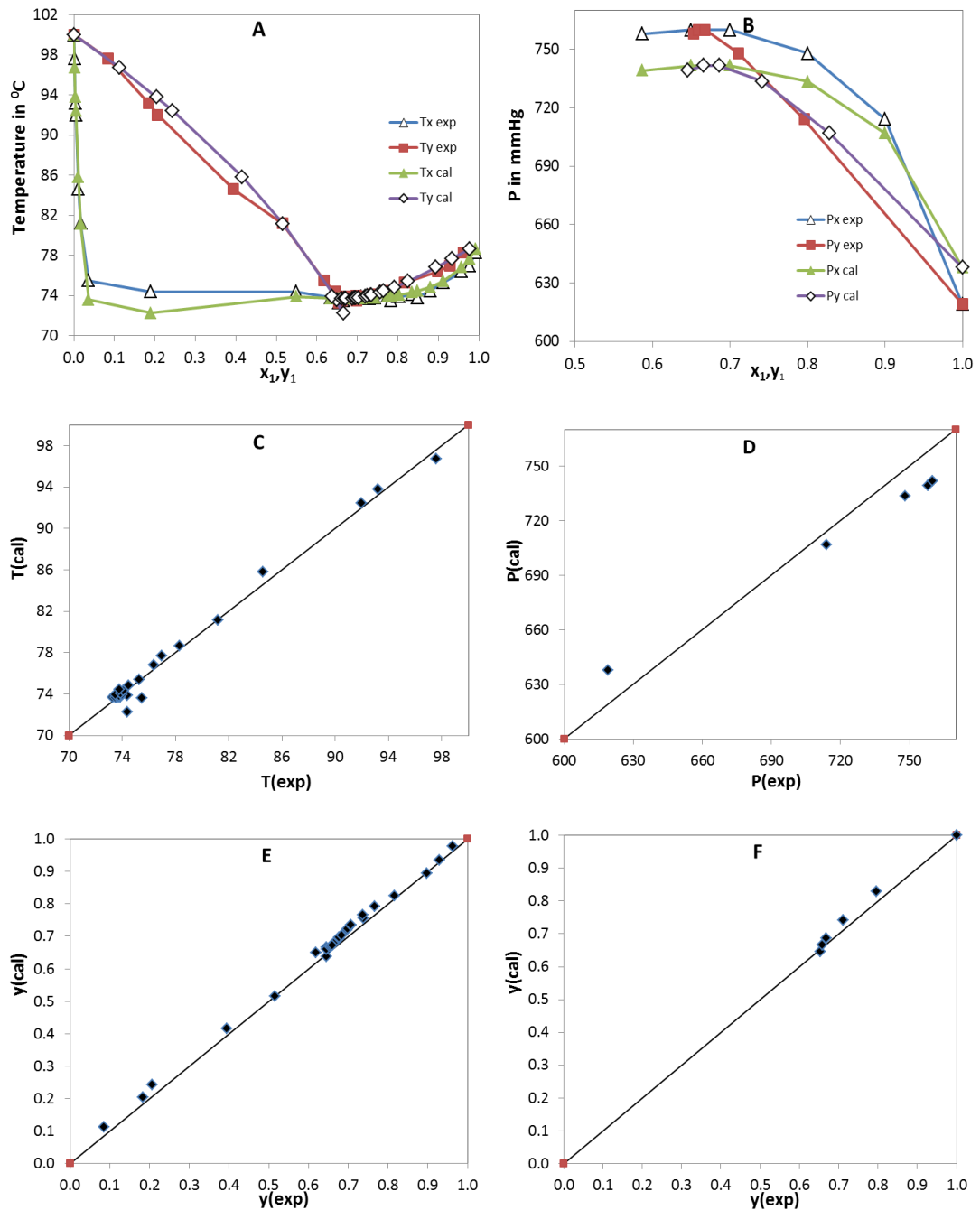


Figure 4.5: A&B: isobaric VLE at 760 mmHg and isothermal at 73.80°C for the system MEK (1)-water (2) respectively. C&E: comparison of experimental (solid symbols) and estimated (hollowed symbols) equilibrium temperature and composition for isobaric condition. D&F: comparison of experimental and correlated equilibrium pressure (mmHg) and composition for isothermal condition.

Binary VLE water-hexanol

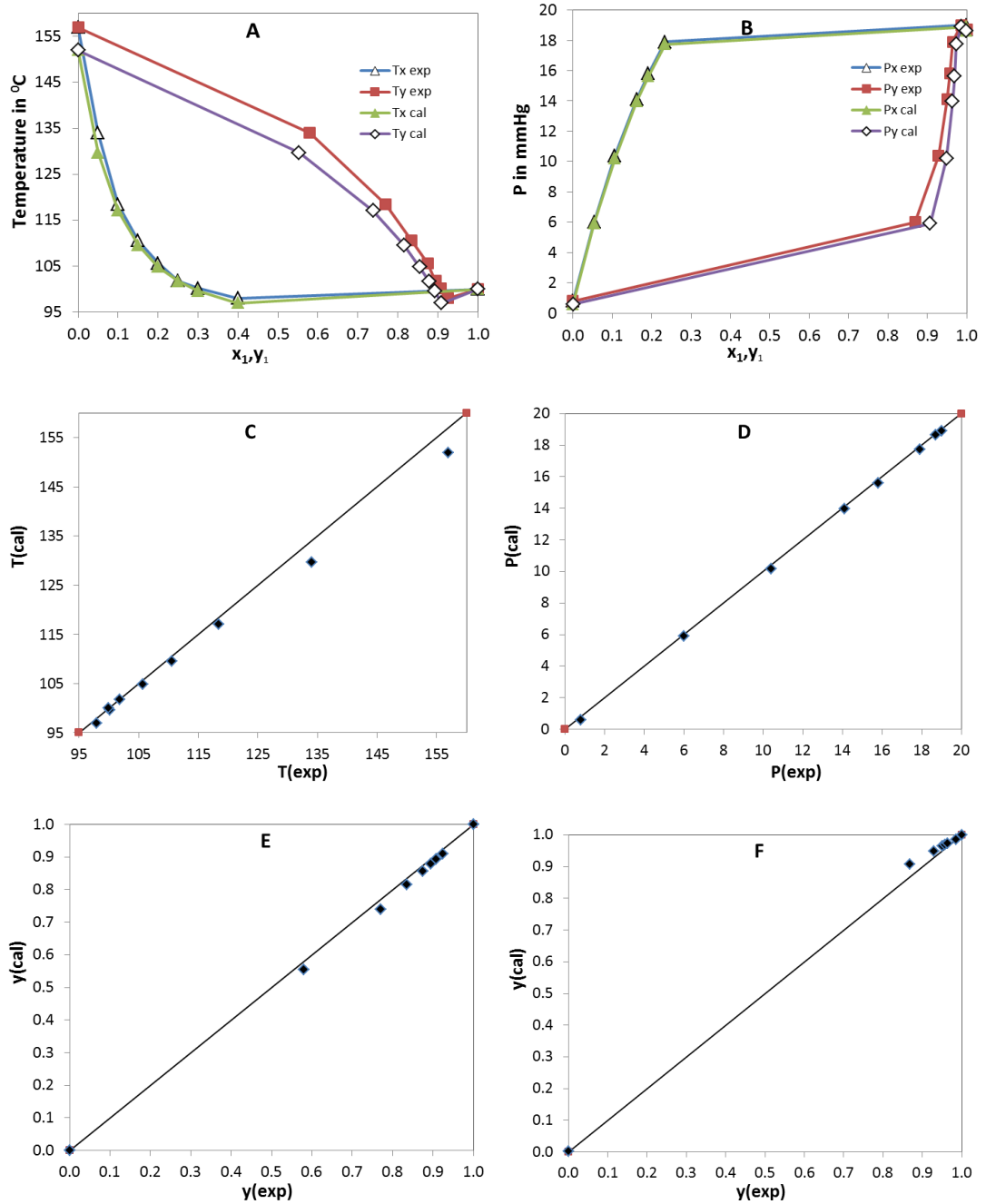


Figure 4.6: A&B: isobaric VLE at 760 mmHg and isothermal at 21.0°C for the system water (1)-1-hexanol (2) respectively. C&E: comparison of experimental (solid symbols) and estimated (hollowed symbols) equilibrium temperature and composition for isobaric condition. D&F: comparison of experimental and correlated equilibrium pressure (mmHg) and composition for isothermal condition.

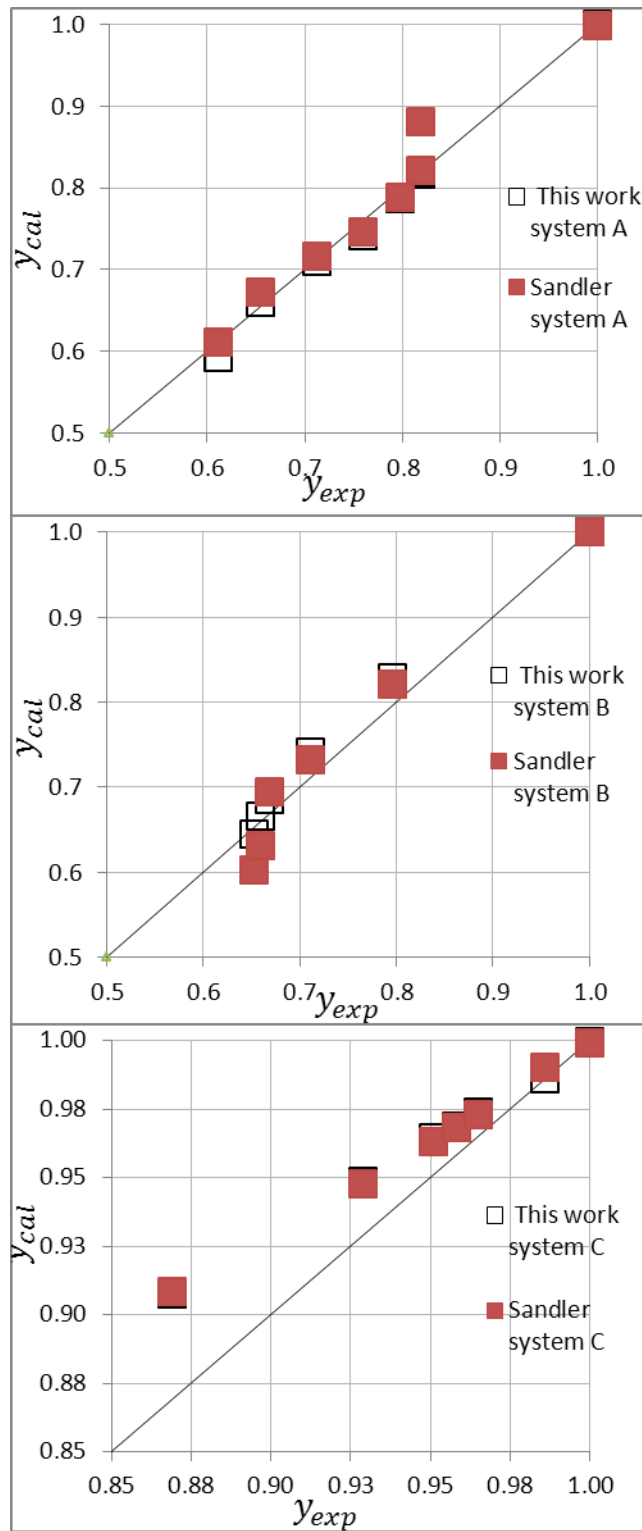


Figure 4.7: Experimental versus calculated values for vapour phase composition for binary VLE systems, the solid icon represents the value when the Sandler's programme was used and the hollowed icon represents the value obtained by this work (PRSV+WSMR model). A. VLE isothermal data at 35.0°C for the system water(1)-n-butanol(2) B. Binary VLE isothermal data at 73.80°C for the system MEK(1)-water(2), C. Binary VLE isothermal data at 21.0°C for the system water(1)-1-hexanol(2).

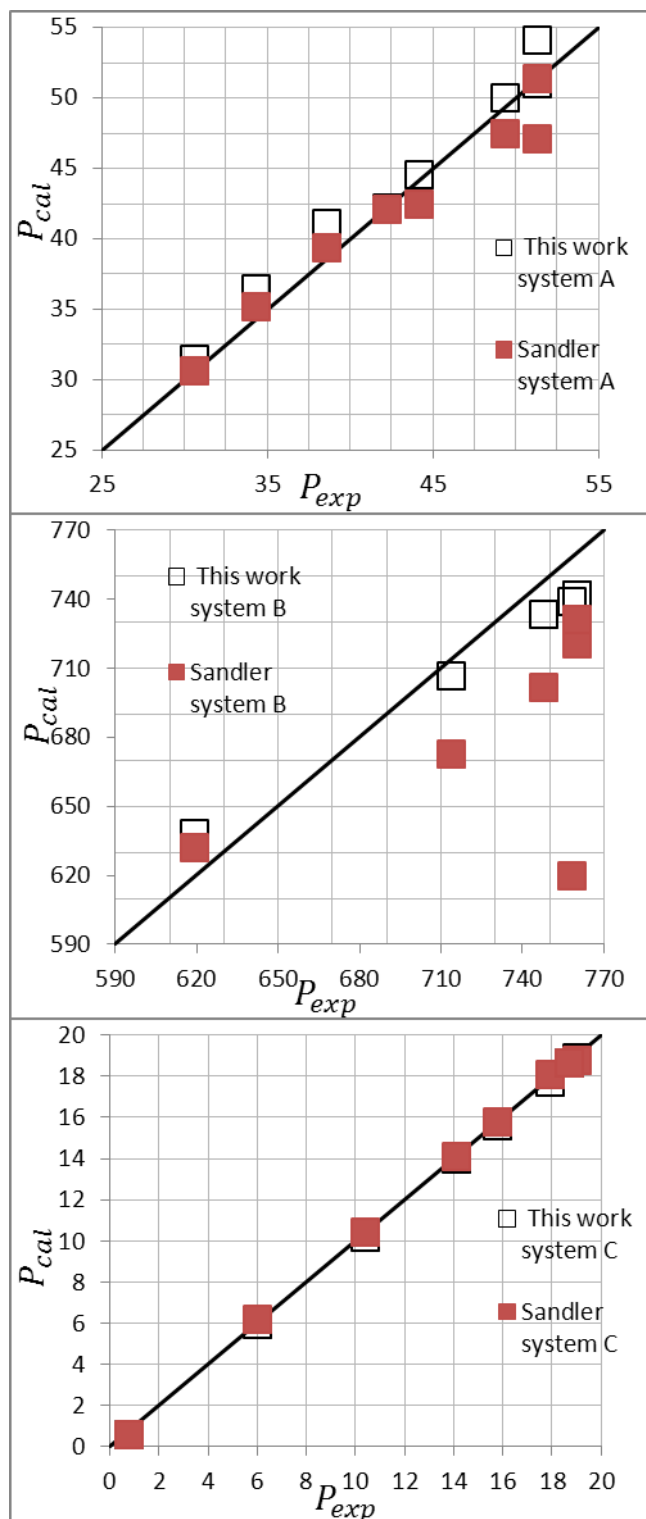


Figure 4.8: Experimental versus calculated values for pressure (mmHg) for binary VLE systems, the solid icon represents the AD value when the Sandler's programme was used and the hollowed icon represents the AD value obtained by this work (PRSV+WSMR model). A. VLE isothermal data at 35.0°C for the system water(1)-n-butanol(2) B. Binary VLE isothermal data at 73.80°C for the system MEK(1)-water(2), C. Binary VLE isothermal data at 21.0°C for the system water(1)-1-hexanol(2).

4.2.3 Conclusions on PRSV+WSMR

Generally ranges of binary VLE systems have been modelled using the PRSV + WSMR through UNIQUAC activity coefficient as excess Gibbs energy function. This covers the range from homogenous slightly non-ideal to strongly non-ideal heterogeneous mixtures at low and moderate pressures and this model shows the capability to represent these complex systems. Despite some limitations for highly asymmetric systems, this conclusion is in line with other researchers findings. As the size of the hydrocarbon molecule increases the system becomes more asymmetric and one of the limitations for the WSMR is poor correlation for highly asymmetric systems at high pressure.

One of the main considerations in discussing non-ideality in binary system is the relative strength of the mixture bond. Thus as we consider homologous series for ethanol, propanol, butanol in the presence of water, experimental data indicate that the positive deviations increase as the hydrocarbon chain length increases. The increase in the positive deviations is obviously linked to the availability of the polar –OH group in the alcohol to the –OH group in the water molecule. The length of the hydrocarbon chain makes the availability of the –OH group in the alcohol much less and the mixture bond much weaker to the point where two liquid phases can form rich in each of the separate components. The next section comprises of the results & discussion on further tests which were carried out on PRSV+WSMR for correlation of liquid-liquid and vapour-liquid-liquid equilibrium, for a range of binary systems. The parameters obtained from correlation of data were used in prediction of mutual solubility of these mixtures, applying Gibbs minimisation techniques.

4.3 Prediction models for modelling binary LLE & VLE systems

The Area Method (AM) developed by Eubank et al. (1992) and the Tangent Plane Intersection (TPI) method developed by Hodges et al. (1998) have been applied to two binary systems:

- 1- LLE butanol-water system in the 0-120⁰C temperature range.
- 2- LLE ethyl acetate –water system in the 0-70⁰C temperature range.

The experimental data were acquired from DECHEMA chemistry series (1977-1991).

The prediction results for both systems are shown in table 4.14 and 4.15 respectively; the parameters used were obtained from LLE correlations using PRSV EOS combined with the Wong Sandler mixing rules. The results obtained in this work indicated that, for these data, both Gibbs free minimisation methods (AM & TPI) are reliable and robust for such non-ideal binary systems.

It was observed that the AM was computationally slow compared to the TPI method; this is due to the integration part of the calculation in a search for the maximum positive net area (MPNA) under the Gibbs energy curve and bounded by the tangent plane. Consequently AM was only used for LLE binary systems. It was observed that for the butanol-water system the Gibbs energy curve flattens in the 2 phase region as the temperature increases up to a point where the 2-phase behaviour is almost eliminated (as shown in the figure 4.9). This change was not so pronounced in the Gibbs energy curve for the ethyl acetate- water system. Figure 4.10 shows the ethyl acetate mole fraction verses the Gibbs energy curve for various temperatures. The Absolute Average Deviation (AAD) for the AM and TPI predictions for the butanol-water system are 0.0008 and 0.0019 respectively. The AAD for the AM and the TPI predictions in the ethyl acetate-water system are 0.0033 and 0.0004 respectively.

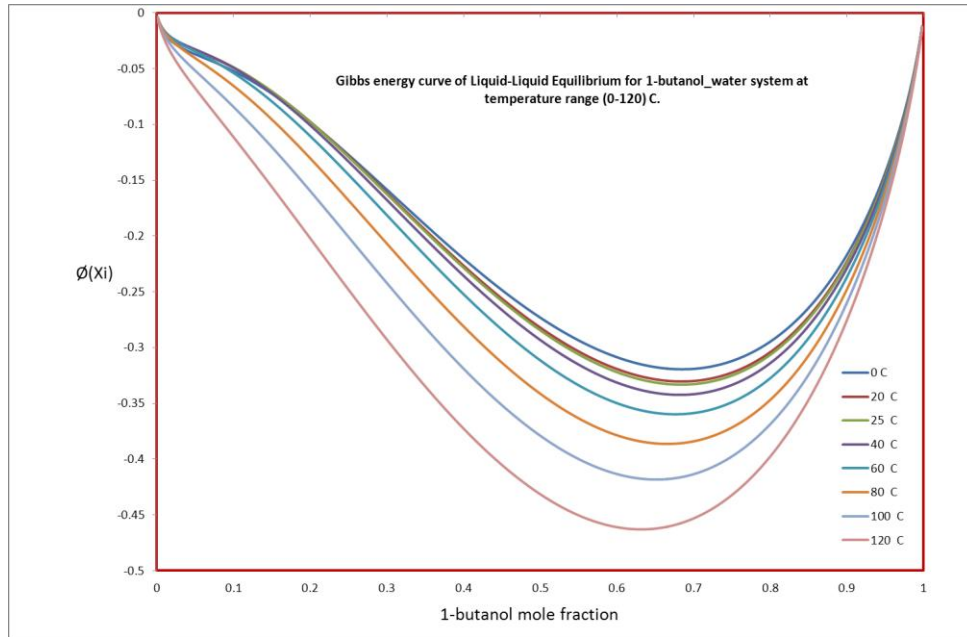


Figure 4.9: Gibbs energy curve of liquid-liquid equilibrium for 1-butanol (1)-water (2) system at temperature range (0-120)⁰C

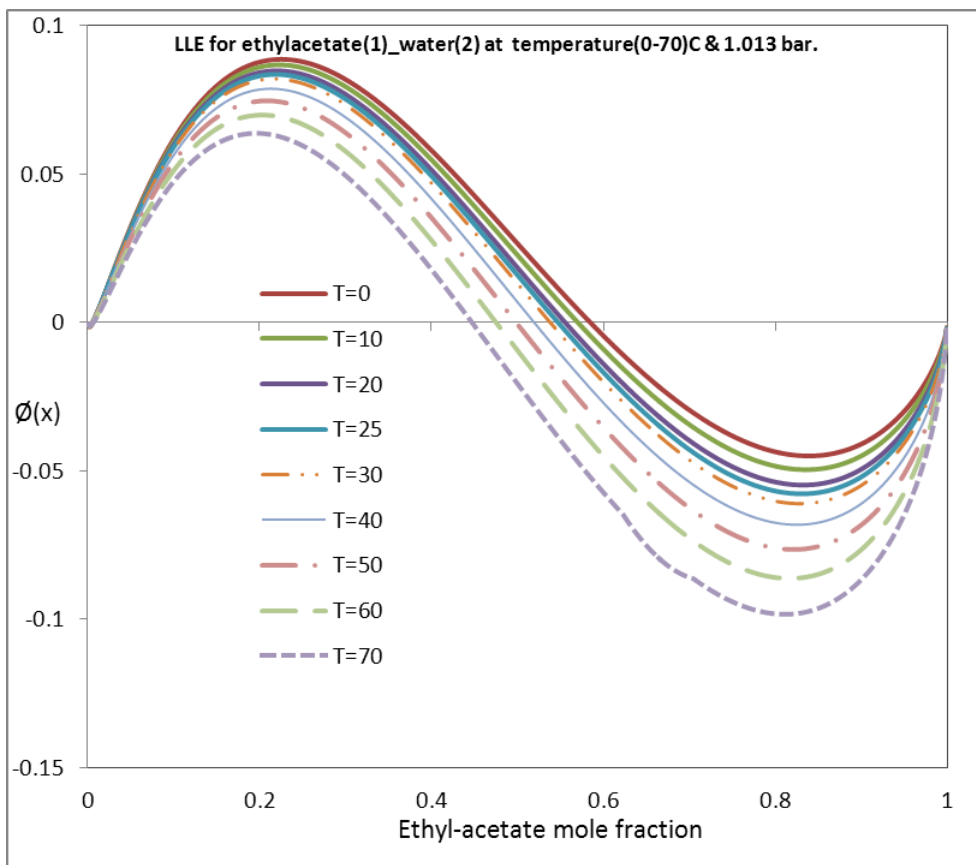


Figure 4.10: Gibbs free energy curve of liquid-liquid equilibrium for ethyl acetate (1)-water (2) system at temperature range (0-70)⁰C

Part of this work is to test the applicability of the TPI method to VLE binary systems. Four binary systems were selected and correlated using PRSV EOS combined with UNIQUAC through WSMR. The VLE binary systems investigated were:

1. Water- n-butyl acetate at 91.85⁰C and 1.013 bar.
2. Ethyl acetate – water at 72.05⁰C and 1.013 bar.
3. n-butanol - water at 36.00⁰C and 0.068 bar.
4. Water-n-butanol at 93.77⁰C and 1.013 bar.

Tables 4.16 (A&B) show the parameters obtained by correlating the experimental data and the predictive values using the TPI method. The TPI search procedure is explained in detail in the theory section (3.10.2). The search is started by defining the grid size (1000), the process then calculates and stores the reduced Gibbs energy of mixing (ϕ) at a fixed pressure and temperature. The cubic root solver function is used to find the compressibility factor (Z) for PRSV EOS, to identify the phase region (liquid or vapour). The initial starting points are selected (2, grid-1) and the following step is the calculation of the tangent slope and $\Delta\tau$ at the corresponding compositions, then (τ) is calculated and stored. The sequential search is conducted for $F(x) = L(x) - \phi(x)$, where $L(x)$ is the value of ϕ on the tangent line at a trial composition x , if $F(x) > 0$ the tangent is above the ϕ curve and τ is updated ($\tau = \tau + \Delta\tau$). The Nelder Mead simplex is used to minimise the τ function by changing α values (α is the length variable which starts from feed composition(z)). The solution for the minimisation procedure is the stationary points, which indicate the compositions of two phases at equilibrium. In the Area method and the TPI applied on LLE binary systems, the search requires the finding of two points; these points are the solution for the global Gibbs free optimisation function. In VLE predictions an extra phase is present and therefore the original 2-Point search technique needs modification. To calculate the equilibrium phase compositions of binary VLE using the TPI method this work has extended the TPI LLE for calculation of VLE (the modified 2-Point search) and developed a direct 3 Point search method. This research has implemented this method for phase equilibrium predictions for the four VLE binary systems indicated previously. The details of these methods are outlined below together with some discussion on the results.

4.3.1 Modified 2 Point and direct 3-point search for TPI binary VLE phase equilibrium calculation

The methods mentioned previously (AM & TPI) have been tested in this research on binary LLE systems exhibiting 2-phase behaviour only. In the LLE binary phase calculation the search is for two stationary points on the tangent line. According to Gibbs criterion in phase equilibrium for a multi-phase binary system at any equilibrium point $(x_\alpha, x_\beta, x_\gamma)$ the tangent plane (as shown in figure (4.11)) equation that passes through these points and uses a reference point in phase α can be written as:

$$(\phi^i - \phi^\alpha) - \sum_{j=1}^{c-1} (x_j^i - x_j^\alpha) \left(\frac{\partial \phi}{\partial x_j} \right)_{\phi, x_{k \neq j}}^\alpha = 0 \quad \text{for } i = \beta, \gamma, \dots, \pi - 1 \quad (4.2)$$

π represents the number of phases and equation (4.1) is valid at any equilibrium point. For 3-phase binary systems the total derivative of the Gibbs energy of mixing with respect to composition at any stationary points must be equal in each phase:

$$\left(\frac{\partial \phi}{\partial x_1} \right)_{TPx_{k \neq 1}}^\alpha = \left(\frac{\partial \phi}{\partial x_1} \right)_{TPx_{k \neq 1}}^\beta = \left(\frac{\partial \phi}{\partial x_1} \right)_{TPx_{k \neq 1}}^\gamma \quad (4.3)$$

The 2-point search approach has been modified in this work to predict three phase equilibrium. The first step in doing this is the division of the composition space into a grid and then the calculation of the Gibbs energy of mixing at each grid point, followed by identification of the composition of the cusps where the phase changes at the phase boundaries (as shown in figure 4.11). The constrained search simplex (Nelder-Mead) is used to minimise a ϕ –tangent plane intersection quantity (τ) in composition range (0, cusp2) by changing a set of independent variables (α_1, α_2). The results obtained from the search are (x_α, x_β) . According to equation (4.3) phase (α or β) can be taken as a reference phase and the partial derivatives with respect to x must be equal at all the equilibrium points. It follows that for VLE in the binary system, the three points representing the equilibrium compositions for each phase lie on a tangent line with the Gibbs free energy at its

minimum value. A Second search is conducted to find the third point(x_γ) by using a constrained simplex between (Cusp2, 1).

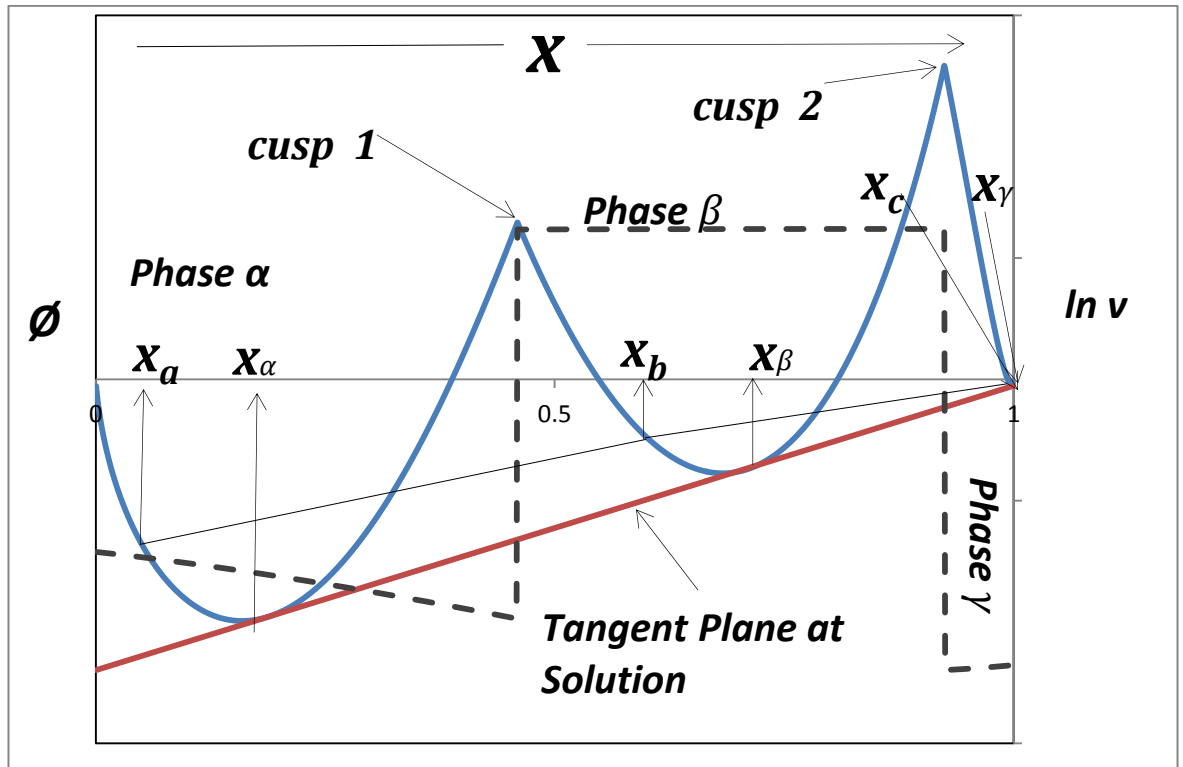


Figure 4.11: Schematic representation of a 3-phase binary at fixed T and P, showing the solution tangent line

The direct 3-point search has been developed in this work from the TPI for 2-phases developed by Hodges et al. (1998). This method mathematically represents the tangent line with three points rather than two. A part of the TPI algorithm is to construct a tangent plane and test for its location with respect to the Gibbs free energy curve (ϕ); if the tangent is above the ϕ curve τ function must be updated with $\Delta\tau$. As mentioned previously in section (3.10.2), for binary systems $\Delta\tau = x_{i\text{grid}}\sqrt{1 + (m_{iTP})^2}$ where m_{iTP} is the slope of the tangent line. In the 2-phase equilibrium prediction using TPI the slope is given by equation (4.4):

$$\frac{\Delta\phi}{\Delta x} = \frac{(\phi(x_b) - \phi(x_a))}{(x_b - x_a)} \quad (4.4)$$

In the presence of an extra phase in VLLE considering equation (4.3), the slope can be given by equation (4.5):

$$\frac{\Delta\phi}{\Delta x} = \frac{(\phi(x_c) - \phi(x_a))}{(x_c - x_a)} = \frac{(\phi(x_b) - \phi(x_a))}{(x_b - x_a)} = \frac{(\phi(x_c) - \phi(x_b))}{(x_c - x_b)} \quad (4.5)$$

In the above equation (4.5), if the terms are theoretically identical, they can be combined by determination of the mean average deviation which produces one slope and replaces m_{iTP} in the $\Delta\tau$ equation with this new value. Any two parts of these terms can be used.

$$\frac{\Delta\phi}{\Delta x} = \left(\frac{(\phi(x_c) - \phi(x_a))}{(x_c - x_a)} + \frac{(\phi(x_b) - \phi(x_a))}{(x_b - x_a)} \right) / 2 \quad (4.6)$$

Or can be written as:

$$\frac{\Delta\phi}{\Delta x} = \left(\frac{(\phi(x_b) - \phi(x_a))}{(x_b - x_a)} + \frac{(\phi(x_c) - \phi(x_b))}{(x_c - x_b)} \right) / 2 \quad (4.7)$$

Now the tangent line equation is expressed mathematically using three points.

The initial values are important for stable solutions for the τ function. This work has established a new method for the initialisation of VLLE binary system calculations. This new method depends on the detection of phase boundaries, as shown in the schematic graph for a VLLE binary system (figure 4.11). Knowing the phase change composition (cusp1, cusp2) between phases in such operational conditions is advantageous compared to searching randomly for (x_a, x_b, x_c) values. This work has found that using a random initial generator increases the risk of the TPI method finding trivial solution sensitivity and produces slightly different results compared to the fixed initial point. The AAD results for testing the TPI method with the random initial generator can be seen in table 4.17 and it is obvious from the figure 4.12 that this method produces inconsistent and fluctuating results. For this reason a more reliable and stable initial continuous generator has been suggested. The three initial values are estimated as follows: $x_a = (1/Grid\ No.) * \sqrt{2}$, $x_b = cusp1 + 0.0001$ and $x_c = cusp2 + 0.0001$. From these values the arm's length (α) of the search is calculated; $\alpha_1 = z - x_a$, $\alpha_2 = x_b - z$ and $\alpha_3 = x_c - z$.

Table 4.17: The AAD values using the TPI method with initial random generator, the test was carried out 10 times on four VLLE systems, at a fixed feed composition 0.5 and grid number 1000

Test No.	System			
	1	2	3	4
1	0.0609	0.0020	0.0166	0.0065
2	0.0005	0.0023	0.0219	0.0059
3	0.0053	0.0017	0.0356	0.0087
4	0.0031	0.0017	0.0231	0.0066
5	0.0044	0.0013	0.0279	0.0597
6	0.0006	0.0013	0.0194	0.0116
7	0.0083	0.0020	0.0154	0.0028
8	0.0006	0.0017	0.0103	0.0062
9	0.0006	0.0027	0.0196	0.0083
10	0.0024	0.0017	0.0128	0.0196

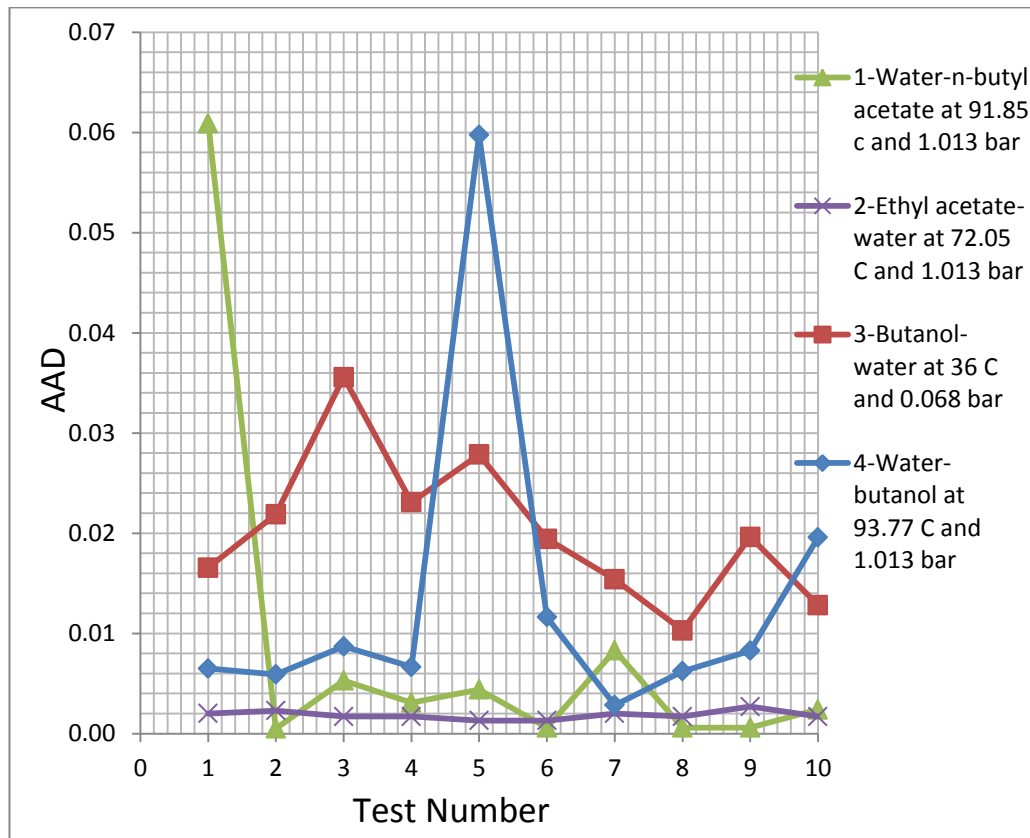


Figure 4.12: The fluctuations in the results for the TPI method using random initial generator in prediction of VLLE for four binary systems

This work has applied the modified 2-point search method and direct 3-point search on the four VLLE systems mentioned previously. The prediction results and AAD for each system are shown in table (4.16B).

The TPI method mentioned was used for modelling binary VLLE systems. As shown in figure (4.14 A) the water-n-butyl acetate system exhibits three phases at temperature 364 K and atmospheric pressure. The tangent line should intersect the ϕ curve at three stationary points; at these points the Gibbs free energy is at a global minimum and τ values theoretically should be zero. It was found that the tangent line touches the Gibbs energy curve at only two points, the position of the line in respect of the third point can be below or above the curve. The inconsistency of the TPI method is apparent in systems with three phases. In the water (1)-n-butyl acetate (2) system, the tangent drawn between organic and aqueous phases will be above the Gibbs energy curve with respect to the third phase. Alternatively if a tangent is drawn between organic and vapour phase, it will be under the curve and will not touch the curve at the third point in the aqueous region. This problem can be demonstrated graphically for four VLLE binary systems that were investigated, for instance in the water (1)-n butyl acetate (2) system if a tangent is drawn from the first equilibrium point in the aqueous phase to the second equilibrium point in the vapour phase it will not intersect in the organic phase, as shown in figure (4.13). When plotting the Gibbs energy curve and the tangent line versus composition the circle outlining the area shows that the tangent line does not intersect with the (ϕ) curve in the organic phase region.

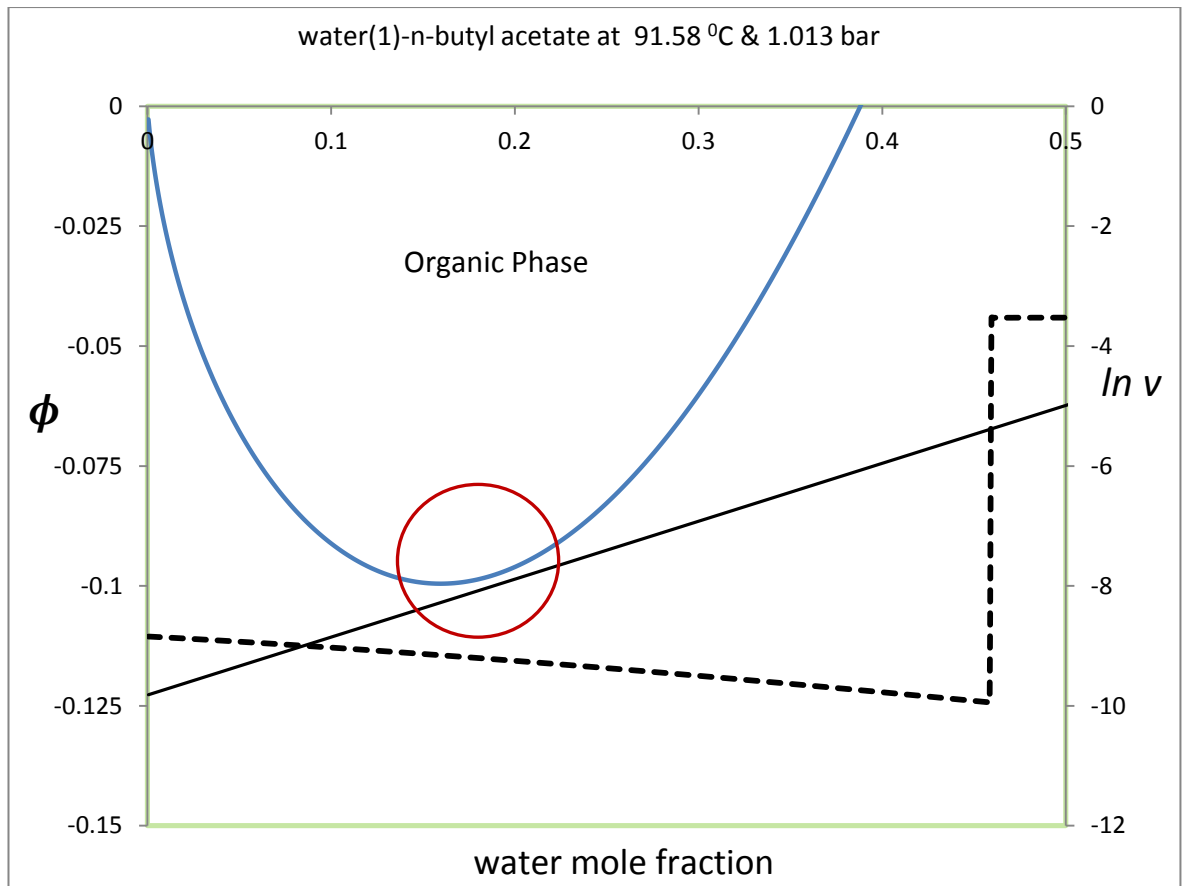


Figure 4.13: Organic part of Gibbs energy curve (ϕ) for VLLE water(1)-n-butyl acetate(2) system at 91.85 °C & 1.013 bar, the circled area is expected for the tangent line to intersect with the energy curve (ϕ)

The theory assumes that three stationary points should touch the energy curve which matches the minimum Gibbs free energy and equality of the first derivative at these points. The representation of Gibbs free energy using the PRSV EOS and WSMR shows that at each equilibrium point there is a possibility for the tangent line to touch the curve at more than one point, this is due to the shape of the curve. However in global optimisation methods such as TPI, the points calculated will be the solutions to the minimisation of the τ function.

This work has found that the TPI search methods for three phase binary systems are efficient for predictions for the compositions of stationary points. The reliability remains a critical issue as it depends on the shape of the Gibbs energy curve. This work also found the slope of the tangent line between phases of organic-vapour; organic-aqueous and aqueous-vapour are not equal. In practice, for the systems

considered, it appears mathematically impossible to draw a line that touches the ϕ curve at the three points, whereas this appears not to be a problem in 2 Phase binary systems. This could be affected by the correlating equations used for representing data and experimental error which occurred whilst measuring these data.

The results for the four VLLE binary systems using the TPI 2-point search and 3-point direct search methods are listed in table (4.16B) with their AAD and computational duration in seconds. The overall AAD of the results for four systems, in the direct 3-point method is 0.0018 and 0.004 for the 2-point search method, this indicates that the direct 3-point performs better than the other method. This can be related to the search pattern considered in the 2-point method by finding the equilibrium compositions of first and second phase in ascending order in the first construction of the tangent line and fixing the second phase composition whilst searching for the third point. The figures (4.14, 4.15, 4.16 & 4.17) show graphical representations of four VLLE binary systems. It can be seen that with water-butanol system shown in figure (4.17), a section of the ϕ curve flattens to almost a straight line above a composition of 0.5 in the organic phase, and such graphical behaviour increases the difficulty of heterogeneous modelling.

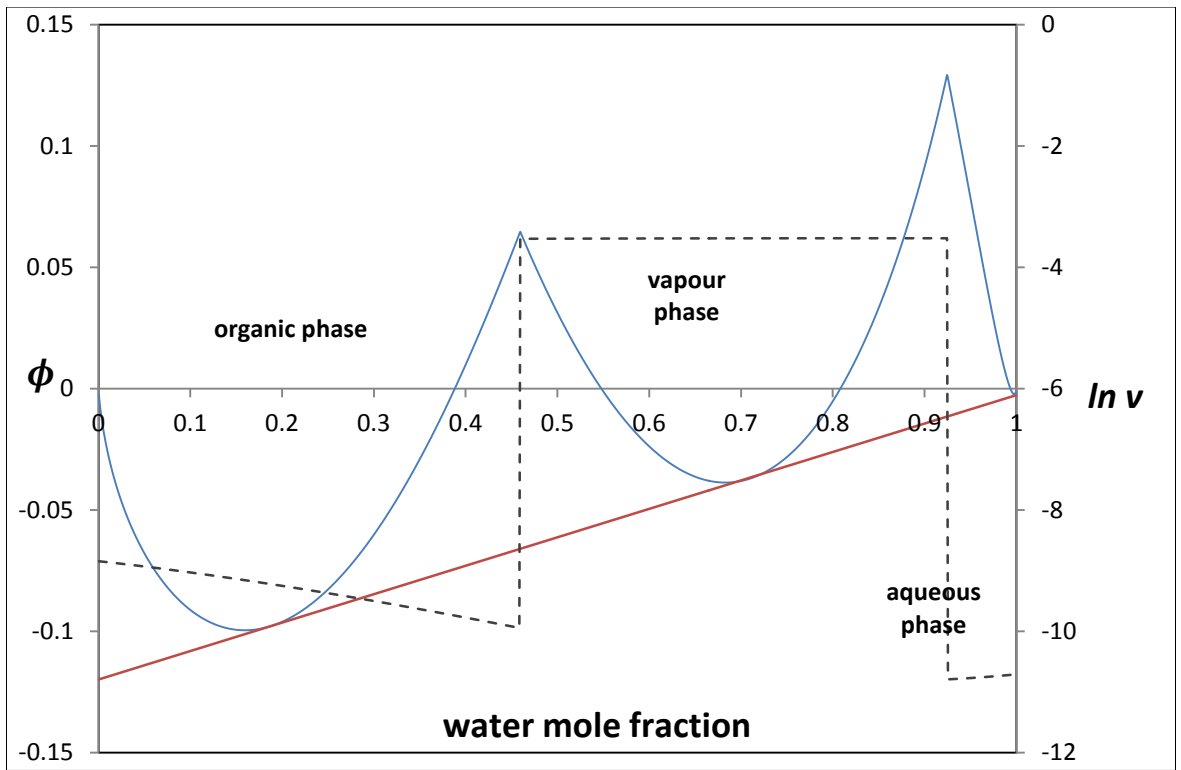


Figure 4.14: VLLE water (1)-n butyl acetate (2) system at 91.85°C and 1.013 bar, showing the tangent line and Gibbs free energy curve

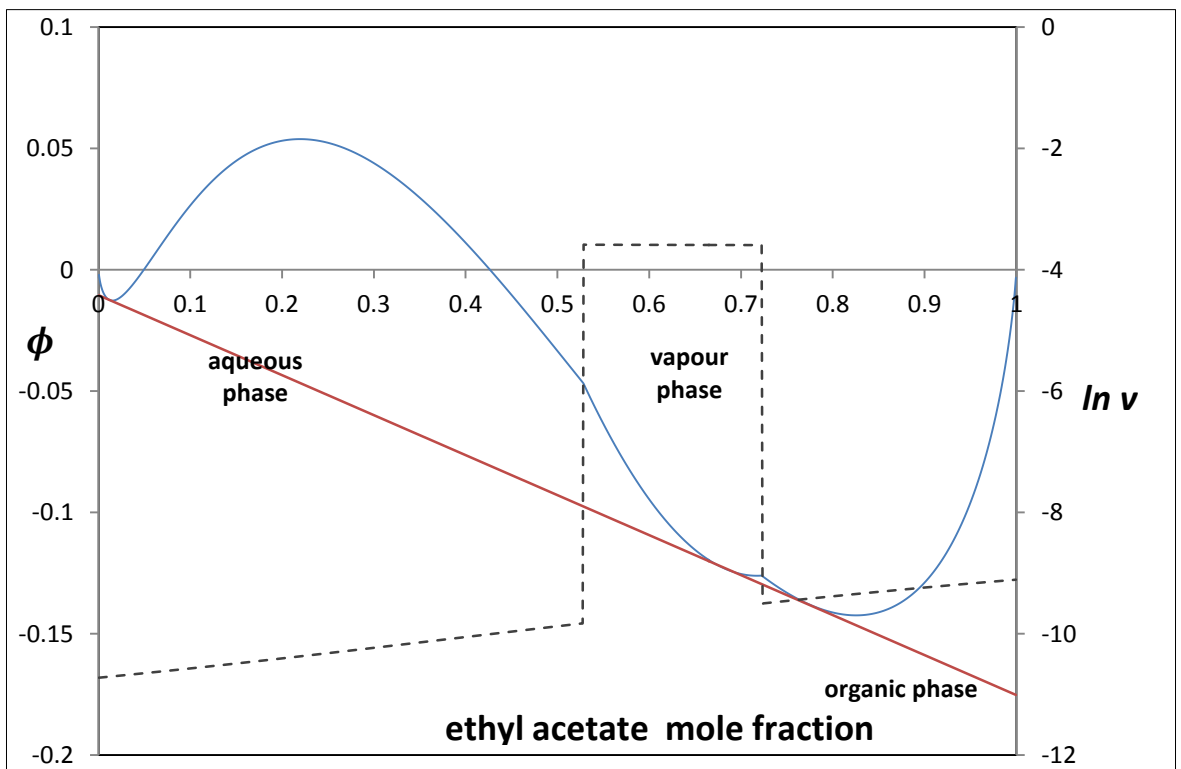


Figure 4.15: VLLE ethyl acetate (1)-water (2) system at 72.05°C and 1.013 bar, showing the tangent line and Gibbs free energy curve

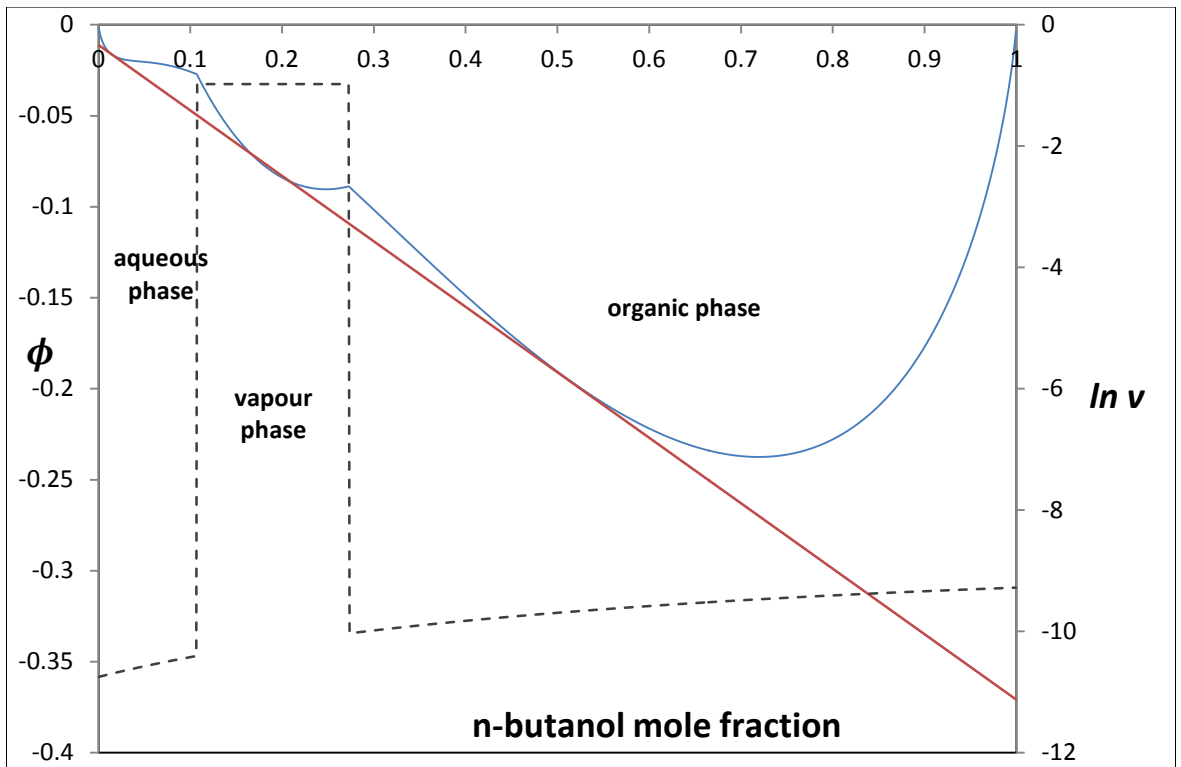


Figure 4.16: VLE n-butanol (1)-water (2) system at 36°C and 0.068 bar, showing the tangent line and Gibbs free energy curve

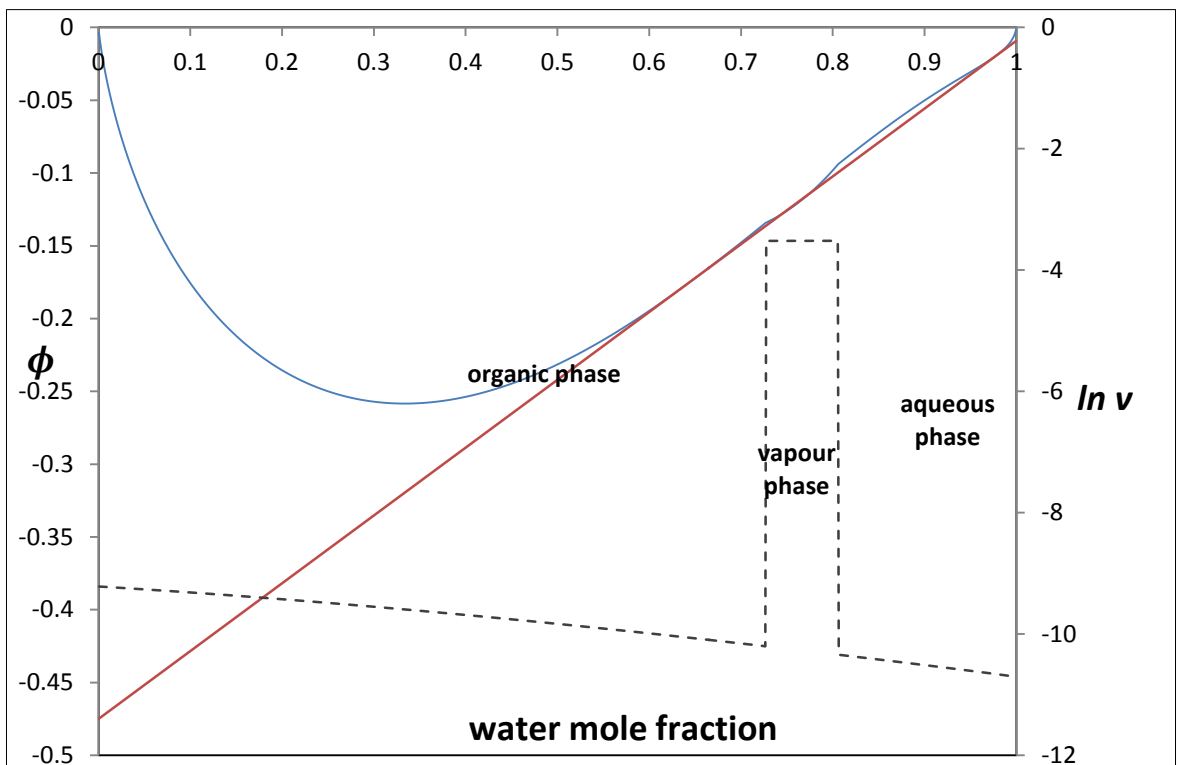


Figure 4.17: VLE Water (1)-n-butanol (2) system at 93.77°C and 1.013 bar, showing the tangent line and Gibbs free energy curve

4.3.2 Conclusions on prediction models for LLE and VLLE binary systems

Initially this work modelled non-ideal binary systems, with and without heterogeneous behaviour, using PRSV+WSMR; it has also demonstrated the applicability of the Area Method and the TPI prediction method for LLE heterogeneous systems. The two methods were tested for two binary LLE systems in various temperatures and the results indicate that these methods are effective for modelling such binary systems.

This work extended the TPI method to binary VLLE prediction and successfully applied this method to four VLLE binary systems. This work has also demonstrated the sensitivity of the TPI method to random initial values. At each run the program produces results with slightly different solutions when compared to the results for fixed initial values. The new method recommended for fixed initial value depends on phase change (Cusps) compositions. The new initial scheme was tested using the extended 2-point and 3-point direct search methods on VLLE binary systems. The Nelder-Mead optimisation simplex was utilised in all the minimisation processes. Due to the computational time consumption, the Area method was only applied on the LLE systems.

This work will now investigate the applicability of the TPI method in phase equilibrium prediction for VLLE ternary systems.

4.4 VLLLE Ternary System Results

The correlation and predictions for four ternary VLLLE systems were carried out using data published by Younis et al. (2007). The methods used were:

1. Flash calculation
2. Tangent Plane Intersection(TPI)
3. Tangent Plane Distance Function(TPDF)
4. Systematic Initial Generator(SIG)

In the flash calculation, a feed composition (z_1) is calculated from the arithmetic mean of each experimental data point using the following equation:

$$z_i = (x_{i\ aq}^{exp} + x_{i\ org}^{exp} + y_i^{exp})/nc \quad (4.8. a)$$

where nc is the number of the components and $i = 1$

At equilibrium the two liquid phases are connected by a tie line and the relative change between the two components at the overall feed compositions along a tie line is constant:

$$D_{ij} = \frac{dx_j}{dx_i} = \frac{(x_j - z_j)}{(x_i - z_i)} \quad (4.8. b)$$

where $i \neq j$

The second component feed composition (z_2) is calculated from the equation of the tie line (4.8.b).

The VLLLE flash calculation using PRSV+WSMR is explained in the theory chapter section (3.9). The Nelder-Mead simplex was used for optimisation in the data correlation and the estimated parameters from this correlation procedure are shown in table (4.21) and were used in the prediction methods.

Initially the TPI method was tested on two artificial 3 phase systems of Shyu et al. (1995), the test included various values of feed compositions inside 2 phase and 3 phase region. The results are shown in table (4.18) and (4.19) for system 1 & 2 respectively.

The tables below (4.22 - 4.49) show the summary of results for the flash calculation, TPI and TPDF prediction methods for the following VLLE ternary systems:

1. VLLE water-acetone-MEK at pressure 760 mmHg
2. VLLE water-ethanol-MEK at pressure 760 mmHg
3. VLLE water-acetone-n-butyl acetate at pressure:
 - 3.1 360 mmHg
 - 3.2 600 mmHg
 - 3.3 760 mmHg
4. VLLE water- ethanol-n-butyl acetate at pressure:
 - 4.1 360 mmHg
 - 4.2 600 mmHg
 - 4.3 760 mmHg

Table (4.20) shows the AAD for the flash calculations, TPDF and TPI predictions for four systems using the PRSV+WSMR model. The simplex algorithm used for three phase flash calculations can be found in appendix A.

Table 4.18: Results for the TPI method for system 1 of Shyu et al. at various feed composition (inside and outside heterogeneous regions), a set of initial values and fixed grid number

Grid = 100x 100		Phase I		Phase II		Phase III	
Z_1	Z_2	X_1	X_2	X_1	X_2	X_1	X_2
Solution by Shyu et al							
		0.0739	0.1731	0.1491	0.6290	0.8416	0.1002
Inside heterogeneous region							
Initial values							
		0.0100	0.1000	0.0100	0.9700	0.9800	0.0050
This work							
0.20	0.30	0.0734	0.1711	0.1489	0.6324	0.8428	0.1008
0.20	0.40	0.0740	0.1738	0.1217	0.6934	0.8410	0.1009
0.20	0.50	0.0730	0.1714	0.1457	0.6308	0.8443	0.0988
0.30	0.30	0.0736	0.1736	0.1463	0.6370	0.8417	0.1014
0.30	0.40	0.9790	0.0169	0.0195	0.9795	0.9834	0.0144
0.30	0.50	0.0740	0.1734	0.1352	0.6502	0.8417	0.1002
0.35	0.35	0.0749	0.1731	0.1471	0.6348	0.8449	0.0970
0.45	0.40	0.0690	0.1664	0.1435	0.6347	0.8528	0.0960
0.50	0.30	0.0727	0.1718	0.1479	0.6362	0.8409	0.1003
0.50	0.35	0.0729	0.1724	0.1502	0.6259	0.8417	0.1013
Outside heterogeneous region							
This work							
0.01	0.90	0.7594	0.2378	0.0225	0.9702	0.7583	0.2391
0.01	0.95	0.1697	0.6047	0.1691	0.5969	0.6852	0.2115
0.05	0.85	0.8014	0.1968	0.0236	0.9730	0.7980	0.2010
0.05	0.90	0.7514	0.1943	0.1246	0.7870	0.7500	0.1930
0.10	0.85	0.7984	0.1351	0.1416	0.6868	0.7992	0.1358

Table 4.19: Results for the TPI method for system 1 of Shyu et al. at various feed composition (inside and outside heterogeneous regions), a set of initial values and fixed grid number

Grid = 100x 100		Phase I		Phase II		Phase III	
Z_1	Z_2	X_1	X_2	X_1	X_2	X_1	X_2
Solution by Shyu et al							
		0.2077	0.2582	0.0652	0.7380	0.7861	0.0568
Inside heterogeneous region							
Initial values							
		0.0100	0.1000	0.0100	0.9700	0.9800	0.0050
This work							
0.20	0.40	0.2083	0.2563	0.0649	0.7420	0.7901	0.0547
0.20	0.50	0.1981	0.2656	0.0653	0.7393	0.7841	0.0573
0.30	0.35	0.2088	0.2558	0.0646	0.7387	0.7879	0.0565
0.30	0.40	0.2083	0.2563	0.0649	0.7420	0.7901	0.0547
0.30	0.45	0.2054	0.2606	0.0653	0.7414	0.7902	0.0563
0.30	0.50	0.2085	0.2555	0.0650	0.7408	0.7879	0.0550
0.30	0.55	0.2089	0.2595	0.0653	0.7406	0.7887	0.0555
0.35	0.45	0.2091	0.2568	0.0660	0.7389	0.7893	0.0550
0.35	0.50	0.2078	0.2582	0.0657	0.7400	0.7890	0.0565
0.40	0.45	0.2047	0.2592	0.0654	0.7388	0.7813	0.0575
Outside heterogeneous region							
This work							
0.65	0.05	0.0631	0.7314	0.0609	0.7573	0.8006	0.0500
0.70	0.05	0.0622	0.7497	0.0622	0.7544	0.8025	0.0500
0.80	0.15	0.0672	0.7371	0.0624	0.7479	0.7906	0.0567
0.85	0.05	0.0839	0.6879	0.0879	0.6964	0.8707	0.0313
0.90	0.05	0.1121	0.6238	0.1149	0.6339	0.9037	0.0218

Table 4.20: The summary table for the VLE ternary systems: Absolute Average Deviation (AAD) for the Flash calculations, the TPDF and TPI predictions

System	System NO.	Temperature range In °C	Pressure mmHg	Method	AAD		
					organic	aqueous	vapour
water-acetone-MEK	1	70.10-73.10	760	Flash	0.0016	0.0017	0.0026
				TPDF	0.0041	0.0024	0.0058
				TPI	0.0655	0.0088	0.0573
water-ethanol-MEK	2	71.20-73.20	760	Flash	0.0052	0.0046	0.0074
				TPDF	0.0336	0.0203	0.0161
				TPI	0.0806	0.0211	0.0258
water-acetone-n butyl acetate	3	45.10-59.00	360	Flash	0.0072	0.007	0.0081
				TPDF	0.0159	0.0111	0.0178
				TPI	0.0335	0.0204	0.0289
	4	56.20-69.20	600	Flash	0.0079	0.0077	0.0151
				TPDF	0.0064	0.0117	0.0258
				TPI	0.0658	0.0265	0.0252
	5	66.10-86.10	760	Flash	0.0046	0.0031	0.0041
				TPDF	0.0055	0.0026	0.0037
				TPI	0.0222	0.0205	0.0458
water-ethanol-n butyl acetate	6	62.20-71.10	360	Flash	0.0091	0.0052	0.0118
				TPDF	0.0118	0.0080	0.0146
				TPI	0.0502	0.0106	0.0267
	7	74.20-81.00	600	Flash	0.0047	0.0047	0.0031
				TPDF	0.0212	0.0152	0.0216
				TPI	0.0304	0.0173	0.038
	8	82.80-88.20	760	Flash	0.0045	0.0052	0.0070
				TPDF	0.0179	0.0092	0.0069
				TPI	0.0558	0.0152	0.0608

Table 4.21: UNIQUAC parameters and PRSV EOS interaction parameters for four VLLE ternary systems using flash calculations

System	Pressure mmHg	UNIQUAC Parameters						EOS interaction Parameters		
		A_{12}	A_{21}	A_{23}	A_{32}	A_{31}	A_{13}	K_{12}	K_{23}	K_{13}
water-acetone-MEK	760	101.48	-67.77	292.61	-364.94	525.73	273.54	0.5587	0.9150	1.74E-05
water-ethanol-MEK	760	-481.95	1484.17	63.99	2420.92	599.20	257.12	0.7767	0.0033	0.0001
water-acetone-n butyl acetate	360	-70.75	616.16	-269.95	663.49	2124.50	-120.44	0.1114	1.00E-05	0.9305
	600	61.57	618.57	-355.96	1161.59	2588.11	800.82	1.00E-05	0.3883	0.2317
	760	180.44	294.50	1871.19	-419.96	799.09	404.92	1.00E-05	0.4085	0.2831
water-ethanol-n butyl acetate	360	-87.01	3443.77	-178.49	377.69	794.66	856.13	1.00E-05	0.0799	0.0019
	600	-86.30	802.03	-102.64	468.79	895.85	696.22	0.1310	1.00E-05	0.0243
	760	179.96	-263.45	-300.59	728.63	756.49	469.5948	0.6342	0.6667	0.3781

4.4.1 VLE system: water (1)-acetone (2)-MEK (3) at pressure 760 mmHg

Table 4.22: VLE ternary system water (1)-acetone (2)-methyl ethyl ketone (3) at 760 mmHg, flash calculation, TPDF & TPI predictions

Temperature in C	Experimental			Flash calculation			TPDF Prediction			TPI Prediction		
	water	acetone	MEK	water	acetone	MEK	water	acetone	MEK	water	acetone	MEK
Organic Phase												
73.10	0.450	0.016	0.534	0.445	0.017	0.539	0.444	0.015	0.542	0.432	0.005	0.563
72.60	0.451	0.032	0.518	0.451	0.030	0.519	0.452	0.028	0.520	0.440	0.011	0.549
72.20	0.465	0.044	0.490	0.466	0.043	0.491	0.473	0.042	0.485	0.470	0.025	0.505
71.80	0.502	0.066	0.432	0.506	0.063	0.431	0.510	0.065	0.425	0.504	0.046	0.450
71.30	0.549	0.085	0.366	0.550	0.083	0.367	0.559	0.085	0.356	0.517	0.055	0.429
70.90	0.578	0.093	0.330	0.578	0.091	0.331	0.573	0.094	0.333	0.618	0.059	0.323
70.30	0.613	0.096	0.291	0.611	0.097	0.292	0.609	0.095	0.296	0.620	0.070	0.310
70.10	0.684	0.089	0.227	0.683	0.092	0.225	0.682	0.090	0.229	0.721	0.083	0.197
Aqueous Phase												
73.10	0.947	0.003	0.049	0.954	0.002	0.044	0.950	0.003	0.047	0.967	0.009	0.024
72.60	0.948	0.006	0.046	0.950	0.005	0.045	0.951	0.006	0.043	0.961	0.014	0.025
72.20	0.939	0.010	0.051	0.942	0.008	0.050	0.943	0.009	0.048	0.948	0.020	0.033
71.80	0.926	0.017	0.056	0.928	0.015	0.057	0.929	0.016	0.054	0.935	0.022	0.043
71.30	0.907	0.027	0.066	0.908	0.025	0.066	0.908	0.027	0.065	0.908	0.027	0.065
70.90	0.896	0.033	0.071	0.897	0.031	0.072	0.892	0.034	0.074	0.896	0.037	0.067
70.30	0.876	0.041	0.083	0.877	0.040	0.083	0.881	0.039	0.080	0.875	0.041	0.083
70.10	0.823	0.059	0.118	0.825	0.059	0.117	0.817	0.061	0.122	0.824	0.059	0.117
Vapour Phase												
73.10	0.352	0.031	0.617	0.351	0.032	0.618	0.346	0.034	0.620	0.272	0.026	0.702
72.60	0.351	0.060	0.590	0.344	0.060	0.596	0.341	0.060	0.598	0.263	0.047	0.689
72.20	0.343	0.087	0.569	0.337	0.087	0.576	0.331	0.095	0.573	0.287	0.094	0.619
71.80	0.338	0.135	0.527	0.328	0.135	0.537	0.323	0.133	0.544	0.278	0.131	0.591
71.30	0.314	0.186	0.500	0.315	0.187	0.499	0.312	0.190	0.499	0.279	0.161	0.560
70.90	0.311	0.209	0.480	0.311	0.209	0.480	0.306	0.214	0.480	0.294	0.181	0.525
70.30	0.305	0.231	0.464	0.307	0.231	0.462	0.300	0.229	0.471	0.299	0.234	0.468
70.10	0.304	0.250	0.446	0.307	0.246	0.447	0.294	0.251	0.455	0.295	0.250	0.455

Table 4.23: VLLE water (1)-acetone (2)-MEK (3) sensitivity of TPI and TPDF methods to different initial values at various temperatures and 760 mmHg

Temp	Initial values						TPI predictions						TPDF predictions					
	organic		aqueous		vapour		organic		aqueous		vapour		organic		aqueous		vapour	
	x_1	x_2	x_1	x_2	y_1	y_2	Δx_1	Δx_2	Δx_1	Δx_2	Δy_1	Δy_2	Δx_1	Δx_2	Δx_1	Δx_2	Δy_1	Δy_2
73.10 °C	0.120	0.010	0.810	0.010	0.120	0.010	0.330	0.006	0.004	0.021	0.233	0.021	0.006	0.002	0.002	0.000	0.006	0.003
	0.140	0.010	0.820	0.010	0.140	0.010	0.327	0.007	0.039	0.018	0.247	0.021	0.006	0.002	0.002	0.000	0.006	0.003
	0.160	0.010	0.840	0.010	0.160	0.010	0.394	0.006	0.103	0.013	0.200	0.022	0.006	0.002	0.002	0.000	0.006	0.003
	0.180	0.010	0.860	0.010	0.180	0.010	0.302	0.009	0.057	0.037	0.238	0.021	0.006	0.002	0.002	0.000	0.006	0.003
	0.200	0.010	0.880	0.010	0.200	0.010	0.281	0.011	0.037	0.027	0.215	0.021	0.006	0.002	0.002	0.000	0.006	0.003
	0.220	0.010	0.900	0.010	0.220	0.010	0.287	0.002	0.040	0.027	0.157	0.023	0.006	0.002	0.002	0.000	0.006	0.003
	0.240	0.010	0.920	0.010	0.240	0.010	0.327	0.011	0.029	0.001	0.114	0.028	0.006	0.002	0.002	0.000	0.006	0.003
	0.260	0.010	0.940	0.010	0.260	0.010	0.300	0.002	0.007	0.022	0.147	0.031	0.006	0.002	0.002	0.000	0.006	0.003
	0.280	0.010	0.950	0.010	0.280	0.010	0.277	0.005	0.027	0.005	0.100	0.027	0.006	0.002	0.002	0.000	0.006	0.003
	0.300	0.010	0.960	0.010	0.300	0.010	0.150	0.007	0.015	0.013	0.053	0.022	0.006	0.002	0.002	0.000	0.006	0.003
72.60 °C	0.100	0.010	0.800	0.010	0.100	0.010	0.154	0.289	0.006	0.020	0.350	0.040	0.001	0.004	0.003	0.001	0.009	0.001
	0.110	0.010	0.810	0.010	0.110	0.010	0.190	0.320	0.120	0.040	0.276	0.040	0.002	0.004	0.003	0.001	0.009	0.001
	0.120	0.010	0.820	0.010	0.120	0.010	0.122	0.264	0.007	0.016	0.299	0.060	0.001	0.004	0.003	0.001	0.010	0.001
	0.130	0.010	0.830	0.010	0.130	0.010	0.130	0.266	0.017	0.011	0.239	0.055	0.001	0.004	0.003	0.001	0.010	0.001
	0.140	0.010	0.840	0.010	0.140	0.010	0.205	0.319	0.070	0.055	0.237	0.058	0.001	0.004	0.003	0.001	0.010	0.001
	0.150	0.010	0.850	0.010	0.150	0.010	0.302	0.023	0.021	0.004	0.198	0.051	0.001	0.004	0.003	0.001	0.009	0.001
	0.160	0.010	0.860	0.010	0.160	0.010	0.119	0.255	0.014	0.021	0.241	0.049	0.001	0.004	0.003	0.001	0.009	0.001
	0.170	0.010	0.870	0.010	0.170	0.010	0.312	0.031	0.042	0.028	0.247	0.045	0.001	0.004	0.003	0.001	0.009	0.001
	0.180	0.010	0.880	0.010	0.180	0.010	0.117	0.253	0.004	0.020	0.229	0.045	0.001	0.004	0.003	0.001	0.009	0.001
	0.190	0.010	0.890	0.010	0.190	0.010	0.115	0.245	0.013	0.025	0.148	0.055	0.002	0.004	0.003	0.001	0.009	0.001
72.20 °C	0.100	0.010	0.800	0.010	0.100	0.010	0.407	0.153	0.011	0.019	0.016	0.168	0.008	0.002	0.002	0.001	0.012	0.008
	0.110	0.010	0.810	0.010	0.110	0.010	0.253	0.012	0.028	0.027	0.017	0.202	0.007	0.002	0.003	0.001	0.012	0.008
	0.120	0.010	0.820	0.010	0.120	0.010	0.193	0.291	0.031	0.004	0.214	0.087	0.007	0.002	0.003	0.001	0.012	0.008
	0.130	0.010	0.830	0.010	0.130	0.010	0.136	0.254	0.009	0.023	0.337	0.086	0.007	0.002	0.003	0.001	0.012	0.008
	0.140	0.010	0.840	0.010	0.140	0.010	0.152	0.254	0.027	0.004	0.208	0.064	0.007	0.002	0.003	0.001	0.012	0.008
	0.150	0.010	0.850	0.010	0.150	0.010	0.149	0.256	0.017	0.010	0.188	0.087	0.007	0.002	0.003	0.001	0.012	0.008
	0.160	0.010	0.860	0.010	0.160	0.010	0.136	0.245	0.041	0.036	0.215	0.087	0.007	0.002	0.003	0.001	0.012	0.008
	0.170	0.010	0.870	0.010	0.170	0.010	0.143	0.251	0.003	0.017	0.220	0.083	0.007	0.002	0.003	0.001	0.012	0.008
	0.180	0.010	0.880	0.010	0.180	0.010	0.136	0.249	0.015	0.024	0.287	0.087	0.007	0.002	0.003	0.001	0.012	0.008
	0.190	0.010	0.890	0.010	0.190	0.010	0.135	0.242	0.027	0.029	0.171	0.087	0.007	0.002	0.003	0.001	0.012	0.008

Temp	Initial values						TPI predictions						TPDF predictions					
	organic		aqueous		Vapour		organic		aqueous		vapour		organic		aqueous		vapour	
	x_1	x_2	x_1	x_2	y_1	y_2	Δx_1	Δx_2	Δx_1	Δx_2	Δy_1	Δy_2	Δx_1	Δx_2	Δx_1	Δx_2	Δy_1	Δy_2
71.80 °C	0.100	0.010	0.820	0.010	0.100	0.010	0.286	0.343	0.027	0.035	0.251	0.089	0.009	0.001	0.003	0.001	0.015	0.002
	0.110	0.010	0.830	0.010	0.110	0.010	0.184	0.230	0.020	0.028	0.225	0.096	0.009	0.001	0.003	0.001	0.015	0.002
	0.120	0.010	0.840	0.010	0.120	0.010	0.184	0.235	0.014	0.026	0.285	0.117	0.009	0.001	0.003	0.001	0.015	0.002
	0.130	0.010	0.850	0.010	0.130	0.010	0.183	0.226	0.015	0.025	0.190	0.094	0.009	0.001	0.003	0.001	0.016	0.002
	0.140	0.010	0.860	0.010	0.140	0.010	0.261	0.306	0.017	0.028	0.197	0.088	0.009	0.001	0.003	0.001	0.015	0.002
	0.150	0.010	0.870	0.010	0.150	0.010	0.179	0.230	0.001	0.017	0.255	0.095	0.008	0.001	0.003	0.001	0.016	0.002
	0.160	0.010	0.880	0.010	0.160	0.010	0.182	0.237	0.004	0.016	0.263	0.135	0.009	0.001	0.003	0.001	0.015	0.002
	0.170	0.010	0.890	0.010	0.170	0.010	0.184	0.238	0.015	0.026	0.319	0.097	0.009	0.001	0.002	0.001	0.015	0.002
	0.180	0.010	0.900	0.010	0.180	0.010	0.182	0.231	0.008	0.021	0.196	0.133	0.009	0.001	0.003	0.001	0.015	0.002
0.190	0.010	0.910	0.010	0.190	0.010	0.179	0.231	0.014	0.026	0.222	0.135	0.009	0.001	0.003	0.001	0.015	0.002	
71.30 °C	0.100	0.010	0.890	0.010	0.100	0.010	0.239	0.217	0.001	0.016	0.130	0.185	0.010	0.000	0.001	0.000	0.002	0.003
	0.110	0.010	0.900	0.010	0.110	0.010	0.256	0.245	0.011	0.012	0.313	0.166	0.010	0.000	0.000	0.000	0.002	0.003
	0.120	0.010	0.910	0.010	0.120	0.010	0.243	0.226	0.038	0.003	0.275	0.186	0.010	0.000	0.001	0.000	0.002	0.003
	0.130	0.010	0.920	0.010	0.130	0.010	0.243	0.226	0.004	0.016	0.312	0.141	0.010	0.000	0.001	0.000	0.002	0.003
	0.140	0.010	0.930	0.010	0.140	0.010	0.243	0.226	0.040	0.002	0.313	0.153	0.010	0.000	0.000	0.000	0.002	0.003
	0.150	0.010	0.940	0.010	0.150	0.010	0.233	0.225	0.023	0.006	0.285	0.185	0.010	0.000	0.001	0.000	0.002	0.003
	0.160	0.010	0.950	0.010	0.160	0.010	0.237	0.219	0.063	0.041	0.281	0.184	0.010	0.000	0.001	0.000	0.002	0.003
	0.170	0.010	0.960	0.010	0.170	0.010	0.227	0.212	0.213	0.093	0.313	0.134	0.010	0.000	0.001	0.000	0.002	0.003
	0.180	0.010	0.970	0.010	0.180	0.010	0.209	0.188	0.312	0.112	0.180	0.138	0.010	0.000	0.001	0.000	0.002	0.003
0.190	0.010	0.980	0.010	0.190	0.010	0.331	0.303	0.201	0.085	0.150	0.130	0.009	0.000	0.001	0.000	0.002	0.003	
70.90 °C	0.110	0.010	0.900	0.010	0.110	0.010	0.548	0.093	0.027	0.000	0.000	0.000	0.004	0.002	0.004	0.002	0.005	0.006
	0.120	0.010	0.910	0.010	0.120	0.010	0.502	0.092	0.022	0.000	0.000	0.000	0.005	0.002	0.004	0.002	0.005	0.006
	0.130	0.010	0.920	0.010	0.130	0.010	0.466	0.154	0.189	0.000	0.000	0.000	0.004	0.002	0.004	0.002	0.005	0.006
	0.140	0.010	0.930	0.010	0.140	0.010	0.552	0.070	0.008	0.000	0.000	0.000	0.004	0.002	0.004	0.002	0.005	0.006
	0.150	0.010	0.940	0.010	0.150	0.010	0.429	0.081	0.274	0.000	0.000	0.000	0.004	0.002	0.004	0.002	0.005	0.006
	0.160	0.010	0.950	0.010	0.160	0.010	0.433	0.088	0.277	0.000	0.000	0.000	0.004	0.002	0.004	0.002	0.005	0.006
	0.170	0.010	0.960	0.010	0.170	0.010	0.425	0.081	0.299	0.000	0.000	0.000	0.004	0.002	0.004	0.002	0.005	0.006
	0.180	0.010	0.970	0.010	0.180	0.010	0.396	0.062	0.313	0.000	0.000	0.000	0.004	0.002	0.004	0.002	0.005	0.006
	0.190	0.010	0.980	0.010	0.190	0.010	0.377	0.052	0.073	0.000	0.000	0.000	0.004	0.002	0.004	0.002	0.005	0.006
0.200	0.010	0.985	0.010	0.200	0.010	0.372	0.089	0.085	0.000	0.000	0.000	0.004	0.002	0.004	0.002	0.005	0.006	

Table 4.24: The SIG, TPI and TPDF results on VLLE ternary system of water (1)-acetone (2)MEK (3) at 760 mm Hg, different sets of feed composition were chosen outside heterogeneous region with various temperatures

z_1	z_2	T in $^{\circ}\text{C}$	Method	Phase I		Phase II		Phase III		No Phases
				x_1	x_2	x_1	x_2	y_1	y_2	
0.500	0.300	73.10	SIG	0.9490	0.0317	0.9490	0.0316	0.3400	0.3960	2
			TPI	0.0207	0.0001	0.9483	0.0237	0.3314	0.3020	3
			TPDF	0.9490	0.0316	0.9490	0.0316	0.3400	0.3956	2
0.600	0.300	72.60	SIG	0.9482	0.0392	0.9483	0.0392	0.3314	0.5021	2
			TPI	0.0035	0.0658	0.9555	0.0221	0.3166	0.3002	3
			TPDF	0.9483	0.0391	0.9483	0.0391	0.3314	0.5012	2
0.700	0.200	72.20	SIG	0.9440	0.0379	0.9444	0.0377	0.3260	0.4502	2
			TPI	0.5331	0.0243	0.9445	0.0184	0.0233	0.2222	3
			TPDF	0.9445	0.0376	0.9445	0.0376	0.3261	0.4484	2
0.300	0.500	71.80	SIG	0.9271	0.0517	0.9271	0.0517	0.3177	0.5339	2
			TPI	0.4694	0.4525	0.9269	0.0678	0.2462	0.6234	3
			TPDF	0.9271	0.0517	0.9271	0.0517	0.2984	0.5012	2
0.200	0.700	71.30	SIG	0.4012	0.5174	0.4012	0.5174	0.1903	0.6677	2
			TPI	0.3077	0.4136	0.3504	0.6359	0.1233	0.7003	3
			TPDF	0.4012	0.5174	0.4012	0.5174	0.1996	0.7004	2
0.250	0.650	70.90	SIG	0.8570	0.1185	0.8570	0.1185	0.2574	0.6743	2
			TPI	0.4077	0.5865	0.9362	0.0413	0.1494	0.6905	3
			TPDF	0.8570	0.1185	0.8570	0.1185	0.2486	0.6512	2
0.100	0.650	70.30	SIG	0.1869	0.5843	0.1869	0.5844	0.1247	0.8120	2
			TPI	0.0030	0.6004	0.1949	0.5966	0.3096	0.6707	3
			TPDF	0.1868	0.5844	0.1868	0.5844	0.0998	0.6501	2
0.150	0.750	70.10	SIG	0.2720	0.6412	0.2720	0.6412	0.1415	0.7090	2
			TPI	0.2697	0.4095	0.2697	0.7280	0.1008	0.7504	3
			TPDF	0.2720	0.6412	0.2720	0.6412	0.1497	0.7502	2

4.4.2 VLE system: Water (1)-Ethanol (2)-Methyl Ethyl Ketone (3) at pressure 760 mmHg

Table 4.25: VLE ternary system (water-ethanol-methyl ethyl ketone) at 760 mmHg flash calculation, TPDF & TPI predictions

Temperature in °C	Experimental			Flash calculation			TPDF Prediction			TPI Prediction		
	water	Ethanol	MEK	water	ethanol	MEK	water	ethanol	MEK	water	ethanol	MEK
Organic Phase												
73.20	0.461	0.012	0.527	0.461	0.012	0.528	0.46	0.013	0.527	0.404	0.012	0.584
72.80	0.518	0.029	0.453	0.526	0.027	0.447	0.51	0.038	0.453	0.478	0.032	0.49
72.10	0.548	0.037	0.415	0.554	0.034	0.412	0.541	0.046	0.414	0.438	0.039	0.523
71.60	0.637	0.045	0.319	0.646	0.043	0.310	0.563	0.058	0.379	0.464	0.053	0.483
71.20	0.72	0.044	0.236	0.736	0.043	0.221	0.561	0.058	0.382	0.496	0.056	0.448
Aqueous Phase												
73.20	0.95	0.005	0.045	0.953	0.004	0.043	0.956	0.004	0.040	0.973	0.009	0.018
72.80	0.934	0.012	0.054	0.937	0.01	0.053	0.94	0.014	0.046	0.933	0.033	0.035
72.10	0.911	0.017	0.072	0.918	0.015	0.066	0.935	0.018	0.047	0.913	0.043	0.044
71.60	0.892	0.025	0.083	0.899	0.024	0.078	0.922	0.026	0.053	0.905	0.043	0.052
71.20	0.84	0.033	0.127	0.854	0.032	0.114	0.922	0.025	0.052	0.869	0.054	0.077
Vapour Phase												
73.20	0.364	0.013	0.623	0.353	0.015	0.632	0.352	0.017	0.632	0.343	0.015	0.642
72.80	0.367	0.031	0.603	0.355	0.035	0.610	0.342	0.051	0.608	0.334	0.06	0.606
72.10	0.361	0.04	0.599	0.351	0.044	0.605	0.338	0.061	0.601	0.322	0.07	0.608
71.60	0.361	0.053	0.585	0.350	0.059	0.591	0.332	0.077	0.591	0.316	0.096	0.588
71.20	0.361	0.06	0.578	0.350	0.064	0.586	0.331	0.077	0.592	0.322	0.115	0.563

Table 4.26: VLE water (1)-ethanol (2)-MEK (3) sensitivity of TPI and TPDF methods to different initial values at temperatures; 73.2, 72.8 & 72.1⁰C, pressure 760 mmHg

Temp	Initial values						TPI predictions						TPDF predictions					
	organic		aqueous		vapour		organic		aqueous		vapour		organic		aqueous		vapour	
	X ₁	X ₂	X ₁	X ₂	y ₁	y ₂	Δx ₁	Δx ₂	Δx ₁	Δx ₂	Δy ₁	Δy ₂	Δx ₁	Δx ₂	Δx ₁	Δx ₂	Δy ₁	Δy ₂
73.20 ⁰ C	0.010	0.01	0.725	0.01	0.050	0.01	0.376	0.205	0.257	0.221	0.064	0.267	0.001	0.000	0.007	0.001	0.012	0.004
	0.025	0.01	0.750	0.01	0.075	0.01	0.318	0.205	0.238	0.153	0.321	0.251	0.001	0.000	0.007	0.001	0.012	0.004
	0.050	0.01	0.775	0.01	0.100	0.01	0.407	0.002	0.152	0.144	0.268	0.011	0.001	0.000	0.007	0.001	0.012	0.004
	0.075	0.01	0.800	0.01	0.125	0.01	0.398	0.016	0.172	0.159	0.229	0.009	0.001	0.000	0.007	0.001	0.012	0.004
	0.100	0.01	0.825	0.01	0.150	0.01	0.361	0.010	0.170	0.142	0.221	0.004	0.001	0.000	0.007	0.001	0.012	0.004
	0.125	0.01	0.850	0.01	0.175	0.01	0.336	0.003	0.214	0.195	0.220	0.008	0.001	0.000	0.007	0.001	0.012	0.004
	0.150	0.01	0.875	0.01	0.200	0.01	0.320	0.013	0.228	0.209	0.194	0.005	0.001	0.000	0.007	0.001	0.012	0.004
	0.175	0.01	0.900	0.01	0.225	0.01	0.277	0.008	0.050	0.005	0.139	0.003	0.001	0.000	0.007	0.001	0.012	0.004
	0.200	0.01	0.925	0.01	0.250	0.01	0.298	0.007	0.025	0.005	0.114	0.003	0.001	0.000	0.007	0.001	0.012	0.004
72.80 ⁰ C	0.010	0.01	0.800	0.01	0.050	0.01	0.480	0.125	0.322	0.309	0.094	0.311	0.009	0.009	0.007	0.002	0.025	0.019
	0.025	0.01	0.820	0.01	0.075	0.01	0.316	0.029	0.302	0.282	0.127	0.316	0.009	0.009	0.007	0.002	0.025	0.019
	0.050	0.01	0.840	0.01	0.100	0.01	0.450	0.212	0.269	0.238	0.079	0.266	0.009	0.009	0.007	0.002	0.025	0.02
	0.075	0.01	0.860	0.01	0.125	0.01	0.444	0.008	0.248	0.237	0.268	0.016	0.009	0.009	0.007	0.002	0.025	0.019
	0.100	0.01	0.880	0.01	0.150	0.01	0.421	0.016	0.284	0.269	0.251	0.014	0.009	0.009	0.007	0.002	0.025	0.019
	0.125	0.01	0.900	0.01	0.175	0.01	0.395	0.016	0.302	0.288	0.224	0.021	0.009	0.009	0.007	0.002	0.025	0.02
	0.150	0.01	0.920	0.01	0.200	0.01	0.370	0.007	0.314	0.306	0.196	0.022	0.009	0.009	0.007	0.002	0.025	0.02
	0.175	0.01	0.940	0.01	0.225	0.01	0.354	0.003	0.295	0.276	0.185	0.026	0.009	0.009	0.007	0.002	0.025	0.02
	0.200	0.01	0.960	0.01	0.250	0.01	0.319	0.020	0.351	0.341	0.129	0.029	0.009	0.009	0.007	0.002	0.025	0.02
72.10 ⁰ C	0.010	0.01	0.980	0.01	0.275	0.01	0.349	0.068	0.275	0.248	0.128	0.010	0.009	0.009	0.007	0.002	0.025	0.02
	0.025	0.01	0.980	0.01	0.275	0.01	0.349	0.068	0.275	0.248	0.128	0.010	0.009	0.009	0.007	0.002	0.025	0.02
	0.050	0.01	0.800	0.01	0.100	0.01	0.237	0.263	0.156	0.170	0.292	0.037	0.008	0.009	0.023	0.001	0.023	0.021
	0.075	0.01	0.820	0.01	0.125	0.01	0.274	0.266	0.274	0.244	0.089	0.001	0.008	0.009	0.024	0.001	0.024	0.021
	0.100	0.01	0.840	0.01	0.150	0.01	0.279	0.274	0.286	0.267	0.115	0.016	0.007	0.009	0.023	0.001	0.024	0.021
	0.125	0.01	0.860	0.01	0.175	0.01	0.295	0.287	0.276	0.256	0.125	0.004	0.008	0.009	0.024	0.001	0.023	0.021
	0.150	0.01	0.880	0.01	0.200	0.01	0.261	0.263	0.057	0.104	0.146	0.004	0.007	0.009	0.024	0.001	0.023	0.021
	0.175	0.01	0.900	0.01	0.225	0.01	0.229	0.234	0.081	0.096	0.083	0.005	0.008	0.009	0.024	0.001	0.024	0.021
	0.200	0.01	0.920	0.01	0.250	0.01	0.269	0.270	0.202	0.184	0.082	0.001	0.007	0.009	0.023	0.001	0.023	0.021
72.10 ⁰ C	0.216	0.01	0.940	0.01	0.275	0.01	0.264	0.264	0.007	0.062	0.087	0.011	0.008	0.009	0.024	0.001	0.023	0.021
	0.219	0.01	0.960	0.01	0.300	0.01	0.101	0.372	0.047	0.009	0.067	0.004	0.008	0.009	0.023	0.001	0.024	0.021
	0.222	0.01	0.980	0.01	0.325	0.01	0.105	0.363	0.068	0.008	0.036	0.004	0.008	0.009	0.024	0.001	0.023	0.021

Table 4.27: Results for SIG, TPI and TPDF methods on VLLE ternary system of water (1)-ethanol (2)MEK (3) at 760 mm Hg. different sets of fixed values of feed composition were chosen outside heterogeneous region with various temperatures

z_1	z_2	T in $^{\circ}\text{C}$	Method	Phase I		Phase II		Phase III		No Phases
				x_1	x_2	x_1	x_2	y_1	y_2	
0.200	0.500	73.20	SIG	0.3199	0.5564	0.3199	0.5564	0.2084	0.5216	2
			TPI	0.0556	0.6486	0.4324	0.4555	0.3098	0.6070	3
			TPDF	0.3199	0.5564	0.3199	0.5564	0.1997	0.4998	2
0.500	0.200	72.80	SIG	0.6312	0.1728	0.6314	0.1727	0.3142	0.2386	2
			TPI	0.3688	0.2272	0.8317	0.0905	0.3686	0.2273	3
			TPDF	0.6313	0.1727	0.6313	0.1727	0.3142	0.2386	2
0.650	0.150	72.10	SIG	0.5858	0.1601	0.5859	0.1601	0.3024	0.2046	2
			TPI	0.3524	0.0221	0.6887	0.1500	0.6617	0.1617	3
			TPDF	0.5859	0.1601	0.5859	0.1601	0.3024	0.2046	2
0.700	0.150	71.60	SIG	0.5347	0.1743	0.5347	0.1743	0.2868	0.2108	2
			TPI	0.5026	0.0712	0.7344	0.0918	0.3159	0.1507	3
			TPDF	0.5347	0.1743	0.5347	0.1743	0.2868	0.2108	2
0.200	0.600	71.20	SIG	0.2426	0.6433	0.2425	0.6438	0.1439	0.5388	2
			TPI	0.1138	0.6428	0.3633	0.5066	0.2045	0.6985	3
			TPDF	0.2417	0.6446	0.2417	0.6446	0.1434	0.5395	2

4.4.3 VLE system: Water (1)-Acetone (2)-n Butyl Acetate (3)

Table 4.28: VLE ternary system (water-acetone-n-butyl acetate) at 360 mmHg, flash calculation, TPDF and TPI predictions

Temperature in °C	Experimental			Flash calculation			TPDF Prediction			TPI Prediction		
	Water	acetone	n-butyl acetate	water	acetone	n-butyl acetate	water	acetone	n-butyl acetate	water	acetone	n-butyl acetate
Organic Phase												
59.00	0.159	0.231	0.610	0.141	0.238	0.621	0.158	0.231	0.611	0.160	0.230	0.610
52.80	0.197	0.367	0.436	0.197	0.366	0.437	0.176	0.356	0.469	0.202	0.377	0.421
49.40	0.245	0.435	0.320	0.250	0.428	0.321	0.214	0.431	0.354	0.239	0.441	0.320
48.20	0.303	0.461	0.236	0.305	0.451	0.244	0.298	0.464	0.237	0.222	0.463	0.315
46.20	0.384	0.451	0.165	0.384	0.436	0.180	0.374	0.478	0.149	0.373	0.555	0.072
45.10	0.470	0.414	0.117	0.470	0.400	0.130	0.478	0.449	0.073	0.492	0.487	0.022
Aqueous Phase												
59.00	0.965	0.033	0.002	0.967	0.033	0.000	0.965	0.033	0.002	0.965	0.032	0.003
52.80	0.931	0.066	0.003	0.939	0.060	0.001	0.932	0.065	0.003	0.927	0.071	0.003
49.40	0.898	0.097	0.005	0.905	0.093	0.002	0.896	0.098	0.005	0.907	0.091	0.003
48.20	0.865	0.128	0.006	0.879	0.118	0.004	0.858	0.135	0.007	0.895	0.101	0.004
46.20	0.825	0.165	0.011	0.842	0.150	0.008	0.847	0.146	0.007	0.898	0.100	0.002
45.10	0.761	0.215	0.024	0.776	0.205	0.019	0.828	0.165	0.007	0.827	0.171	0.001
Vapour Phase												
59.00	0.377	0.484	0.139	0.372	0.480	0.148	0.386	0.485	0.129	0.387	0.485	0.128
52.80	0.294	0.615	0.091	0.290	0.617	0.094	0.288	0.633	0.079	0.279	0.652	0.069
49.40	0.259	0.672	0.069	0.251	0.683	0.066	0.233	0.716	0.051	0.256	0.695	0.050
48.20	0.246	0.699	0.055	0.228	0.720	0.052	0.215	0.737	0.048	0.223	0.738	0.040
46.20	0.232	0.723	0.045	0.218	0.739	0.043	0.208	0.749	0.043	0.197	0.776	0.026
45.10	0.225	0.738	0.037	0.214	0.748	0.038	0.201	0.763	0.036	0.162	0.835	0.003

Table 4.29: VLE water (1)-acetone (2)-n-butyl acetate (3) sensitivity of TPI and TPDF methods to different initial values at various temperatures and 360 mmHg

Temp	Initial values						TPI predictions						TPDF predictions					
	organic		aqueous		vapour		organic		aqueous		vapour		organic		aqueous		vapour	
	x_1	x_2	x_1	x_2	y_1	y_2	Δx_1	Δx_2	Δx_1	Δx_2	Δy_1	Δy_2	Δx_1	Δx_2	Δx_1	Δx_2	Δy_1	Δy_2
59.00°C	0.100	0.010	0.850	0.010	0.100	0.010	0.027	0.038	0.003	0.005	0.130	0.160	0.001	0.000	0.000	0.000	0.009	0.000
	0.110	0.010	0.860	0.010	0.110	0.010	0.080	0.025	0.002	0.005	0.119	0.139	0.001	0.000	0.000	0.000	0.009	0.000
	0.120	0.010	0.870	0.010	0.120	0.010	0.001	0.025	0.024	0.002	0.019	0.014	0.001	0.000	0.000	0.000	0.009	0.000
	0.130	0.010	0.880	0.010	0.130	0.010	0.010	0.061	0.079	0.062	0.013	0.008	0.001	0.000	0.000	0.000	0.009	0.000
	0.140	0.010	0.890	0.010	0.140	0.010	0.009	0.047	0.022	0.020	0.004	0.001	0.001	0.000	0.000	0.000	0.009	0.000
	0.150	0.010	0.900	0.010	0.150	0.010	0.005	0.025	0.010	0.002	0.008	0.000	0.001	0.000	0.000	0.000	0.009	0.000
	0.160	0.010	0.910	0.010	0.160	0.010	0.002	0.025	0.012	0.010	0.010	0.001	0.001	0.000	0.000	0.000	0.009	0.000
	0.170	0.010	0.920	0.010	0.170	0.010	0.006	0.025	0.016	0.015	0.015	0.004	0.001	0.000	0.000	0.000	0.009	0.000
	0.180	0.010	0.930	0.010	0.180	0.010	0.015	0.025	0.023	0.030	0.028	0.027	0.001	0.000	0.000	0.000	0.009	0.000
0.190	0.010	0.940	0.010	0.190	0.010	0.013	0.032	0.031	0.013	0.008	0.002	0.001	0.000	0.000	0.000	0.009	0.000	
52.80°C	0.100	0.010	0.850	0.010	0.100	0.010	0.043	0.102	0.009	0.014	0.013	0.030	0.021	0.011	0.001	0.001	0.006	0.018
	0.110	0.010	0.860	0.010	0.110	0.010	0.064	0.102	0.183	0.163	0.017	0.035	0.021	0.011	0.001	0.001	0.006	0.018
	0.120	0.010	0.870	0.010	0.120	0.010	0.049	0.102	0.082	0.061	0.007	0.023	0.021	0.011	0.001	0.001	0.006	0.018
	0.130	0.010	0.880	0.010	0.130	0.010	0.012	0.114	0.055	0.057	0.052	0.074	0.021	0.011	0.001	0.001	0.006	0.018
	0.140	0.010	0.890	0.010	0.140	0.010	0.119	0.103	0.018	0.020	0.041	0.055	0.021	0.011	0.001	0.001	0.006	0.018
	0.150	0.010	0.900	0.010	0.150	0.010	0.110	0.103	0.013	0.014	0.031	0.052	0.021	0.011	0.001	0.001	0.006	0.018
	0.160	0.010	0.910	0.010	0.160	0.010	0.042	0.102	0.056	0.054	0.019	0.036	0.021	0.011	0.001	0.001	0.006	0.018
	0.170	0.010	0.920	0.010	0.170	0.010	0.044	0.102	0.028	0.028	0.013	0.029	0.021	0.011	0.001	0.001	0.006	0.018
	0.180	0.010	0.930	0.010	0.180	0.010	0.034	0.102	0.031	0.030	0.028	0.048	0.021	0.011	0.001	0.001	0.006	0.018
0.190	0.010	0.940	0.010	0.190	0.010	0.030	0.102	0.024	0.022	0.024	0.048	0.021	0.011	0.001	0.001	0.006	0.018	
49.40°C	0.100	0.010	0.850	0.010	0.100	0.010	0.007	0.146	0.077	0.061	0.006	0.002	0.030	0.002	0.003	0.002	0.027	0.045
	0.110	0.010	0.860	0.010	0.110	0.010	0.031	0.144	0.023	0.019	0.013	0.001	0.031	0.002	0.003	0.002	0.027	0.045
	0.120	0.010	0.870	0.010	0.120	0.010	0.006	0.145	0.058	0.054	0.020	0.048	0.030	0.002	0.003	0.002	0.027	0.045
	0.130	0.010	0.880	0.010	0.130	0.010	0.009	0.144	0.048	0.048	0.004	0.023	0.030	0.002	0.003	0.002	0.027	0.045
	0.140	0.010	0.890	0.010	0.140	0.010	0.036	0.153	0.047	0.043	0.049	0.062	0.030	0.002	0.003	0.002	0.027	0.045
	0.150	0.010	0.900	0.010	0.150	0.010	0.034	0.144	0.032	0.036	0.046	0.066	0.030	0.002	0.003	0.002	0.027	0.045
	0.160	0.010	0.910	0.010	0.160	0.010	0.007	0.145	0.027	0.028	0.021	0.039	0.030	0.002	0.003	0.002	0.027	0.045
	0.170	0.010	0.920	0.010	0.170	0.010	0.054	0.144	0.011	0.001	0.063	0.087	0.030	0.002	0.003	0.002	0.027	0.045
	0.180	0.010	0.930	0.010	0.180	0.010	0.066	0.144	0.036	0.037	0.066	0.082	0.030	0.002	0.003	0.002	0.027	0.045
0.190	0.010	0.940	0.010	0.190	0.010	0.105	0.144	0.054	0.053	0.025	0.055	0.030	0.002	0.003	0.002	0.027	0.045	

Temp	Initial values						TPI predictions						TPDF predictions					
	organic		aqueous		vapour		organic		aqueous		vapour		organic		aqueous		vapour	
	x_1	x_2	x_1	x_2	y_1	y_2	Δx_1	Δx_2	Δx_1	Δx_2	Δy_1	Δy_2	Δx_1	Δx_2	Δx_1	Δx_2	Δy_1	Δy_2
48.20°C	0.100	0.200	0.850	0.010	0.100	0.200	0.078	0.141	0.025	0.029	0.021	0.024	0.005	0.003	0.007	0.007	0.031	0.037
	0.110	0.200	0.860	0.010	0.110	0.200	0.111	0.142	0.028	0.027	0.053	0.060	0.005	0.003	0.007	0.007	0.031	0.037
	0.120	0.200	0.870	0.010	0.120	0.200	0.196	0.142	0.066	0.063	0.028	0.028	0.005	0.003	0.007	0.007	0.031	0.037
	0.130	0.200	0.880	0.010	0.130	0.200	0.077	0.141	0.029	0.029	0.020	0.022	0.005	0.003	0.007	0.007	0.031	0.037
	0.140	0.200	0.890	0.010	0.140	0.200	0.117	0.141	0.054	0.054	0.060	0.056	0.005	0.003	0.007	0.007	0.031	0.037
	0.150	0.200	0.900	0.010	0.150	0.200	0.091	0.141	0.019	0.025	0.033	0.038	0.005	0.003	0.007	0.007	0.031	0.037
	0.160	0.200	0.910	0.010	0.160	0.200	0.114	0.141	0.041	0.041	0.054	0.051	0.005	0.003	0.007	0.007	0.031	0.037
	0.170	0.200	0.920	0.010	0.170	0.200	0.075	0.141	0.003	0.007	0.008	0.018	0.005	0.003	0.007	0.007	0.031	0.037
	0.180	0.200	0.930	0.010	0.180	0.200	0.110	0.142	0.052	0.049	0.052	0.055	0.005	0.003	0.007	0.007	0.031	0.037
	0.190	0.200	0.940	0.010	0.190	0.200	0.053	0.005	0.085	0.078	0.005	0.005	0.005	0.003	0.007	0.007	0.031	0.037
46.20°C	0.100	0.200	0.850	0.010	0.100	0.200	0.165	0.330	0.098	0.091	0.144	0.437	0.010	0.027	0.022	0.019	0.024	0.026
	0.110	0.200	0.860	0.010	0.110	0.200	0.154	0.136	0.104	0.051	0.003	0.015	0.010	0.027	0.022	0.019	0.024	0.026
	0.120	0.200	0.870	0.010	0.120	0.200	0.254	0.392	0.109	0.102	0.410	0.403	0.010	0.027	0.022	0.019	0.024	0.026
	0.130	0.200	0.880	0.010	0.130	0.200	0.268	0.131	0.077	0.137	0.056	0.013	0.010	0.027	0.022	0.019	0.024	0.026
	0.140	0.200	0.890	0.010	0.140	0.200	0.296	0.131	0.066	0.158	0.061	0.017	0.010	0.027	0.022	0.019	0.024	0.026
	0.150	0.200	0.900	0.010	0.150	0.200	0.248	0.131	0.120	0.157	0.069	0.027	0.010	0.027	0.022	0.019	0.024	0.026
	0.160	0.200	0.910	0.010	0.160	0.200	0.242	0.131	0.123	0.125	0.065	0.021	0.010	0.027	0.022	0.019	0.024	0.026
	0.170	0.200	0.920	0.010	0.170	0.200	0.229	0.131	0.100	0.151	0.084	0.040	0.010	0.027	0.022	0.019	0.024	0.026
	0.180	0.200	0.930	0.010	0.180	0.200	0.204	0.249	0.105	0.155	0.090	0.047	0.010	0.027	0.022	0.019	0.024	0.026
	0.190	0.200	0.940	0.010	0.190	0.200	0.146	0.133	0.166	0.156	0.086	0.041	0.010	0.027	0.022	0.019	0.024	0.026
45.10°C	0.100	0.200	0.850	0.010	0.100	0.200	0.298	0.399	0.123	0.133	0.363	0.419	0.008	0.035	0.067	0.050	0.024	0.025
	0.110	0.200	0.860	0.010	0.110	0.200	0.202	0.319	0.101	0.215	0.167	0.408	0.008	0.035	0.067	0.050	0.024	0.025
	0.120	0.200	0.870	0.010	0.120	0.200	0.211	0.327	0.136	0.198	0.120	0.408	0.008	0.035	0.067	0.050	0.024	0.025
	0.130	0.200	0.880	0.010	0.130	0.200	0.190	0.306	0.114	0.214	0.151	0.408	0.008	0.035	0.067	0.050	0.024	0.025
	0.140	0.200	0.890	0.010	0.140	0.200	0.180	0.296	0.188	0.197	0.102	0.408	0.008	0.035	0.067	0.050	0.024	0.025
	0.150	0.200	0.900	0.010	0.150	0.200	0.176	0.293	0.190	0.167	0.047	0.410	0.008	0.035	0.067	0.050	0.024	0.025
	0.160	0.200	0.910	0.010	0.160	0.200	0.166	0.283	0.195	0.206	0.082	0.408	0.008	0.035	0.067	0.050	0.024	0.025
	0.170	0.200	0.920	0.010	0.170	0.200	0.159	0.276	0.201	0.208	0.073	0.408	0.008	0.035	0.067	0.050	0.024	0.025
	0.180	0.200	0.930	0.010	0.180	0.200	0.153	0.269	0.177	0.198	0.063	0.408	0.008	0.035	0.067	0.050	0.024	0.025
	0.190	0.200	0.940	0.010	0.190	0.200	0.159	0.276	0.173	0.215	0.055	0.451	0.008	0.035	0.067	0.050	0.024	0.025

Table 4.30: SIG, TPI and TPDF results on VLLE ternary system of water (1) acetone (2) n-butyl acetate (3) at 360 mm Hg. Different sets of fixed values of feed composition were chosen outside heterogeneous region with various temperatures

z_1	z_2	T in °C	Method	Phase I		Phase II		Phase III		No. Phases
				x_1	x_2	x_1	x_2	y_1	y_2	
0.100	0.600	59.00	SIG	0.0216	0.3412	0.0216	0.3412	0.1358	0.7181	2
			TPI	0.1152	0.5736	0.1148	0.5324	0.1009	0.7823	3
			TPDF	0.0216	0.3412	0.0216	0.3412	0.1358	0.7181	2
0.150	0.600	52.80	SIG	0.0870	0.4372	0.0870	0.4372	0.1949	0.7159	2
			TPI	0.1236	0.4292	0.1967	0.3912	0.1967	0.7134	3
			TPDF	0.0870	0.4372	0.0870	0.4372	0.1949	0.7159	2
0.150	0.650	49.40	SIG	0.1160	0.5089	0.1160	0.5089	0.1771	0.7622	2
			TPI	0.1435	0.4876	0.2065	0.4549	0.2065	0.7359	3
			TPDF	0.1160	0.5089	0.1160	0.5089	0.1771	0.7622	2
0.150	0.700	48.20	SIG	0.1194	0.5379	0.1194	0.5379	0.1656	0.7826	2
			TPI	0.1288	0.5252	0.1604	0.5179	0.1604	0.7881	3
			TPDF	0.1194	0.5379	0.1194	0.5379	0.1656	0.7826	2
0.100	0.700	46.20	SIG	0.0851	0.6109	0.0851	0.6109	0.1231	0.8381	2
			TPI	0.0951	0.6074	0.1331	0.5684	0.1331	0.8279	3
			TPDF	0.0851	0.6109	0.0851	0.6109	0.1231	0.8381	2
0.200	0.700	45.10	SIG	0.2423	0.5511	0.2424	0.5511	0.1722	0.7976	2
			TPI	0.1704	0.5913	0.2000	0.5740	0.1706	0.7969	3
			TPDF	0.2423	0.5511	0.2423	0.5511	0.1722	0.7976	2

Table 4.31: VLLE ternary system (water-acetone-n-butyl acetate) at 600 mmHg, flash calculation, TPDF and TPI predictions

Temperature in °C	Experimental			Flash calculation			TPDF Prediction			TPI Prediction		
	water	acetone	n-butyl acetate	water	acetone	n-butyl acetate	water	acetone	n-butyl acetate	water	acetone	n-butyl acetate
Organic Phase												
69.20	0.188	0.229	0.583	0.176	0.221	0.603	0.192	0.227	0.582	0.190	0.230	0.581
62.40	0.231	0.363	0.406	0.232	0.361	0.408	0.235	0.368	0.397	0.232	0.371	0.398
60.30	0.281	0.420	0.299	0.287	0.412	0.301	0.283	0.419	0.298	0.224	0.440	0.335
58.10	0.352	0.435	0.213	0.352	0.425	0.223	0.343	0.444	0.213	0.362	0.519	0.119
56.50	0.428	0.420	0.151	0.428	0.400	0.172	0.406	0.443	0.151	0.289	0.434	0.277
56.20	0.518	0.376	0.106	0.518	0.367	0.116	0.526	0.378	0.095	0.226	0.495	0.279
Aqueous Phase												
69.20	0.968	0.030	0.002	0.972	0.028	0.000	0.969	0.030	0.002	0.970	0.030	0.001
62.40	0.936	0.062	0.003	0.943	0.056	0.001	0.941	0.057	0.002	0.940	0.058	0.002
60.30	0.905	0.091	0.004	0.912	0.085	0.004	0.934	0.065	0.002	0.934	0.062	0.003
58.10	0.872	0.122	0.006	0.886	0.107	0.006	0.892	0.104	0.004	0.864	0.055	0.080
56.50	0.846	0.143	0.010	0.860	0.130	0.009	0.866	0.127	0.006	0.914	0.086	0.000
56.20	0.785	0.198	0.017	0.805	0.175	0.020	0.814	0.173	0.013	0.846	0.143	0.011
Vapour Phase												
69.20	0.395	0.463	0.143	0.367	0.465	0.168	0.376	0.481	0.143	0.372	0.486	0.142
62.40	0.313	0.597	0.091	0.287	0.605	0.108	0.271	0.628	0.101	0.268	0.632	0.100
60.30	0.277	0.652	0.070	0.256	0.666	0.078	0.248	0.682	0.070	0.250	0.695	0.055
58.10	0.253	0.692	0.055	0.232	0.709	0.060	0.213	0.733	0.054	0.186	0.703	0.110
56.50	0.244	0.709	0.047	0.223	0.726	0.051	0.192	0.764	0.044	0.289	0.704	0.006
56.20	0.231	0.730	0.040	0.212	0.746	0.042	0.187	0.775	0.038	0.226	0.730	0.044

Table 4.32: SIG, TPI and TPDF results on VLLE ternary system of water (1)-acetone (2)n-butyl acetate (3) at 600 mm Hg. Different sets of fixed values of feed composition were chosen outside heterogeneous region with various temperatures

z_1	z_2	T in °C	Method	Phase I		Phase II		Phase III		No Phases
				x_1	x_2	x_1	x_2	y_1	y_2	
0.100	0.650	69.20	SIG	0.0163	0.3387	0.0163	0.3387	0.1203	0.7255	2
			TPI	0.0292	0.3338	0.1848	0.6466	0.2529	0.7448	3
			TPDF	0.0162	0.3388	0.0162	0.3388	0.1203	0.7255	2
0.150	0.650	62.40	SIG	0.0741	0.4567	0.0741	0.4567	0.1804	0.7275	2
			TPI	0.0292	0.3338	0.1848	0.6466	0.2529	0.7448	3
			TPDF	0.0741	0.4567	0.0741	0.4567	0.1804	0.7275	2
0.200	0.650	60.30	SIG	0.1700	0.4691	0.1700	0.4691	0.2109	0.7156	2
			TPI	0.1291	0.5391	0.3618	0.6351	0.1368	0.7455	3
			TPDF	0.1700	0.4691	0.1700	0.4691	0.2109	0.7156	2
0.200	0.700	58.10	SIG	0.2176	0.5086	0.2177	0.5086	0.1953	0.7505	2
			TPI	0.1960	0.4785	0.2017	0.4793	0.1992	0.7490	3
			TPDF	0.2177	0.5086	0.2177	0.5086	0.1953	0.7505	2
0.100	0.700	56.50	SIG	0.0858	0.6282	0.0858	0.6281	0.1258	0.8306	2
			TPI	0.0976	0.6083	0.1155	0.6022	0.1155	0.7723	3
			TPDF	0.0858	0.6281	0.0858	0.6281	0.1258	0.8306	2
0.100	0.600	56.20	SIG	0.1040	0.6257	0.1040	0.6256	0.1348	0.8235	2
			TPI	0.0975	0.5626	0.1217	0.5526	0.0982	0.8003	3
			TPDF	0.1040	0.6257	0.1040	0.6257	0.1348	0.8235	2

Table 4.33: VLLE ternary system (water-acetone-n-butyl acetate) at 760 mmHg, flash calculation, TPDF and TPI predictions

Temperature in °C	Experimental			Flash calculation			TPDF Prediction			TPI Prediction		
	water	acetone	n-butyl acetate	water	acetone	n-butyl acetate	water	acetone	n-butyl acetate	water	acetone	n-butyl acetate
Organic Phase												
86.10	0.173	0.077	0.751	0.171	0.076	0.753	0.171	0.077	0.753	0.175	0.061	0.764
82.10	0.178	0.146	0.675	0.179	0.148	0.673	0.169	0.147	0.683	0.172	0.123	0.705
79.20	0.194	0.204	0.572	0.194	0.208	0.598	0.187	0.205	0.608	0.192	0.176	0.632
77.00	0.206	0.265	0.518	0.210	0.256	0.535	0.204	0.266	0.530	0.201	0.210	0.589
73.80	0.228	0.332	0.440	0.232	0.328	0.439	0.226	0.333	0.441	0.233	0.256	0.511
71.30	0.265	0.376	0.360	0.265	0.374	0.360	0.266	0.373	0.361	0.272	0.371	0.357
69.50	0.291	0.408	0.302	0.291	0.407	0.303	0.292	0.405	0.302	0.264	0.336	0.400
68.00	0.325	0.425	0.250	0.324	0.419	0.258	0.324	0.417	0.260	0.336	0.412	0.252
67.10	0.382	0.427	0.191	0.378	0.418	0.204	0.407	0.403	0.191	0.383	0.425	0.192
66.40	0.467	0.406	0.127	0.463	0.408	0.129	0.467	0.406	0.127	0.468	0.403	0.130
66.10	0.512	0.378	0.110	0.512	0.368	0.120	0.512	0.387	0.102	0.506	0.388	0.106
Aqueous Phase												
86.10	0.990	0.008	0.002	0.989	0.009	0.002	0.990	0.008	0.002	0.982	0.014	0.004
82.10	0.982	0.016	0.002	0.978	0.019	0.003	0.981	0.017	0.002	0.977	0.001	0.023
79.20	0.972	0.027	0.001	0.968	0.029	0.003	0.971	0.028	0.002	0.959	0.001	0.040
77.00	0.964	0.034	0.002	0.959	0.038	0.003	0.964	0.035	0.002	0.924	0.000	0.076
73.80	0.946	0.051	0.002	0.941	0.055	0.003	0.946	0.052	0.002	0.937	0.037	0.026
71.30	0.931	0.067	0.003	0.925	0.071	0.004	0.932	0.065	0.003	0.936	0.055	0.009
69.50	0.913	0.083	0.004	0.909	0.086	0.005	0.915	0.081	0.004	0.903	0.066	0.031
68.00	0.895	0.100	0.005	0.893	0.101	0.006	0.902	0.093	0.005	0.889	0.093	0.018
67.10	0.869	0.125	0.007	0.871	0.121	0.008	0.892	0.104	0.005	0.869	0.121	0.010
66.40	0.820	0.168	0.013	0.825	0.164	0.012	0.820	0.168	0.013	0.800	0.187	0.014
66.10	0.807	0.178	0.016	0.819	0.166	0.015	0.811	0.176	0.013	0.711	0.256	0.034

Temperature in °C	Experimental			Flash calculation			TPDF Prediction			TPI Prediction		
	water	acetone	n-butyl acetate	water	acetone	n-butyl acetate	water	acetone	n-butyl acetate	water	acetone	n-butyl acetate
Vapour Phase												
86.10	0.586	0.188	0.226	0.586	0.183	0.232	0.586	0.188	0.226	0.550	0.126	0.324
82.10	0.484	0.336	0.179	0.497	0.320	0.183	0.485	0.335	0.179	0.496	0.333	0.171
79.20	0.424	0.423	0.153	0.437	0.412	0.151	0.427	0.423	0.150	0.414	0.425	0.161
77.00	0.394	0.474	0.133	0.397	0.475	0.128	0.394	0.474	0.131	0.425	0.502	0.072
73.80	0.338	0.562	0.100	0.342	0.561	0.097	0.341	0.564	0.095	0.350	0.579	0.071
71.30	0.304	0.614	0.081	0.309	0.611	0.079	0.309	0.610	0.081	0.273	0.570	0.157
69.50	0.282	0.650	0.068	0.287	0.647	0.066	0.283	0.648	0.069	0.264	0.617	0.119
68.00	0.276	0.665	0.059	0.274	0.667	0.059	0.267	0.664	0.069	0.236	0.642	0.122
67.10	0.267	0.682	0.051	0.262	0.685	0.052	0.262	0.679	0.059	0.197	0.636	0.166
66.40	0.247	0.712	0.041	0.246	0.713	0.041	0.247	0.712	0.041	0.184	0.651	0.165
66.10	0.262	0.693	0.046	0.256	0.698	0.046	0.237	0.718	0.045	0.182	0.655	0.163

Table 4.34: Results for the SIG, TPI and TPDF methods on VLLE ternary system of water (1)-acetone (2)-n-butyl acetate (3) at 760 mm Hg. Different sets of fixed values of feed composition were chosen outside heterogeneous region with various temperatures

z_1	z_2	T in °C	Method	Phase I		Phase II		Phase III		No Phases
				x_1	x_2	x_1	x_2	y_1	y_2	
0.200	0.500	86.10	SIG	0.0513	0.2153	0.0513	0.2153	0.2319	0.5611	2
			TPI	0.0513	0.2153	0.2611	0.4681	0.2752	0.7007	3
			TPDF	0.0514	0.2152	0.0514	0.2152	0.2319	0.5611	2
0.200	0.600	82.10	SIG	0.0572	0.2686	0.0572	0.2686	0.2110	0.6256	2
			TPI	0.0981	0.1785	0.4384	0.5605	0.0894	0.8637	3
			TPDF	0.0572	0.2686	0.0572	0.2686	0.2110	0.6255	2
0.200	0.700	79.20	SIG	0.0894	0.3817	0.0894	0.3817	0.2103	0.7360	2
			TPI	0.1731	0.2043	0.2030	0.6961	0.0763	0.8279	3
			TPDF	0.0894	0.3816	0.0894	0.3816	0.2003	0.7008	2
0.200	0.500	77.00	SIG	0.1043	0.3163	0.1043	0.3163	0.2622	0.6193	2
			TPI	0.1974	0.2424	0.2053	0.2404	0.0885	0.7721	3
			TPDF	0.1044	0.3162	0.1044	0.3162	0.2622	0.6193	2
0.200	0.600	73.80	SIG	0.1129	0.3787	0.1129	0.3787	0.2305	0.6775	2
			TPI	0.1045	0.3766	0.2881	0.5728	0.0120	0.6950	3
			TPDF	0.1128	0.3787	0.1128	0.3787	0.2305	0.6775	2
0.250	0.650	71.30	SIG	0.1692	0.4074	0.1692	0.4074	0.2566	0.6699	2
			TPI	0.0978	0.4388	0.2933	0.5874	0.0193	0.6962	3
			TPDF	0.1692	0.4074	0.1692	0.4074	0.2566	0.6699	2
0.100	0.650	69.50	SIG	0.0746	0.5025	0.0746	0.5025	0.1277	0.8108	2
			TPI	0.0810	0.4891	0.2677	0.6222	0.0267	0.6976	3
			TPDF	0.0746	0.5025	0.0746	0.5025	0.1277	0.8108	2

z_1	z_2	T in °C	Method	Phase I		Phase II		Phase III		No Phases
				x_1	x_2	x_1	x_2	y_1	y_2	
0.150	0.750	68.00	SIG	0.1113	0.5181	0.1113	0.5181	0.1568	0.7908	2
			TPI	0.0601	0.3867	0.1704	0.7428	0.0473	0.7717	3
			TPDF	0.1113	0.5181	0.1113	0.5181	0.1568	0.7908	2
0.100	0.750	67.10	SIG	0.0768	0.5592	0.0768	0.5592	0.1111	0.8414	2
			TPI	0.0649	0.4341	0.1327	0.7309	0.0093	0.7644	3
			TPDF	0.0768	0.5592	0.0768	0.5592	0.1111	0.8414	2
0.150	0.800	66.40	SIG	0.1232	0.5528	0.1232	0.5528	0.1507	0.8061	2
			TPI	0.1133	0.5080	0.1514	0.7185	0.1133	0.7342	3
			TPDF	0.1232	0.5528	0.1232	0.5528	0.1507	0.8061	2
0.100	0.650	66.10	SIG	0.1997	0.5279	0.1997	0.5279	0.1974	0.7626	2
			TPI	0.1996	0.4033	0.2411	0.3886	0.0884	0.7909	3
			TPDF	0.1997	0.5279	0.1997	0.5279	0.1974	0.7626	2

4.4.4 VLE system: Water (1)-Ethanol (2)-n Butyl Acetate (3)

Table 4.35: VLE ternary system (water-ethanol-n-butyl acetate) at 360 mmHg, flash calculation, TPDF and TPI predictions

Temperature in °C	Experimental			Flash calculation			TPDF Prediction			TPI Prediction		
	water	ethanol	n butyl acetate	water	ethanol	n butyl acetate	water	ethanol	n butyl acetate	water	ethanol	n butyl acetate
Organic Phase												
71.10	0.153	0.069	0.778	0.158	0.092	0.750	0.158	0.068	0.775	0.202	0.027	0.770
68.20	0.228	0.184	0.587	0.227	0.198	0.575	0.224	0.183	0.593	0.220	0.133	0.647
67.00	0.266	0.205	0.530	0.260	0.217	0.523	0.263	0.212	0.525	0.251	0.190	0.559
66.00	0.328	0.261	0.411	0.321	0.261	0.418	0.321	0.264	0.416	0.287	0.242	0.471
65.50	0.362	0.267	0.371	0.351	0.262	0.387	0.328	0.273	0.399	0.308	0.268	0.424
65.00	0.446	0.284	0.270	0.439	0.279	0.281	0.408	0.297	0.295	0.334	0.293	0.374
62.20	0.616	0.253	0.132	0.623	0.249	0.128	0.591	0.250	0.159	0.453	0.256	0.291
Aqueous Phase												
71.10	0.976	0.023	0.001	0.968	0.029	0.003	0.972	0.024	0.004	0.990	0.008	0.003
68.20	0.937	0.059	0.004	0.928	0.067	0.005	0.929	0.064	0.007	0.957	0.039	0.004
67.00	0.931	0.066	0.002	0.922	0.072	0.006	0.921	0.072	0.007	0.932	0.062	0.006
66.00	0.906	0.090	0.004	0.898	0.094	0.008	0.896	0.096	0.009	0.906	0.086	0.008
65.50	0.899	0.097	0.005	0.895	0.097	0.008	0.889	0.102	0.009	0.890	0.100	0.010
65.00	0.871	0.120	0.009	0.871	0.117	0.011	0.870	0.120	0.011	0.871	0.118	0.011
62.20	0.814	0.160	0.025	0.828	0.150	0.022	0.854	0.130	0.015	0.871	0.116	0.013
Vapour Phase												
71.10	0.606	0.143	0.251	0.597	0.160	0.243	0.603	0.126	0.271	0.647	0.087	0.267
68.20	0.517	0.281	0.201	0.530	0.278	0.192	0.535	0.265	0.200	0.580	0.200	0.220
67.00	0.508	0.305	0.187	0.524	0.294	0.183	0.528	0.289	0.183	0.543	0.265	0.192
66.00	0.478	0.345	0.177	0.497	0.340	0.163	0.500	0.343	0.157	0.510	0.321	0.169
65.50	0.480	0.352	0.168	0.496	0.342	0.162	0.493	0.354	0.153	0.494	0.349	0.157
65.00	0.462	0.377	0.161	0.484	0.371	0.145	0.478	0.388	0.134	0.477	0.378	0.145
62.20	0.456	0.398	0.146	0.477	0.388	0.134	0.425	0.396	0.179	0.427	0.386	0.188

Table 4.36: SIG, TPI and TPDF results on VLLE ternary system of water (1)-ethanol (2) n-butyl acetate (3) at 360 mm Hg. Different sets of fixed values of feed composition were chosen outside heterogeneous region with various temperatures

z_1	z_2	T in °C	Method	Phase I		Phase II		Phase III		No Phases
				x_1	x_2	x_1	x_2	y_1	y_2	
0.100	0.600	71.10	SIG	0.0184	0.4408	0.0183	0.4408	0.1384	0.6736	2
			TPI	0.0001	0.3027	0.1001	0.3983	0.0859	0.6620	3
			TPDF	0.0165	0.4427	0.0165	0.4427	0.1379	0.6737	2
0.150	0.600	68.20	SIG	0.0328	0.4789	0.0328	0.4789	0.1985	0.6499	2
			TPI	0.0364	0.6445	0.1560	0.4612	0.1552	0.8165	3
			TPDF	0.0330	0.4787	0.0330	0.4787	0.1983	0.6499	2
0.150	0.650	67.00	SIG	0.0310	0.5324	0.0310	0.5324	0.1866	0.6851	2
			TPI	0.1489	0.4211	0.3094	0.3800	0.1848	0.7597	3
			TPDF	0.0314	0.5319	0.0314	0.5319	0.1857	0.6852	2
0.150	0.700	66.00	SIG	0.0282	0.5834	0.0283	0.5833	0.1737	0.7190	2
			TPI	0.0094	0.6404	0.1607	0.4577	0.1607	0.6920	3
			TPDF	0.0264	0.5852	0.0264	0.5852	0.1707	0.7196	2
0.100	0.700	65.50	SIG	0.0227	0.6233	0.0227	0.6232	0.1518	0.7510	2
			TPI	0.0363	0.7312	0.1002	0.5746	0.1002	0.8003	3
			TPDF	0.0217	0.6243	0.0217	0.6243	0.1515	0.7510	2
0.200	0.700	65.00	SIG	0.0377	0.5927	0.0378	0.5926	0.2023	0.7048	2
			TPI	0.0653	0.6396	0.2000	0.4860	0.1993	0.7518	3
			TPDF	0.0376	0.5928	0.0376	0.5928	0.2004	0.7003	2
0.150	0.700	62.20	SIG	0.0493	0.6701	0.0508	0.6689	0.2171	0.7188	2
			TPI	0.0275	0.8054	0.1502	0.6085	0.1502	0.7750	3
			TPDF	0.0488	0.6706	0.0488	0.6706	0.2152	0.7191	2

Table 4.37: VLLE ternary system (water-ethanol-n-butyl acetate) at 600 mmHg, flash calculation, TPDF and TPI predictions

Temperature in °C	Experimental			Flash calculation			TPDF Prediction			TPI Prediction		
	water	ethanol	n butyl acetate	water	ethanol	n butyl acetate	water	ethanol	n butyl acetate	water	ethanol	n butyl acetate
Organic Phase												
81.00	0.205	0.069	0.727	0.203	0.053	0.744	0.198	0.043	0.759	0.135	0.090	0.775
77.30	0.289	0.172	0.539	0.286	0.167	0.547	0.292	0.167	0.541	0.247	0.170	0.583
76.10	0.295	0.202	0.503	0.301	0.195	0.504	0.303	0.197	0.501	0.302	0.224	0.474
75.50	0.373	0.247	0.380	0.371	0.247	0.382	0.367	0.257	0.376	0.346	0.256	0.399
75.10	0.387	0.260	0.353	0.388	0.259	0.353	0.379	0.266	0.355	0.369	0.277	0.354
74.40	0.483	0.271	0.246	0.475	0.268	0.258	0.437	0.315	0.249	0.401	0.324	0.275
74.20	0.660	0.231	0.108	0.658	0.235	0.107	0.553	0.343	0.104	0.631	0.281	0.088
Aqueous Phase												
81.00	0.976	0.021	0.002	0.977	0.022	0.000	0.986	0.014	0.000	0.986	0.014	0.000
77.30	0.941	0.056	0.003	0.946	0.054	0.001	0.958	0.041	0.000	0.956	0.041	0.003
76.10	0.931	0.065	0.003	0.933	0.066	0.001	0.951	0.049	0.000	0.944	0.053	0.003
75.50	0.906	0.089	0.005	0.911	0.086	0.003	0.936	0.064	0.001	0.935	0.065	0.001
75.10	0.903	0.093	0.004	0.909	0.088	0.003	0.933	0.066	0.001	0.927	0.072	0.001
74.40	0.873	0.117	0.009	0.885	0.108	0.007	0.909	0.090	0.001	0.903	0.095	0.002
74.20	0.815	0.159	0.026	0.832	0.147	0.020	0.823	0.168	0.009	0.877	0.100	0.023
Vapour Phase												
81.00	0.611	0.144	0.245	0.604	0.144	0.252	0.626	0.126	0.248	0.486	0.264	0.250
77.30	0.521	0.282	0.197	0.517	0.283	0.200	0.522	0.282	0.196	0.501	0.303	0.196
76.10	0.517	0.300	0.183	0.504	0.307	0.188	0.502	0.310	0.188	0.483	0.336	0.181
75.50	0.484	0.348	0.169	0.483	0.348	0.169	0.476	0.359	0.165	0.472	0.359	0.168
75.10	0.485	0.352	0.162	0.479	0.359	0.162	0.472	0.367	0.161	0.462	0.379	0.159
74.40	0.473	0.372	0.155	0.472	0.373	0.155	0.444	0.421	0.135	0.401	0.460	0.140
74.20	0.466	0.391	0.143	0.469	0.388	0.144	0.404	0.508	0.088	0.374	0.470	0.156

Table 4.38: SIG, TPI and TPDF results on VLLE ternary system of water (1)-ethanol (2) n-butyl acetate (3) at 600 mm Hg. Different sets of fixed values of feed composition were chosen outside heterogeneous region with various temperatures

z_1	z_2	T in °C	Method	Phase I		Phase II		Phase III		No Phases
				x_1	x_2	x_1	x_2	y_1	y_2	
0.100	0.600	81.00	SIG	0.0241	0.3926	0.0241	0.3926	0.1247	0.6678	2
			TPI	0.0389	0.3311	0.1872	0.5946	0.1872	0.8020	3
			TPDF	0.0194	0.3973	0.0194	0.3973	0.1248	0.6678	2
0.150	0.600	77.30	SIG	0.0528	0.4783	0.0528	0.4783	0.1906	0.6508	2
			TPI	0.0702	0.4267	0.2323	0.5986	0.2447	0.7497	3
			TPDF	0.0529	0.4782	0.0529	0.4782	0.1906	0.6508	2
0.150	0.650	76.10	SIG	0.0464	0.5131	0.0464	0.5131	0.1711	0.6779	2
			TPI	0.0586	0.4741	0.2006	0.6390	0.2063	0.7477	3
			TPDF	0.0464	0.5132	0.0464	0.5132	0.1711	0.6779	2
0.150	0.700	75.50	SIG	0.0497	0.6027	0.0497	0.6027	0.1650	0.7145	2
			TPI	0.0524	0.6032	0.1612	0.6955	0.2620	0.7190	3
			TPDF	0.0493	0.6031	0.0493	0.6031	0.1650	0.7145	2
0.100	0.700	75.10	SIG	0.0437	0.6482	0.0437	0.6482	0.1478	0.7440	2
			TPI	0.0601	0.5938	0.1852	0.6976	0.2003	0.7320	3
			TPDF	0.0437	0.6482	0.0437	0.6482	0.1478	0.7440	2
0.200	0.700	74.40	SIG	0.0769	0.6337	0.0769	0.6337	0.2042	0.7138	2
			TPI	0.0922	0.5595	0.3034	0.6955	0.1075	0.7766	3
			TPDF	0.0769	0.6337	0.0769	0.6337	0.2003	0.7002	2
0.200	0.600	74.20	SIG	0.1116	0.5449	0.1116	0.5449	0.2512	0.6319	2
			TPI	0.1458	0.4921	0.2000	0.4534	0.1862	0.7716	3
			TPDF	0.1116	0.5449	0.1116	0.5449	0.2512	0.6319	2

Table 4.39: VLLE ternary system (water-ethanol-n-butyl acetate) at 760 mmHg, flash calculation, TPDF and TPI predictions

Temperature in °C	Experimental			Flash calculation			TPDF Prediction			TPI Prediction		
	water	ethanol	n-butyl acetate	water	ethanol	n-butyl acetate	water	ethanol	n-butyl acetate	water	ethanol	n-butyl acetate
Organic Phase												
88.20	0.188	0.058	0.754	0.191	0.068	0.741	0.189	0.068	0.743	0.213	0.060	0.727
86.10	0.226	0.118	0.656	0.229	0.125	0.645	0.224	0.126	0.650	0.228	0.109	0.663
85.00	0.290	0.188	0.522	0.294	0.185	0.521	0.279	0.184	0.537	0.250	0.188	0.562
84.50	0.303	0.206	0.491	0.310	0.206	0.485	0.311	0.206	0.483	0.274	0.209	0.517
84.10	0.385	0.253	0.362	0.386	0.248	0.365	0.384	0.248	0.368	0.291	0.225	0.485
83.50	0.408	0.256	0.336	0.406	0.252	0.342	0.410	0.254	0.337	0.292	0.262	0.446
83.20	0.500	0.265	0.235	0.497	0.266	0.237	0.490	0.281	0.230	0.370	0.273	0.357
83.10	0.533	0.265	0.202	0.531	0.266	0.203	0.504	0.277	0.218	0.422	0.278	0.300
82.80	0.650	0.233	0.117	0.647	0.242	0.111	0.608	0.292	0.100	0.482	0.301	0.217
Aqueous Phase												
88.20	0.978	0.020	0.002	0.976	0.017	0.007	0.974	0.019	0.007	0.975	0.018	0.007
86.10	0.956	0.042	0.002	0.954	0.037	0.009	0.954	0.039	0.007	0.947	0.031	0.022
85.00	0.942	0.055	0.002	0.933	0.057	0.010	0.929	0.062	0.009	0.933	0.059	0.008
84.50	0.935	0.062	0.002	0.923	0.067	0.010	0.919	0.072	0.009	0.932	0.064	0.003
84.10	0.911	0.084	0.005	0.898	0.090	0.012	0.897	0.093	0.010	0.924	0.104	0.028
83.50	0.898	0.093	0.009	0.888	0.098	0.014	0.896	0.094	0.010	0.917	0.076	0.007
83.20	0.876	0.115	0.009	0.870	0.114	0.015	0.876	0.113	0.011	0.842	0.132	0.026
83.10	0.867	0.122	0.011	0.862	0.121	0.017	0.880	0.109	0.011	0.899	0.096	0.005
82.80	0.825	0.149	0.025	0.825	0.149	0.026	0.830	0.153	0.017	0.876	0.102	0.022
Vapour Phase												
88.20	0.619	0.139	0.243	0.628	0.111	0.260	0.618	0.120	0.262	0.627	0.113	0.260
86.10	0.556	0.217	0.227	0.580	0.194	0.226	0.569	0.205	0.227	0.433	0.362	0.206
85.00	0.532	0.274	0.194	0.541	0.268	0.192	0.530	0.276	0.194	0.407	0.355	0.238
84.50	0.521	0.300	0.178	0.528	0.292	0.180	0.520	0.298	0.182	0.415	0.367	0.218
84.10	0.493	0.340	0.167	0.500	0.340	0.159	0.501	0.339	0.160	0.407	0.379	0.214
83.50	0.496	0.344	0.160	0.498	0.345	0.158	0.501	0.342	0.157	0.460	0.372	0.168
83.20	0.481	0.368	0.151	0.488	0.367	0.145	0.488	0.367	0.145	0.345	0.472	0.183
83.10	0.481	0.374	0.145	0.485	0.372	0.143	0.491	0.364	0.145	0.321	0.520	0.159
82.80	0.471	0.387	0.141	0.476	0.383	0.141	0.471	0.394	0.135	0.473	0.387	0.140

Table 4.40: Results for SIG, TPI and TPDF methods on VLE ternary system of water (1)-ethanol (2) n-butyl acetate (3) at 760 mm Hg. Different sets of fixed values of feed composition were chosen outside heterogeneous region with various temperatures

z_1	z_2	T in $^{\circ}\text{C}$	Method	Phase I		Phase II		Phase III		No Phases
				x_1	x_2	x_1	x_2	y_1	y_2	
0.200	0.500	88.20	SIG	0.0851	0.2084	0.0851	0.2084	0.2163	0.5414	2
			TPI	0.1506	0.1542	0.5388	0.3817	0.3026	0.6892	3
			TPDF	0.0852	0.2083	0.0852	0.2083	0.2163	0.5414	2
0.200	0.600	86.10	SIG	0.1072	0.2867	0.1072	0.2867	0.2068	0.6207	2
			TPI	0.1822	0.1985	0.3300	0.5768	0.2138	0.6932	3
			TPDF	0.1073	0.2865	0.1073	0.2865	0.2003	0.6008	2
0.200	0.700	85.00	SIG	0.2031	0.6185	0.2031	0.6185	0.2041	0.7141	2
			TPI	0.0932	0.2201	0.2769	0.6985	0.0932	0.7063	3
			TPDF	0.2030	0.6187	0.2030	0.6187	0.2000	0.7002	2
0.200	0.500	84.50	SIG	0.1332	0.3019	0.1332	0.3019	0.2284	0.5842	2
			TPI	0.1797	0.2306	0.5534	0.4273	0.1843	0.6831	3
			TPDF	0.1332	0.3018	0.1332	0.3018	0.2284	0.5842	2
0.200	0.600	84.10	SIG	0.1236	0.3220	0.1236	0.3220	0.2039	0.6142	2
			TPI	0.1982	0.2190	0.3926	0.5760	0.2012	0.7549	3
			TPDF	0.1241	0.3216	0.1241	0.3216	0.2039	0.6142	2
0.250	0.650	83.50	SIG	0.2599	0.5566	0.2599	0.5567	0.2706	0.7024	2
			TPI	0.1664	0.2548	0.3736	0.5717	0.2087	0.6538	3
			TPDF	0.2595	0.5570	0.2595	0.5570	0.2500	0.6502	2
0.100	0.650	83.20	SIG	0.0704	0.3826	0.0704	0.3826	0.1078	0.7205	2
			TPI	0.1000	0.2687	0.2382	0.6483	0.3486	0.6500	3
			TPDF	0.0704	0.3826	0.0704	0.3826	0.1078	0.7204	2
0.150	0.750	83.10	SIG	0.1506	0.6786	0.1506	0.6787	0.1627	0.8123	2
			TPI	0.1360	0.7203	0.1935	0.2553	0.0698	0.7635	3
			TPDF	0.1504	0.6789	0.1504	0.6789	0.1500	0.7502	2
0.100	0.750	82.80	SIG	0.0775	0.4623	0.0775	0.4623	0.1047	0.7838	2
			TPI	0.0995	0.2881	0.1334	0.7424	0.1069	0.7426	3
			TPDF	0.0774	0.4624	0.0774	0.4624	0.1001	0.7508	2

4.5 Equilibrium Phase prediction at a fixed T & P

The tables below are the prediction results for the SIG, TPI and TPDF methods on the VLLE ternary systems measured and published by Younis et al. (2007). The predictions are based on given experimental temperature and pressure for a particular system without knowing the feed compositions. The summary of the results for the methods used are listed in table 4.41.

Table 4.41: Summary table for VLLE ternary systems shows Absolute Average Deviation (AAD) for SIG, TPDF and TPI predictions. These predictions are based on temperature and pressure

System	System NO.	Temperature range in °C	Pressure mmHg	Method	AAD		
					organic	aqueous	vapour
water-acetone-MEK	1	70.10-73.10	760	SIG	0.0159	0.0243	0.0118
				TPDF	0.0209	0.0160	0.0121
				TPI	0.0725	0.0163	0.0392
water-ethanol-MEK	2	71.20-73.20	760	SIG	0.0252	0.0495	0.0398
				TPDF	0.0302	0.0182	0.0330
				TPI	0.1379	0.0345	0.0926
water-acetone-n butyl acetate	3	45.10-59.00	360	SIG	0.0429	0.0161	0.0305
				TPDF	0.0173	0.0166	0.0304
				TPI	0.0779	0.0539	0.0516
	4	56.20-69.20	600	SIG	0.0361	0.0279	0.0367
				TPDF	0.0406	0.0352	0.0464
				TPI	0.2304	0.0539	0.1589
	5	66.10-86.10	760	SIG	0.0266	0.0283	0.0102
				TPDF	0.0270	0.0283	0.0100
				TPI	0.1144	0.0782	0.0519
water-ethanol-n butyl acetate	6	62.20-71.10	360	SIG	0.0579	0.2027	0.0903
				TPDF	0.0408	0.0446	0.0489
				TPI	0.0684	0.0681	0.0845
	7	74.20-81.00	600	SIG	0.0393	0.0608	0.0410
				TPDF	0.0200	0.0186	0.0288
				TPI	0.1386	0.0566	0.1144
	8	82.80-88.20	760	SIG	0.0363	0.0137	0.0164
				TPDF	0.0231	0.0152	0.0174
				TPI	0.1583	0.0898	0.1422

4.5.1 Water (1)–acetone (2)-MEK (3)

Table 4.42: VLLE prediction values for VLLE water (1)-acetone (2) MEK (3) system at 760 mmHg using SIG, TPI and TPDF methods

T in $^{\circ}\text{C}$	z_1	z_2	Method	Organic		Aqueous		Vapour	
				x_1	x_2	x_1	x_2	y_1	y_2
73.10	0.684	0.014	SIG	0.4107	0.0181	0.9523	0.0034	0.3421	0.0359
			TPI	0.3998	0.0184	0.9590	0.0089	0.3266	0.0279
			TPDF	0.4116	0.0181	0.9524	0.0034	0.3414	0.0419
72.60	0.709	0.028	SIG	0.4549	0.0546	0.9455	0.0110	0.3337	0.1140
			TPI	0.4606	0.0208	0.9473	0.0214	0.3173	0.0752
			TPDF	0.4599	0.0542	0.9458	0.0109	0.3356	0.0948
72.20	0.697	0.031	SIG	0.4544	0.0375	0.9444	0.0079	0.3289	0.0769
			TPI	0.4385	0.0649	0.9581	0.0101	0.3423	0.0926
			TPDF	0.4575	0.0527	0.9428	0.0112	0.3283	0.1102
71.80	0.720	0.041	SIG	0.4875	0.0649	0.9380	0.0147	0.3223	0.1383
			TPI	0.4940	0.0234	0.9426	0.0197	0.3041	0.1039
			TPDF	0.4877	0.0653	0.9381	0.0148	0.3223	0.1387
71.30	0.724	0.050	SIG	0.5098	0.0805	0.9309	0.0199	0.3148	0.1759
			TPI	0.5444	0.0325	0.9346	0.0197	0.2896	0.1438
			TPDF	0.5135	0.0800	0.9314	0.0197	0.3148	0.1743
70.90	0.735	0.057	SIG	0.5426	0.0906	0.9251	0.0242	0.3090	0.2029
			TPI	0.5395	0.0110	0.9313	0.0239	0.2784	0.1496
			TPDF	0.5353	0.0928	0.9249	0.0247	0.3089	0.2032
70.30	0.751	0.069	SIG	0.6051	0.1067	0.7334	0.0830	0.3018	0.2563
			TPI	0.4436	0.0134	0.9190	0.0303	0.2109	0.1593
			TPDF	0.5885	0.1095	0.9145	0.0332	0.3005	0.2526
70.10	0.757	0.072	SIG	0.6431	0.1018	0.7437	0.0814	0.2993	0.2573
			TPI	0.2037	0.1694	0.7713	0.0650	0.2670	0.1321
			TPDF	0.5966	0.1131	0.9101	0.0359	0.2973	0.2629

4.5.2 Water (1) –ethanol (2)-MEK (3)

Table 4.43: VLE prediction values for VLE water (1)-ethanol (2) MEK (3) system at 760 mmHg using SIG, TPI and TPDF methods

T in $^{\circ}\text{C}$	z_1	z_2	Method	Organic		Aqueous		Vapour	
				x_1	x_2	x_1	x_2	y_1	y_2
73.20	0.705	0.009	SIG	0.4594	0.0441	0.9432	0.0151	0.3389	0.0694
			TPI	0.1376	0.0901	0.8970	0.0016	0.5242	0.0429
			TPDF	0.4313	0.0463	0.9419	0.0166	0.3473	0.0198
72.80	0.726	0.021	SIG	0.5276	0.0460	0.9359	0.0159	0.3329	0.0661
			TPI	0.1584	0.0818	0.9005	0.0014	0.5164	0.0411
			TPDF	0.4954	0.0550	0.9344	0.0192	0.3382	0.0452
72.10	0.713	0.041	SIG	0.5190	0.0539	0.9137	0.0221	0.3222	0.0741
			TPI	0.4915	0.0547	0.9537	0.0029	0.4441	0.0626
			TPDF	0.5189	0.0575	0.9149	0.0231	0.3219	0.0791
71.60	0.695	0.055	SIG	0.5585	0.0686	0.5587	0.0686	0.3208	0.0922
			TPI	0.5704	0.0142	0.8608	0.0643	0.3627	0.0944
			TPDF	0.5692	0.0710	0.9024	0.0298	0.3206	0.0955
71.20	0.780	0.061	SIG	0.7441	0.0645	0.7778	0.0590	0.3086	0.1023
			TPI	0.3819	0.1001	0.7629	0.0748	0.7826	0.0667
			TPDF	0.6994	0.0690	0.7416	0.0633	0.3033	0.1045

4.5.3 Water (1) –acetone (2)-n-butyl acetate (3)

Table 4.44: VLLE prediction values for VLLE water (1)-acetone (2)-n-butyl acetate (3) system at 360 mmHg using SIG, TPI and TPDF methods

T in °C	z ₁	z ₂	Method	Organic		Aqueous		Vapour	
				x ₁	x ₂	x ₁	x ₂	y ₁	y ₂
59.00	0.560	0.122	SIG	0.1542	0.2121	0.9663	0.0313	0.3879	0.4499
			TPI	0.1750	0.2491	0.9451	0.0517	0.2998	0.6291
			TPDF	0.1604	0.2141	0.9661	0.0315	0.3878	0.4519
52.80	0.572	0.219	SIG	0.2121	0.3723	0.9321	0.0648	0.2820	0.6281
			TPI	0.2341	0.3668	0.9368	0.0560	0.2698	0.6413
			TPDF	0.2129	0.3727	0.9320	0.0648	0.2820	0.6287
49.40	0.572	0.271	SIG	0.2441	0.4457	0.9004	0.0955	0.2343	0.7047
			TPI	0.2451	0.4456	0.8745	0.1196	0.2512	0.6846
			TPDF	0.2441	0.4474	0.9003	0.0956	0.2343	0.7071
48.20	0.571	0.291	SIG	0.2582	0.4703	0.8847	0.1108	0.2189	0.7315
			TPI	0.2544	0.4736	0.8908	0.1073	0.2578	0.6974
			TPDF	0.2580	0.4707	0.8847	0.1108	0.2189	0.7319
46.20	0.569	0.324	SIG	0.2892	0.5031	0.8491	0.1451	0.1947	0.7697
			TPI	0.1719	0.5227	0.5902	0.3241	0.2924	0.6894
			TPDF	0.3322	0.4831	0.8525	0.1421	0.1953	0.7673
45.10	0.517	0.370	SIG	0.3140	0.5153	0.8205	0.1724	0.1821	0.7890
			TPI	0.2633	0.7143	0.8212	0.1720	0.2633	0.5572
			TPDF	0.4697	0.4295	0.8207	0.1722	0.1821	0.7892

Table 4.45: VLLE prediction values for VLLE water (1)-acetone (2)-n-butyl acetate (3) system at 600 mmHg using SIG, TPI and TPDF methods

T in $^{\circ}\text{C}$	z_1	z_2	Method	Organic		Aqueous		Vapour	
				x_1	x_2	x_1	x_2	y_1	y_2
69.20	0.553	0.163	SIG	0.1069	0.2016	0.9729	0.0268	0.3730	0.4452
			TPI	0.3799	0.5604	0.9052	0.0852	0.1004	0.8440
			TPDF	0.2709	0.1576	0.9851	0.0148	0.4716	0.3401
62.40	0.670	0.202	SIG	0.2847	0.3730	0.9419	0.0571	0.2700	0.6376
			TPI	0.2155	0.7830	0.9351	0.0637	0.1806	0.3823
			TPDF	0.2878	0.3717	0.9419	0.0570	0.2700	0.6385
60.30	0.674	0.223	SIG	0.3327	0.4050	0.9263	0.0721	0.2431	0.6861
			TPI	0.2155	0.7830	0.9351	0.0637	0.1806	0.3823
			TPDF	0.3359	0.4038	0.9263	0.0721	0.2431	0.6869
58.10	0.646	0.261	SIG	0.3881	0.4283	0.9031	0.0943	0.2172	0.7327
			TPI	0.2171	0.7327	0.9031	0.0943	0.1469	0.7747
			TPDF	0.3901	0.4272	0.9031	0.0943	0.2171	0.7331
56.50	0.657	0.276	SIG	0.4356	0.4343	0.8776	0.1185	0.1995	0.7636
			TPI	0.3597	0.6358	0.7853	0.2105	0.2788	0.6931
			TPDF	0.4367	0.4036	0.9098	0.0882	0.2168	0.7355
56.20	0.651	0.294	SIG	0.4452	0.4342	0.8715	0.1243	0.1963	0.7691
			TPI	0.2256	0.7456	0.5980	0.2939	0.1328	0.5497
			TPDF	0.4481	0.4323	0.8715	0.1243	0.1963	0.7693

Table 4.46: VLLE prediction values for VLLE water (1)-acetone (2)-n-butyl acetate (3) system at 760 mmHg using SIG, TPI and TPDF methods

T in °C	z ₁	z ₂	Method	Organic		Aqueous		Vapour	
				x ₁	x ₂	x ₁	x ₂	y ₁	y ₂
86.10	0.584	0.045	SIG	0.1819	0.0843	0.9908	0.0079	0.5906	0.1941
			TPI	0.1075	0.1129	0.6543	0.3211	0.6899	0.2031
			TPDF	0.1734	0.0766	0.9915	0.0072	0.5909	0.1827
82.10	0.585	0.084	SIG	0.1862	0.1510	0.9834	0.0152	0.5020	0.3193
			TPI	0.1410	0.1694	0.7984	0.0399	0.4746	0.4273
			TPDF	0.1915	0.1529	0.9833	0.0154	0.5019	0.3224
79.20	0.586	0.115	SIG	0.1966	0.2080	0.9764	0.0222	0.4444	0.4114
			TPI	0.1966	0.2079	0.7916	0.0416	0.4444	0.4114
			TPDF	0.2013	0.2093	0.9763	0.0224	0.4444	0.4122
77.00	0.589	0.141	SIG	0.2072	0.2524	0.9702	0.0284	0.4044	0.4736
			TPI	0.1608	0.2115	0.9380	0.0395	0.4122	0.5571
			TPDF	0.2097	0.2533	0.9701	0.0285	0.4044	0.4743
73.80	0.594	0.180	SIG	0.2289	0.3198	0.9591	0.0394	0.3514	0.5553
			TPI	0.1952	0.2299	0.9473	0.0451	0.4114	0.5841
			TPDF	0.2305	0.3209	0.9590	0.0395	0.3514	0.5562
71.30	0.601	0.212	SIG	0.2559	0.3740	0.9476	0.0507	0.3139	0.6133
			TPI	0.2076	0.2727	0.9548	0.0362	0.3870	0.5940
			TPDF	0.2556	0.3748	0.9476	0.0507	0.3139	0.6139
69.50	0.609	0.237	SIG	0.2824	0.4116	0.9369	0.0613	0.2889	0.6518
			TPI	0.2105	0.2969	0.9518	0.0411	0.4139	0.5789
			TPDF	0.2816	0.4124	0.9368	0.0613	0.2889	0.6524
68.00	0.618	0.256	SIG	0.3119	0.4398	0.9252	0.0728	0.2692	0.6825
			TPI	0.1608	0.6740	0.8810	0.1135	0.2960	0.4281
			TPDF	0.3109	0.4405	0.9252	0.0728	0.2691	0.6828
67.10	0.626	0.267	SIG	0.3345	0.4535	0.9163	0.0815	0.2578	0.7001
			TPI	0.1147	0.7993	0.9267	0.0687	0.2848	0.6692
			TPDF	0.3334	0.4542	0.9164	0.0815	0.2578	0.7003
66.40	0.632	0.276	SIG	0.3562	0.4615	0.9079	0.0898	0.2492	0.7137
			TPI	0.2397	0.6988	0.9069	0.0904	0.2397	0.6988
			TPDF	0.3548	0.4622	0.9080	0.0897	0.2492	0.7136
66.10	0.635	0.279	SIG	0.3669	0.4636	0.9037	0.0938	0.2455	0.7190
			TPI	0.6350	0.3099	0.6898	0.2513	0.2210	0.6550
			TPDF	0.3654	0.4645	0.9038	0.0937	0.2455	0.7193

4.5.4 Water (1)–ethanol (2)-n-butyl acetate (3)

Table 4.47: VLLE prediction values for VLLE water (1)-ethanol (2)-n-butyl acetate (3) system at 360 mmHg using SIG, TPI and TPDF methods

T in $^{\circ}\text{C}$	z_1	z_2	Method	Organic		Aqueous		Vapour	
				x_1	x_2	x_1	x_2	y_1	y_2
71.10	0.559	0.082	SIG	0.1443	0.0507	0.1449	0.0507	0.6313	0.0882
			TPI	0.1441	0.0521	0.8756	0.0821	0.5673	0.0035
			TPDF	0.1760	0.0382	0.9899	0.0099	0.6280	0.0876
68.20	0.593	0.094	SIG	0.2392	0.0683	0.2398	0.0683	0.6647	0.0996
			TPI	0.2427	0.0378	0.6827	0.0390	0.8744	0.0942
			TPDF	0.1972	0.1285	0.9669	0.0326	0.5887	0.1865
67.00	0.593	0.105	SIG	0.3459	0.0896	0.3756	0.0907	0.6733	0.1186
			TPI	0.2315	0.1819	0.9205	0.0783	0.5553	0.2477
			TPDF	0.2309	0.1832	0.9504	0.0486	0.5505	0.2519
66.00	0.597	0.147	SIG	0.2589	0.2329	0.9324	0.0660	0.5193	0.3055
			TPI	0.2153	0.2450	0.9452	0.0538	0.4627	0.3676
			TPDF	0.2656	0.2337	0.9322	0.0662	0.5192	0.3060
65.50	0.598	0.160	SIG	0.2799	0.2571	0.9217	0.0762	0.5038	0.3326
			TPI	0.5981	0.2372	0.7266	0.1292	0.6357	0.3150
			TPDF	0.2844	0.2576	0.9214	0.0764	0.5038	0.3331
65.00	0.606	0.184	SIG	0.3618	0.2082	0.6520	0.1775	0.5471	0.2641
			TPI	0.3052	0.2792	0.8763	0.1179	0.4920	0.3565
			TPDF	0.3066	0.2805	0.9090	0.0880	0.4884	0.3602
62.20	0.657	0.261	SIG	0.5751	0.3244	0.6301	0.2965	0.3987	0.5224
			TPI	0.4910	0.3013	0.9175	0.0556	0.4910	0.4364
			TPDF	0.6144	0.3040	0.6144	0.3040	0.3993	0.5202

Table 4.48: VLLE prediction values for VLLE water (1)-ethanol (2)-n-butyl acetate (3) system at 600 mmHg using SIG, TPI and TPDF methods

T in °C	z ₁	z ₂	Method	Organic		Aqueous		Vapour	
				x ₁	x ₂	x ₁	x ₂	y ₁	y ₂
81.00	0.591	0.045	SIG	0.2432	0.0215	0.2443	0.0215	0.6915	0.0527
			TPI	0.2207	0.0513	0.7623	0.0880	0.6061	0.1212
			TPDF	0.2220	0.0349	0.9887	0.0106	0.6099	0.1326
77.30	0.615	0.114	SIG	0.2813	0.1747	0.9457	0.0525	0.5126	0.2914
			TPI	0.2737	0.1746	0.8855	0.0623	0.5102	0.2941
			TPDF	0.2875	0.1765	0.9454	0.0528	0.5125	0.2926
76.10	0.613	0.134	SIG	0.3361	0.2318	0.9256	0.0716	0.4810	0.3460
			TPI	0.4724	0.3971	0.9493	0.0141	0.4713	0.5277
			TPDF	0.3371	0.2325	0.9254	0.0717	0.4810	0.3465
75.50	0.639	0.168	SIG	0.3727	0.2615	0.9121	0.0842	0.4652	0.3746
			TPI	0.4573	0.4834	0.8652	0.1259	0.3077	0.6882
			TPDF	0.3696	0.2620	0.9120	0.0843	0.4652	0.3749
75.10	0.645	0.176	SIG	0.3999	0.2803	0.9010	0.0944	0.4547	0.3943
			TPI	0.4467	0.5070	0.8152	0.1826	0.4258	0.5671
			TPDF	0.3952	0.2811	0.9009	0.0945	0.4546	0.3947
74.40	0.678	0.194	SIG	0.4552	0.3083	0.8747	0.1183	0.4357	0.4314
			TPI	0.5514	0.4474	0.8379	0.1530	0.3753	0.6211
			TPDF	0.4506	0.3095	0.8747	0.1183	0.4357	0.4316
74.20	0.738	0.195	SIG	0.4732	0.3144	0.8646	0.1273	0.4302	0.4427
			TPI	0.3852	0.6000	0.8537	0.1442	0.5654	0.4335
			TPDF	0.6889	0.2339	0.6889	0.2339	0.4354	0.4353

Table 4.49: VLLE prediction values for VLLE water (1)-ethanol (2)-n-butyl acetate (3) system at 760 mmHg using SIG, TPI and TPDF methods

T in °C	z ₁	z ₂	Method	Organic		Aqueous		Vapour	
				x ₁	x ₂	x ₁	x ₂	y ₁	y ₂
88.20	0.575	0.038	SIG	0.1816	0.0882	0.9684	0.0309	0.6252	0.1843
			TPI	0.3257	0.3366	0.8267	0.0061	0.3257	0.1597
			TPDF	0.1843	0.0618	0.9784	0.0209	0.6260	0.1150
86.10	0.480	0.096	SIG	0.2635	0.1289	0.9584	0.0403	0.5723	0.2075
			TPI	0.2906	0.2236	0.7257	0.0954	0.2906	0.4541
			TPDF	0.2666	0.1311	0.9581	0.0406	0.5722	0.2081
85.00	0.507	0.100	SIG	0.3075	0.1744	0.9424	0.0557	0.5409	0.2611
			TPI	0.4490	0.5463	0.6743	0.0868	0.2407	0.1814
			TPDF	0.3081	0.1754	0.9421	0.0560	0.5408	0.2616
84.50	0.506	0.099	SIG	0.3254	0.1953	0.9336	0.0641	0.5267	0.2860
			TPI	0.3629	0.4505	0.8969	0.0919	0.2188	0.2597
			TPDF	0.3288	0.1889	0.9367	0.0610	0.5338	0.2816
84.10	0.637	0.143	SIG	0.3485	0.2144	0.9257	0.0716	0.5153	0.3061
			TPI	0.2235	0.1973	0.7973	0.0669	0.4906	0.4962
			TPDF	0.3474	0.2147	0.9255	0.0717	0.5153	0.3064
83.50	0.646	0.163	SIG	0.3804	0.2425	0.9116	0.0847	0.4982	0.3370
			TPI	0.2648	0.2176	0.7801	0.0492	0.3850	0.5996
			TPDF	0.3791	0.2427	0.9115	0.0849	0.4981	0.3373
83.20	0.645	0.235	SIG	0.3990	0.2572	0.9033	0.0926	0.4896	0.3530
			TPI	0.2423	0.2194	0.8940	0.0022	0.5978	0.3551
			TPDF	0.4515	0.2596	0.9106	0.0861	0.5025	0.3466
83.10	0.580	0.245	SIG	0.4057	0.2623	0.9002	0.0954	0.4866	0.3585
			TPI	0.2599	0.1964	0.8009	0.0021	0.5427	0.4476
			TPDF	0.5129	0.2524	0.9189	0.0785	0.5169	0.3340
82.80	0.700	0.244	SIG	0.5754	0.3070	0.8652	0.1294	0.4671	0.4475
			TPI	0.2895	0.2694	0.6898	0.2043	0.6042	0.2918
			TPDF	0.6274	0.2853	0.8647	0.1297	0.4734	0.4059

4.6 Discussion on VLLE ternary systems

The main intention of this section of research has been to apply the TPI developed by Hodges et al. (1998) to recently available new VLLE ternary experimental data. Further tests examine the reliability and efficiency of this method in predicting the phase equilibrium for heterogeneous multicomponent systems.

In the application of the TPI method to VLLE binary systems, (τ) was defined as the part of the Tangent line bounded by the Gibbs energy curve (ϕ) and to minimise the Gibbs free energy, the (τ) function has to be minimised.

There are two independent variables in binary systems (α_1, α_2) when a 2-point search method is used. This number increases to three if the direct 3-point search method is used. However applying the TPI to ternary systems is more complicated than binary systems, as the tangent changes to a 2D area of intersection with the (ϕ) surface in a 3D composition space; in this environment the (τ) function has to be minimised.

The number of variables required in a ternary 3-phase search increases to six $(\alpha_1, \alpha_2, \alpha_3, \theta_1, \theta_2$ and $\theta_3)$, where α_i represents the length of an arm extending from the feed composition (z_i) at an angle (θ_i) . The Nelder-Mead algorithm is constrained to search for optimum values for both variables (α_i is constrained to stay in the physical composition space and θ_i values in a range of (0-360)). The tangent plane now represents the area of a 2D composition plane and the slopes of this tangent plane (m_{1TP}, m_{2TP}) are determined by solving the objective function $(\tau = \tau + \Delta\tau)$. The Nelder-Mead technique requires a set of initial values to set up the simplex. The minimisation algorithm evaluates the value of the (τ) function for a number of iterations and generates new variables based on four coefficient factors (reflection, expansion, contraction and shrinkage). This process reduces the function value to zero by rejecting the largest value and replacing the variables with new evaluated values. The initial composition and the feed composition are used to calculate the starting values for these variables (α_i, θ_i) . If the (τ) value is reduced to zero, this indicates solutions have been found and the global Gibbs free energy is at the minimum

level. The Nelder-Mead minimisation procedure is explained in a previous chapter (3.12) and its algorithm can be found in appendix C.

The $\Delta\tau$ for ternary systems now takes the form of the following equation;

$$\Delta\tau = h_1\sqrt{(1 + (m_{1TP})^2)} h_2\sqrt{(1 + (m_{2TP})^2)} \quad (4.9)$$

where h_1 and h_2 are the width of a unit of the search grid, m_{1TP} and m_{2TP} are the slopes of the tangent plane.

4.6.1 Application of the TPI and TPDF methods on artificial ternary systems

Shyu et al. (1995) designed two hypothetical ternary systems using the Margules excess Gibbs energy model which is based on three binary constants. Initially the TPI method was applied to these two ternary 3-phase systems (artificial test systems; 1 and 2 of Shyu et.al (1995)), at a grid size (100x100) using fixed initial compositions and various (z_1, z_2) overall feed compositions.

TPI requires the division of the composition space into a number of grids. A number of sets of the grid were tested in a range of (50-500). It was found that using the small grid number produces $\tau > 0$ and the large number greatly increases the computational time without further improvement in the results. This work has selected the optimum grid number (100 x100). When the selected grid failed in producing $\tau = 0$ solution, the number was increased to a higher value. Figure 4.18 shows various grid numbers versus overall AAD for composition for both systems of Shyu et al. (1995).

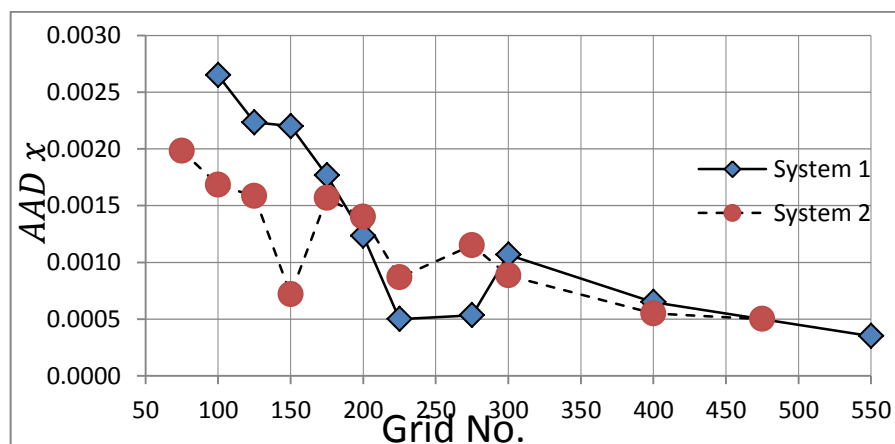


Figure 4.18: A plot of the grid number against the Absolute Average Deviation for composition for the artificial systems of Shyu et al. (1995)

The method was applied by calculating the initial values of the distance between the corners of the 3-phase region (α_1 , α_2 and α_3) and the respective angles of the length variables (θ_1 , θ_2 and θ_3). The Nelder-Mead optimisation simplex minimised the (τ) function by allowing six variables to be adjusted simultaneously. The Margules excess Gibbs energy expression was used in both systems, the values of the binary constants which appear in the equation were given by Shyu et al. (1995):

$$\frac{G^E}{RT} = 2.8x_1x_2 + 3.4x_1x_3 + 2.5x_2x_3 \quad \text{system1} \quad (4.10)$$

$$\frac{G^E}{RT} = 3.6x_1x_2 + 2.4x_1x_3 + 2.3x_2x_3 \quad \text{system2} \quad (4.11)$$

$$\phi = \frac{G^E}{RT} + \sum_i^n x_i \ln x_i \quad (4.12)$$

Where ϕ is the reduced Gibbs energy of the mixture and the global minimum of ϕ solution has to be found. Tables 4.18 and 4.19 show the results for systems 1 and 2. The tables show the solution of Shyu et al. (1995) and the predicted composition values using the TPI method. The predicted values agree up to three decimal places when compared with their results.

It was found that adjusting six variables using Nelder-Mead made the simplex sensitive to the initial values. A set of initial values to start the Nelder-Mead optimisation simplex were chosen in a systematic way based on the intuitive knowledge of actual data. It was discovered that for a range of initial values the algorithm failed to predict the correct number of phases and converged to unrealistic values when compared to Shyu et al. predictions. It was believed that this problem could be solved by regrouping the variables into two main groups (α_i and θ_i) and changing the algorithm to adjust the first group while the second is fixed and vice versa until the τ solution reaches zero (Hodges 1998). However applying the TPI method on both artificial systems using the regrouped variable method did not have any effect on the sensitivity issue but increased the computational time in the minimisation procedure. By inspection

of these initial values shown in tables (4.18 & 4.19), a set of values was selected to start the Nelder-Mead simplex and conclusions were drawn about the behaviour of the TPI method. The necessity of a systematic approach to the selection of Nelder-Mead initial values emphasised by this work and a systematic approach is proposed for real systems later in this chapter.

Two different sets of feed compositions were selected for both systems; the values of the first set were inside the 3-phase region and the second sets of values were outside the 3-phase region. The TPI test results for the first region showed that the prediction values are in the 3-phase heterogeneous region. It was noticed that the TPI method procedure could converge to solutions that gave two identical phase compositions when the feed compositions were outside the 3-phase region. In this case the objective function produced shows $\tau > 0$.

When the feed compositions are outside the 3-phase region, the results indicate that the TPI predictions are consistent with a 2-phase region. However, according to the phase diagram published by Shyu et al. (1995) for these systems, some of these feed compositions are in the single phase region which TPI fails to identify. These results show that the TPI method is capable of differentiating between 3-phase and 2-phase regions. But there are problems over the whole phase range.

In order to apply the TPDF method on both hypothetical systems, the excess Gibbs energy equation should be changed to an activity coefficient form because the TPDF Gibbs free minimisation function suggested by Michelsen(1982 a) takes the following form:

$$\frac{F(y)}{RT} = \sum_i y_i (\ln y_i + \ln \gamma_i(y) - \ln z_i - \ln \gamma_i(z)) \quad (4.13)$$

The simplified Margules equation for excess Gibbs energy for a ternary system is based on consideration of the three components being chemically similar and the assumption that they have similar molecular size. The equation has three binary constants (A_{12} , A_{13} & A_{23}):

$$\frac{g^E}{RT} = A_{12} x_1 x_2 + A_{13} x_1 x_3 + A_{23} x_2 x_3 \quad (4.14)$$

The activity coefficients equations given by Prausnitz et al. (1998) are:

$$\ln \gamma_1 = A_{12}x_2^2 + A_{13}x_3^2 + (A_{12} + A_{13} - A_{23})x_2x_3 \quad (4.15)$$

$$\ln \gamma_2 = A_{12}x_1^2 + A_{23}x_3^2 + (A_{12} + A_{23} - A_{13})x_1x_3 \quad (4.16)$$

$$\ln \gamma_3 = A_{13}x_1^2 + A_{23}x_2^2 + (A_{13} + A_{23} - A_{12})x_1x_2 \quad (4.17)$$

When the TPDF method was applied to both theoretical systems of Shyu et al. (1995), with a set of feed composition values inside the 3-phase region, it was discovered that the method predicts two phases instead of three. Shyu used an activity coefficient based model and he represented activity data using the second order Margules equation. When this equation is used to predict activity coefficients, the form of the equation is such that it can only predict regular systems behaviour and is not capable of representing or predicting two phase liquid behaviour. If a more advanced form of the Margules equations had been used, then these equations would have required more constants than were available from the work of Shyu et al. For this reason no further attempt was made to apply the TPDF method to Shyu et al. systems.

However testing the TPI method with various feed compositions based on selected values inside the 3-phase region showed that this method was capable of finding a zero τ solution for these hypothetical ternary 3-phase systems of Shyu. Further tests were required on 3-phase real systems to validate the above statement and examine the problem relating to sensitivity to the initial values.

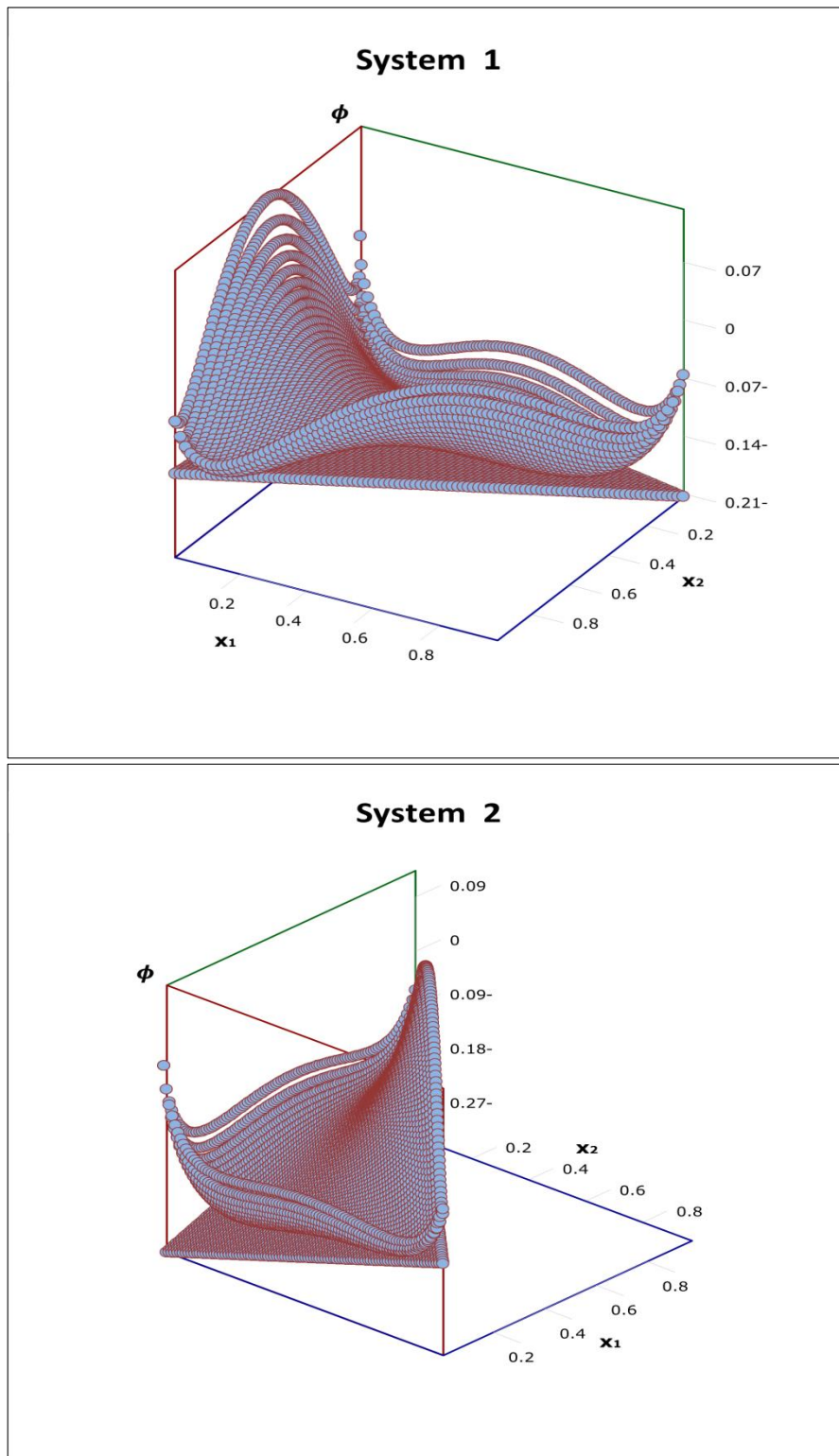


Figure 4.19: A plot showing Gibbs energy surface and the tangent plane under the surface for two ternary 3-phase systems of Shyu et al. (System 1 & System 2)

Figure 4.19 shows the Gibbs energy surface (ϕ) for the LLE ternary artificial systems of Shyu et al. (1995). Note that, in contrast to a binary, the ϕ curve is now a surface in a 3 dimensional composition space. The tangent plane (shaded triangle) lies under the Gibbs energy surface and the Global solution is

obtained when τ is zero. It is important to observe the difficulty of locating the boundaries between these phases. The initialisation procedure used in the binary system based on the location of phase boundaries is difficult to apply to 3-phase ternary systems. In the binary VLE phase calculations for the majority of the heterogeneous systems, the vapour phase lies between two other liquid phases on the ϕ curve. Sometimes the location of the boundaries on the Gibbs energy surface is not clearly defined, particularly in these types of LLE hypothetical mixtures and a mathematical approach to find the phase boundaries is not available, especially when the activity coefficient model (Margules) is used in describing the Gibbs energy surface.

In terms of applying the TPI and TPDF methods to real systems it should be noted that Shyu only worked in theoretical phases and did not identify the nature of the phase. The following work clearly works with vapour-liquid-liquid systems.

4.6.2 The sensitivity of TPI method to initial values

One of the deficiencies of the TPI method when used in conjunction with the Nelder-Mead simplex was found to be its sensitivity to the initial values. This was found when applying the method to VLLE binary systems (Section 4.3.1). An Initial attempt to judge the effect of the starting values on the performance of the TPI method on ternary VLLE data was carried out on three ternary systems.

The TPI method was applied to the VLLE data for water(1)-acetone(2)-methyl ethyl ketone(3) system [system 1] at 760 mmHg and six different temperatures (range between 73.10 - 70.10 °C). The minimisation procedure (Nelder-Mead simplex) allowed the adjustment of the six variables (α_i, θ_i) simultaneously. The PRSV+WSMR was used to represent the Gibbs energy of the system utilising the parameters obtained (table: 4.21) from 3-phase flash calculations.

This work has investigated the effect of different initial values on the performance of the TPI method in ternary VLLE for the stated system. The initial composition of the first component (water) is increased by (0.01 or 0.02) increments whilst the second composition (acetone) is fixed at 0.01. This scheme was applied to all the phases. Table (4.23) shows the initial values in each phase at specified temperatures and the corresponding results of the TPI method in absolute differences $[\Delta x_i = |x_i^{exp} - x_i^{pred}|]$, where *exp* is experimental and *pred* is predicted using the TPI method. It can be seen from table (4.23) that 10 different sets of initial values were used for each data point.

Observing the initial values used in table (4.23) and the final results of the TPI method, it is obvious that if the initial values are closer to the actual solution the differences, Δx_i , are smaller and better results are produced. If the initial values are not close to the actual solution the TPI simplex usually converges to an incorrect solution for the stated physical conditions. The main reason for this behaviour, as found by previous researchers (Hodges et al., 1998), is the flattened shape of the (ϕ) surface around the solution compositions which allows a zero τ solution to be obtained in areas which are significantly different to the actual solution. Figure (4.20) shows the change of the Δx_1 versus the

starting values used for all the phases at two different temperatures (73.10 °C & 72.60 °C) for system 1.

The initialisation scheme previously outlined was applied to VLLE water (1) ethanol (2) methyl ethyl ketone (3) [system 2] at three different temperatures and a pressure of 760 mmHg. The TPI prediction results with the starting values are listed in table (4.26) for this system. Figure (4.21) shows the difference between experimental and predicted composition values (Δx_1) for the first component at each set of initial values used for system 2 at two different temperatures (73.20°C & 72.80°C). It is obvious that the relationship between predicted results for the TPI method and the initial values is proportional. As the set of initial values shifts closer to the expected solution so the TPI results also shift closer to the actual solution.

The third system tested was VLLE water (1)-acetone (2)-n-butyl acetate (3) at six different temperatures and a pressure of 360 mmHg. Table (4.29) shows the results of the TPI method with the starting values. Results for this system were found to be similar to those of other systems which were investigated when examining the TPI method for sensitivity issues.

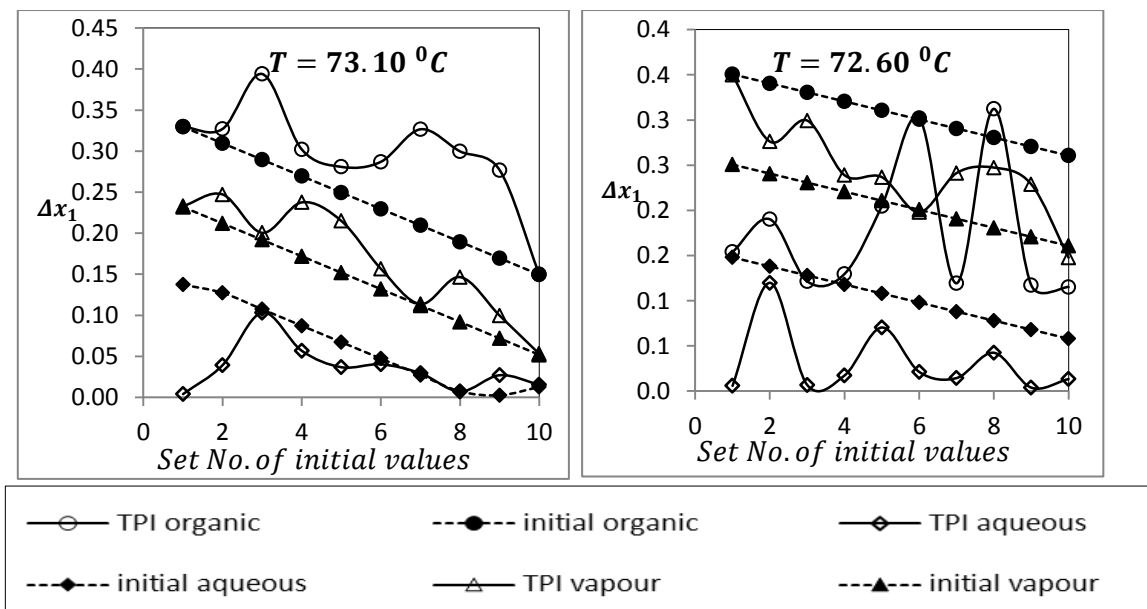


Figure 4.20: TPI method predictions for 10 sets of initial values of VLLE water (1)-acetone (2)-MEK (3) at temperature 73.10 & 72.60°C and pressure of 760 mmHg. The solid line represents TPI values and the dotted line the initial values

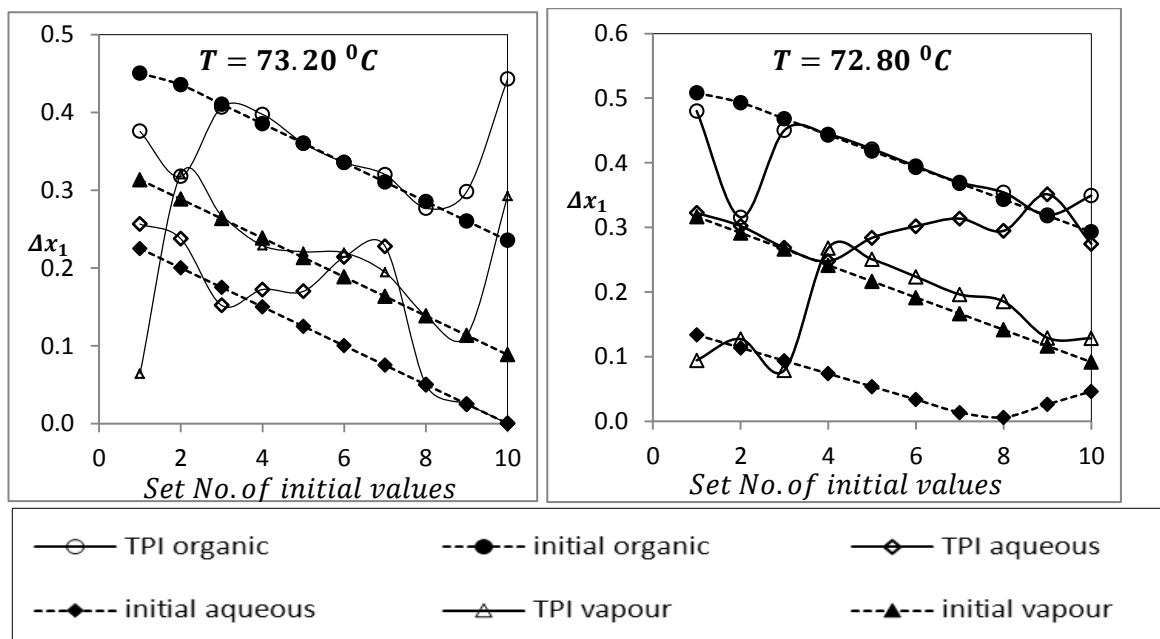


Figure 4.21: TPI method predictions for 10 sets of initial values of VLE water (1)-ethanol (2)-MEK (3) at temperature 73.20 & 72.80°C and pressure of 760 mmHg. The solid line represents TPI values and the dotted line the initial values

The prediction results for the TPI method are more accurate for the third system when compared to the other two systems. Figures (4.22, 4.23 & 4.24) show the Gibbs energy surface(ϕ), tangent plane and the predicted equilibrium compositions for all phases (the 3-phase Systematic Initial Generator used to calculate the starting compositions) for all three systems respectively. By visual observation of these graphs the location of the equilibrium points for the organic and vapour phases can be seen for system 1 & 2, these points are on the phase boundaries. For system 3 the minima on the ϕ curve are more clearly defined and hence it is easier to fix the correct position for the tangent plane. The distribution of the points on system 3 are spread wide and not on the edge of the phase boundaries. For this reason the TPI method produces smaller AAD for system 3 when compared to the AAD for other systems. This could be the main reason behind the failure of the TPI found throughout this work.

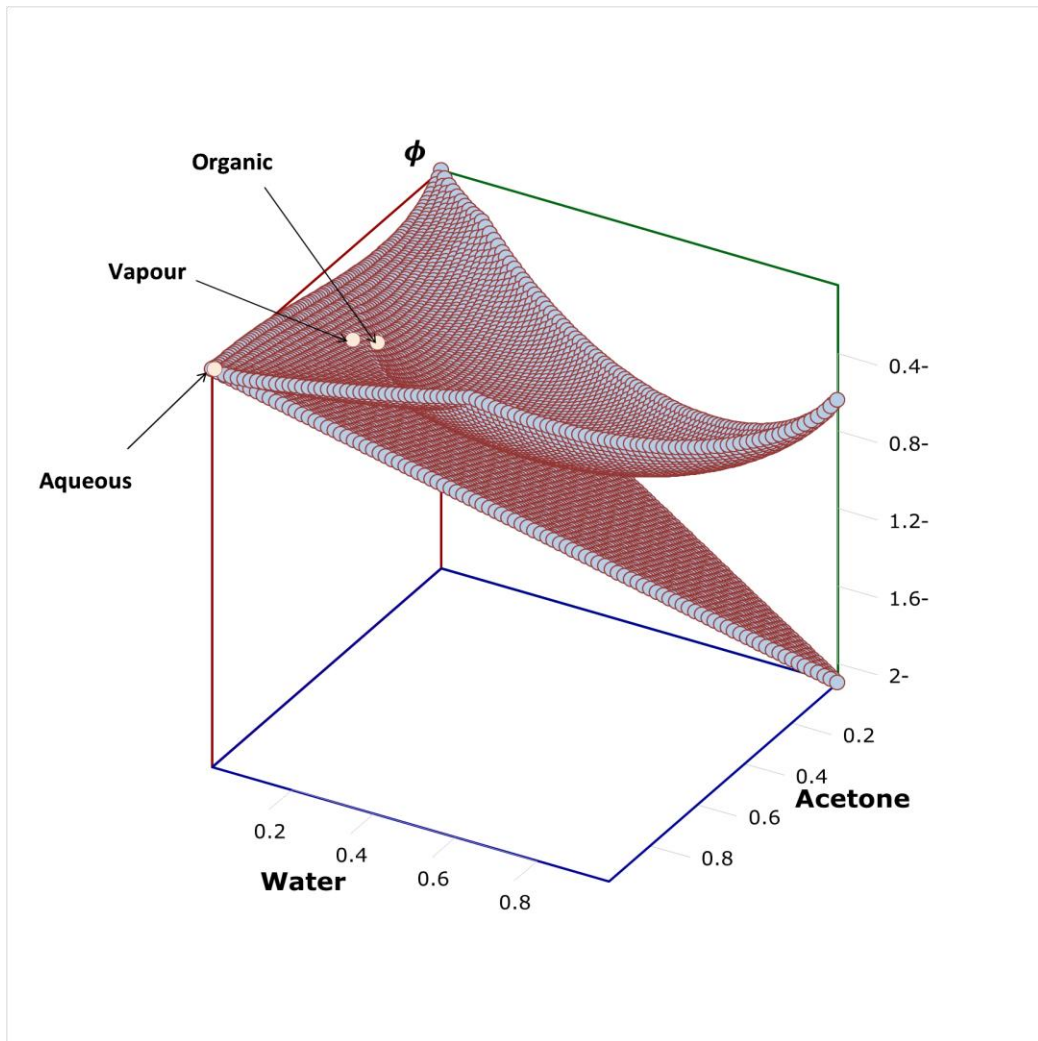


Figure 4.22: Gibbs energy surface (ϕ) with the tangent plane under the ϕ surface is intersecting in three stationary points for the VLLE water(1)-acetone(2)-MEK system at 760 mmHg and temperature of 73.10⁰C

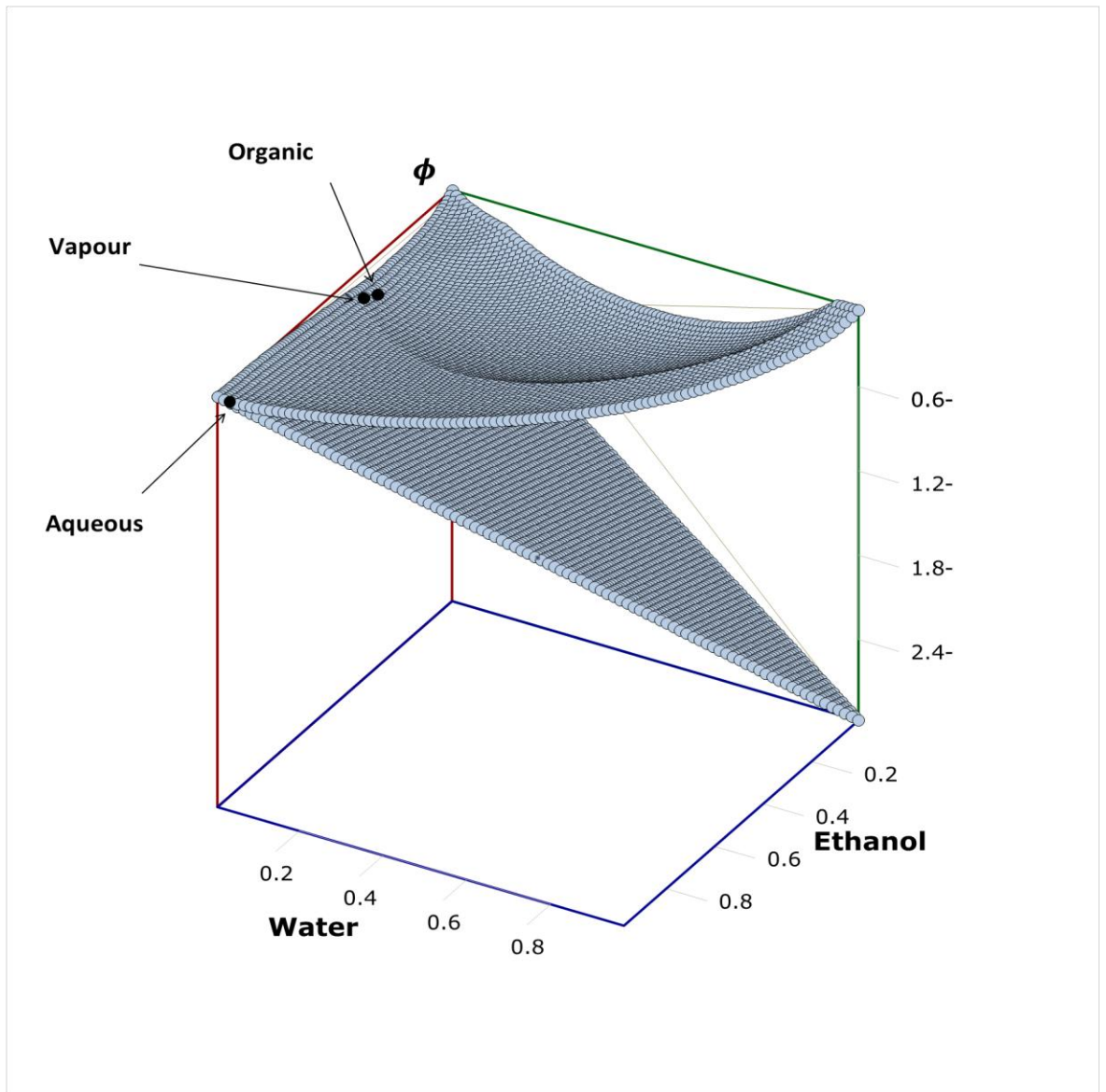


Figure 4.23: Gibbs energy surface (ϕ) with the tangent plane under the ϕ surface is intersecting in three stationary points, for the VLLE water(1)-ethanol(2)-MEK system at 760 mmHg and temperature of 73.20°C

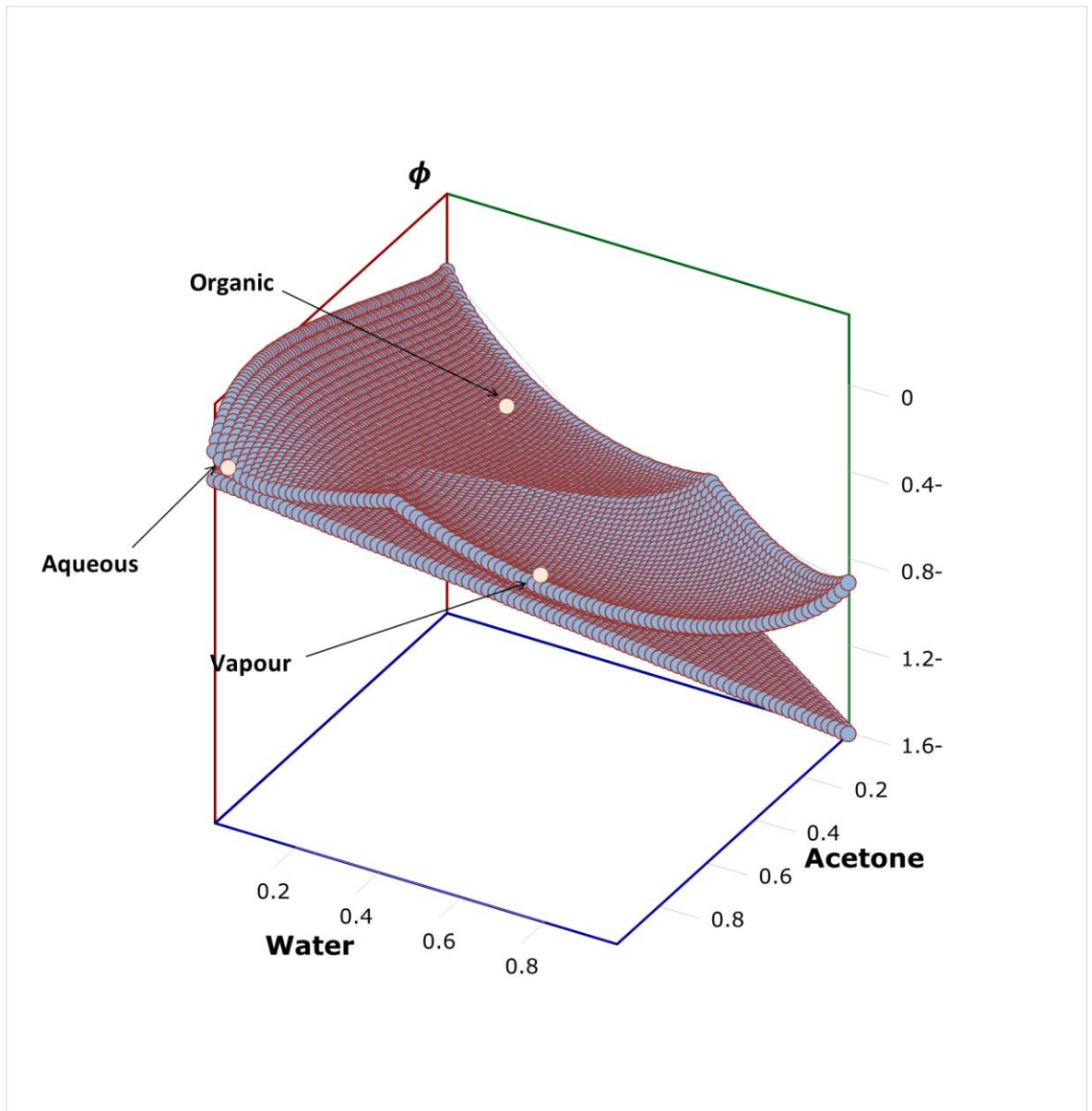


Figure 4.24: Gibbs energy surface (ϕ) with the tangent plane under the ϕ surface is intersecting in three stationary points for the VLLE water(1)-acetone(2)-n-butyl acetate system at 360 mmHg and temperature of 59.00°C

Another suggested possible reason for the TPI sensitivity issue is the fact that the objective function to be minimised (τ) might have many local minima which increases the possibility for the minimisation simplex to converge to zero resulting in incorrect phase equilibrium composition values.

To overcome this problem of initial value sensitivity an algorithm has been developed which generates values close to the real solution (Systematic Initial Generator).

4.6.3 Systematic Initial Generator (SIG)

The sensitivity of the TPI method to initial values is due to the method of formulating this mathematical problem (Gibbs energy minimisation). The main idea of the TPI method suggested by Hodges et al. (1998) is the calculation and minimisation of a hyper-tangent plane that is bounded by Gibbs energy surface quantity (τ) via the repeated search of a tangent distance function $F(x)$ value to adjust the tangent position in relation to the (ϕ) surface.

In the literature survey section (2.5), it is clearly outlined that in Gibbs minimisation methods of phase equilibrium calculations there is a possibility for the optimisation to converge to a trivial or local rather than a global solution, when a poor initial estimate is supplied. Many researchers have related this problem to the non-convex non-linear properties of the objective function with several local minima. The survey also concluded that the methods and strategies selected depend on the type of phase calculations (LLE, VLE, and VLLE), complexity of the systems (level of non-ideality) and the operating conditions (temperature and pressure).

In phase equilibrium calculations on VLE hydrocarbon systems at low and moderate pressures, Michelsen (1982 b) used two sets of initial estimates which are calculated from a relative volatility (K-factor) expression using the Wilson correlation. (See literature survey section (2.5.1)). This initial estimation is based on the critical pressure, critical temperature and acentric factor for pure component at the system temperature. Other researchers suggested a different initialisation scheme for the LLE calculation on ternary systems; however the initialisation scheme for VLLE multi-component calculations for the polar non-ideal systems of interest has not been thoroughly investigated.

Some of the initialisation methods rely on a 2 phase stability test and phase split as an initial estimate for 3 phase calculations; however the direct initialisation method for VLLE multicomponent heterogeneous systems (in particular the systems investigated in this work) is not covered in the literature. For this reason and in an attempt to improve the reliability of the TPI method for 3-phase calculations of ternary systems, this work suggests and applies a direct initialisation algorithm for VLLE multicomponent systems. The details of the

suggested method of initialisation can be found in the theory section (3.11.2). This work has adopted the VLLE initialisation method for 3-phase flash calculations. This method combines the LLE and VLE initialisation strategies using UNIQUAC as an activity coefficient model, PRSV+WSMR as EOS and the Rachford-Rice equation as a 3-phase flash calculation. The main objective function in the algorithm minimises relative volatilities of the component in the mixture.

The initialisation method developed in this work was applied to the VLLE ternary data for the systems listed at the beginning of this section. The systematic initial values have a positive effect on the final results for the TPI method. The SIG apparently supplies the TPI method with more realistic and logical starting values.

The effect of SIG can be seen for system 1: water (1)-acetone (2)-MEK (3) at 760 mmHg; when the results for the TPI method (Δx_i) in table (4.22) are compared to (Δx_i) in table (4.23). The prediction results for the TPI method with embedded SIG are significantly improved if compared to the results when arbitrary initial values are used. This statement can be applied to the other systems investigated. Tables (4.25, 4.26) and (4.28, 4.29) show the results for system 2: water (1)-ethanol (2)-MEK (3) at 760 mmHg and system 3: water (1)-acetone (2) - n-butyl acetate (3) at pressure of 360 mmHg respectively.

This section shows that the accuracy of the final prediction results for the TPI method strongly depends on initial estimates. This has been demonstrated when a number of sets of initial values were tested using the TPI method on three VLLE ternary systems at different temperatures. At each temperature data point 10 sets of initial values were used to measure the sensitivity of the TPI method. The effects of the Systematic Initial Generator on the final results of the TPI method have been demonstrated.

This research has also examined another Gibbs minimisation method suggested by Michelsen known as Tangent Plane Distance Function (TPDF).

4.6.4 Application of the Tangent Plane Distance Function for prediction of 3 phase equilibrium

The concept of the tangent plane criterion by Michelsen (1982) was used in testing the thermodynamic stability of a phase, to estimate the number of phases present at equilibrium. Considering a multicomponent mixture at a fixed temperature and pressure with mole fraction (z_1, z_2, \dots, z_n) split into M number of phases, the thermodynamic criterion for the stability of this mixture is that the Gibbs energy should be at a global minimum. The Gibbs energy can be written in terms of chemical potential as explained in the theory section (3.10), hence the change of energy for such a mixture is described in the form of fugacity coefficients (Michelsen 1982) and the equation used is as follows:

$$\frac{F(y)}{RT} = \sum_i y_i (\ln y_i + \ln \phi_i(y) - \ln z_i - \ln \phi_i(z)) \quad (4.18)$$

As shown in figure (4.25) $F(y)$ is the vertical distance from the tangent line to the (ϕ) surface at a feed composition to the (ϕ) surface at composition y . To find the stationary points (equilibrium points) the above equation should be minimised simultaneously for all the phases present in the equilibrium, whilst the sum of the mole fraction for each phase must equal one.

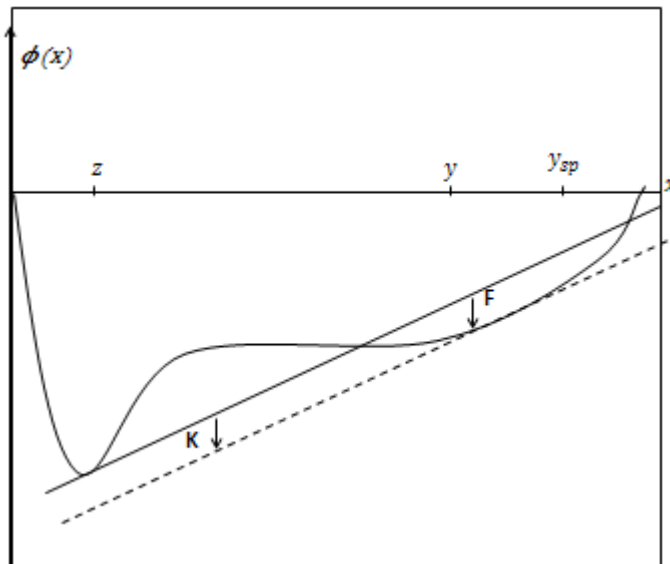


Figure 4.25: Gibbs energy of mixing for a hypothetical binary system showing the tangent line at feed composition (z) and tangent distance F at trial composition (y) and the parallel tangent at the stationary point

This work has applied the TPDF method in the form of fugacity coefficients suggested by Michelsen (1982) and expressed in equation 4.16, for the

prediction of VLLE for all the ternary systems previously cited. The TPDF method was tested for sensitivity issues and the same initial values used for the TPI were also used here.

The subsequent results were compared with the TPI method. Tables (4.23, 4.26 and 4.29) show the TPI and the TPDF results for three VLLE systems investigated. These tables show at each temperature a set of 10 different initial values used and the $[\Delta x_i = |x_i^{exp} - x_i^{pred}|]$ calculated from the predictions using both methods.

Analysis of these tables shows that the TPDF predictions give consistently more satisfactory results when compared to the TPI method which produces significantly less accurate results. The Absolute Average Deviation (AAD) was 0.004 from the experimental data for the water (1) acetone (2)-MEK (3) [system 1] compared to an AAD for the TPI method of 0.128. The results for system1 are presented in table (4.23). The TPDF predictions for VLLE water (1)-ethanol (2)-methyl ethyl ketone (3) [system 2] at 760 mmHg can be seen in table (4.26) and the AAD for this system is 0.01, compared to an AAD of the TPI of 0.175 for the same system. Table (4.29) contains the TPDF and the TPI results for VLLE water (1) acetone (2)-n-butyl acetate (3) [system 3] at 360 mmHg and the AAD for all data points is 0.017 and 0.096 for TPDF and TPI respectively. It can be seen that the AAD values produced by both methods are relatively low. This is consistent with the nature of the ϕ surface for the systems which have been discussed previously. The AAD values for the three systems studied indicate that the TPDF method is more effective than the TPI method in prediction of phase equilibrium compositions for heterogeneous high polar systems based on the known experimental data. In addition a positive feature of the TPDF method is it is less sensitive to the initial values which make this method efficient and reliable in the prediction of phase equilibria.

4.6.5 The SIG ,TPI and TPDF as Phase predictors

The TPI, TPDF and SIG were tested on the four ternary VLE systems of Younis et al. (2007) at a specific temperature and at a system pressure with different sets of overall feed composition outside the 3-phase region. The TPI initial starting values were obtained from SIG results. The results for these methods as phase predictor for four systems are shown: in table (4.24) for water (1)-acetone (2)-MEK (3) at pressure of 760 mmHg, in table (4.27) for water (1)-ethanol (2)-MEK (3) at pressure of 760 mmHg, in tables: (4.30,4.32 and 4.34) for water (1)-acetone (2)-n-butyl acetate (3) at pressures of 360, 600 and 760 mmHg respectively and in tables (4.36, 4.38 and 4.40) for water (1)-ethanol (2)-n-butyl acetate (3) at pressures of 360, 600 and 760 mmHg respectively.

The results indicate that the SIG and TPDF methods can predict the number of phases when the feed composition is outside the 3-Phase region (by producing the single liquid phase composition). However the TPI is not capable of identifying the 2-phase region even though the TPI starting values were obtained from the SIG which had already indicated the 2-phase region. The reason for the failure of the TPI to predict the correct number of phases is due to the search pattern of the TPI algorithm using the angle variable (θ_i) which is related to the length variable (α_i). Each angle is related to a phase which rotates between (0 - 360) degrees and for the TPI to converge to a 3-phase solution each angle has to be constrained in a range of values dependant on the prior knowledge of the heterogeneous system whilst the (α_i) values were constrained between (0 -1).

The TPDF method was used as a phase predictor by testing a number of sets of values of feed compositions outside the 3-phase region. The results indicate a single liquid phase with compositions which differ from the feed composition values for both of these systems of water-acetone-n-butyl acetate and water-ethanol-n-butyl acetate. However the TPDF method displayed unpredictable behaviour only outside the 3-phase region for the two systems water-acetone-MEK and water-ethanol-MEK. The values of the single liquid phase results were the same as the feed compositions. When an attempt at convergence for this method was further explored it was found that the method pushed the initial

values to a range of different values but for these systems the values always returned to the feed composition values initially supplied. It should be noted that this behaviour was not observed for systems containing water-n-butyl acetate, for these systems the TPDF method converged to results correctly predicting the phases present.

For the systems containing the water-MEK binary, the TPDF method was capable of correct phase predictions when the initial feed compositions lay within the heterogeneous region. The problem with this system only arose when the initial values lay outside the known heterogeneous region. It appears that the representation of the ϕ curve for systems containing the MEK-water binary is of such a nature that the TPDF method is not able to easily recognise the phase boundaries. This aspect of these systems requires further research and analysis.

A sub-procedure was developed based on minimisation of relative volatility values (K_i) in the Flash calculation. The values of phase compositions of the TPDF method were used as initial values for this calculation and the K_i are calculated and stored. The fractions of molar rate of organic and aqueous liquid phases were calculated in an internal loop then the new values of K_i were calculated and compared with the stored values $|K_i^{old} - K_i^{new}|$ and the value (10^{-5}) of the absolute difference was used as the stopping condition. The use of the additional sub-procedure has improved the reliability of the TPDF as a phase predictor.

4.6.6 The Flash ,TPI and TPDF Phase Equilibrium results

The VLLE flash calculation was applied to the ternary systems of interest and the parameters obtained were used in the SIG, TPI and TPDF prediction methods for VLLE phase equilibrium calculations. A set of feed compositions were chosen inside the 3-Phase heterogeneous region for each experimental temperature which lies on the experimental tie line. The results of the Flash , TPI and TPDF for these ternary systems can be found in: table (4.22) for water (1)-acetone (2)-MEK (3) at pressure of 760 mmHg , table (4.25) for water (1)-ethanol (2)-MEK (3) at pressure of 760 mmHg ,tables (4.28,4.31 and 4.33) for water (1)-acetone (2)-n-butyl acetate(3) at pressures of 360, 600 760 mmHg

respectively and tables (4.35,4.37 and 4.39) for water (1)-ethanol (2)-n-butyl acetate(3 at pressures of 360, 600 760 mmHg respectively. As mentioned the UNIQUAC parameters and PRSV EOS interaction parameters are obtained from flash calculation at isobaric condition for each VLE ternary system.

By applying the TPI to real systems, it was found that, if the angles lay in a range (0-360) degrees, the TPI minimisation procedure converges to a trivial solution. This behaviour was not apparent when the TPI method was applied to the artificial hypothetical systems; however, for the real systems studied the different behaviour of the TPI is probably due to the nature of the Gibbs energy surface which has a flattened shape which does not allow the global minima to be clearly defined. This is linked to the problems highlighted in the previous paragraph where the angle changes in the method and TPI cannot detect the flattened structure. In contrast the global minima of the ϕ surface for the artificial systems of Shyu et al. are better defined and the TPI method is capable of finding these minima.

The graphical representation for the VLE flash calculation and the TPI and TPDF predictions compared with experimental data for each ternary system of Younis et al. (2007) can be seen in the following figures; the symbols used in these ternary plots are: [◆: exp. organic, ◇:pred. organic, ●: exp. aqueous, ○: pred. aqueous, ▲: exp. vapour, △: pred. vapour], where “exp” is experimental and “pred” is predicted values.

1. water (1)-acetone (2)-MEK (3) at 760 mmHg

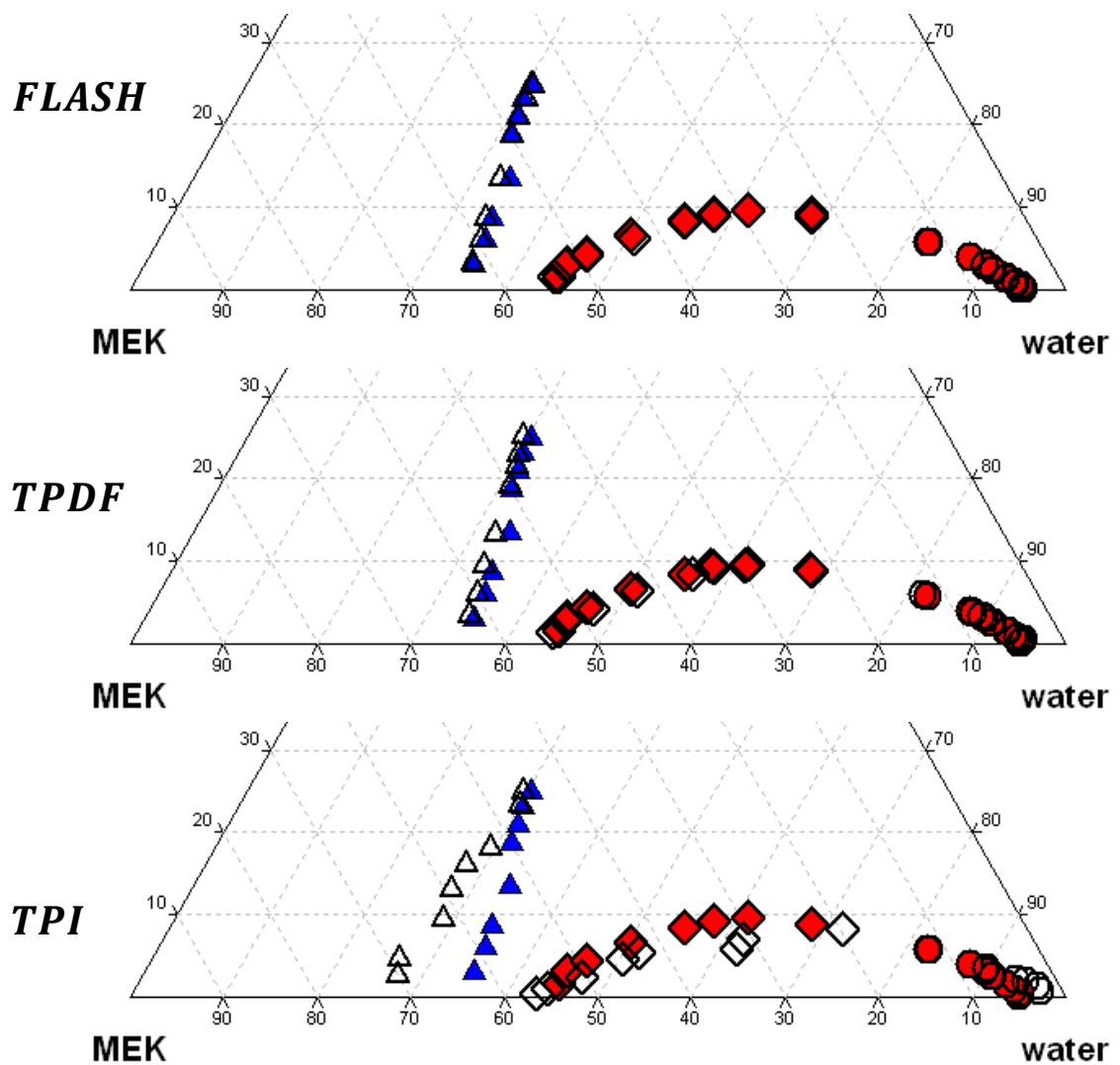


Figure 4.26: VLE (mole fraction) representation for ternary system (water (1)-acetone (2)-MEK (3) at 760 mmHg. The diagram shows the comparison of experimental data, correlated using flash calculation and predicted values using TPDF and TPI

2. water (1)-acetone (2)-MEK (3) at 760 mmHg

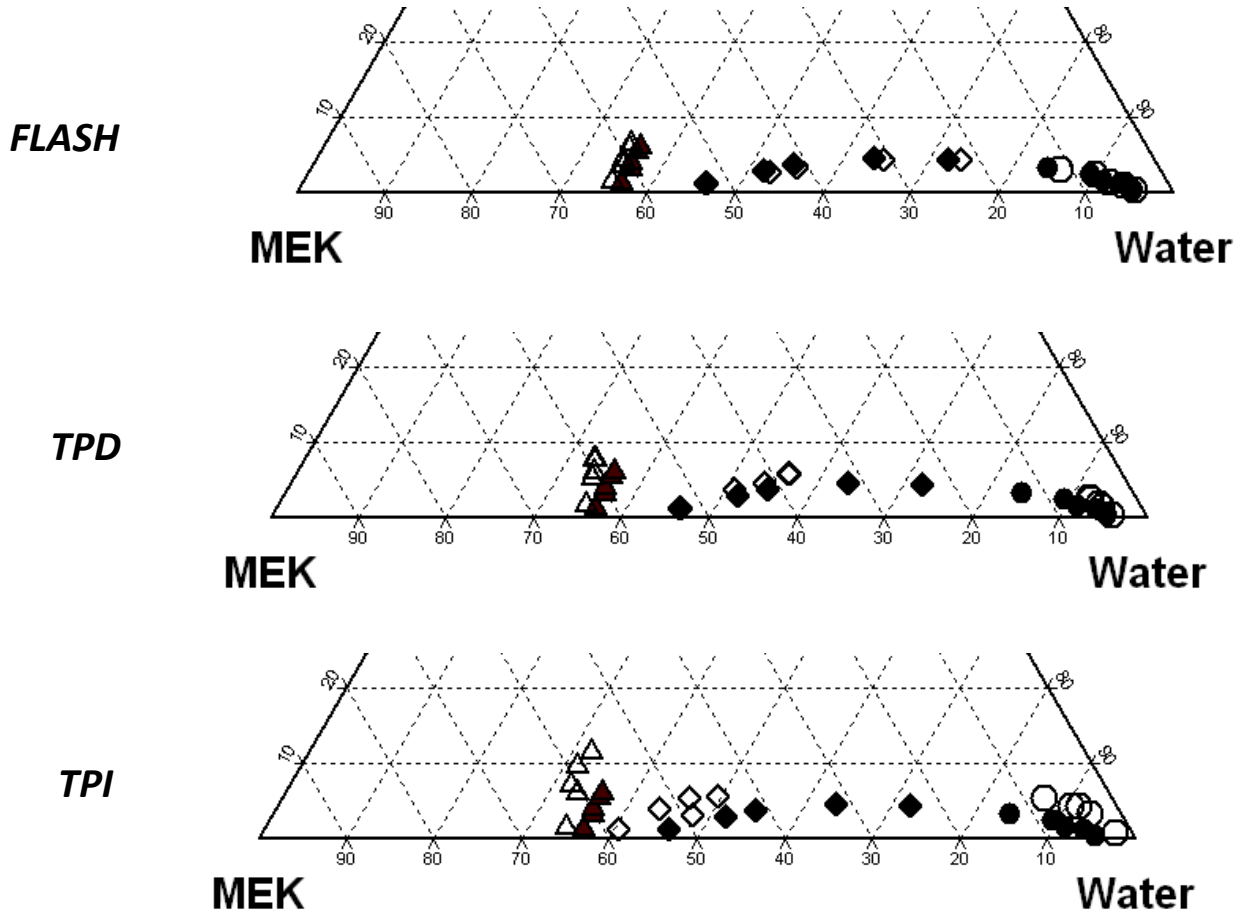


Figure 4.27: VLLE (mole fraction) representation for ternary system (water (1)-ethanol (2)-MEK (3) at 760 mmHg. The diagram shows the comparison of experimental data, correlated using flash calculation and predicted values using TPDF and TPI

3. water (1)-acetone (2)-n-butyl acetate(3)

The flash calculation, the TPI and TPDF results for the third system VLLE water (1) – acetone (2)-n-butyl acetate (3) at pressure 360, 600 and 760 mmHg are listed in tables (4.28, 4.31 and 4.33) respectively. Figures 4.28 through 4.36 below present the graphical representation for calculated results using the 3-phase flash calculation values, the predicted composition values for the TPDF and the TPI respectively.

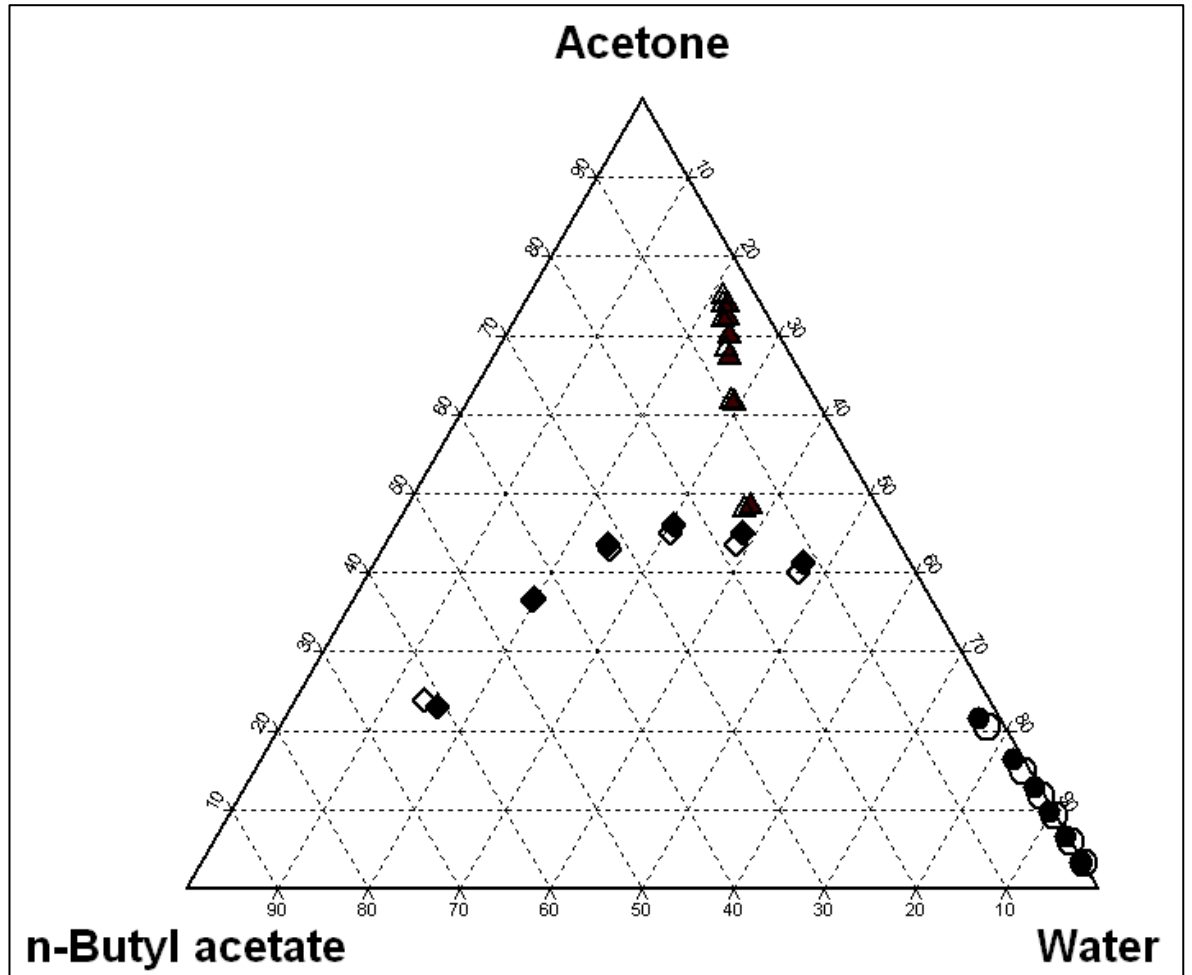


Figure 4.28: VLE (mole fraction) representation for ternary system (water (1)-acetone (2)-n-butyl acetate (3) at 360 mmHg. The diagram shows the comparison of experimental data, correlated using flash calculation

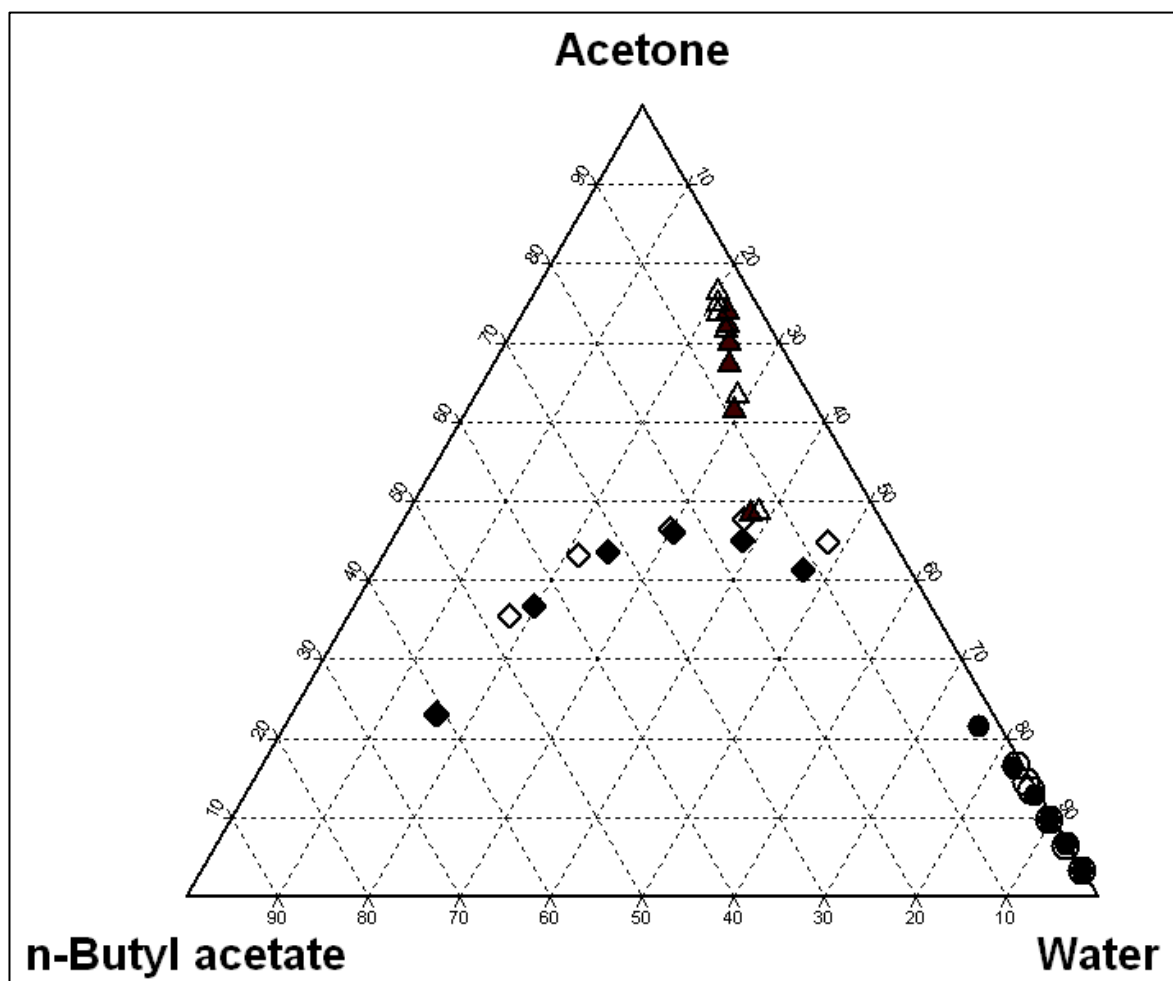


Figure 4.29: VLE (mole fraction) representation for ternary system (water (1)-acetone (2)-n-butyl acetate (3) at 360 mmHg. The diagram shows the comparison of experimental data, correlated using flash calculation and predicted values using TPDF

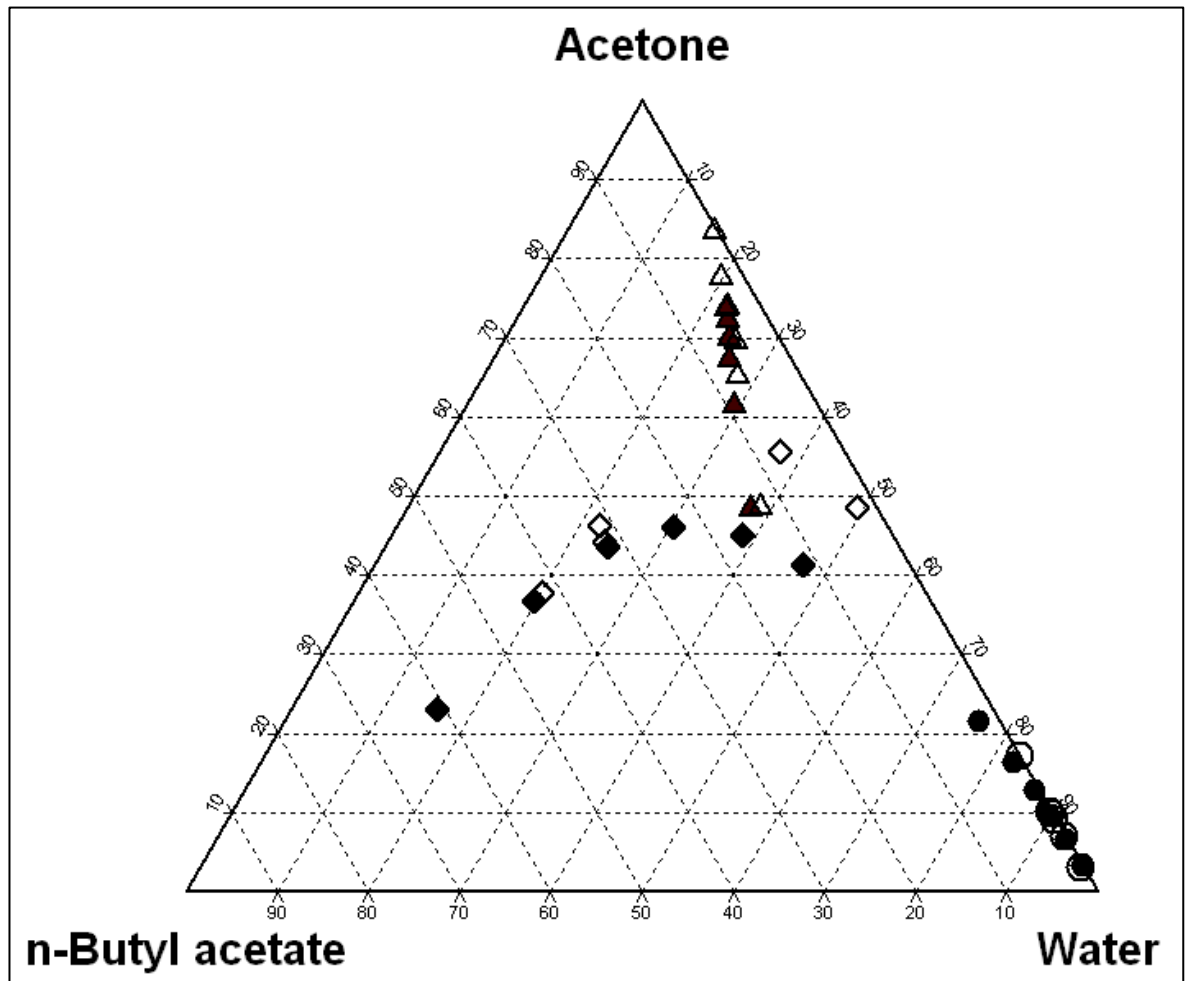


Figure 4.30: VLLE (mole fraction) representation for ternary system (water (1)-acetone (2)-n-butyl acetate (3) at 360 mmHg. The diagram shows the comparison of experimental data, correlated using flash calculation and predicted values using TPI

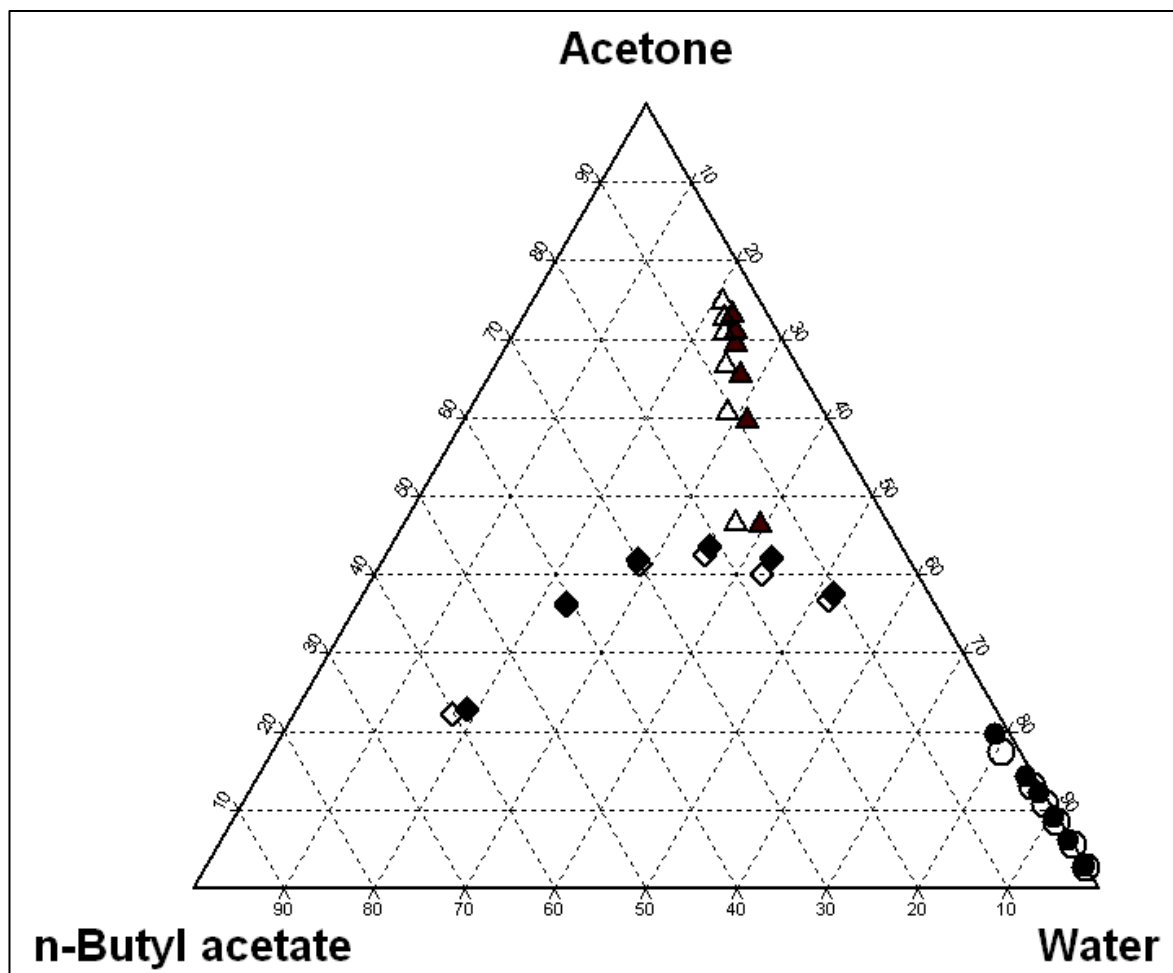


Figure 4.31: VLE (mole fraction) representation for ternary system (water (1)-acetone (2)-n-butyl acetate (3) at 600 mmHg. The diagram shows the comparison of experimental data, correlated using flash calculation

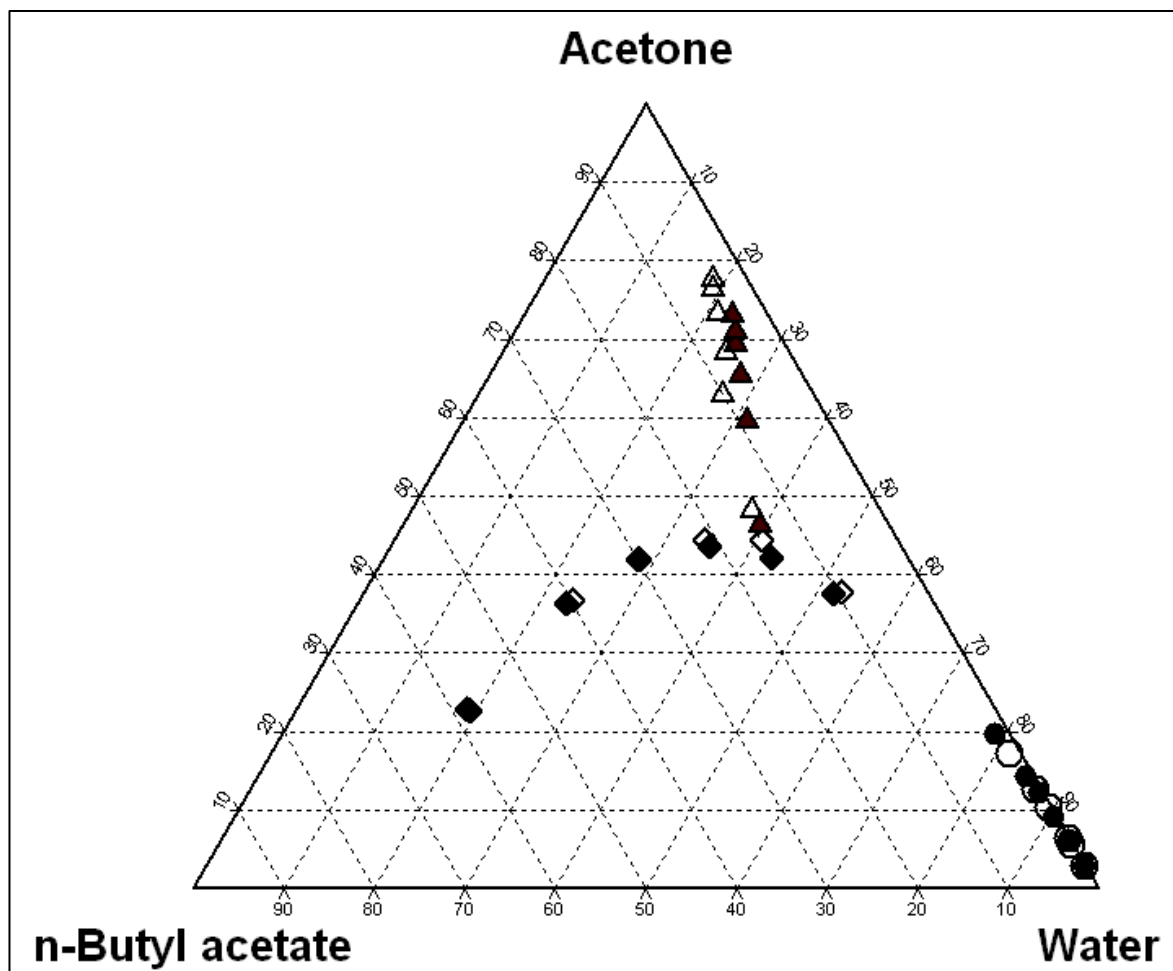


Figure 4.32: VLE (mole fraction) representation for ternary system (water (1)-acetone (2)-n-butyl acetate (3) at 600 mmHg. The diagram shows the comparison of experimental data, correlated using flash calculation and predicted values using TPDF

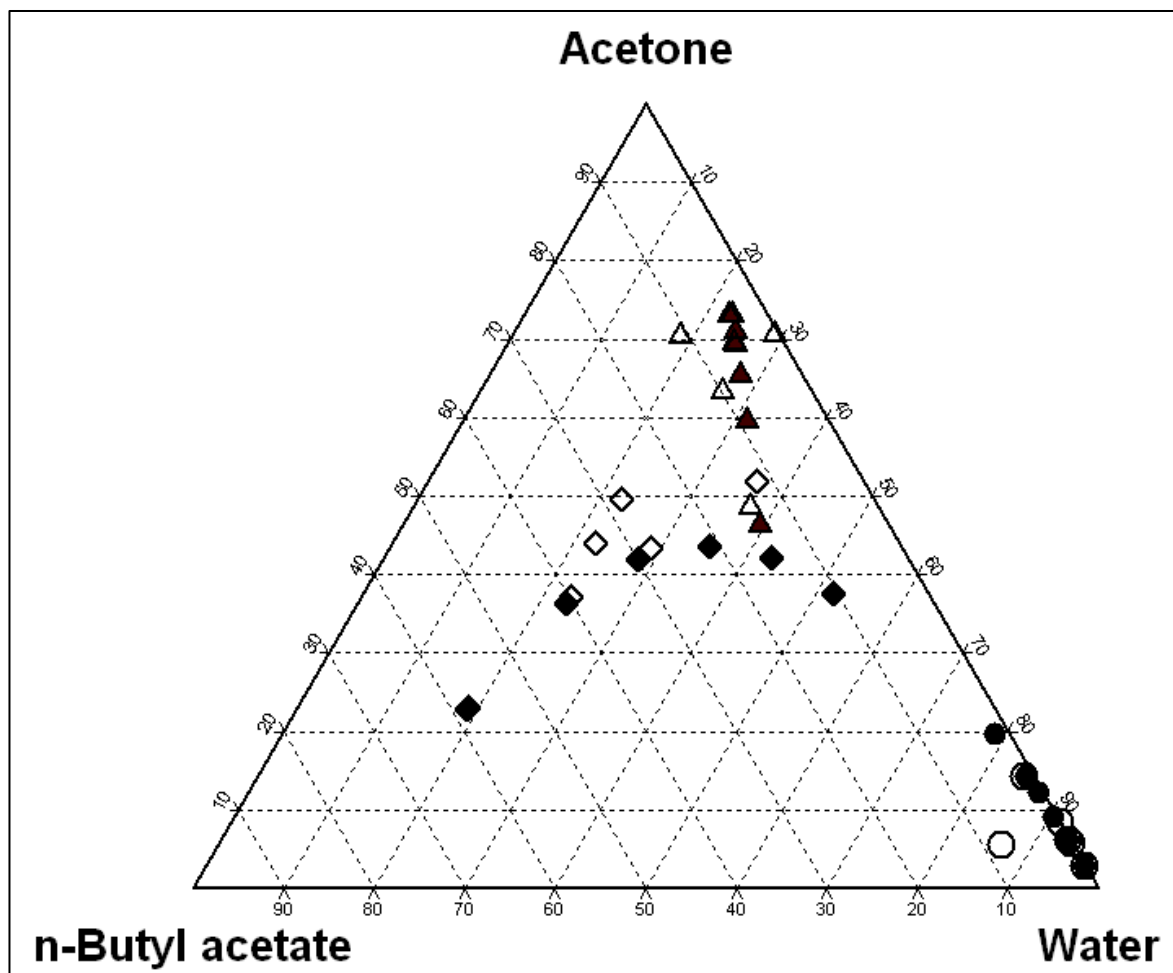


Figure 4.33: VLLE (mole fraction) representation for ternary system (water (1)-acetone (2)-n-butyl acetate (3) at 600 mmHg. The diagram shows the comparison of experimental data, correlated using flash calculation and predicted values using TPI

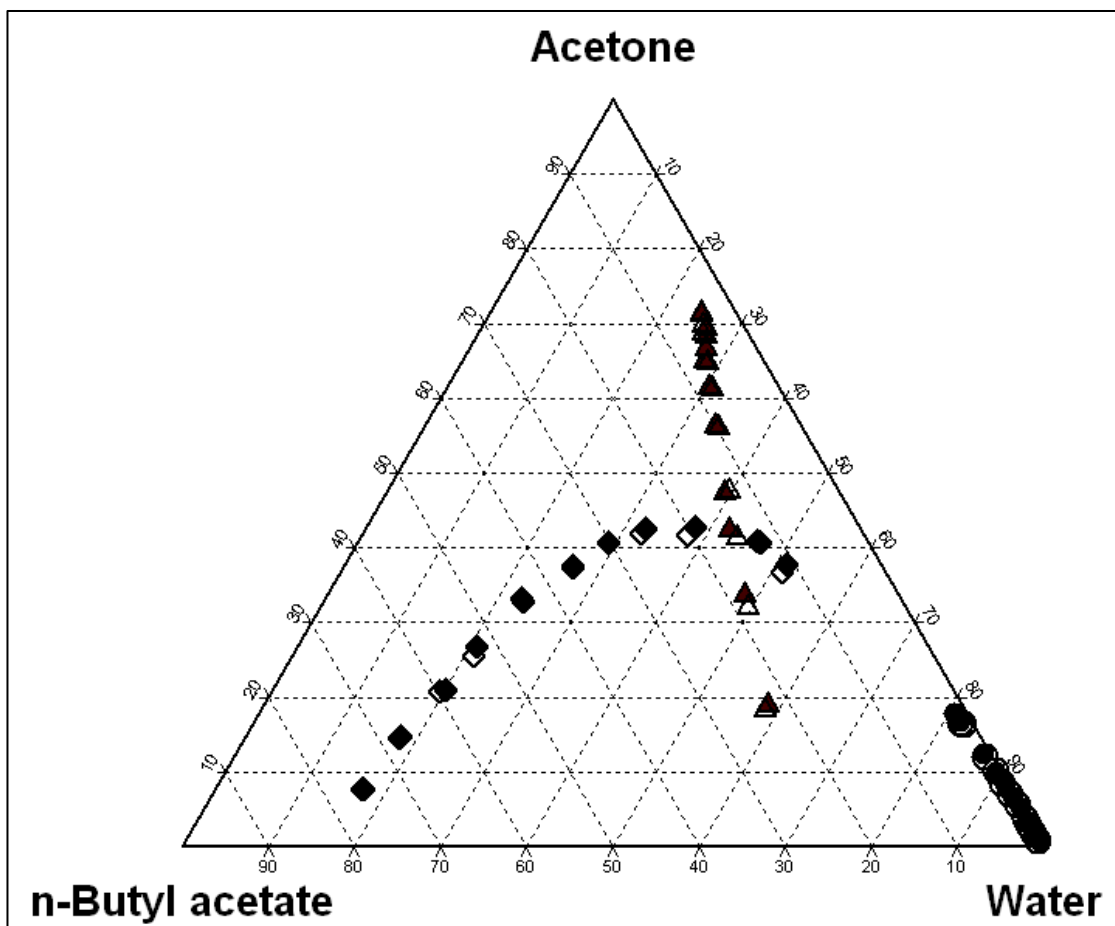


Figure 4.34: VLLE (mole fraction) representation for ternary system (water (1)-acetone (2)-n-butyl acetate (3) at 760 mmHg. The diagram shows the comparison of experimental data, correlated using flash calculation

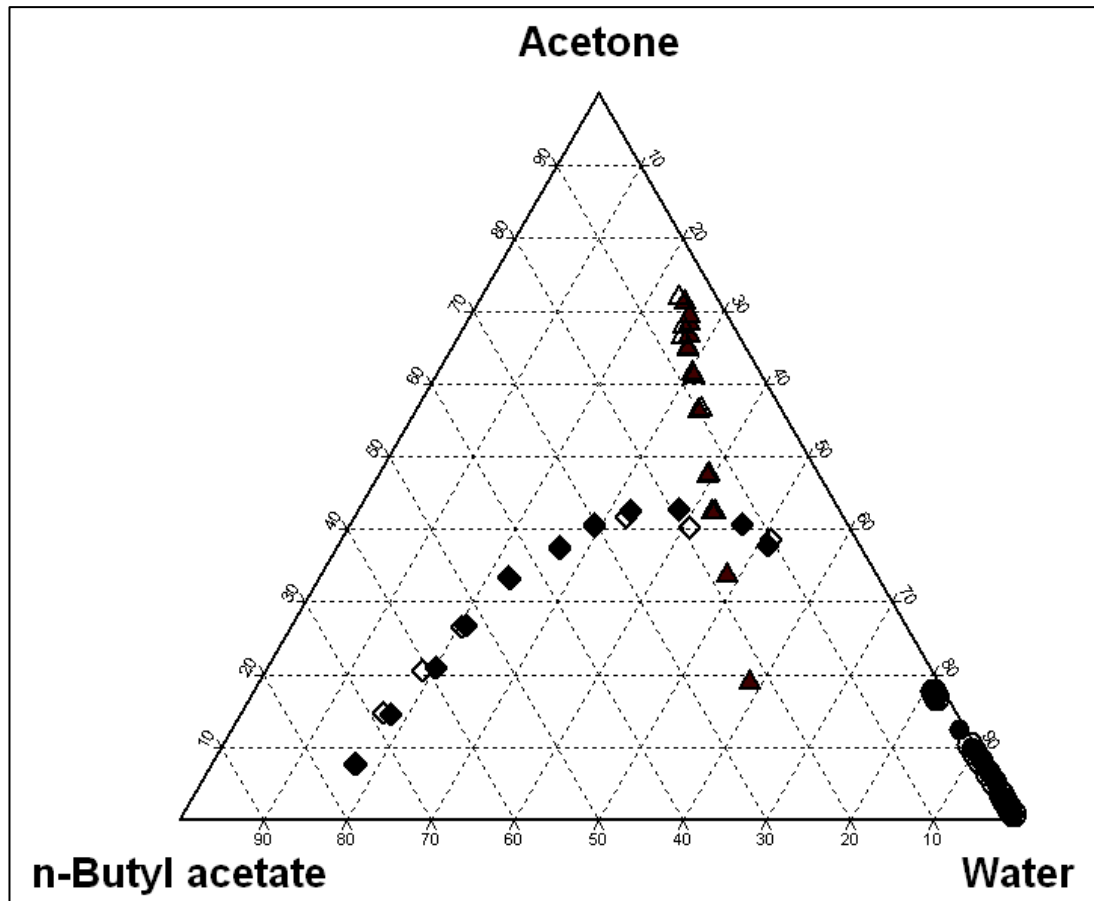


Figure 4.35: VLLE (mole fraction) representation for ternary system (water (1)-acetone (2)-n-butyl acetate (3) at 760 mmHg. The diagram shows the comparison of experimental data , correlated using flash calculation and predicted values using TPDF

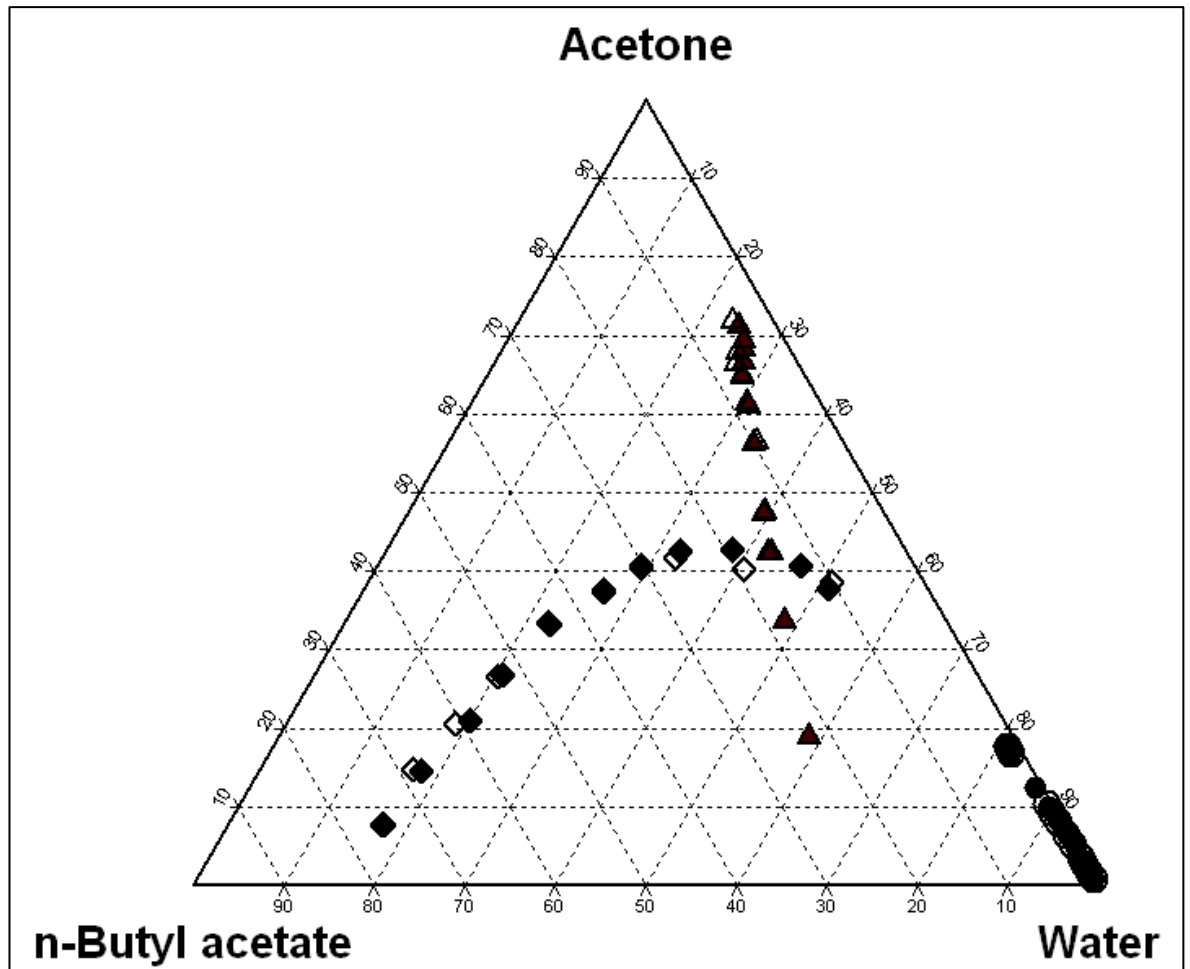
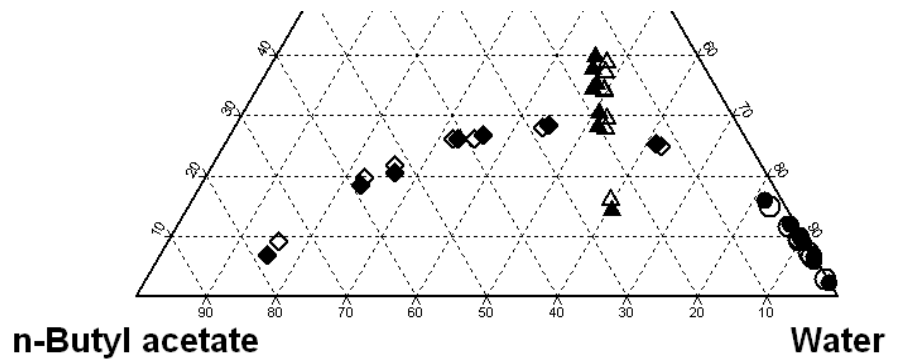


Figure 4.36: VLLE (mole fraction) representation for ternary system (water (1)-acetone (2)-n-butyl acetate (3) at 760 mmHg. The diagram shows the comparison of experimental data, correlated using flash calculation and predicted values using TPI

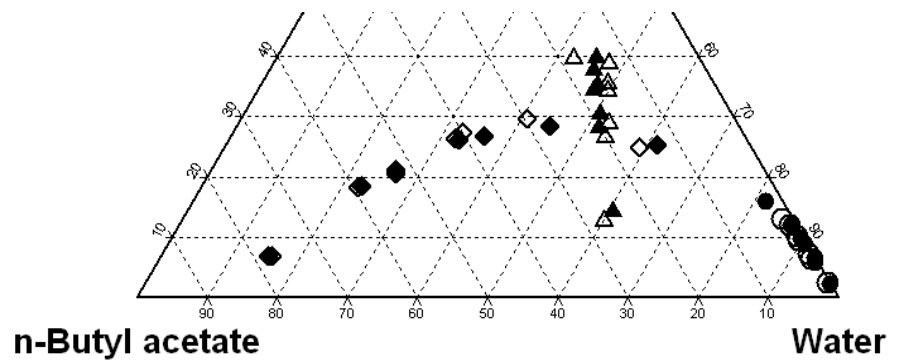
4. water (1)-ethanol (2)-n-butyl acetate(3)

The flash calculation, the TPI and TPDF results for the third system VLLE water (1) – ethanol (2)-n-butyl acetate (3) at pressure 360, 600 and 760 mmHg are listed in table (4.35, 4.37 and 4.39) respectively. Figures (4.37, 4.38 & 4.39) below present the graphical representation for calculated results using the 3-phase flash calculation, the predicted composition values for the TPDF and the TPI respectively.

FLASH



TPDF



TPI

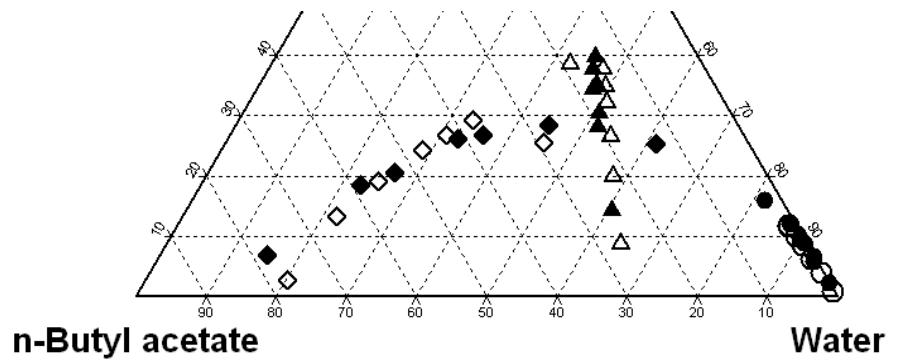
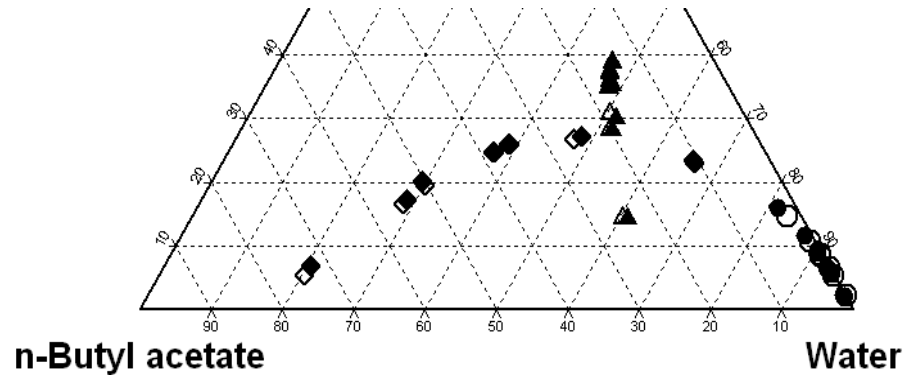
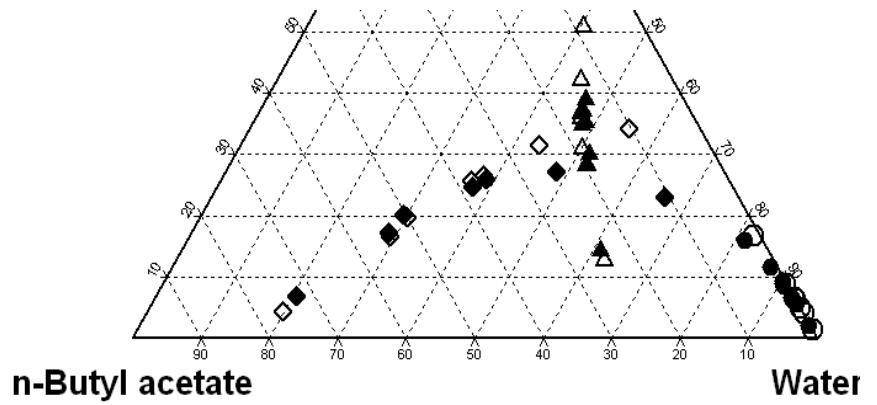


Figure 4.37: VLE (mole fraction) representation for ternary system (water (1)-ethanol (2)-n-butyl acetate (3) at 360 mmHg. The diagram shows the comparison of experimental data, correlated using flash calculation and predicted values using TPDF and TPI

FLASH



TPDF



TPI

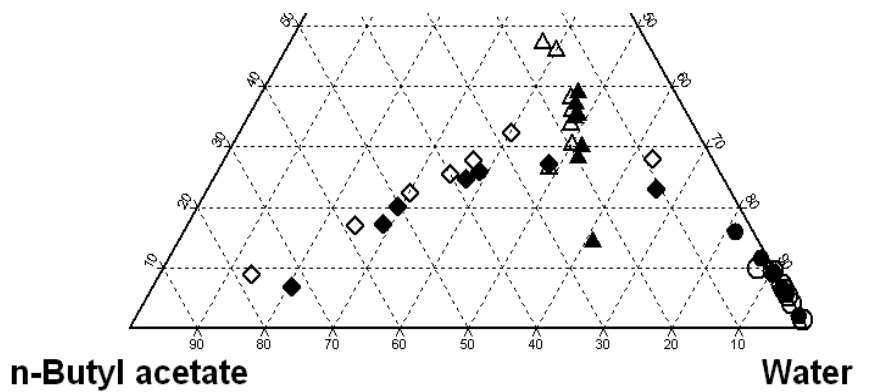
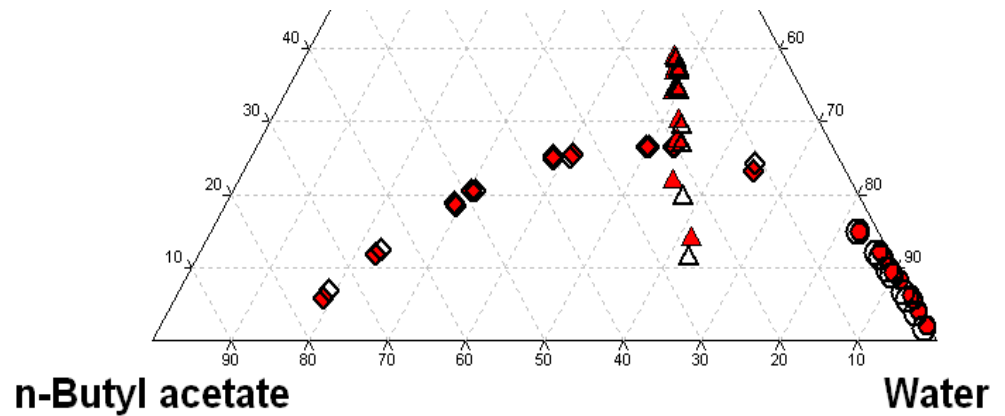
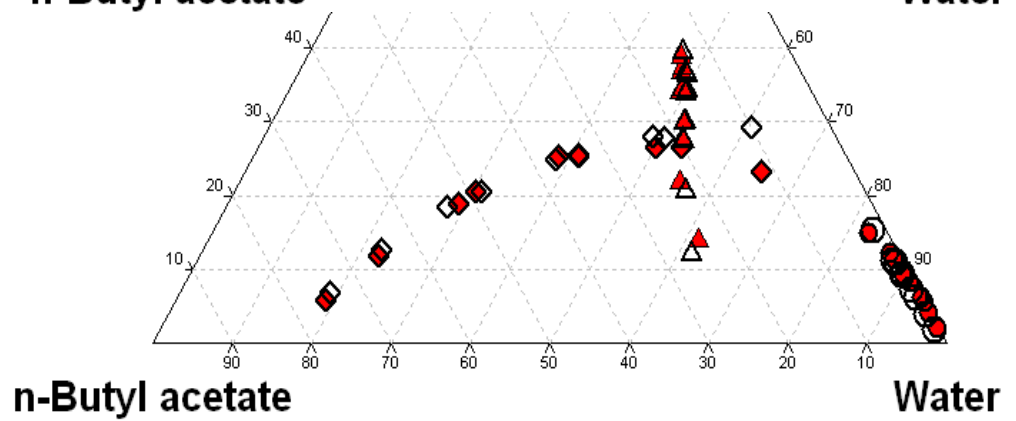


Figure 4.38: VLE (mole fraction) representation for ternary system (water (1)-ethanol (2)-n-butyl acetate (3) at 600 mmHg. The diagram shows the comparison of experimental data, correlated using flash calculation and predicted values using TPDF and TPI

FLASH



TPDF



TPI

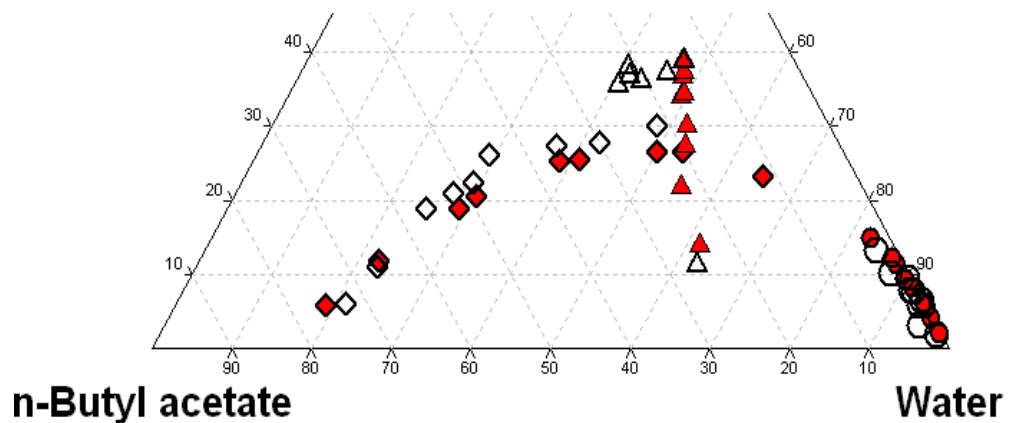


Figure 4.39: VLE (mole fraction) representation for ternary system (water (1)-ethanol (2)-n-butyl acetate (3) at 760 mmHg. The diagram shows the comparison of experimental data, correlated using flash calculation and predicted values using TPDF and TPI

All the prediction methods used up to this point were based on known temperature, pressure and feed compositions. In order to take the prediction method a step further, the challenge was to predict the VLLE phase equilibrium if only the temperature and pressure were known. Thus another investigation was carried out to predict phase equilibrium for a system when the only conditions known are pressure and the temperature. An approach was adopted based on equality of the fugacity of the components over the three phases. From the results obtained the feed compositions were calculated using the tie-line equation for liquid-liquid equilibrium. The tables in section (4.5) show the results for the ternary systems of interest using the SIG, TPI and TPDF methods as follows: table (4.42) for water (1)-acetone (2)-MEK (3) at pressure of 760 mmHg , table (4.43) for water (1)-ethanol (2)-MEK (3) at pressure of 760 mmHg , tables (4.44, 4.45 and 4.46) for water (1)-acetone (2)-n-butyl acetate(3) at pressures of 360, 600 760 mmHg respectively and tables (4.47, 4.48 and 4.49) for water (1)-ethanol (2)-n-butyl acetate(3 at pressures of 360, 600 760 mmHg respectively.

The summary of the results using SIG, TPI and TPDF methods to predict VLLE for ternary systems at a fixed temperature and pressure can be seen in table (4.41). Overall the results are comparable to those listed in table (4.21) in the beginning of this section. Figure (4.40) shows the Absolute Average Deviation (AAD) for each system using both methods.

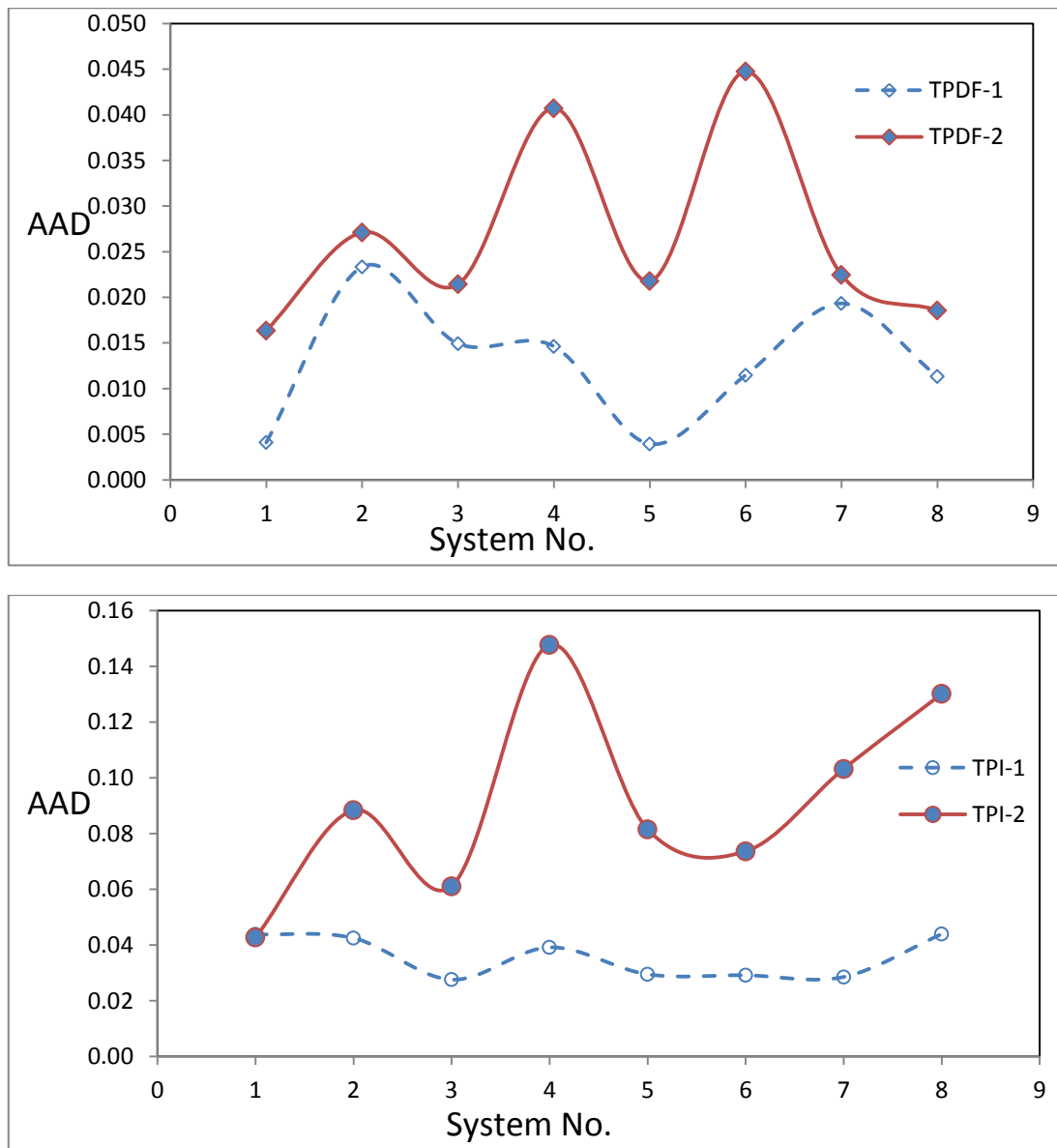


Figure 4.40: AAD for VLE predictions for ternary systems showing the TPI and TPDF methods where TPI-1 and TPDF-1 indicates that the predicted values obtained at known temperature , pressure and feed compositions , TPI-2 and TPDF-2 indicates that the prediction values are obtained from knowing temperature and pressure of the system

4.7 Conclusions on phase equilibrium for ternary VLE

From the attempt to model the polar heterogeneous systems, using PRSV EOS with Wong Sandler combining rules and the UNIQUAC equation to express the excess energy, it can be concluded that this type of mixture can be modelled using the same equation (Equation of State) for describing the vapour and liquid phase fugacities. Four ternary VLE systems of (Younis et al. (2007)) were correlated using flash calculations. The graphical visualisation of the correlated results and the experimental values show that the modelling package (PRSV+WSMR) adequately represents multi-component, multi-phase heterogeneous systems. Parameters required for subsequent prediction were obtained at this stage.

Testing the TPI method on two hypothetical 3-phase systems, the results showed the method to be capable of finding global solutions. When the TPDF method was applied to the systems of Shyu et al., it was discovered that the TPDF was predicting 2 phases in the 3-Phase region. This was due to the use of a simplified version of the Margules activity coefficient equation which was used for the Gibbs energy minimisation function suggested by Michelsen (TPDF). The numbers of the binary constants given by Shyu et al. were not sufficient to allow a more advanced version of the Margules equation to be utilised.

The sensitivity to the starting values for three VLE systems of Younis et al. (2007) was investigated and it was discovered that the TPI method converges to incorrect solutions even if the initial values are theoretically within the heterogeneous region. The TPI method is extremely sensitive to initial values whichever part of the heterogeneous region is selected as a starting point. An explanation for this behaviour was found to be the flattened shape of the ϕ curve around the real solution which causes the minimisation procedure to converge to an incorrect τ zero solution. The geometrical based minimisation of the TPI method influences the search pattern which becomes trapped in local minima and this controls and directs the search procedure to converge to incorrect solutions. To overcome this issue it was suggested that the angle variables be constrained in a way to redefine the composition search region of

each phase in the minimisation to avoid the convergence to a local minima. This was found to be effective and improved the results for the TPI method.

A further contributing factor to the TPI sensitivity issue is the location of the stationary equilibrium points relative to the phase boundaries. The graphical representation for the Gibbs energy surface for system 1 & 2 of Younis et al. (2007) showed the stationary points for the organic and vapour phase compositions to be on the phase boundaries (ternary systems which have MEK). By contrast, for system 3 these points are relatively far apart on the ϕ surface.

In an attempt to provide the TPI minimisation method simplex with realistic initial values, this research suggested a Systematic Initial Generator (SIG) as a direct initialisation scheme for VLLE multi-component systems. The SIG method was tested on four VLLE ternary systems and it has been demonstrated that this method produces an overall improvement in the TPI results.

The differences between the two methods of Gibbs minimisation techniques (TPI & TPDF) have been discussed. Both methods represent the thermodynamic criterion aspect for equilibrium by constructing an objective function to be minimised, but each method uses a different mathematical approach. The TPI method converts the problem to a geometrical shape through construction of the ϕ curve and tangent hyper-plane. The search procedure finds the location of the tangent hyper-plane in relation to the ϕ surface. When the tangent is located under the ϕ surface a part of the tangent which intersects with the ϕ will be reduced to zero.

Alternatively the TPDF method formulates the problem mathematically by minimising the Gibbs energy of the mixture expressed in the form of fugacity coefficients. This approach was developed by Michelsen (1982a) and was essentially derived from chemical potential criteria. The function is expressed in the form of the differences between the ϕ surface and the two parallel tangent hyper planes at feed compositions and at trial compositions. The solution for these rigorous mathematical problems is to minimise these differences with the constraint that the sum of the compositions in each phase must be equal to one. The results are the compositions of the stationary points for all phases.

From the analytical observation of both methods, the TPDF method apparently has less local minima which allow the minimisation to converge to solutions with less computational effort. A further advantage of the TPDF method is that it can be applied to quaternary systems without any major change in the method when compared to the TPI method. The TPDF method is robust and reliable and can usually be applied successfully to systems of interest without showing inconsistency and sensitivity to the initial values for the simplex.

The SIG, TPI and TPDF methods were investigated as phase predictors on the systems of Younis et al (2007). A set of feed compositions were selected outside the heterogeneous region. The results for SIG and TPDF methods correctly indicated when the system forms a single liquid phase at a fixed temperature and pressure. However the TPI results indicated that for the same feed compositions the liquid splits into two phases when in fact only a single liquid phase is present.

Applying the TPI to quaternary 3 phase systems introduces an extra degree of freedom to the system according to phase rule and increases the total number of variable compositions from 6 to 8. The base-case calculation is required to calculate the global solution which splits into two ternary pseudo systems and two hyper planes to be adjusted simultaneously as the Gibbs energy only exists in a 3-dimensional space. This increases the complexity of the method and also increases the sensitivity to the initial values to start the simplex. For this reason the TPI is only applied to VLLE ternary systems.

Overall, for ternary systems, this work has demonstrated that the PRSV equation of state with WS mixing rules is capable of satisfactorily correlating real heterogeneous system data. When attempting to use the Tangent Plane Intersection (TPI) and the Tangent Plane Distance Function (TPDF) method it has been demonstrated that, for four heterogeneous VLLE systems these methods give variable prediction results. Usually the TPDF method is capable of accurate predictions inside and outside the heterogeneous regions. The behaviour of the TPI method was much more variable. This method is also sensitive to the initial starting values supplied to the simplex method. Attempts were carried out to supply more realistic starting values. The details of these findings have been given in this conclusion section.

4.8 Quaternary systems

The correlation and predictions for two quaternary VLE systems were carried out using data published by Younis et al. (2007). The methods used were:

1. Flash calculation
2. Tangent Plane Distance Function (TPDF)
3. Systematic Initial Generator(SIG)

In the VLE flash calculation using PRSV+WSMR, the objective function (AAD between the correlated and experimental composition values) was minimised with the Nelder-Mead simplex. The estimated parameters from this correlation procedure were used in the TPDF prediction and the SIG methods. Table (4.50) shows the summary of results for the Flash, TPDF and SIG methods for VLE quaternary systems. The estimated UNIQUAC and PRSV interaction parameters are listed in table (4.51).

The VLE quaternary systems modelled are:

1. Water(1)-ethanol(2)-acetone(3)-MEK(4) at 760 mmHg
2. Water(1)-ethanol(2)-acetone(3)-n-butyl acetate(4):
 - 2.1 760 mmHg
 - 2.2 600 mmHg
 - 2.3 360 mmHg

The results for two VLE heterogeneous quaternary systems are shown in the tables below (n-butyl acetate is shown as n-BA in table header). The overall feed composition was calculated from the mean average deviation of the experimental data.

Table 4.50: Summary table for VLLE quaternary systems, over all Absolute Average Deviation (AAD) for the flash calculations, the TPDF and SIG predictions

System	Temperature range in °C	P mmHg	Method	AAD		
				organic	aqueous	vapour
VLLE water(1) ethanol(2) acetone(3) MEK(4)	70.60-73.80	760	Flash	0.0044	0.0072	0.0081
			TPDF	0.0247	0.0161	0.0164
			SIG	0.0697	0.0158	0.0213
VLLE water (1) ethanol (2) acetone (3) n-butyl acetate (4)	72.20-92.00	760	Flash	0.0109	0.0086	0.0156
			TPDF	0.0265	0.0099	0.0353
			SIG	0.0835	0.0270	0.0362
VLLE water (1) ethanol (2) acetone (3) n-butyl acetate (4)	61.00-80.20	600	Flash	0.0093	0.0057	0.0152
			TPDF	0.0133	0.0097	0.0114
			SIG	0.1297	0.0278	0.0480
VLLE water (1) ethanol (2) acetone (3) n-butyl acetate (4)	48.10-70.00	360	Flash	0.0096	0.0034	0.0146
			TPDF	0.0157	0.0079	0.0093
			SIG	0.0981	0.0168	0.0352

Table 4.51: Shows UNIQUAC and PRSV EOS interaction parameters for two VLLE quaternary systems using flash calculations

Parameters	water(1) ethanol(2) acetone(3) MEK(4)	water (1) ethanol (2) acetone (3) n-butyl acetate (4)			
	760 mmHg	760 mmHg	600 mmHg	360 mmHg	
UNIQUAC	A ₁₂	74.396	-57.65	-18.66	-10.79
	A ₂₁	-91.49	285.36	499.27	394.34
	A ₂₃	-636.00	2644.90	-258.50	-193.20
	A ₃₂	565.33	-278.50	1074.7	639.13
	A ₃₁	-64.73	583.58	308.19	285.95
	A ₁₃	770.30	-6.809	175.61	114.08
	A ₂₄	199.50	-105.90	-145.30	-115.00
	A ₄₂	421.71	238.41	485.55	379.63
	A ₃₄	1211.20	-86.82	632.92	701.77
	A ₄₃	-137.30	123.53	-289.30	-295.20
	A ₁₄	280.52	626.47	441.94	428.63
	A ₄₁	526.35	818.91	1176.10	958.92
	PRSV EOS	k ₁₂	0.4779	0.2107	0.1348
k ₂₃		3E-05	0.2617	1E-05	0.0450
k ₁₃		8E-05	0.0577	8E-05	4E-06
K ₁₄		1E-07	0.0699	0.1224	0.1069
K ₃₄		0.2925	0.0434	0.3132	0.1742
K ₂₄		0.0457	0.3303	0.1149	0.0897

4.8.1 VLE water (1) ethanol(2) acetone(3) MEK(4)

Table 4.52: VLE quaternary system water (1)-ethanol (2)-acetone (3)-MEK (4) at 760 mmHg, experimental Flash, TPDF and SIG predictions

Temperature in °C	Experimental			Flash calculation			TPDF Prediction			SIG Prediction		
	water	ethanol	MEK	water	ethanol	MEK	water	ethanol	MEK	water	ethanol	MEK
Organic Phase												
73.80	0.44924	0.00890	0.53944	0.45317	0.00833	0.53604	0.44625	0.00413	0.54719	0.39455	0.00329	0.60032
73.40	0.47183	0.01552	0.50844	0.47499	0.01623	0.50449	0.46562	0.00693	0.52401	0.37766	0.00485	0.61492
73.00	0.49451	0.02182	0.47772	0.49756	0.02403	0.47241	0.49450	0.01433	0.48483	0.37743	0.01054	0.60556
72.70	0.52253	0.02768	0.44238	0.52559	0.03175	0.43508	0.51614	0.02538	0.44939	0.38116	0.01822	0.59081
72.50	0.56038	0.03270	0.39862	0.56513	0.03929	0.38671	0.51549	0.03060	0.44388	0.38109	0.02360	0.58317
72.20	0.59520	0.03766	0.35788	0.59577	0.04801	0.34524	0.52037	0.03345	0.43418	0.38288	0.02503	0.57825
72.00	0.63979	0.04010	0.31028	0.63810	0.05583	0.29532	0.52973	0.02930	0.42795	0.38444	0.02148	0.57872
73.20	0.43084	0.00557	0.55942	0.42994	0.00320	0.56393	0.42591	0.00584	0.56436	0.37390	0.00563	0.61589
73.00	0.46087	0.01249	0.51739	0.46156	0.00760	0.52381	0.45580	0.00720	0.52840	0.38130	0.00652	0.60213
72.70	0.49983	0.01911	0.46882	0.50109	0.01223	0.47604	0.47553	0.01360	0.49905	0.38679	0.01203	0.58595
72.40	0.54560	0.02704	0.40864	0.55177	0.01942	0.41210	0.53451	0.01925	0.42804	0.40800	0.02092	0.54799
72.00	0.59385	0.03196	0.35231	0.59965	0.02460	0.35466	0.55422	0.03549	0.38852	0.43449	0.03754	0.50047
71.70	0.69458	0.03347	0.25115	0.70219	0.02922	0.24618	0.55282	0.02959	0.38238	0.42173	0.02862	0.50499
72.80	0.44568	0.00618	0.53796	0.44647	0.00376	0.54216	0.43800	0.00807	0.54127	0.39767	0.01687	0.57053
72.30	0.47550	0.01149	0.49378	0.47917	0.00741	0.49833	0.46997	0.01373	0.49444	0.39561	0.02565	0.55203
72.00	0.50381	0.01668	0.45231	0.51117	0.01130	0.45549	0.50390	0.02007	0.44801	0.41659	0.02331	0.52670
71.80	0.54129	0.02090	0.40440	0.54949	0.01524	0.40665	0.54074	0.02809	0.39958	0.42106	0.03026	0.50893
71.30	0.58878	0.02416	0.34942	0.60040	0.01914	0.34635	0.52817	0.01622	0.41695	0.39888	0.01705	0.53516
71.10	0.66484	0.02534	0.27237	0.67725	0.02243	0.26371	0.57009	0.05000	0.34026	0.44217	0.04809	0.45905
72.40	0.42993	0.00310	0.55902	0.42863	0.00185	0.56382	0.45901	0.00833	0.37197	0.45522	0.00835	0.38535
72.10	0.45538	0.00542	0.51894	0.45682	0.00346	0.52451	0.48471	0.01217	0.35999	0.44398	0.01435	0.38487
71.80	0.47431	0.00774	0.48632	0.47988	0.00526	0.49069	0.48372	0.01315	0.45003	0.40628	0.01517	0.51660
71.30	0.50064	0.01003	0.44822	0.50636	0.00704	0.45413	0.51649	0.02692	0.39597	0.43897	0.03024	0.45998
71.10	0.56792	0.01376	0.36233	0.57658	0.01122	0.36371	0.54331	0.01952	0.38324	0.39963	0.01842	0.51313
70.60	0.60641	0.01560	0.31803	0.61664	0.01355	0.31604	0.55813	0.01680	0.36559	0.47129	0.01312	0.43324

Temperature in °C	Experimental			Flash calculation			TPDF Prediction			SIG Prediction		
	water	ethanol	MEK	water	ethanol	MEK	water	ethanol	MEK	water	ethanol	MEK
Aqueous Phase												
73.80	0.97782	0.01587	0.00276	0.97034	0.00552	0.02380	0.95650	0.00719	0.03606	0.95431	0.00667	0.03881
73.40	0.95793	0.03283	0.00323	0.95732	0.01171	0.02949	0.95209	0.01150	0.03597	0.94810	0.01043	0.04111
73.00	0.93925	0.04815	0.00407	0.94585	0.01817	0.03256	0.93879	0.02234	0.03760	0.93015	0.02321	0.04509
72.70	0.92240	0.06228	0.00398	0.93440	0.02486	0.03468	0.91767	0.03817	0.04120	0.90504	0.04064	0.05033
72.50	0.90451	0.07599	0.00544	0.91864	0.03216	0.03957	0.90640	0.04638	0.04325	0.88561	0.05349	0.05438
72.20	0.87972	0.09528	0.00690	0.89784	0.04205	0.04370	0.89981	0.05053	0.04444	0.88021	0.05626	0.05572
72.00	0.84392	0.11829	0.01356	0.87196	0.05470	0.05122	0.90915	0.04333	0.04262	0.88976	0.04911	0.05345
73.20	0.94841	0.00264	0.04797	0.94776	0.00242	0.04934	0.95107	0.01084	0.03760	0.94471	0.01236	0.04221
73.00	0.93641	0.00537	0.05601	0.93718	0.00584	0.05553	0.94946	0.01240	0.03696	0.94093	0.01427	0.04307
72.70	0.92178	0.00782	0.06748	0.92414	0.00931	0.06383	0.93600	0.02260	0.03891	0.92148	0.02687	0.04731
72.40	0.91102	0.01350	0.06947	0.91314	0.01486	0.06671	0.93540	0.01291	0.04848	0.91757	0.01801	0.06043
72.00	0.89970	0.01612	0.07680	0.90113	0.01851	0.07273	0.91344	0.02457	0.05725	0.88962	0.03230	0.07222
71.70	0.84018	0.02334	0.12433	0.84686	0.02501	0.11421	0.91918	0.02038	0.05306	0.89744	0.02526	0.06815
72.80	0.94301	0.00291	0.05175	0.94352	0.00293	0.05220	0.94446	0.00612	0.04759	0.92319	0.01464	0.05970
72.30	0.93945	0.00499	0.05113	0.93858	0.00574	0.05272	0.93853	0.00999	0.04806	0.91469	0.02233	0.05847
72.00	0.92097	0.00756	0.06397	0.92246	0.00923	0.06255	0.93151	0.01413	0.04948	0.91266	0.01995	0.06133
71.80	0.91195	0.00980	0.06818	0.91274	0.01234	0.06636	0.92169	0.01941	0.05258	0.89910	0.02646	0.06653
71.30	0.89300	0.01273	0.08025	0.89577	0.01580	0.07565	0.93655	0.01101	0.04569	0.91870	0.01507	0.05777
71.10	0.87386	0.01560	0.09246	0.87863	0.01868	0.08535	0.88464	0.03680	0.06754	0.84361	0.04553	0.09624
72.40	0.94984	0.00172	0.04676	0.94886	0.00143	0.04884	0.91337	0.00709	0.04613	0.91434	0.00712	0.04756
72.10	0.93941	0.00265	0.05346	0.93990	0.00283	0.05441	0.91404	0.00982	0.04598	0.89966	0.01285	0.05264
71.80	0.93508	0.00381	0.05366	0.93490	0.00445	0.05565	0.93537	0.00959	0.04617	0.91946	0.01332	0.05633
71.30	0.90985	0.00480	0.07364	0.91263	0.00642	0.07160	0.91573	0.01965	0.05225	0.89317	0.02626	0.06529
71.10	0.89973	0.00725	0.07384	0.90001	0.01019	0.07347	0.92960	0.01337	0.04668	0.90759	0.01691	0.06230
70.60	0.88460	0.00915	0.08215	0.88555	0.01236	0.08048	0.90322	0.02660	0.04927	0.84763	0.03371	0.07225

Temperature in °C	Experimental			Flash calculation			TPDF Prediction			SIG Prediction		
	water	ethanol	MEK	water	ethanol	MEK	water	ethanol	MEK	water	ethanol	MEK
Vapour Phase												
73.80	0.35983	0.00869	0.62717	0.35582	0.01965	0.61700	0.35840	0.00695	0.62945	0.35114	0.00631	0.63859
73.40	0.35687	0.01536	0.61977	0.34835	0.03582	0.60334	0.35663	0.01101	0.62509	0.34375	0.00958	0.64112
73.00	0.35717	0.02206	0.60918	0.34246	0.04989	0.59095	0.34989	0.02050	0.61651	0.33354	0.02000	0.63289
72.70	0.35739	0.02872	0.59878	0.33807	0.06213	0.57956	0.33955	0.03309	0.60947	0.32354	0.03276	0.62382
72.50	0.35884	0.03556	0.58651	0.33677	0.07286	0.56743	0.33407	0.03920	0.60751	0.31657	0.04124	0.61810
72.20	0.35232	0.04181	0.58311	0.32846	0.08450	0.55960	0.33041	0.04151	0.60533	0.31387	0.04289	0.61588
72.00	0.35113	0.04699	0.57628	0.32448	0.09484	0.55387	0.33354	0.03565	0.60546	0.31643	0.03671	0.61606
73.20	0.35332	0.00517	0.63403	0.35154	0.00776	0.63146	0.35104	0.01015	0.63056	0.34012	0.01107	0.63896
73.00	0.35073	0.01224	0.61905	0.34583	0.01667	0.61648	0.35080	0.01128	0.61967	0.33662	0.01215	0.62967
72.70	0.34821	0.01902	0.60437	0.34126	0.02443	0.60404	0.34453	0.01958	0.61143	0.32819	0.02111	0.61880
72.40	0.34799	0.02798	0.58186	0.33619	0.03428	0.58452	0.34335	0.02943	0.60131	0.32914	0.03681	0.60683
72.00	0.33927	0.03461	0.57171	0.32959	0.03963	0.57571	0.33188	0.05053	0.58447	0.32095	0.05941	0.58536
71.70	0.33939	0.04131	0.55419	0.32446	0.04391	0.56986	0.33314	0.04306	0.56987	0.32010	0.04752	0.57702
72.80	0.35393	0.00611	0.61983	0.34865	0.00852	0.61910	0.34567	0.01438	0.62472	0.33123	0.03044	0.62110
72.30	0.34832	0.01145	0.60088	0.34131	0.01479	0.59881	0.34271	0.02294	0.60644	0.32183	0.04574	0.60137
72.00	0.34841	0.01635	0.57896	0.33558	0.02008	0.58101	0.33930	0.03151	0.59088	0.32643	0.03995	0.59323
71.80	0.34185	0.02093	0.56404	0.32949	0.02408	0.56676	0.33455	0.04145	0.57711	0.32228	0.05048	0.57846
71.30	0.34500	0.02514	0.54110	0.32761	0.02712	0.55153	0.34033	0.02524	0.57872	0.32488	0.03075	0.58578
71.10	0.34382	0.02895	0.52413	0.32495	0.02881	0.54141	0.31943	0.06757	0.54731	0.30961	0.07236	0.55157
72.40	0.35013	0.00286	0.63192	0.34940	0.00440	0.62801	0.32477	0.01462	0.43127	0.32505	0.01468	0.44798
72.10	0.34624	0.00539	0.60783	0.34104	0.00717	0.60450	0.32610	0.02037	0.44248	0.31895	0.02497	0.43713
71.80	0.34306	0.00776	0.58584	0.33399	0.00960	0.58299	0.33961	0.02180	0.56695	0.32664	0.02741	0.57029
71.30	0.33662	0.00987	0.56837	0.32563	0.01124	0.56684	0.32940	0.04087	0.54088	0.31854	0.04909	0.53995
71.10	0.32576	0.01398	0.53112	0.31450	0.01359	0.53218	0.33576	0.02968	0.55271	0.31885	0.03276	0.56383
70.60	0.32433	0.01567	0.51380	0.31128	0.01452	0.51911	0.31543	0.01288	0.54136	0.29880	0.01112	0.51396

4.8.2 VLLE water (1) ethanol (2) acetone (3) n-butyl acetate (4) at 760 mmHg

Table 4.53: VLLE quaternary system water (1)-ethanol (2)-acetone (3)-n butyl acetate (4) at 760 mmHg, experimental, Flash, TPDF and SIG predictions

Temperature in °C	Experimental			Flash calculation			TPD Prediction			SIG Prediction		
	water	ethanol	n-BA	water	ethanol	n-BA	water	ethanol	n-BA	water	ethanol	n-BA
Organic Phase												
92.00	0.16469	0.01355	0.80283	0.18537	0.01798	0.77699	0.17048	0.01942	0.79253	0.28224	0.03824	0.66530
89.50	0.19652	0.04823	0.72539	0.20837	0.06273	0.69783	0.19709	0.04550	0.71496	0.32743	0.10326	0.54945
88.50	0.27541	0.10092	0.58033	0.27183	0.12253	0.56213	0.27439	0.09491	0.53622	0.34279	0.13233	0.50236
87.10	0.26244	0.05023	0.65177	0.26542	0.06607	0.63105	0.26657	0.05202	0.63295	0.35909	0.12782	0.47551
84.50	0.28607	0.14653	0.51273	0.28950	0.16284	0.49576	0.29220	0.10553	0.49677	0.45132	0.19620	0.29139
84.20	0.25866	0.09718	0.59530	0.28042	0.11033	0.56247	0.25714	0.05235	0.64195	0.41200	0.16137	0.34618
83.10	0.36187	0.19826	0.37565	0.36285	0.20633	0.36991	0.36034	0.13580	0.36324	0.51344	0.21260	0.20365
82.00	0.26897	0.14371	0.52492	0.28700	0.15427	0.50019	0.26506	0.09804	0.54022	0.48137	0.18180	0.23598
81.00	0.36188	0.19797	0.37027	0.36383	0.20623	0.36307	0.36397	0.13142	0.37027	0.57670	0.19056	0.13786
79.50	0.48265	0.22013	0.23030	0.47523	0.22670	0.23410	0.48161	0.15849	0.19561	0.68267	0.17681	0.05909
90.20	0.20647	0.03665	0.71251	0.21599	0.04915	0.68844	0.20108	0.04743	0.70708	0.29519	0.06323	0.61072
85.40	0.23931	0.07160	0.61384	0.24739	0.08761	0.58861	0.23349	0.07821	0.61261	0.37041	0.12599	0.43201
82.10	0.26103	0.09985	0.54214	0.26686	0.11649	0.51969	0.26572	0.09805	0.53952	0.41683	0.14235	0.31809
81.20	0.29952	0.12445	0.46271	0.31246	0.13513	0.44623	0.29729	0.11602	0.46969	0.44932	0.15815	0.26504
80.10	0.33120	0.14454	0.39734	0.34419	0.15217	0.39004	0.33410	0.12889	0.40546	0.48531	0.16567	0.21419
79.50	0.36552	0.15907	0.34260	0.36667	0.16819	0.34267	0.36752	0.14763	0.33043	0.59412	0.15492	0.13098
79.20	0.40288	0.16801	0.29551	0.40046	0.17664	0.29744	0.39653	0.15845	0.27704	0.59999	0.16177	0.11970
78.00	0.45325	0.17248	0.24309	0.44804	0.18048	0.24963	0.46806	0.16345	0.19760	0.57350	0.16090	0.12443
92.50	0.21427	0.00569	0.76653	0.22358	0.00926	0.75206	0.21743	0.01404	0.75597	0.32658	0.01475	0.64915
88.50	0.21563	0.02924	0.69216	0.22324	0.04011	0.67032	0.21324	0.06459	0.66032	0.30220	0.04750	0.60855
84.10	0.26352	0.05227	0.58771	0.26334	0.06803	0.56739	0.26293	0.10016	0.53721	0.35236	0.09152	0.44775
80.20	0.25845	0.07241	0.53666	0.25847	0.09270	0.49619	0.25647	0.12942	0.47837	0.39547	0.10192	0.33011
79.10	0.28079	0.08924	0.47252	0.28021	0.10310	0.45385	0.28504	0.14634	0.41098	0.43225	0.12067	0.26924
77.00	0.32806	0.11432	0.36544	0.33191	0.12449	0.36269	0.32349	0.14860	0.37137	0.47669	0.12096	0.20282
75.00	0.40023	0.12822	0.27078	0.39967	0.13628	0.27483	0.39913	0.16570	0.25928	0.54486	0.11850	0.13159
73.50	0.48180	0.13083	0.19381	0.47749	0.13833	0.20191	0.48012	0.17397	0.16270	0.62181	0.11108	0.07552
88.10	0.17686	0.01749	0.74106	0.19519	0.02422	0.71253	0.17904	0.04905	0.72579	0.30378	0.03580	0.61477
80.10	0.22959	0.03780	0.56319	0.24239	0.04686	0.54387	0.23465	0.12271	0.51458	0.36016	0.06049	0.38573

Temperature in °C	Experimental			Flash calculation			TPD Prediction			SIG Prediction		
	water	ethanol	n-BA	water	ethanol	n-BA	water	ethanol	n-BA	water	ethanol	n-BA
79.30	0.24802	0.04594	0.50126	0.25758	0.05514	0.49118	0.23067	0.12228	0.51972	0.37429	0.06824	0.35377
78.00	0.25618	0.05308	0.45705	0.26829	0.06207	0.45285	0.26373	0.14475	0.43490	0.39386	0.07273	0.31149
77.00	0.29935	0.05937	0.39213	0.30750	0.06817	0.39501	0.29749	0.15691	0.37364	0.41202	0.07717	0.27716
76.20	0.30382	0.06385	0.35987	0.31789	0.07219	0.36615	0.29441	0.14994	0.39561	0.42208	0.07492	0.25746
75.00	0.33468	0.06753	0.31661	0.35226	0.07692	0.33176	0.32259	0.16259	0.33810	0.44133	0.07277	0.22521
74.10	0.39870	0.07429	0.24804	0.41560	0.08379	0.26620	0.40466	0.16346	0.26005	0.47622	0.07964	0.18398
72.20	0.45790	0.07523	0.18248	0.46148	0.08162	0.19266	0.46716	0.17127	0.18285	0.54222	0.07365	0.11712
Aqueous Phase												
92.00	0.99098	0.00496	0.00116	0.98981	0.00606	0.00140	0.98972	0.00408	0.00334	0.98419	0.01203	0.00175
89.50	0.97927	0.01469	0.00232	0.96960	0.02313	0.00224	0.97948	0.00989	0.00352	0.95876	0.03508	0.00297
88.50	0.96068	0.03113	0.00189	0.94360	0.04554	0.00317	0.95353	0.02373	0.00460	0.94459	0.04757	0.00391
87.10	0.97672	0.01587	0.00172	0.96935	0.02243	0.00227	0.97977	0.01026	0.00278	0.94476	0.04503	0.00364
84.50	0.94223	0.04559	0.00320	0.91806	0.06662	0.00476	0.94940	0.02637	0.00421	0.88255	0.09086	0.00974
84.20	0.96105	0.02990	0.00216	0.94944	0.03945	0.00311	0.98029	0.01013	0.00255	0.90735	0.06724	0.00663
83.10	0.90928	0.06956	0.00696	0.88085	0.09541	0.00802	0.92228	0.04031	0.00544	0.83515	0.12041	0.01728
82.00	0.94491	0.04358	0.00214	0.92437	0.06025	0.00417	0.95561	0.02331	0.00371	0.85992	0.09388	0.01254
81.00	0.91178	0.06872	0.00493	0.88324	0.09280	0.00721	0.93054	0.03664	0.00451	0.80961	0.12311	0.02078
79.50	0.86849	0.09827	0.01156	0.84153	0.12255	0.01307	0.87713	0.06330	0.00762	0.68413	0.17635	0.05843
90.20	0.98171	0.01181	0.00102	0.97292	0.01750	0.00211	0.97842	0.01043	0.00363	0.97246	0.02063	0.00224
85.40	0.96646	0.02199	0.00176	0.95138	0.03232	0.00284	0.96506	0.01798	0.00373	0.93610	0.04617	0.00413
82.10	0.95164	0.03170	0.00236	0.93185	0.04552	0.00376	0.95563	0.02330	0.00373	0.90082	0.06143	0.00701
81.20	0.93670	0.04109	0.00322	0.91894	0.05403	0.00468	0.94342	0.02973	0.00418	0.87694	0.07571	0.00966
80.10	0.92136	0.05006	0.00426	0.90293	0.06454	0.00590	0.93353	0.03503	0.00443	0.84901	0.08926	0.01351
79.50	0.90691	0.05860	0.00549	0.88259	0.07732	0.00744	0.91021	0.04656	0.00581	0.84077	0.09243	0.01374
79.20	0.89141	0.06725	0.00738	0.86713	0.08632	0.00915	0.88914	0.05661	0.00733	0.81767	0.10500	0.01804
78.00	0.87296	0.07631	0.01052	0.85028	0.09566	0.01193	0.86924	0.06687	0.00824	0.78394	0.11271	0.02546
92.50	0.99498	0.00262	0.00084	0.99313	0.00306	0.00157	0.99273	0.00263	0.00282	0.99281	0.00451	0.00137
88.50	0.98159	0.00955	0.00150	0.97288	0.01418	0.00209	0.97026	0.01485	0.00393	0.97732	0.01477	0.00184
84.10	0.96862	0.01718	0.00147	0.95504	0.02436	0.00266	0.95210	0.02483	0.00423	0.94438	0.03236	0.00340
80.20	0.95565	0.02396	0.00210	0.93200	0.03544	0.00311	0.92405	0.03846	0.00618	0.91140	0.04212	0.00561
79.10	0.94239	0.03007	0.00253	0.92010	0.04146	0.00401	0.90282	0.04846	0.00777	0.88520	0.05610	0.00815
77.00	0.91472	0.04244	0.00432	0.89302	0.05522	0.00614	0.91039	0.04623	0.00591	0.85081	0.06528	0.01215

Temperature in °C	Experimental			Flash calculation			TPD Prediction			SIG Prediction		
	water	ethanol	n-BA	water	ethanol	n-BA	water	ethanol	n-BA	water	ethanol	n-BA
75.00	0.88454	0.05429	0.00792	0.86291	0.06843	0.00931	0.88130	0.06087	0.00729	0.79322	0.07987	0.02157
73.50	0.84760	0.06677	0.01469	0.82962	0.08093	0.01509	0.83492	0.08268	0.01100	0.67534	0.10316	0.05347
88.10	0.98562	0.00613	0.00099	0.97889	0.00855	0.00182	0.97701	0.01115	0.00374	0.98120	0.01077	0.00162
80.10	0.96333	0.01281	0.00166	0.94983	0.01709	0.00264	0.92897	0.03588	0.00605	0.93427	0.02250	0.00375
79.30	0.95263	0.01576	0.00217	0.93661	0.02115	0.00322	0.93004	0.03546	0.00586	0.92429	0.02664	0.00440
78.00	0.94253	0.01880	0.00252	0.92571	0.02472	0.00376	0.90294	0.04812	0.00799	0.91026	0.03038	0.00540
77.00	0.93120	0.02173	0.00327	0.91458	0.02818	0.00450	0.88613	0.05613	0.00908	0.89654	0.03436	0.00653
76.20	0.92617	0.02433	0.00388	0.90673	0.03061	0.00459	0.90534	0.04812	0.00669	0.88860	0.03463	0.00719
75.00	0.90877	0.02740	0.00506	0.89618	0.03453	0.00629	0.88420	0.05803	0.00824	0.87340	0.03602	0.00860
74.10	0.92313	0.03131	0.00554	0.89622	0.03718	0.00415	0.88897	0.05767	0.00638	0.84787	0.04390	0.01159
72.20	0.85094	0.03913	0.01146	0.83749	0.04666	0.01246	0.85912	0.07236	0.00820	0.79205	0.05008	0.01926
Vapour Phase												
92.00	0.64474	0.02817	0.28236	0.65411	0.02230	0.27976	0.63155	0.02309	0.30229	0.66241	0.04305	0.26409
89.50	0.58179	0.09763	0.25022	0.61019	0.07315	0.24978	0.59288	0.05077	0.25807	0.62196	0.11143	0.22426
88.50	0.52579	0.16927	0.21062	0.56774	0.13103	0.20925	0.52617	0.09644	0.18326	0.60208	0.14157	0.20795
87.10	0.60571	0.09414	0.21888	0.61930	0.07111	0.23099	0.60775	0.05523	0.22948	0.59037	0.13229	0.19616
84.50	0.49598	0.21060	0.18411	0.53576	0.17069	0.18374	0.50970	0.10454	0.16774	0.51213	0.20023	0.13935
84.20	0.60134	0.13715	0.16742	0.59132	0.11465	0.19855	0.60451	0.05528	0.22978	0.51400	0.15738	0.14676
83.10	0.46594	0.24639	0.15268	0.50244	0.21090	0.14974	0.46273	0.13052	0.12623	0.47377	0.22138	0.11380
82.00	0.52771	0.18839	0.16389	0.54194	0.15929	0.17786	0.51591	0.09747	0.17959	0.45919	0.17647	0.11230
81.00	0.45971	0.24329	0.14756	0.49609	0.20892	0.14532	0.46992	0.12634	0.12986	0.42992	0.19667	0.09149
79.50	0.43582	0.26852	0.12930	0.47345	0.23678	0.12163	0.40933	0.15631	0.08583	0.39536	0.20994	0.07255
90.20	0.57741	0.07434	0.24414	0.60379	0.05512	0.24207	0.59063	0.05271	0.25500	0.62883	0.06828	0.23769
85.40	0.52529	0.11768	0.19372	0.55240	0.08984	0.20071	0.54421	0.08119	0.20863	0.54940	0.12356	0.17262
82.10	0.47852	0.14701	0.16958	0.51299	0.11430	0.17508	0.51614	0.09748	0.17951	0.47171	0.12967	0.12644
81.20	0.48989	0.15232	0.14268	0.50207	0.12770	0.15241	0.48928	0.11232	0.15547	0.44887	0.14443	0.11136
80.10	0.47249	0.16448	0.13478	0.48199	0.14181	0.13660	0.47073	0.12290	0.13678	0.42380	0.15138	0.09651
79.50	0.42056	0.18529	0.13263	0.45315	0.15578	0.12484	0.43741	0.13834	0.11357	0.41272	0.15166	0.08678
79.20	0.40759	0.19157	0.12261	0.43952	0.16281	0.11449	0.41642	0.14782	0.09874	0.40360	0.16050	0.08204
78.00	0.40008	0.19727	0.11719	0.43314	0.16889	0.10686	0.39912	0.15757	0.08320	0.38004	0.15103	0.07304
92.50	0.67104	0.01509	0.27821	0.67825	0.01096	0.27763	0.66598	0.01598	0.28883	0.67861	0.01659	0.28437
88.50	0.56340	0.05909	0.23036	0.58785	0.04292	0.22980	0.56208	0.06950	0.23062	0.62742	0.04975	0.23421

Temperature in °C	Experimental			Flash calculation			TPD Prediction			SIG Prediction		
	water	ethanol	n-BA	water	ethanol	n-BA	water	ethanol	n-BA	water	ethanol	n-BA
84.10	0.50587	0.09008	0.18594	0.53774	0.06594	0.19096	0.51150	0.09998	0.17861	0.52573	0.08440	0.16430
80.20	0.42253	0.11612	0.12972	0.46712	0.08261	0.15280	0.45022	0.12248	0.14832	0.44053	0.08493	0.11584
79.10	0.42230	0.11931	0.14483	0.44741	0.08994	0.14062	0.42472	0.13422	0.12627	0.41499	0.10045	0.09949
77.00	0.38926	0.12880	0.11980	0.41698	0.10458	0.11324	0.42854	0.13588	0.11883	0.37492	0.09790	0.07867
75.00	0.36480	0.13562	0.10219	0.39132	0.11264	0.09326	0.39771	0.15077	0.09174	0.33864	0.09646	0.06053
73.50	0.35416	0.13839	0.09152	0.37690	0.11641	0.08166	0.36756	0.16334	0.07099	0.31261	0.09506	0.04814
88.10	0.57500	0.03641	0.23621	0.59123	0.02676	0.23803	0.57576	0.05525	0.25964	0.63250	0.03700	0.23394
80.10	0.45988	0.05510	0.15534	0.47729	0.04108	0.15948	0.45484	0.11769	0.15894	0.44572	0.04832	0.12447
79.30	0.41673	0.06133	0.14439	0.44139	0.04584	0.13962	0.45391	0.11714	0.15986	0.42869	0.05371	0.11427
78.00	0.39762	0.06556	0.13331	0.41778	0.04975	0.12444	0.42058	0.13237	0.13066	0.40315	0.05566	0.10016
77.00	0.38454	0.06871	0.12201	0.40231	0.05278	0.11049	0.40504	0.14040	0.11343	0.38398	0.05806	0.08960
76.20	0.37545	0.06986	0.11147	0.38739	0.05472	0.09945	0.41928	0.13553	0.12133	0.37006	0.05531	0.08277
75.00	0.39004	0.07534	0.11129	0.38822	0.05861	0.09356	0.39819	0.14395	0.10477	0.34960	0.05246	0.07272
74.10	0.37108	0.07919	0.09873	0.37850	0.06397	0.08243	0.40144	0.14926	0.09332	0.33300	0.05767	0.06356
72.20	0.31902	0.07336	0.07489	0.32944	0.05931	0.06301	0.37558	0.15942	0.07662	0.29908	0.05296	0.04720

4.8.3 VLE water (1) ethanol (2) acetone (3) n-butyl acetate (4) at 600 mmHg

Table 4.54: VLE quaternary system water (1)-ethanol (2)-acetone (3)-n butyl acetate (4) at 600 mmHg, experimental, Flash, TPDF and SIG predictions

Temperature in °C	Experimental			Flash calculation			TPDF Prediction			SIG Prediction		
	water	ethanol	n-BA	water	ethanol	n-BA	water	ethanol	n-BA	water	ethanol	n-BA
Organic Phase												
80.20	0.17837	0.05833	0.73417	0.19193	0.04862	0.73006	0.17209	0.03623	0.76152	0.33343	0.07413	0.56804
77.10	0.23142	0.08733	0.64718	0.23997	0.08422	0.63554	0.23284	0.08369	0.64031	0.43962	0.14908	0.36312
74.00	0.27089	0.12788	0.55599	0.28288	0.12365	0.54227	0.28179	0.12642	0.53620	0.59864	0.15482	0.17698
73.00	0.27371	0.17160	0.49911	0.29793	0.15638	0.48725	0.27557	0.12757	0.54069	0.58589	0.15572	0.17312
72.10	0.31928	0.20500	0.41665	0.35044	0.18362	0.40912	0.32393	0.15004	0.46825	0.46626	0.17391	0.23747
71.10	0.48147	0.23427	0.22280	0.49853	0.21905	0.22030	0.48382	0.19367	0.27022	0.68553	0.15553	0.07718
80.00	0.16721	0.03265	0.76384	0.17439	0.03018	0.75077	0.17471	0.03512	0.75124	0.33084	0.07145	0.56665
76.20	0.21375	0.06469	0.65750	0.22253	0.06022	0.64267	0.21236	0.06702	0.63302	0.42322	0.12484	0.37377
74.10	0.23452	0.09786	0.57972	0.25198	0.08633	0.56892	0.23244	0.08313	0.58250	0.46385	0.14022	0.29156
73.10	0.26047	0.12160	0.51455	0.28102	0.10902	0.50197	0.27579	0.10529	0.50777	0.55939	0.14312	0.19941
69.50	0.30336	0.14145	0.44206	0.32220	0.12829	0.43129	0.30991	0.12920	0.44313	0.62977	0.13209	0.11175
68.30	0.39554	0.16886	0.31079	0.41216	0.15607	0.30621	0.40025	0.16083	0.32485	0.69036	0.12696	0.06690
67.20	0.51850	0.16708	0.19930	0.51883	0.16608	0.19696	0.52230	0.17461	0.19226	0.72741	0.12109	0.04212
66.10	0.59206	0.16670	0.13399	0.59492	0.16633	0.13243	0.57238	0.16449	0.14133	0.69581	0.12522	0.04591
79.50	0.14914	0.02279	0.77611	0.15821	0.02026	0.75923	0.14148	0.02190	0.77802	0.30319	0.05361	0.58697
75.40	0.17993	0.04322	0.68137	0.19126	0.03733	0.66297	0.17721	0.04052	0.66130	0.38340	0.09051	0.41052
73.10	0.20151	0.06218	0.60149	0.22070	0.05220	0.58975	0.22361	0.06708	0.56956	0.50655	0.11773	0.25525
70.50	0.22613	0.07936	0.53508	0.24652	0.06667	0.52211	0.24491	0.06701	0.50842	0.55079	0.10758	0.19153
69.10	0.25521	0.09225	0.46927	0.27764	0.07959	0.45956	0.25439	0.07515	0.48596	0.59405	0.10676	0.14076
65.40	0.38340	0.12677	0.27455	0.39983	0.11605	0.27144	0.38875	0.12002	0.28019	0.63150	0.11053	0.07770
64.10	0.45740	0.13289	0.20136	0.46743	0.12572	0.19938	0.43914	0.13098	0.22346	0.61188	0.11212	0.07041
77.00	0.15368	0.01205	0.76725	0.16232	0.00967	0.75380	0.15306	0.01057	0.73954	0.30153	0.03084	0.53848
74.50	0.16678	0.02231	0.68488	0.17970	0.01800	0.66787	0.16936	0.01457	0.65052	0.31655	0.03818	0.47139
71.40	0.18238	0.03139	0.61330	0.19879	0.02505	0.59695	0.18224	0.02042	0.60043	0.34261	0.05181	0.38443
68.30	0.20152	0.04024	0.54472	0.21912	0.03221	0.52845	0.19580	0.03110	0.53656	0.39465	0.07024	0.28086
66.20	0.22289	0.04533	0.49184	0.23979	0.03742	0.47746	0.21114	0.03505	0.49840	0.44138	0.07264	0.21405
64.00	0.27036	0.05757	0.38681	0.28936	0.04813	0.37996	0.24533	0.04130	0.41748	0.52704	0.07121	0.13367
63.00	0.31810	0.06603	0.30710	0.33537	0.05741	0.30371	0.30549	0.06113	0.32055	0.60519	0.07350	0.07988

Temperature in °C	Experimental			Flash calculation			TPD Prediction			SIG Prediction		
	water	ethanol	n-BA	water	ethanol	n-BA	water	ethanol	n-BA	water	ethanol	n-BA
Organic Phase												
62.10	0.37480	0.07027	0.24010	0.38876	0.06374	0.24035	0.35509	0.07939	0.26836	0.60648	0.08095	0.06827
61.00	0.43729	0.07155	0.18604	0.44110	0.06782	0.19119	0.38259	0.07628	0.23515	0.58670	0.07396	0.06581
Aqueous Phase												
80.20	0.97880	0.01544	0.00279	0.97436	0.01821	0.00541	0.97464	0.01607	0.00703	0.96199	0.02750	0.00827
77.10	0.96206	0.02979	0.00302	0.95502	0.03322	0.00811	0.94846	0.03689	0.01038	0.91297	0.06353	0.01535
74.00	0.94665	0.04392	0.00192	0.93541	0.04880	0.01003	0.91709	0.05939	0.01597	0.87129	0.08391	0.02121
73.00	0.92919	0.05724	0.00364	0.91678	0.06326	0.01217	0.91602	0.06033	0.01603	0.86171	0.08670	0.02163
72.10	0.90958	0.07034	0.00722	0.89519	0.07898	0.01617	0.89906	0.07210	0.01946	0.79998	0.11318	0.04033
71.10	0.86039	0.10660	0.01171	0.84652	0.11193	0.02319	0.84488	0.10727	0.03241	0.80698	0.11540	0.02829
80.00	0.98308	0.01101	0.00151	0.97802	0.01276	0.00595	0.97433	0.01573	0.00697	0.96240	0.02667	0.00808
76.20	0.96578	0.02258	0.00278	0.95945	0.02597	0.00773	0.94827	0.03270	0.00995	0.92323	0.05231	0.01242
74.10	0.95031	0.03329	0.00268	0.94326	0.03741	0.00917	0.93459	0.04161	0.01173	0.89869	0.06484	0.01525
73.10	0.93781	0.04233	0.00232	0.92906	0.04724	0.01016	0.91638	0.05317	0.01462	0.88367	0.07196	0.01731
69.50	0.92272	0.05200	0.00311	0.91329	0.05696	0.01204	0.89448	0.06725	0.01812	0.83757	0.08396	0.02232
68.30	0.88041	0.07226	0.01409	0.86921	0.08117	0.02016	0.85719	0.08891	0.02596	0.81851	0.09205	0.02206
67.20	0.85699	0.08771	0.01224	0.84908	0.09125	0.02200	0.79998	0.11500	0.03901	0.73616	0.11875	0.03931
66.10	0.80871	0.10856	0.02544	0.80436	0.11196	0.03256	0.78098	0.11739	0.03981	0.70486	0.12310	0.04307
79.50	0.98344	0.00786	0.00269	0.98036	0.00922	0.00584	0.97770	0.01103	0.00669	0.96754	0.02060	0.00701
75.40	0.96965	0.01466	0.00347	0.96575	0.01776	0.00685	0.95809	0.02184	0.00820	0.93807	0.03755	0.00928
73.10	0.95725	0.02137	0.00290	0.95338	0.02498	0.00753	0.93741	0.03553	0.01046	0.91056	0.05265	0.01218
70.50	0.94182	0.02808	0.00451	0.93733	0.03348	0.00907	0.93048	0.03628	0.01012	0.89937	0.05138	0.01196
69.10	0.92687	0.03427	0.00610	0.92179	0.04134	0.01060	0.92244	0.04112	0.01103	0.89299	0.05211	0.01051
65.40	0.87695	0.05639	0.00766	0.87073	0.06372	0.01523	0.85435	0.07147	0.02024	0.79730	0.08012	0.02270
64.10	0.84324	0.06815	0.01348	0.83752	0.07595	0.02018	0.82594	0.08263	0.02500	0.76732	0.08590	0.02287
77.00	0.98683	0.00466	0.00127	0.98509	0.00438	0.00523	0.98207	0.00535	0.00535	0.97031	0.01265	0.00559
74.50	0.97513	0.00805	0.00157	0.97413	0.00890	0.00564	0.97098	0.00825	0.00586	0.96010	0.01641	0.00578
71.40	0.96383	0.01128	0.00217	0.96321	0.01319	0.00616	0.96297	0.01186	0.00601	0.94188	0.02365	0.00647
68.30	0.95209	0.01450	0.00223	0.95106	0.01775	0.00661	0.94559	0.01950	0.00728	0.91389	0.03413	0.00798
66.20	0.94148	0.01744	0.00267	0.94072	0.02127	0.00722	0.93987	0.02176	0.00721	0.89916	0.03605	0.00809
64.00	0.91815	0.02324	0.00371	0.91798	0.02836	0.00859	0.92420	0.02590	0.00772	0.88537	0.03573	0.00759

Temperature in °C	Experimental			Flash calculation			TPD Prediction			SIG Prediction		
	water	ethanol	n-BA	water	ethanol	n-BA	water	ethanol	n-BA	water	ethanol	n-BA
Aqueous Phase												
63.00	0.89606	0.02815	0.07040	0.89511	0.03481	0.01005	0.89018	0.03867	0.01077	0.82812	0.04823	0.01432
62.10	0.87191	0.03306	0.00773	0.87245	0.03973	0.01213	0.87245	0.04826	0.01252	0.79696	0.05777	0.01658
61.00	0.84409	0.03800	0.01131	0.84529	0.04465	0.01571	0.87861	0.04354	0.01009	0.75072	0.05897	0.02224
Vapour Phase												
80.20	0.60054	0.09750	0.24638	0.60090	0.09590	0.25193	0.59954	0.07792	0.26905	0.58626	0.12483	0.24174
77.10	0.54390	0.16585	0.20232	0.55520	0.14580	0.22712	0.54196	0.14780	0.23105	0.50175	0.20855	0.17918
74.00	0.48981	0.21042	0.18682	0.51425	0.18986	0.20005	0.49532	0.19465	0.20142	0.43377	0.20802	0.12875
73.00	0.47531	0.22952	0.16947	0.48595	0.22167	0.17944	0.49215	0.19672	0.20110	0.41448	0.19947	0.11504
72.10	0.45293	0.25634	0.16173	0.47389	0.24529	0.16343	0.47778	0.21569	0.18684	0.39538	0.20437	0.10431
71.10	0.41397	0.28295	0.12648	0.42907	0.28213	0.12372	0.45140	0.25737	0.15193	0.37568	0.21273	0.08196
80.00	0.58319	0.07341	0.24539	0.60323	0.06398	0.25543	0.59204	0.07519	0.26351	0.58172	0.12031	0.23806
76.20	0.51124	0.12447	0.19972	0.54339	0.10854	0.21631	0.50746	0.12117	0.21126	0.48613	0.17193	0.16916
74.10	0.47785	0.15046	0.17260	0.50391	0.13870	0.18895	0.47908	0.13887	0.19252	0.44028	0.17738	0.13652
73.10	0.44913	0.16794	0.15389	0.47181	0.15972	0.16720	0.45615	0.15808	0.17290	0.41964	0.17841	0.12286
69.50	0.42435	0.18075	0.13280	0.44665	0.17332	0.15008	0.43014	0.17715	0.15522	0.35530	0.15146	0.08227
68.30	0.39751	0.19330	0.11579	0.41399	0.18956	0.12239	0.40998	0.19864	0.13306	0.33394	0.15255	0.06719
67.20	0.38474	0.19776	0.10446	0.38959	0.19582	0.10404	0.38276	0.20535	0.10477	0.31501	0.15219	0.05457
66.10	0.37658	0.20441	0.09223	0.37849	0.20184	0.09043	0.35779	0.18772	0.08681	0.29860	0.14187	0.04647
79.50	0.57763	0.04978	0.23891	0.59597	0.04493	0.25043	0.57552	0.05147	0.26554	0.57224	0.09313	0.22919
75.40	0.49974	0.07839	0.19324	0.52980	0.07218	0.20773	0.49132	0.08061	0.20679	0.47438	0.12616	0.16160
73.10	0.45485	0.09528	0.16907	0.48884	0.09017	0.17714	0.45412	0.11275	0.17597	0.42457	0.14370	0.12887
70.50	0.41709	0.10617	0.14272	0.44895	0.10333	0.15266	0.41730	0.10326	0.14824	0.37850	0.11888	0.10143
69.10	0.39356	0.11429	0.13056	0.42104	0.11208	0.13293	0.40506	0.11077	0.14083	0.35710	0.11239	0.08058
65.40	0.33358	0.12571	0.09387	0.35439	0.12535	0.08707	0.34205	0.12875	0.08992	0.29488	0.10557	0.04980
64.10	0.32018	0.12933	0.08442	0.33535	0.12638	0.07353	0.32837	0.13188	0.07881	0.27507	0.09857	0.03769
77.00	0.56866	0.02518	0.23283	0.59911	0.02196	0.24863	0.55454	0.02468	0.24212	0.51791	0.05192	0.18849
74.50	0.48395	0.04057	0.18281	0.52505	0.03702	0.20138	0.47456	0.03071	0.19220	0.46351	0.05789	0.15283
71.40	0.43050	0.04915	0.14742	0.47207	0.04658	0.16727	0.43644	0.03956	0.16640	0.40194	0.06721	0.11466
68.30	0.39260	0.05369	0.12373	0.42452	0.05361	0.13835	0.38573	0.05338	0.13649	0.34657	0.07490	0.08209
66.20	0.36501	0.05701	0.10960	0.39618	0.05699	0.12042	0.36648	0.05565	0.12172	0.31396	0.06768	0.06423
64.00	0.33777	0.05880	0.08842	0.35304	0.06084	0.09091	0.32937	0.05563	0.09447	0.28238	0.05752	0.04843

Temperature in °C	Experimental			Flash calculation			TPD Prediction			SIG Prediction		
	water	ethanol	n-BA	water	ethanol	n-BA	water	ethanol	n-BA	water	ethanol	n-BA
Vapour Phase												
64.00	0.33777	0.05880	0.08842	0.35304	0.06084	0.09091	0.32937	0.05563	0.09447	0.28238	0.05752	0.04843
63.00	0.30813	0.06175	0.07642	0.32337	0.06220	0.07188	0.30151	0.06650	0.07259	0.27007	0.05790	0.03817
62.10	0.30520	0.06197	0.07509	0.30671	0.06094	0.05971	0.29628	0.07782	0.06604	0.25521	0.06264	0.03324
61.00	0.28827	0.06194	0.06382	0.29159	0.05871	0.05264	0.28645	0.06960	0.05815	0.24231	0.05322	0.02789

4.8.4 VLE water (1) ethanol (2) acetone (3) n-butyl acetate (4) at 360 mmHg

Table 4.55: VLE quaternary system water (1)-ethanol (2)-acetone (3)-n butyl acetate (4) at 360 mmHg, experimental, Flash, TPDF and SIG predictions

Temperature in °C	Experimental			Flash calculation			TPDF Prediction			SIG Prediction		
	water	ethanol	n-BA	water	ethanol	n-BA	water	ethanol	n-BA	water	ethanol	n-BA
Organic Phase												
70.00	0.14377	0.04416	0.78578	0.16081	0.04264	0.76969	0.15432	0.04989	0.76908	0.26840	0.05748	0.66438
66.50	0.17470	0.09238	0.69352	0.19640	0.08341	0.68155	0.18054	0.09398	0.67884	0.37955	0.14123	0.45192
64.10	0.23522	0.13400	0.58052	0.25243	0.12741	0.56922	0.23264	0.12589	0.58409	0.66928	0.14104	0.15749
63.10	0.26314	0.17306	0.50515	0.28474	0.16154	0.49620	0.29744	0.16003	0.48168	0.55704	0.18505	0.20521
62.20	0.31052	0.20001	0.42807	0.33001	0.18834	0.41977	0.36187	0.17162	0.40303	0.57870	0.18355	0.17626
61.10	0.39213	0.22718	0.31596	0.40502	0.21817	0.31001	0.41336	0.18961	0.32940	0.58713	0.18881	0.15132
60.00	0.48229	0.23995	0.21497	0.49257	0.23041	0.21294	0.48088	0.20723	0.24648	0.65684	0.17770	0.09507
72.00	0.15625	0.03162	0.77872	0.17361	0.02902	0.76538	0.15993	0.03083	0.77556	0.25182	0.03450	0.70145
69.00	0.24326	0.05781	0.64329	0.24654	0.05941	0.63601	0.23879	0.06115	0.63734	0.29507	0.05855	0.62549
66.20	0.21561	0.09248	0.60684	0.23786	0.08678	0.59303	0.22410	0.08700	0.60610	0.36024	0.12036	0.47632
62.30	0.29191	0.10955	0.50243	0.29984	0.10832	0.49509	0.28975	0.10331	0.50532	0.41999	0.15240	0.32947
61.10	0.27286	0.14193	0.46923	0.30090	0.12500	0.46771	0.30976	0.10774	0.48596	0.43586	0.15396	0.29455
57.20	0.41687	0.17854	0.26928	0.42815	0.17206	0.26720	0.42297	0.16483	0.28105	0.58862	0.15914	0.12241
56.10	0.54924	0.18004	0.14924	0.55584	0.17536	0.15066	0.52605	0.18029	0.17015	0.67785	0.14687	0.06378
70.10	0.15883	0.02349	0.76789	0.17434	0.01958	0.75674	0.15510	0.02332	0.76391	0.26159	0.02767	0.68968
65.30	0.02474	0.03706	0.65409	0.08733	0.03309	0.79201	0.15233	0.03928	0.70662	0.32531	0.07956	0.51224
62.30	0.19185	0.05792	0.62519	0.20935	0.05351	0.61060	0.19387	0.04793	0.61030	0.34184	0.09209	0.43178
59.20	0.23281	0.07745	0.53325	0.25067	0.07108	0.52425	0.20196	0.06975	0.57159	0.41070	0.12097	0.30242
57.20	0.24561	0.08813	0.49099	0.26573	0.08129	0.48479	0.22431	0.08643	0.51284	0.41070	0.12097	0.30242
54.10	0.36118	0.12596	0.29405	0.37295	0.11939	0.29097	0.30140	0.11608	0.36638	0.74687	0.09160	0.04373
52.10	0.42339	0.13379	0.22356	0.43489	0.12804	0.22379	0.32448	0.12431	0.32993	0.73723	0.08938	0.03439
68.50	0.15421	0.01405	0.76583	0.16819	0.01100	0.75072	0.15313	0.01322	0.74849	0.27049	0.02316	0.65536
64.50	0.15511	0.01949	0.69938	0.17614	0.01775	0.68254	0.14947	0.01679	0.69573	0.29811	0.03803	0.53984
62.40	0.19132	0.02756	0.61040	0.20647	0.02602	0.59670	0.19212	0.02608	0.59873	0.30957	0.05285	0.48151
58.60	0.23197	0.03470	0.53351	0.24071	0.03270	0.52305	0.21319	0.03349	0.53346	0.33799	0.06638	0.37915
55.50	0.21603	0.04187	0.50074	0.23528	0.03843	0.49075	0.20383	0.03466	0.52594	0.36574	0.06827	0.30127
50.60	0.32271	0.06725	0.29422	0.33660	0.06250	0.29330	0.28663	0.05943	0.33876	0.50758	0.07884	0.12919
49.30	0.35732	0.07061	0.24950	0.36940	0.06592	0.25288	0.32668	0.06677	0.28968	0.52459	0.07637	0.10273
48.10	0.45312	0.07368	0.17832	0.44871	0.07135	0.18998	0.42290	0.07733	0.19486	0.54030	0.07172	0.08051

Temperature in °C	Experimental			Flash calculation			TPD Prediction			SIG Prediction		
	water	ethanol	n-BA	water	ethanol	n-BA	water	ethanol	n-BA	water	ethanol	n-BA
Aqueous Phase												
70.00	0.97782	0.01587	0.00276	0.97573	0.01660	0.00521	0.96351	0.02410	0.00921	0.97096	0.02116	0.00689
66.50	0.95793	0.03283	0.00323	0.95473	0.03345	0.00745	0.92795	0.04978	0.01513	0.92761	0.05630	0.01179
64.10	0.93925	0.04815	0.00407	0.93095	0.05222	0.00976	0.90871	0.06425	0.01730	0.89282	0.07637	0.01840
63.10	0.92240	0.06228	0.00398	0.91321	0.06647	0.01120	0.88284	0.08255	0.02214	0.86111	0.09889	0.02228
62.20	0.90451	0.07599	0.00544	0.89252	0.08160	0.01405	0.88500	0.08262	0.01899	0.84409	0.10640	0.02551
61.10	0.87972	0.09528	0.00690	0.86570	0.10092	0.01701	0.86172	0.09747	0.02331	0.81271	0.12177	0.03160
60.00	0.84392	0.11829	0.01356	0.83177	0.12330	0.02303	0.82201	0.12170	0.03300	0.77478	0.13871	0.03989
72.00	0.98118	0.01163	0.00285	0.97959	0.01167	0.00566	0.97441	0.01426	0.00760	0.97917	0.01307	0.00654
69.00	0.96717	0.02254	0.00172	0.96353	0.02331	0.00662	0.95909	0.02565	0.00787	0.96992	0.02124	0.00666
66.20	0.95051	0.03330	0.00251	0.94589	0.03589	0.00772	0.93375	0.04235	0.01174	0.93625	0.04735	0.01013
62.30	0.93433	0.04423	0.00327	0.92983	0.04596	0.00946	0.92897	0.04583	0.01006	0.89327	0.07069	0.01460
61.10	0.92075	0.05332	0.00342	0.91782	0.05400	0.01046	0.93098	0.04570	0.00928	0.88093	0.07509	0.01579
57.20	0.86644	0.08341	0.00841	0.85938	0.08720	0.01671	0.85547	0.08827	0.01989	0.79300	0.10991	0.02952
56.10	0.80129	0.11221	0.02470	0.79856	0.11526	0.03003	0.78627	0.12121	0.03501	0.72971	0.13270	0.04355
70.10	0.98401	0.00817	0.00157	0.98232	0.00789	0.00508	0.97538	0.01119	0.00701	0.98263	0.00997	0.00545
65.30	0.96894	0.01566	0.00260	0.96657	0.01774	0.00552	0.95580	0.02165	0.00892	0.95056	0.03125	0.00751
62.30	0.95615	0.02279	0.00190	0.95379	0.02396	0.00652	0.94569	0.02529	0.00838	0.93109	0.03946	0.00852
59.20	0.94436	0.02857	0.00207	0.93951	0.03183	0.00700	0.92531	0.03890	0.01087	0.89271	0.05822	0.01195
57.20	0.92821	0.03587	0.00357	0.92580	0.03859	0.00860	0.90293	0.05059	0.01381	0.89271	0.05822	0.01195
54.10	0.87269	0.05882	0.00735	0.86727	0.06379	0.01322	0.83451	0.07783	0.02583	0.81554	0.07512	0.02126
52.10	0.84039	0.07026	0.01252	0.83770	0.07454	0.01755	0.81344	0.08599	0.02977	0.76145	0.08421	0.02738
68.50	0.98412	0.00456	0.00298	0.98334	0.00472	0.00509	0.97775	0.00654	0.00624	0.98169	0.00845	0.00504
64.50	0.97462	0.00793	0.00129	0.97390	0.00797	0.00489	0.96603	0.00944	0.00686	0.96503	0.01512	0.00547
62.40	0.96110	0.01215	0.00183	0.96110	0.01234	0.00548	0.95436	0.01403	0.00676	0.95105	0.02216	0.00612
58.60	0.95020	0.01472	0.00219	0.95005	0.01582	0.00591	0.94297	0.01822	0.00675	0.92556	0.03069	0.00714
55.50	0.93845	0.01800	0.00232	0.93823	0.01980	0.00621	0.93805	0.01977	0.00682	0.90349	0.03404	0.00773
50.60	0.87864	0.03238	0.00598	0.87813	0.03617	0.00959	0.88171	0.03670	0.01004	0.82426	0.04860	0.01291
49.30	0.85597	0.03665	0.00839	0.85759	0.04008	0.01176	0.87615	0.03901	0.00939	0.78459	0.05277	0.01648
48.10	0.81394	0.04374	0.01532	0.81769	0.04773	0.01875	0.86324	0.04227	0.00870	0.62578	0.06718	0.05026

Temperature in °C	Experimental			Flash calculation			TPD Prediction			SIG Prediction		
	water	ethanol	n-BA	water	ethanol	n-BA	water	ethanol	n-BA	water	ethanol	n-BA
Vapour Phase												
70.00	0.57381	0.10075	0.25519	0.60451	0.08389	0.25482	0.57000	0.10075	0.27061	0.61812	0.10086	0.25999
66.50	0.51007	0.17071	0.21427	0.55558	0.14220	0.22103	0.50726	0.16376	0.22742	0.53340	0.20302	0.19735
64.10	0.47397	0.21179	0.18697	0.50969	0.19009	0.19090	0.48396	0.19295	0.19738	0.47137	0.21632	0.16701
63.10	0.45365	0.23545	0.17019	0.47984	0.22248	0.17017	0.46553	0.22136	0.17403	0.44342	0.24515	0.13581
62.20	0.43657	0.25173	0.15757	0.45784	0.24441	0.15365	0.46003	0.22580	0.15982	0.42345	0.23984	0.12334
61.10	0.40670	0.27581	0.13108	0.42768	0.26840	0.13111	0.44035	0.23940	0.14324	0.39829	0.23979	0.10633
60.00	0.39970	0.28252	0.12463	0.40974	0.28441	0.11293	0.42171	0.25784	0.12704	0.37527	0.23798	0.09186
72.00	0.63206	0.06312	0.22922	0.62121	0.05721	0.25476	0.58870	0.06369	0.27481	0.63077	0.06429	0.27854
69.00	0.53645	0.11591	0.20434	0.56113	0.09961	0.21760	0.54655	0.10314	0.21906	0.60618	0.09931	0.24862
66.20	0.49677	0.14022	0.18376	0.51131	0.13420	0.18433	0.48889	0.13904	0.19694	0.52921	0.17429	0.19555
62.30	0.46766	0.15864	0.15337	0.47543	0.15136	0.16425	0.46582	0.14599	0.16692	0.43369	0.18795	0.13406
61.10	0.49906	0.15067	0.12879	0.45581	0.16588	0.14763	0.46986	0.14963	0.16551	0.40829	0.18147	0.11887
57.20	0.35655	0.19455	0.11070	0.37718	0.19182	0.10061	0.37691	0.18499	0.10674	0.33114	0.17276	0.07342
56.10	0.34069	0.19832	0.09669	0.35335	0.19597	0.08237	0.34744	0.19656	0.08492	0.31063	0.17308	0.06068
70.10	0.59055	0.04337	0.23773	0.60878	0.03884	0.24899	0.56460	0.04839	0.26154	0.63589	0.05093	0.26794
65.30	0.48134	0.08025	0.19956	0.50729	0.07310	0.21664	0.48399	0.07522	0.21966	0.51335	0.11714	0.18631
62.30	0.43240	0.09447	0.17255	0.48150	0.08616	0.17491	0.44064	0.07861	0.17373	0.44282	0.12022	0.14285
59.20	0.41113	0.10433	0.14949	0.43999	0.10097	0.14583	0.41015	0.10586	0.15704	0.37608	0.13429	0.10307
57.20	0.38536	0.11291	0.13428	0.41709	0.10894	0.13165	0.37988	0.11871	0.13559	0.37608	0.13429	0.10307
54.10	0.31470	0.12271	0.09451	0.33002	0.12188	0.08059	0.32636	0.12715	0.09375	0.28835	0.10623	0.06068
52.10	0.30232	0.12406	0.08332	0.31500	0.12284	0.06881	0.31335	0.12853	0.08486	0.25855	0.09526	0.04357
68.50	0.54798	0.02379	0.24212	0.59028	0.02204	0.24088	0.54096	0.02743	0.24644	0.60542	0.04120	0.24410
64.50	0.46229	0.03737	0.19266	0.51883	0.03272	0.19582	0.46482	0.03267	0.20602	0.50066	0.05784	0.17834
62.40	0.41177	0.04525	0.15976	0.45734	0.04227	0.15962	0.42399	0.04295	0.16153	0.45077	0.07316	0.14831
58.60	0.37650	0.04956	0.13592	0.41727	0.04727	0.13459	0.38232	0.04906	0.13180	0.37234	0.07711	0.10345
55.50	0.35651	0.05284	0.12122	0.37988	0.05234	0.11388	0.35952	0.04964	0.12290	0.31792	0.06815	0.07472
50.60	0.27712	0.05964	0.07685	0.28876	0.05938	0.06117	0.27647	0.05926	0.06674	0.24352	0.05933	0.03901
49.30	0.26536	0.05800	0.06587	0.27626	0.05831	0.05394	0.26744	0.06077	0.05827	0.22638	0.05437	0.03145
48.10	0.25959	0.05882	0.06056	0.26263	0.05760	0.04951	0.25255	0.06082	0.04533	0.21147	0.04865	0.02529

4.9 Discussion

The correlation and predictions for two quaternary VLLE systems of: water (1) ethanol (2) acetone (3) MEK (4) at pressure of 760 mmHg and water (1) ethanol (2) acetone (3) n-butyl acetate (4) system at pressures of 360, 600 and 760 mmHg have been carried out using the PRSV+WSMR model. The Rachford-Rice method is used in flash calculations and the interaction parameters for PRSV EOS and the UNIQUAC energy parameters obtained were used in the TPDF and SIG prediction methods. A quaternary system requires 18 parameters: 12 energy parameters for the UNIQUAC model and 6 interaction parameters for PRSV EOS. Table (4.51) shows these parameters for both VLLE systems of interest.

From the results obtained for binary and ternary LLE, VLE and VLLE calculations it was found that the PRSV+WSMR combination is capable of correlating the non-ideal polar heterogeneous mixtures and thus it would appear that this can be extended to quaternary systems.

The results obtained for the quaternary systems using: Flash, TPDF and SIG methods indicate the capability of these methods to correlate and hence predict the phase behaviour for quaternary multiphase systems at low and moderate pressures and moderate temperatures. The summary of the results in table (4.50) shows the Absolute Average Deviations (AAD) from experimental values for the Flash, TPDF and SIG in each phase. The TPI method has not been tested on the quaternary systems and the reasons are discussed in the previous section (4.7). Overall the AAD TPDF results for the quaternary system with the constituent binary of MEK-water were less accurate than the system with the constituent binary of n-butyl acetate-water. Table (4.52) shows the results for the VLLE system water (1) ethanol (2) acetone (3) MEK (4) at 760 mmHg. Figure (4.41) gives a graphical representation of the composition of water and MEK components for TPDF predicted values versus the experimental values in three phases. An observation of the summary table (4.50) shows that the TPDF AAD is lower than the SIG. Observation of table (4.50) immediately indicates that the TPDF method gives consistently lower values than the SIG method. As shown in sections (3.11 and 4.6.3) the SIG method can be used to generate initial values for the TPI method and it is also capable of extension to

quaternary systems. The SIG method depends on an initial generation of phase compositions using activity coefficients which are used to generate fugacity coefficients which can then be used to calculate initial (K) values. These are used to calculate relative volatilities which are employed in a flash calculation. The SIG results contrast with the TPDF method which is essentially minimising a function directly related to the Gibbs energy surface. Such an approach emphasises that the TPDF method is reliable and efficient in predicting quaternary data.

Observing the data for the quaternary systems it is noticeable that at all temperatures and pressures there is a consistently high concentration of water in the organic phase even at low concentrations of other organic components. Although the TPDF method can produce acceptably low values of AAD for all phases it is noticeable that the AAD values for the organic phase are consistently higher than for the aqueous phase. This high water content of the organic phase is present for all the measured data and is apparently higher than the theoretical predictions. This is expected as the SIG method is based on the calculation of the relative volatility of component i in the mixture. The behaviour of constituent heterogeneous binaries azeotrope of (water-MEK) and (water-n butyl acetate) have the influence on pseudo ternary systems behaviour. The overall AAD for this system is 0.0065 in Flash calculation, the value in TPDF prediction is 0.019 and 0.035 for the SIG.

The results for the VLLE correlation and predictions using TPDF and SIG for the system of water (1) ethanol (2) acetone (3) n-butyl acetate (4) at pressures of 760, 600, 360 mmHg can be found in tables (4.53, 4.54 and 4.55) respectively. The graphical illustrations for water and n-butyl acetate predictions against measured data are shown in figures (4.42, 4.43 and 4.44) for this system at pressure of 760, 600, 360 mmHg respectively.

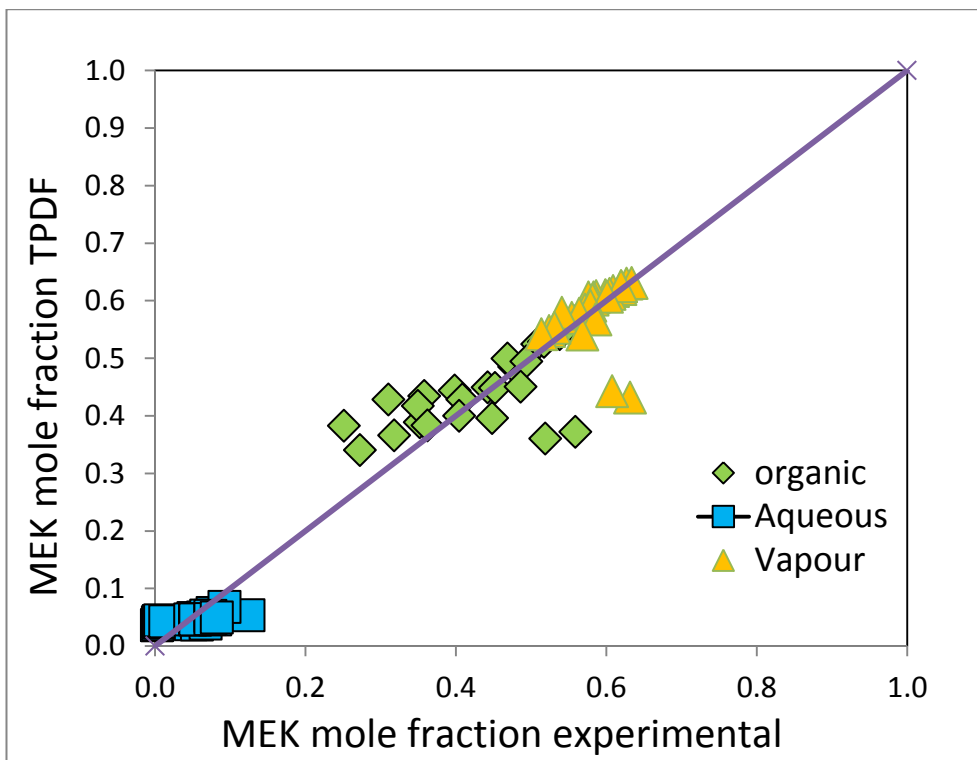
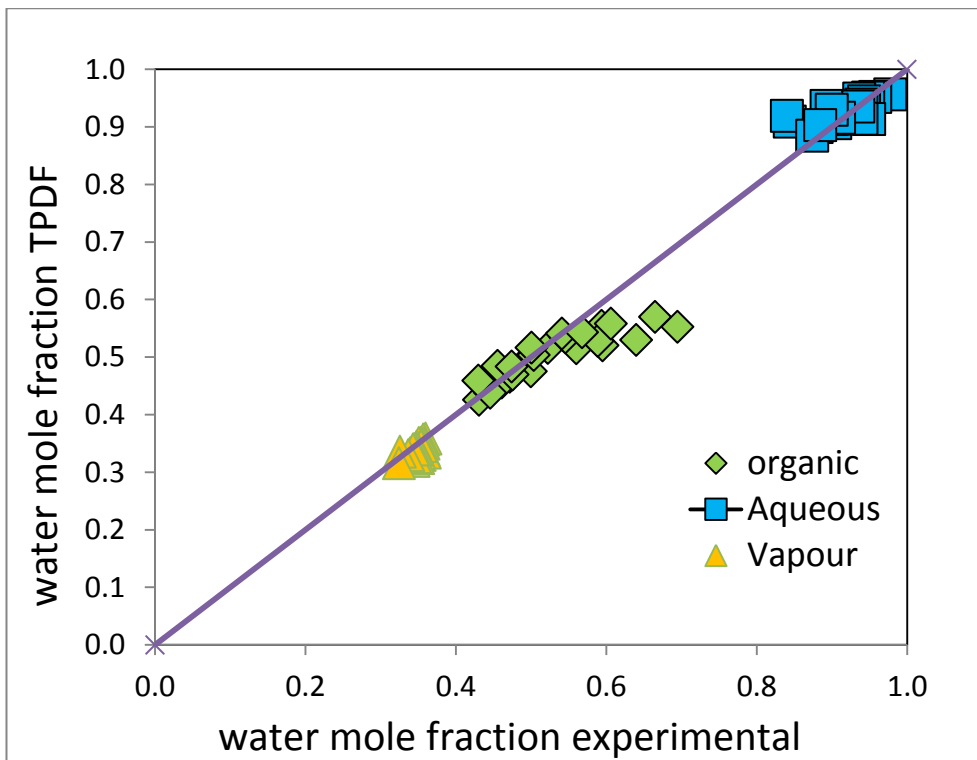


Figure 4.41: VLE quaternary system water (1)-ethanol (2)-acetone (3)-MEK (4) at 760 mmHg, TPDF prediction versus experimental of water and MEK in the organic, aqueous and vapour phases

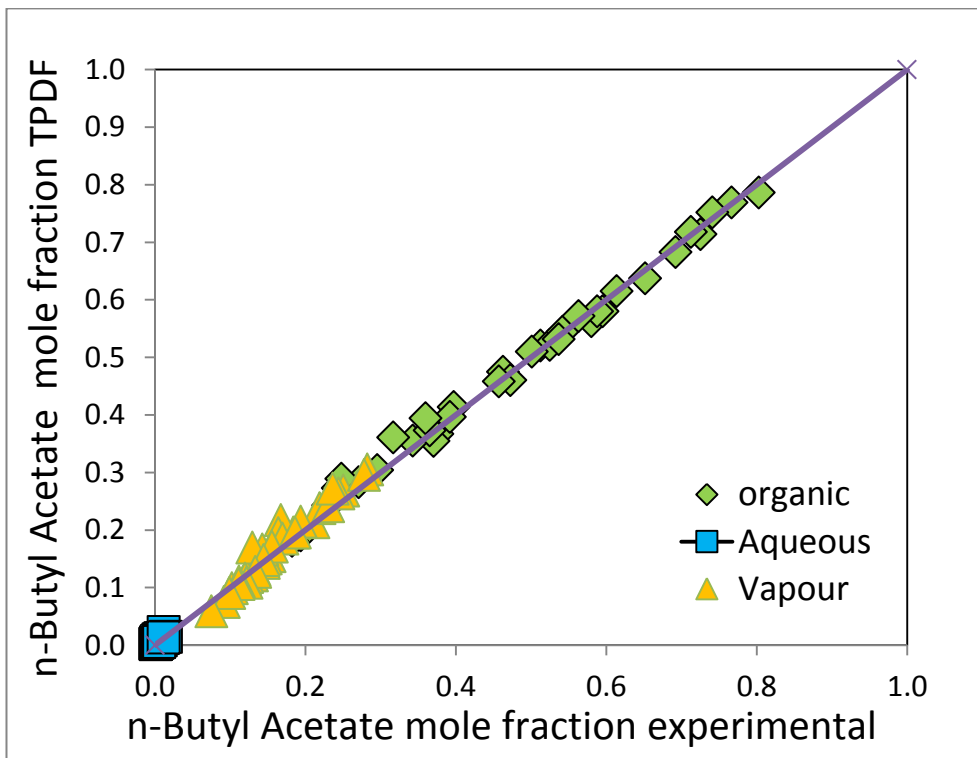
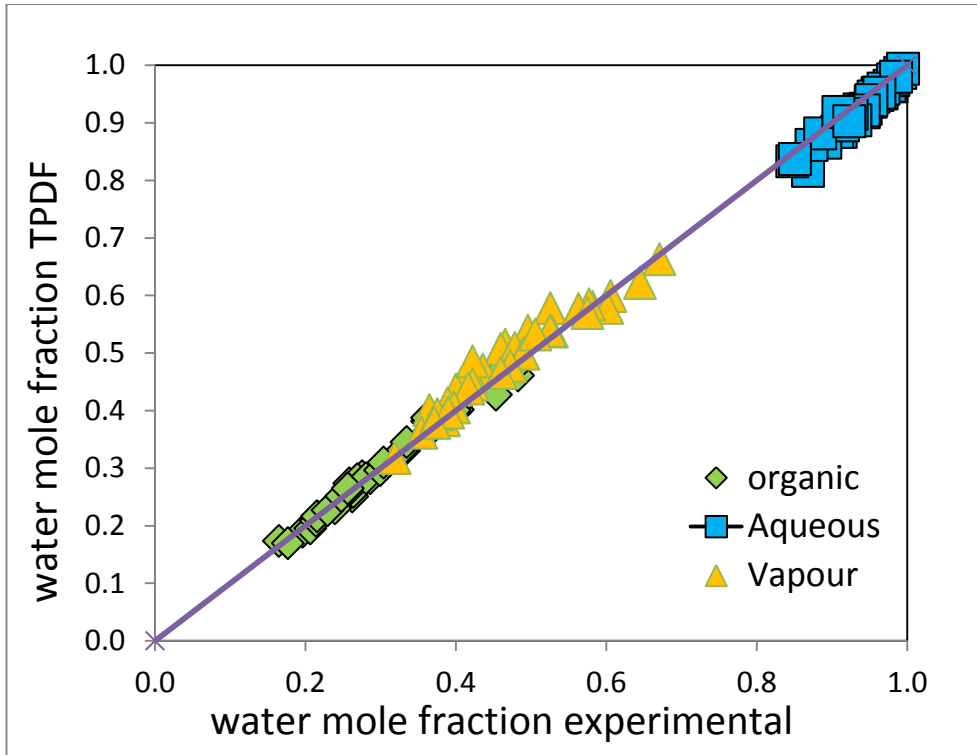


Figure 4.42: VLE quaternary system water(1)-ethanol(2)-acetone(3)-n-butyl acetate(4) at 760 mmHg , TPDF prediction versus experimental of water and n-butyl acetate in the organic ,aqueous and vapour phases

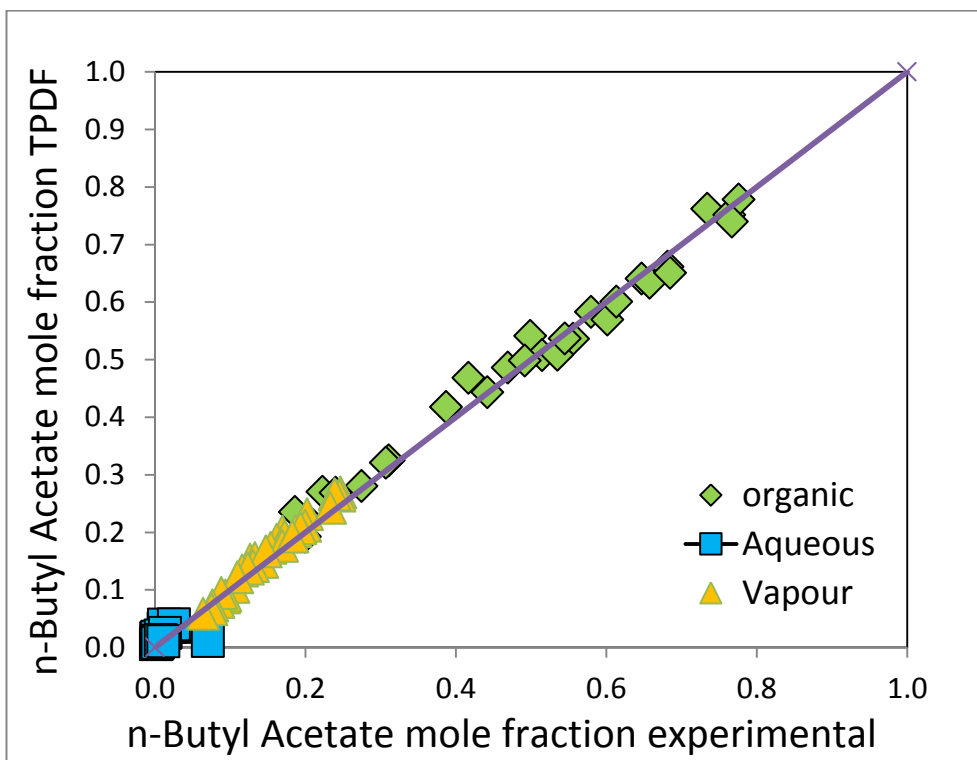
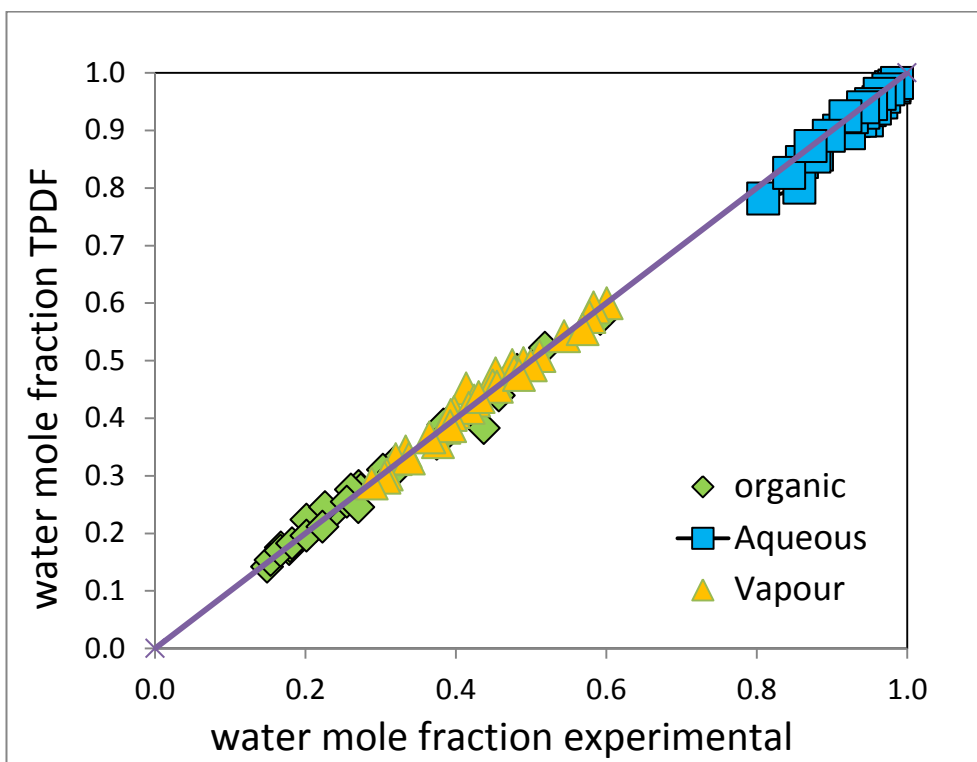


Figure 4.43: VLLE quaternary system water(1)-ethanol(2)-acetone(3)-n-butyl acetate(4) at 600 mmHg , TPDF prediction versus experimental of water and n-butyl acetate in the organic ,aqueous and vapour phases

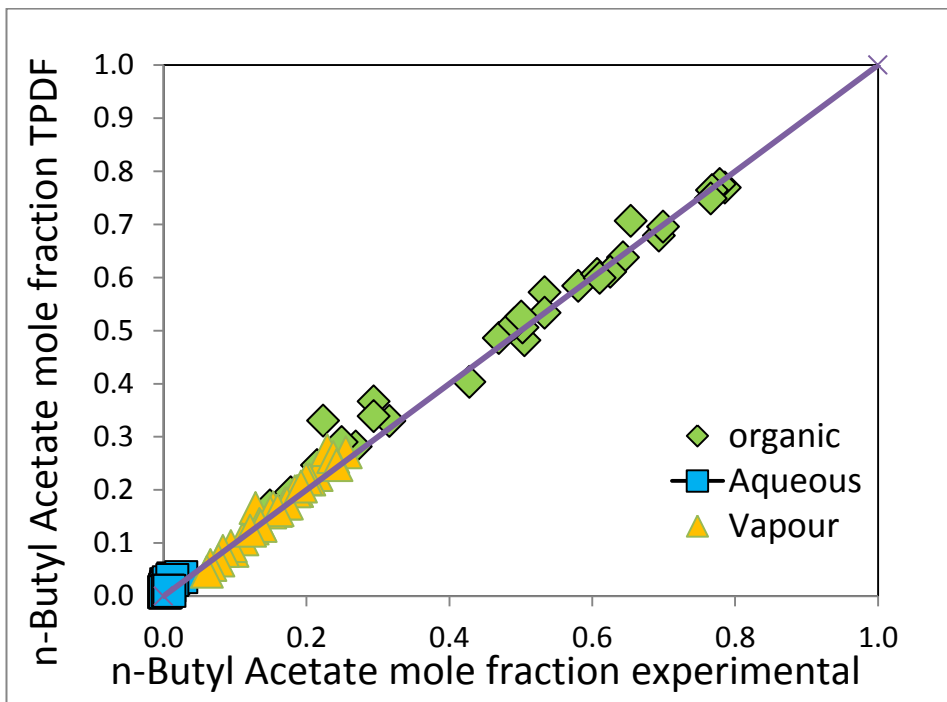
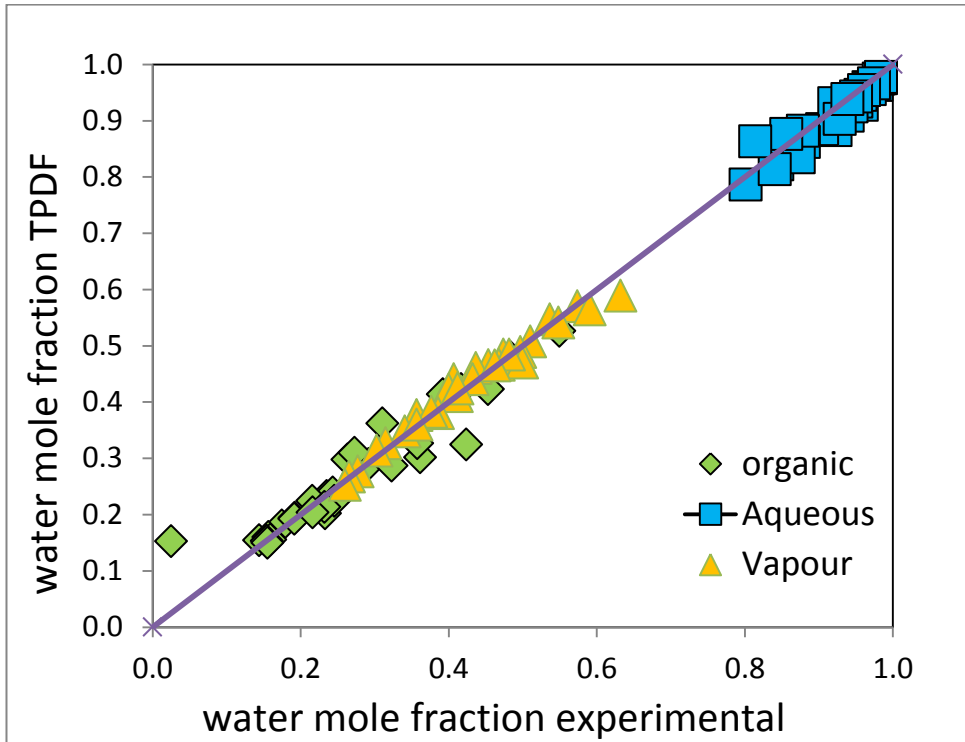


Figure 4.44: VLE quaternary system water(1)-ethanol(2)-acetone(3)-n-butyl acetate(4) at 360 mmHg , TPDF prediction versus experimental of water and n-butyl acetate in the organic ,aqueous and vapour phases

5. Conclusions and Future work

This work has investigated the possibility of thermodynamic modelling of phase equilibria for a range of homogenous and heterogeneous systems particularly for VLLE binary, ternary and quaternary systems by utilising the PRSV EOS combined with WSMR. This modelling package combining PRSV with WSMR was initially tested on the correlation of VLE binary systems under isothermal and isobaric conditions. These mixtures have a range of polar components from moderately polar (MEK, n-butyl acetate) to highly polar (ethanol, propanol) components. The results obtained show that the selected modelling package can successfully and adequately represent the thermodynamic behaviour of fugacity in both liquid and vapour phases.

The Area Method and the TPI method were applied to predict the phase equilibrium of two LLE and four binary VLLE systems and subsequently the TPI method was extended to predict binary VLLE. This was achieved by modifying a 2-point search and a direct 3-point search. Due to the sensitivity of the TPI to initial conditions, this work developed and successfully applied a new scheme of fixed initial values which depend on phase change (Cusps) compositions. The AM method is computationally slower than the TPI due to the integration part of the Gibbs energy curve, for this reason the AM was only applied to LLE binary systems.

In the prediction of VLLE for ternary systems, it was outlined in the literature survey (2.6) that the majority of the optimisation methods require a good initial estimate to improve their reliability and efficiency. A significant achievement of this work was in suggesting a Systematic Initial Generator (SIG) to obtain initial values as close as possible to the real solution. This had a positive effect in decreasing the fitting error of the TPI results. This work has, through modelling, identified a problem (i.e. sensitivity to the starting value) when applying the TPI on VLLE ternary systems. This research has tested another method of Gibbs free minimisation called the TPDF method which was used to predict using the VLLE ternary systems of Younis et al. (2007). This work concludes that the TPDF method is less sensitive to the initial values, computationally faster than the TPI method and

can also be extended to multicomponent multiphase systems with fewer complications.

Another achievement of this work has been in testing the TPI, TPDF and SIG methods as a phase predictor on ternary VLE systems. The TPDF and SIG method were capable of recognising the 2 and 3-Phase regions successfully, however the TPI method failed to identify the 2-phase region. This work has made a useful and effective thermodynamic tool available for engineers working in design and optimisation of chemical process operation. The parameters obtained for the VLE ternary systems can be available for designers in the field of separation processes within the chemical industry.

Finally this work has applied the thermodynamic package PRSV+WSMR successfully to two quaternary systems measured by Younis et al. (2007) using flash correlation whilst obtaining reasonable prediction results for the TPDF and SIG methods. All multicomponent systems investigated in this work display highly non-ideal behaviour in that the liquid phase is heterogeneous for a range of compositions. To use an Equation of State for such systems requires applicable and effective mixing rules. It is extremely rare to find examples of an EOS approach to correlating and predicting highly polar, non-ideal, organic-aqueous systems of low pressures. This work has demonstrated that the Wong-Sandler mixing rules (WSMR) combined with the Peng Robinson Stryjek Vera (PRSV) Equation of State, gives an approach which is fully capable of representing such systems and this method allows both liquid and vapour phases to be represented by the same equations.

The Nelder-Mead optimisation simplex was used in correlation and prediction methods. The main advantage of this optimisation is that it can be used directly to an objective function without the need for derivative of the function. It is well known in the thermodynamic field that the Gibbs free minimisation has non-convex and non-linear properties which indicate that this type of function has several local minima. It is recommended that further research be undertaken to investigate the effect and effectiveness of different optimisation methods on the overall results for VLE ternary and quaternary

systems particularly the modified Nelder-Mead mentioned previously in the theory chapter (section 3.2).

To evaluate the success of modelling the organic/aqueous heterogeneous mixtures with partial miscibility using PRSV+WSMR at atmospheric pressure, this work has used absolute average deviation values as defined at appropriate points in the text. The results relating to binary, ternary and quaternary VLE systems can be found in tables 4.16, 4.20 and 4.50 respectively. In order to illustrate the level of success of the correlations and the predictions of the TPI and TPDF methods, the AAD results for a complex mixture of binary VLE water - n-butyl acetate at 91.05°C and 760 mmHg are 0.001 and 0.0005 for correlation and TPI prediction respectively. In the VLE ternary system of water-acetone-n butyl acetate for a temperature range ($66.1\text{-}86.1$) $^{\circ}\text{C}$ and pressure 760 mmHg the overall AAD value related to composition for the correlation results using flash is 0.004, the value is 0.004 for the TPDF method and 0.03 for the TPI prediction method. For VLE quaternary system of water-ethanol-acetone-n-butyl acetate for a temperature range ($48.1\text{-}70$) $^{\circ}\text{C}$ and pressure 360 mmHg the overall AAD for the correlation is 0.009 and 0.011 for the TPDF method. The AAD is used by other researchers as a measure of success in terms of the correlations and predictions. The smaller the AAD value the more successful the results. The figures obtained in conjunction with an inspection of the data indicate the claimed success and superiority of the TPDF method over the TPI method.

To further develop this work the TPDF should be applied to the prediction of VLE ternary and quaternary systems calculation using the UNIFAC and NRTL equation in place of UNIQUAC to calculate the excess Gibbs energy of mixing in the PRSV+WSMR.

This work has exclusively used Wong Sandler Mixing Rules (WSMR) because an examination of the literature indicated that it is the most effective mixing rule when polar molecules are present in a mixture. For future work it is important that other mixing rules are investigated in order to find out the effect on the overall correlation and prediction results.

This work has used the data available from Younis et al (2007) and the data available from DECHEMA. It is noticeable that there is a shortage of data for heterogeneous polar systems at relatively low pressure and yet these systems are of both theoretical and practical importance. It would be useful to produce more experimental data on such systems to allow theoretical models to be tested against a wide range of data.

6. References

Abrams, D.S., Prausnitz, J.M., (1975) 'Statistical thermodynamics of liquid mixture. A new expression for the excess Gibbs energy of partly or completely miscible systems'. AIChE Journal, 21(1), pp. 116-128.

Alvarez, V. H., R. Larico, Y. Ianos, M. Aznar (2008) 'Parameter estimation for VLE calculation by global minimization: the genetic algorithm', Braz. Journal of Chem. Eng.,25, pp. 409-418.

Ammar, M.N., Renon,H.(1987) ' The isothermal flash problems: new methods for phase split calculations', AIChE Journal, 33, pp. 926-939.

Babu, K. S., M.V.P. Kumar, N. Kaistha (2009) 'Controllable optimized designs of an ideal reactive distillation system using genetic algorithm', Chem. Eng. Sci., 64, pp. 4929-4942.

Bollas, G.M., Barton, P.I., Mitsos, A. (2009) 'Bilevel optimization formulation for parameter estimation in vapor-liquid(-liquid) phase equilibrium problems', Chemical Engineering Science, 64, pp. 1768-1783.

Bonilla-Petriciolet , A. (2007) ' Reliable Initialization Strategy for the Equal Area Rule in Flash Calculations of Ternary Systems', Afinidad , 64 (530),pp. 529-534.

Bonilla-Petriciolet, A., Bravo-Sanchez, U.I. , Castillo-Borja,F., Zapiain-Salinas, J.G., Soto Bernal,J.J. (2007) 'The performance of Simulated Annealing in parameter estimation for vapor-liquid equilibrium modeling', Braz. J. Chem. Eng., 24, pp. 151-162.

Bonilla-Petriciolet, A., Rangaiah, G.P., Segovia-Hernández, J.G. (2010) 'Evaluation of stochastic global optimization methods for modeling vapor-liquid equilibrium data', Fluid Phase Equilibria. 287, pp. 111-125.

Burgos-Solorzano, Gabriela I., Brennecke, Joan F. & Stadtherr, Mark A. (2004) 'Validated computing approach for high-pressure chemical and multiphase equilibrium', Fluid Phase Equilibria 219, pp.245–255.

Carrier, B., Rogalski, M., Peneloux, A. (1988) 'Correlation and prediction of physical properties of hydrocarbons with the modified Peng-Robinson equation of state: 1. Low and medium vapor pressure', *Ind. Eng. Chem. Res.* 27, pp. 1714-1721.

Coutsikos, P., Kalospiros, N.S., Tassios, D.P. (1995) 'Capabilities and limitations of the Wong-Sandler mixing rules', *Fluid Phase Equilibria*, 108, pp. 59-78.

Desai, G.H.I, 1986. Measurement and correlation of vapour-liquid equilibrium of heterogeneous system. Ph.D Thesis. Chemical Engineering Department, Teesside Polytechnic.

Eubank P.T., Hall K.R. (1995) 'Equal area rule and algorithm for determining phase compositions', *AIChE Journal*, 41(4), pp. 924-927.

Eubank, P.T. and Barrufet, M.A. (1988) 'A simple algorithm for calculations of phase separation', *Chemical Engineering Education*, 22, pp. 36.

Eubank, P.T. and Hall, K.R. (1995) 'An area rule and algorithm for determining phase compositions', *AIChE Journal*, 41, pp. 924-927.

Eubank, P.T., Elhassan, A.E., Barrufet M.A. and Whiting, W.B. (1992) 'Area method for prediction of fluid phase equilibria', *Ind. Eng. Chem. Res.*, 31, pp. 942-949.

Gao, F., Han, L. (2012) 'Implementing the Nelder-Mead Simplex Algorithm with Adaptive Parameters', *Computational Optimization and Applications*, 51(1), pp. 259-277

Garcia-Flores, B., Águila-Hernández, J., García-Sánchez, F., Aquino-Olivos, M. (2013) '(liquid-liquid) equilibria for ternary and quaternary systems of representative compounds of gasoline + methanol at 293.15 K: Experimental data and correlation', *Fluid Phase Equilibria*, 348, pp. 60 – 69.

Gecegormez, H., Demirel, Y., (2005) 'Phase stability analysis using interval Newton method with NRTL model', *Fluid Phase Equilibria*. 237, pp. 48–58.

Geem, Z.W.; Kim, J.H. & Loganathan, G.V. (2001) ' A new heuristic optimization algorithm: harmony search', *Simulation*, 76(2), pp. 60-68.

Ghosh, P., Taraphdar, T. (1998) 'Prediction of vapor-liquid equilibria of binary systems using PRSV equation of state and Wong Sandler mixing rules', *Chemical Engineering Journal*, 70, pp.15-24.

Gmehling, J., Onken, U. (1977) *Vapor-Liquid Equilibrium Data Collection 1*. DECHEMA, Frankfurt.

Gmehling, J., Onken,U. and Arlt, W. (1981) *Vapor-liquid equilibrium data collection. aqueous-organic systems (Supplement 1)*. Frankfurt/ Main, DECHEMA Chemistry Data Series Vol. 1a, DECHEMA.

Gmehling, J., Onken,U. and Arlt, W. (1982) *Vapor-liquid equilibrium data collection. Alcohols (Supplement 1)*. Frankfurt/Main DECHEMA Chemistry Data Series Vol. 2, DECHEMA.

Gmehling, J., Onken,U. and Arlt, W. (1991) *Vapor-liquid equilibrium data collection. Aqueous-Organic systems (Supplement 1)*. Frankfurt/Main DECHEMA Chemistry Data Series Vol I. Part 1 , DECHEMA.

Green, K.A., Zhou, S. and Luks, K.D. (1993) 'The fractal response of robust solution techniques to the stationary point problem', *Fluid Phase Equilibria*, 84, pp. 49-78.

Haugen, Kjetil B. and Firoozabadi, A. (2011) 'Efficient and Robust Three-Phase Split computations', *AIChE Journal* ,57(9),pp. 2555-2565.

Henderson, N., de Oliveira, J.R., Amaral Souto, H.P. & Pitanga, R. (2001) ' Modeling and analysis of the isothermal flash problem and its calculation with the simulated annealing algorithm', *Industrial Engineering Chemistry Research*, 40(25), pp. 6028-6038.

Hendriks, E.M., van Bergen, A.R.D. (1992) 'Application of a reduction method to phase equilibria calculations', *Fluid Phase Equilibria*. 74, pp. 17–34.

Hinojosa-Gomez, H., Barragan-Aroche J. Fernando , Bazua-Rueda Enrique R. (2010) ' A modification to the Peng–Robinson-fitted equation of state for pure substances', *Fluid Phase Equilibria*, 298, pp.12-23

Hodges, D., Pritchard, D.W., Anwar, M.M. (1997) 'Calculating binary and ternary multiphase Equilibria: extensions of the integral area method', *Fluid Phase Equilibria*, 130, pp. 101-116.

Hodges, D., Pritchard, D.W., Anwar, M.M. (1998) 'Calculating binary and ternary multiphase Equilibria: the tangent plane intersection method', *Fluid Phase Equilibria*, 152, pp. 187–208.

Hsieha, Cheng-Ting, Ming-JerLeeb, Ho-mu Linb, Ju-Chun Chengb, Wan-Yun Ji (2011) 'Multiphase equilibria for mixtures containing water, isopropanol, propionic acid, and isopropyl propionate', *Fluid Phase Equilibria*, 305 , pp. 53–61.

Huron, M. and J. Vidal(1979) 'New Mixing Rules in Simple Equation of State for representing Vapor-Liquid Equilibrium of strongly non-ideal mixtures', *Fluid Phase Equilibria*, 3, pp. 255-271.

Iglesias-Silva , Gustavo A. ,Bonilla-Petriciolet,A., Eubank, Philip T., Holste, James C. , Kenneth R. H. (2003) 'An algebraic method that includes Gibbs minimization for performing phase equilibrium calculations for any number of components or phases ',*Fluid Phase Equilibria*, 210, pp. 229–245.

Justo-García, D., García-Sánchez, F., Díaz-Ramírez, N.,Díaz-Herrera,E. (2010)' Modeling of three-phase vapor–liquid–liquid equilibria for a natural-gas system rich in nitrogen with the SRK and PC-SAFT EoS', *Fluid Phase Equilibria*,298, pp. 92 – 96.

Kangas, J.,Malinen, I.,Tanskanen,J.(2011) 'Modified bounded homotopies in the solving of phase stability problems for liquid–liquid phase-splitting calculations.', *Ind.Eng.Chem.Res*, 50, pp.7003–7018.

Khodakarami, B., Modarress, H. and Lotfollahi,M. N.(2005) 'Study of the High-Pressure Vapor-Liquid Equilibria for Strongly Non-Ideal Binary and

Ternary Mixtures', Canadian Journal of Chemical Engineering, 83(2), pp. 354-357.

Kirkpatrick, S., C. Gelatt, M. Vecchi (1983) 'Optimization by Simulated Annealing', Science, 220, pp. 671-680.

Kontogeorgis, Georgios M. and Rafiqul G. (2004) Computer Aided Property Estimation for Process and Product Design. Computers Aided Chemical Engineering, Volume 19, London, ELSEVIER.

Kosuge ,H., Iwakabe, K.(2005)'Estimation of isobaric vapor–liquid–liquid equilibria for partially miscible mixture of ternary system' , Fluid Phase Equilibria,233, pp. 47 – 55.

Lee, Ming-Tsung, Lin, Shiang-Tai (2007) 'Prediction of mixture vapor-liquid equilibrium from the combined use of Peng-Robinson equation of state and COSMO-SAC activity coefficient model through Wong-Sandler mixing rule', Fluid Phase Equilibria , 254(1-2), pp. 28-34.

Lee, Y.P.; Rangaiah, G.P. & Luus, R. (1999) 'Phase and chemical equilibrium calculations by direct search optimization', Computers and Chemical Engineering, 23(9), pp. 1183-1191.

Leibovici, Claude F. (2006), 'Initialization of vapor–liquid equilibrium constants for non-hydrocarbon liquid phases', Fluid Phase Equilibria, 248, pp. 217–218.

Li, J., Chen,C., Wang, J.(2000)'Vapor–liquid equilibrium data and their correlation for binary systems consisting of ethanol, 2-propanol, 1,2-ethanediol and methyl benzoate', Fluid Phase Equilibria,169, pp. 75 – 84.

Li, Z. and Firoozabadi, A. (2012) ' General strategy for stability testing and phase split calculation in two and three phases', SPE Journal, 17 (4), pp. 1096-1107.

Li, Z., Firoozabadi, A. (2012) 'initialization of phase fractions in Rachford-Rice equations for robust efficient three-phase split calculation', Fluid Phase Equilibria, 332, pp. 21-27.

Lin, B., Miller, D.C. (2004) 'Tabu search algorithm for chemical process optimization', *Comp. Chem. Eng.*, 28, pp. 2287-2306.

Lin, Ming-Hua ,Tsai, Jung-Fa ,Yu, Chian-Son (2012) 'A Review of Deterministic Optimization Methods in Engineering and management', *Mathematical Problems in Engineering* , 2012, pp. 15.

Lin, Y., & Stadtherr, M. A. (2004) 'Advances in interval methods for deterministic global optimization in chemical engineering', *Journal of Global Optimization*, 29,pp. 281–296.

Liu, Y., Kusano,R., Iwai,Y.(2012) 'Correlation of Vapor-Liquid Equilibria of Supercritical Methanol+ Glycerol System', *Journal of Novel Carbon Resource Sciences* , 5, pp. 19-22.

Lopez, J.A., Trejos, V.M., Cardona, C.A. (2006) 'Objective functions analysis in the minimization of binary VLE data for asymmetric mixtures at high pressures ', *Fluid Phase Equilibria*, 248(2), pp. 147–157.

Lotfollahi, M. N., Modarress, H. and Khodakarami, B.(2007) ' VLE Predictions of Strongly Non-Ideal Binary Mixtures by Modifying van Der Waals and Orbey-Sandler Mixing Rules', *Iran. J. Chem.Chem. Eng.*, 26(3), pp. 73-80.

Luus, R., Rangaiah, G.P.(2010) 'Stochastic Global Optimization: Techniques and Applications in Chemical Engineering', *World Scientific*, pp. 17-56.

Malinen, I.,Kangas, J., Tanskanen,J.(2012) 'new Newton homotopy based method for the robust determination of all the stationary points of the tangent plane distance function', *Chemical Engineering Science* ,84 ,pp:266–275.

Mario, Llano-Restrepo, Y. Mauricio Munoz-Munoz, (2011) ' Combined chemical and phase equilibrium for the hydration of ethylene to ethanol calculated by means of the Peng–Robinson–Stryjek–Vera equation of state and the Wong–Sandler mixing rules', *Fluid Phase Equilibria* ,307,pp. 45– 57.

McDonald, C. M. and Floudas, C. A. (1997) 'GLOPEQ: A new computational tool for the phase and chemical equilibrium problem. *Computers & Chemical Engineering*, 21 (1), pp. 1-23.

McDonald, C.M. and Floudas, C. A. (1995) 'Global optimization for the phase and chemical equilibrium problem: Application to the NRTL equation', *Computers & Chemical Engineering*, 19(11), pp. 1111-1139.

McDonald, C.M., Floudas, C.A.(1995) 'Global optimization for the phase stability problem', *AIChE*,41,pp. 1798–1814.

Michelsen, M. L. (1986) 'Simplified flash calculations for cubic equation of state', *Ind. Eng. Chem. Proc. Des. Dev.* 25(1), pp. 184–188.

Michelsen, M. L. (1990) 'A modified Huron-Vidal Mixing Rule for Cubic Equations of State', *Fluid Phase Equilibria*, 60, pp.213-219.

Michelsen, M. L. (1993) 'Phase equilibrium calculations: what is easy and what is difficult?', *computers and chemical engineering*,17, pp. 431-439.

Michelsen, M.L (1982 b) 'The isothermal flash problem. Part II. Phase split calculation', *Fluid Phase Equilibria* , 9,pp. 21-40.

Michelsen, M.L. (1982 a) 'The isothermal flash problem. Part I. Stability', *Fluid Phase Equilibria*, 9, pp. 1-19.

Mokhatab, S. (2003) ' Three-Phase Flash Calculation for Hydrocarbon Systems Containing Water', *Theoretical Foundations of Chemical Engineering*, 37(3), pp. 291-294.

Nasrifar, K.(2010) 'Comparative study of eleven equations of state in predicting the thermodynamic properties of hydrogen', *International journal of hydrogen energy*, 35, pp. 3802–3811.

Nelder, J. A. and Mead, R. (1965) ' A simplex method for function minimization', *Computer Journal*, 7, pp. 308–313.

Nichita, D. V., Gomez, S. (2009) 'Efficient location of multiple global minima for the phase stability problem', *Chemical engineering Journal* , 152, pp.251-263.

Nichita, D., V., Daniel Broseta, Jean-Charles de Hemptinne (2006) ' Multiphase equilibrium calculation using reduced variables', Fluid Phase Equilibria ,246, pp. 15–27.

Nichita, D.V. and Graciaa , A. (2011) 'A new reduction method for phase equilibrium calculations' , Fluid Phase Equilibria, 302, pp. 226–233.

Nichita, D.V. and Minescu, F. (2004) 'Efficient phase equilibrium calculation in a reduced flash context', Can. J. Chem. Eng. 82, pp. 1225–1238.

Nichita, D.V., Gomez, S., Luna, E.(2002) 'Multiphase equilibria calculation by direct minimization of Gibbs free energy with a global optimization method', Computer and Chemical Engineering, 26, pp.1703-1724.

Nishwan, S.M. , Hanif, G.S. Shyu, K.R. Hall, Eubank, P.T. (1996) 'Calculation of multi-phase equilibria using the equal an application to hydrocarbon/water mixtures', Fluid Phase Equilibria, 126, pp. 53-70.

Ohanomah, M. O. and Thompson, D. W. (1984) 'Computation of multicomponent phase equilibria-Part II. Liquid–liquid and solid–liquid equilibria', Computer and Chemical Engineering, 8, pp. 157–162.

Orbey, H. and Sandler, S. I. (1995 a) ' Reformulation of the Wong-Sandler mixing rule for cubic equations of state',AIChE Journal, 41, pp. 683-90.

Orbey, H., Sandler, I.S. (1998) Modeling Vapor-Liquid Equilibria Cubic Equation of State and Their Mixing Rules. USA: Cambridge University Press.

Orbey, H., Sandler, S.I. (1993) 'Accurate equation of state predictions at high temperatures and pressures using the existing UNIFAC model', Fluid Phase Equilibria, 85, pp. 41-54

Pan, H., & Firoozabadi, A. (1998)' Complex multiphase equilibrium calculations by direct minimization of Gibbs free energy by use of simulated annealing', SPE Reservoir Evaluation and Engineering ,1(1)pp. 36-42.

Pham, N., and Wilamowski, B. M. (2011) 'Improved Nelder Mead's Simplex Method and Applications', JOURNAL OF COMPUTING, 3(3), pp. 2151-9617.

Poling, B.E., Prausnitz, J.M., O'Connell, J.P. (2001) *The Properties of Gases and Liquids*. Fifth Edition, McGraw-Hill.

Prausnitz, J. M. , Lichtenthaler, Ruediger N., Gomes de Azevedo E. (1999) *Molecular thermodynamics of fluid-phase equilibria*. 3rd edn. USA: Prentice-Hall, PTR.

Radzysinski, I.F. and Whiting, W.B. (1987) ' Fluid Phase Stability and Equation of State', *Fluid Phase Equilibria*,34, pp. 101.

Rahman, I., Anwesh Kr. Dasb, Raju B. Mankarb, Kulkarnia, B.D. (2009) 'Evaluation of repulsive particle swarm method for phase equilibrium and phase stability problems', *Fluid Phase Equilibria*, 282 , pp. 65–67.

Rangaiah, G.P. (2001) 'Evaluation of genetic algorithms and simulated annealing for phase equilibrium and stability problems', *Fluid Phase Equilibria* 187–188, pp. 83–109.

Renon, H., and Prausnitz ,J. M. (1968) 'Local composition in thermodynamic excess functions for liquid mixtures' , *AIChE Journal*, 14, pp. 135-144.

Rilvia, S. Santiagoa, Geormenny R. Santosb, Martín Aznarc (2010) ' UNIQUAC correlation of liquid–liquid equilibrium in systems involving ionic liquids: The DFT–PCM approach. Part II ', *Fluid Phase Equilibria*, 293, pp. 66–72.

Rogalski, M., Carrier, B., Solimando,R., Peneloux, A. (1990) 'Correlation and prediction of physical properties of hydrocarbons with the modified Peng-Robinson equation of state: 2. Representation of the vapor pressure and of the molar volume', *Ind. Eng. Chem. Res.* 29,pp. 659-666.

Rossi, C.C.R.S., Berezuk,M.E., Cardoz-Filho, L., Guirardello,R. (2011) 'Simultaneous calculation of chemical and phase equilibria using convexity analysis', *Computers and Chemical Engineering*,35, 1226-1237.

Sandler, Stanley I. (1989) *Chemical and Engineering Thermodynamics*. Canada, John Wiley & Sons Inc.

Sandler, Stanley I. (2006) Chemical Biochemical and Engineering Thermodynamics. 4th edn. USA, John Wiley & Sons Inc.

Schnepper, C.A. and Stadtherr, M.A.(1996) 'Robust process simulation using interval methods', computer and chemical engineering,20, pp. 187-199.

Shyu, G.S., Hanif, N.S.M., Alvarado, J.F.J., Hall, K.R. and Eubank, P.T. (1995) ' Equal area rule methods for ternary systems', Ind.Eng.Chem.Res., 34, pp. 4562-4570.

Silva Pinheiro , R., Maia Bessa, A., Amaral de Queiroz, B., Duarte, A., Sant Ana, H., Santiago-Aguiar, R.(2014) 'Optimization of the methylic biodiesel purification process by intermediate of liquid–liquid equilibrium data for ternary systems containing methanol + water + (soybean, corn or brown shell of coconut) biodiesel', Fluid Phase Equilibria,361, pp. 30 – 36.

Sinnott, R.K. (2005) Chemical engineering Design. 4th edn. London, ELSEVIER, Coulson and Richardson chemical engineering series Volume 6.

Sofyan, Y., Ghajar, A. J., Gasem, K. A. M. (2003) 'Multiphase Equilibrium Calculations Using Gibbs Minimization Techniques', Industrial &Engineering Chemistry Research, 42, pp. 3786.

Solorzano-Zavala, M., Barragan-Aroche, F., Bazua, E. R.(1996) 'Comparative study of mixing rules for cubic equation of state in the prediction of multi-component vapor-liquid equilibria', Fluid Phase Equilibria, 122, pp. 99-116.

Sorensen, J.M. and Arlt,W. (1979) Liquid-liquid equilibrium data collection. Frankfort, DECHEMA chemistry data series, Volume. 5, Part 1.

Stadtherr, Mark A. , Xu, G., Burgos-Solorzano,G.I., Haynes, W.D. (2007) 'Reliable computation of phase stability and equilibrium using interval methods' International Journal of Reliability and Safety , 1(4), pp. 465-488.

Stryjek, R. and Vera, J. H. (1986) 'PRSV: An improved Peng—Robinson equation of state for pure compounds and mixtures', The Canadian Journal of Chemical Engineering, 64, pp. 323-333.

Stryjek, R. and Vera, J.H. (1986) ' PRSV - An improved Peng - Robinson equation of state with new mixing rules for strongly non ideal mixtures', Can. J. Chem. Eng. 64(2),pp. 334-340.

Stryjek, R., and Vera, H. (1986) 'PRSV2: A Cubic Equation of State for Accurate Vapor-Liquid Equilibria Calculations', The Canadian Journal of Chemical Engineering,64, pp.820-826.

Sun, Amy C., Seider, Warren D. (1995) 'Homotopy-continuation method for stability analysis in the global minimization of the Gibbs free energy', Fluid Phase Equilibria, 103, pp. 213-249.

Teh, Y. S., & Rangaiah, G. P. (2002) 'A study of equation-solving and Gibbs free energy minimization methods for phase equilibrium calculations', Institute of Chemical Engineers, 80, 745–759.

Teh, Y., G.P. Rangaiah (2003) 'Tabu search for global optimization of continuous functions with application to phase equilibrium calculations', Comp. Chem. Eng., 27, pp. 1665-1679.

Thomsen, K., Maria C. Iliuta, Peter Rasmussen (2004) 'Extended UNIQUAC model for correlation and prediction of vapor–liquid–liquid–solid equilibria in aqueous salt systems containing non-electrolytes. Part B. Alcohol (ethanol, propanol, butanol)–water–salt systems', Chemical Engineering Science, 59, pp. 3631 – 3647.

Trebble, M.A., (1989) 'A Preliminary Evaluation of Two and Three Phase Flash Initiation Procedures', Fluid Phase Equilibria, 53, pp. 113-122.

Twu , C. H., Coon J. E., and Cunningham J. R. (1995a) 'A new generalized alpha function for a cubic equation of state, Part 1. Peng-Robinson equation', Fluid Phase Equilibria, 105, pp. 49–59.

Twu , C. H., Coon J. E., and Cunningham J. R. (1995b) 'A new generalized alpha function for a cubic equation of state, Part 2. Redlich-Kwong equation', Fluid Phase Equilibria. 105, pp. 61–69.

Wanga, P.C. and Shoup, T. E. (2011) 'Parameter sensitivity study of the Nelder–Mead Simplex Method, *Advances in Engineering Software*, 42(7), pp. 529–533.

Wenchuan Wang, Yixin Qu, Chong H. Twu, John E. Coon, 1996, *Comprehensive Comparison and Evaluation of the Mixing Rules of WS, MHV2, Fluid Phase Equilibria* 116, page 488-494.

Wisniak, J. (1993) 'A New Test for the Thermodynamic Consistency of Vapor-Liquid Equilibrium', *Ind. Eng. Chem. Res.*, 32, pp.1531-1533.

Wong, D.S.H. and Sandler, I.S. (1992) 'A theoretically correct mixing rule for cubic equations of state', *AIChE Journal*, 38(5), pp. 671-680.

Wong, D.S.H. and Sandler, S.I. (1992) 'A Theoretically Correct Mixing Rule for Cubic Equations of State', *AIChE Journal*, 38, pp. 671.

Wyczesany, A. (2010) 'calculation of vapour-liquid-liquid equilibria', *Chemical and Process Engineering*, 31, pp. 333-353.

Wyczesany, A. (2012) 'calculation of vapour-liquid-liquid equilibria in quaternary systems', *Chemical and Process Engineering*, 33, pp. 463-477.

Xiang, H. W. (2005) *The Corresponding-States Principle and its Practice Thermodynamic, Transport and Surface Properties of Fluids*. Netherlands: ELSEVIER.

Xu, G., Haynes, W.D., Stadtherr, M.A. (2005) 'Reliable phase stability for asymmetric models', *Fluid Phase Equilibria* .235, pp. 152–165.

Yan, W., Toppoff, M., Rose, C., Gmehling, J. (1999) 'Prediction of vapor–liquid equilibria in mixed-solvent electrolyte systems using the group contribution concept', *Fluid Phase Equilibria*, 162, pp. 97 – 113.

Younis, O.A.D., D.W. Pritchard, M.M. Anwar (2007) 'Experimental isobaric vapour–liquid–liquid equilibrium data for the quaternary systems water (1)–ethanol (2)–acetone (3)–n-butyl acetate (4) and water (1)–ethanol (2)–acetone (3)–methyl ethyl ketone (4) and their partially miscible-constituent ternaries', *Fluid Phase Equilibria*, 251, pp. 149–160.

Zhang, H, Kennedy, D.D., Rangaiah, G.P., Bonilla-Petriciolet, A. (2011) 'Novel bare-bones particle swarm optimization and its performance for modeling vapor-liquid equilibrium data', Fluid Phase Equilibria, 301, pp. 33-45.

Zhang, H. Bonilla-Petriciolet, A., Rangaiah, G.P.(2011) 'review on Global Optimization Methods for Phase Equilibrium Modeling and Calculations' , The Open Thermodynamics Journal, 5, pp. 71-92.

Zhu, Y., Wen, H., Xu, Z. (2000) 'Global stability analysis and phase equilibrium calculations at high pressures using the enhanced simulated annealing algorithm', Chem. Eng. Sci.,55, pp. 3451-3459.

7. Appendix

A. VLE Flash Calculation Algorithm

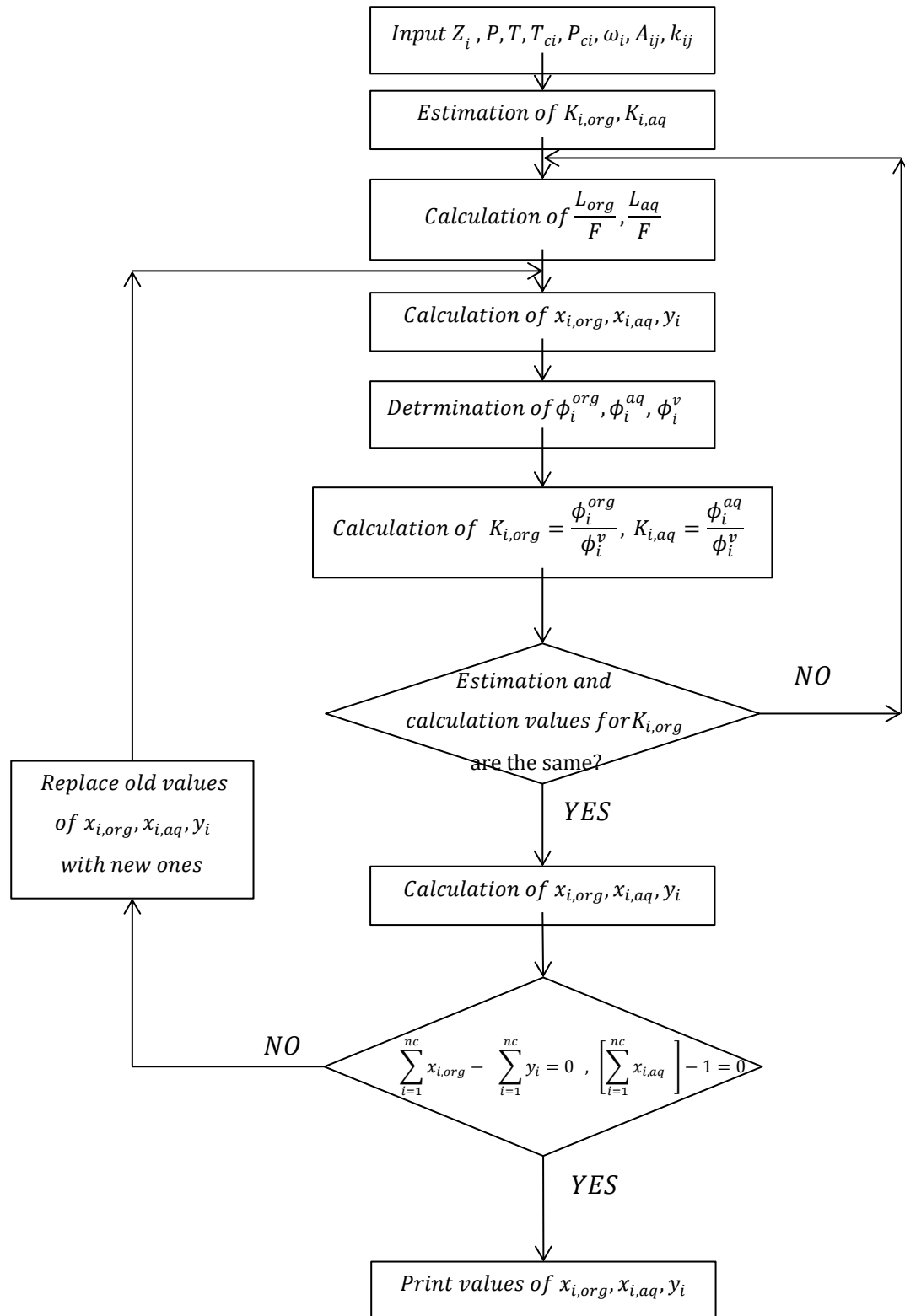


Figure A: The simplex for three Phase Flash calculations

B. Systematic Initial Generator

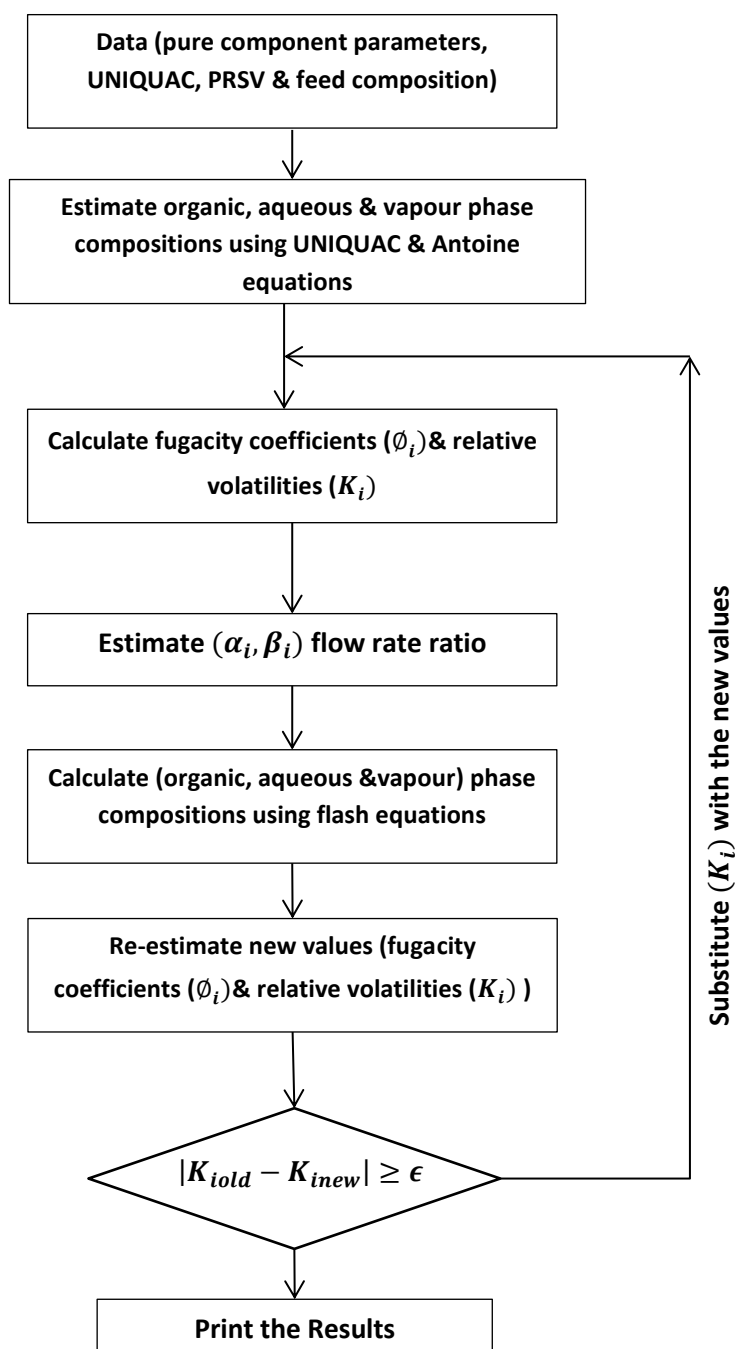


Figure B: Systematic Initial Generator for TPI method

C. Nelder-Mead Simplex

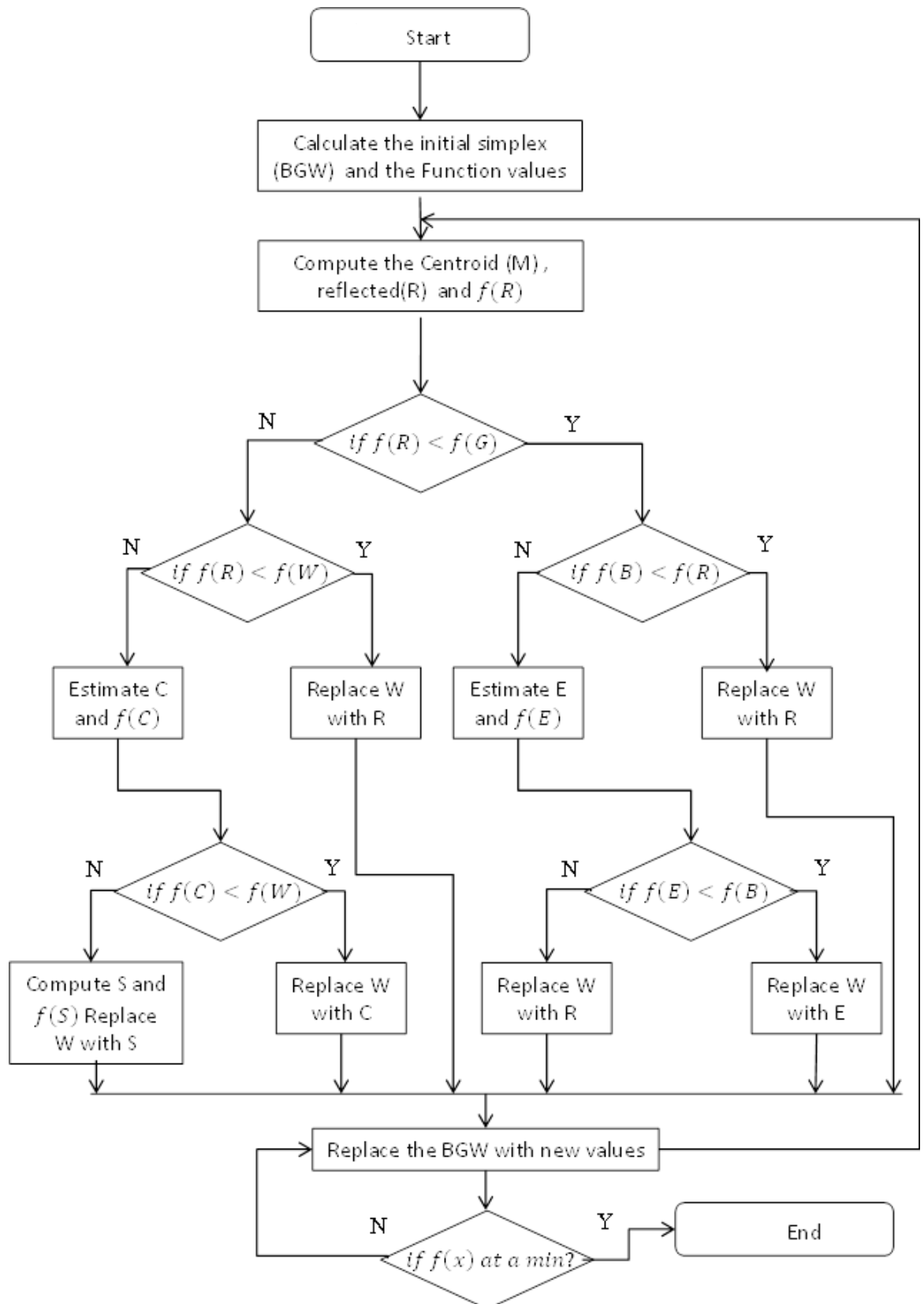


Figure C: Diagram of Nelder-Mead Simplex minimisation procedure

D. Selected VBA program code

D.1 Binary system calculations

D.1.1 VLE Calculations

D.1.2.1 Main program for bubble point calculation

```
Private Sub VLEBINARY_Click()  
Dim result As Variant, STIMER, FTIMER, I  
STIMER = Timer  
  
Call INPUTDATA  
ReDim initParams(1 To 3, 1 To 1)  
  
For I = 1 To 3  
    initParams(I, 1) = Sheet1.Cells(8 + I, 4).Value  
Next I  
  
Dim nelderObj As New Nelder  
    result = nelderObj.SolveMaximum("PRSVUNIQUAC1", initParams)  
  
For I = 1 To 3  
    Sheet1.Cells(8 + I, 5) = result(I, 1)  
Next I  
  
Call WRITERESULTS  
  
'Changing temperature to make sum of vapour mole fractions equals 1  
  
For II = 1 To Points  
  
ReDim initParams(1 To 1, 1 To 1)  
    initParams(1, 1) = TEMPS(II)  
  
result = nelderObj.SolveMaximum("TSUMY", initParams)  
    Sheet1.Cells(30 + II, 24) = result(1, 1)  
Next II  
  
Call WRITERESULTS  
  
FTIMER = Timer  
FTIMER = FTIMER - STIMER  
Sheet1.Cells(14, 12) = FTIMER  
  
End Sub
```

D.1.2.2 Sub program of Peng Robinson Styjrek Vera EOS with Wong Sandler Mixing Rule through UNIQUAC

' The PRSV/WS EOS subprogram for binary VLE

Public Function PRSVUNIQUAC1(X1 As Variant) As Variant

```
Dim PHIBASE#(10), THETABASE#(10), MODTHETABASE#(10), PHI#(10), THETA#(10)
Dim MODTHETA#(10), LI#(10), PART3SUM#(10), PART4SUM#(10)
Dim PART5TOP#(10), PART5BASE#(10), PART5TOT#(10), T#(10, 10)
Dim LNVAPGAMMAP#(10), LNORGGAMMAP#(10), LNAQGAMMAP#(10)
Dim LNAQFUGACITYCOEFFICIENT#(10), LNORGFUGACITYCOEFFICIENT#(10)
Dim VAPFUGCOEFF#(10), LNVAPFUGACITYCOEFFICIENT#(10)
Dim ORGFUGCOEFF#(10), ORGFUGACITYP#(10), AQFUGCOEFF#(10), AQFUGACITYP#(10)
Dim FF1#(10), INTQSUM#(10), EXTQSUM#(10), DSUM#(10)
Dim F12#(50), F22#(50), H12#(50), FF3#(10)
Dim IS12#(50), IS2A2#(50), IS2B2#(50), IS32#(50), IS42#(50)
Dim G1A2#(50), G1B2#(50), G12#(50), G22#(50), VAPFUGACITYP#(10)
Dim CSVC#(10, 10), PUREA#(10, 10), PUREB#(10, 10), PART2C1#(10),
PART2BSUM#(10)
Dim TR#(10), KA0#(10), KA#(10), ALPHA#(10), FF4#(10), FF2#(10)
Dim G32#, GEXCESS#, QORG#, DORG#, BORG#, AORG#
Dim QAQ#, DAQ#, BAQ#, AAQ#, VAQ#, PAQ#, ZAQ#
Dim VNEW#, VOLD#, VORG#, ZORG#, PORG#, QVAP#, AVAP#, BVAP#, DVAP#
Dim VVAP#, ZVAP#, PVAP, PART1F1#, PART2F1#, PART3F1#, PART4F1#
Dim PART1F2#, PART2F2#, PART3F2#, FUNCTION1#, FUNCTION2#
Dim J, K, I, L, COMPONENT, XTRACOMP
Dim PART1#, PART2#, PART3#, PART4#, PART5#
Dim TERM1#, TERM2#, TERM3#, PART3A#, PART3B#, PART3C#
Dim PART2A#, PART2B#, PART2C#, PRESS#, PRESS1#, PRESS2#
Dim OFVALUE#(100), FF11(20), SUMXORGCAL(20, 10), SUMXAQCAL(20, 10)
Dim SUMYORGCAL(20, 10), SUMYAQCAL(20, 10)
Dim AVAP1#, BVAP1#, AAQ1, BAQ1, AORG1, BORG1
```

Call INPUTDATA

```
If (X1(3, 1) > 0 And X1(3, 1) <= 100) Then
For I = 1 To Points
```

'PHYSICAL CONSTANTS AND FIXED PARAMETERS_

```
For J = 1 To TNOC
    TR#(J) = TEMPS(I) / TC(J)
    KA0#(J) = 0.378893 + 1.4897153 * W(J) - 0.1713848 * W(J) ^ 2 +
0.0196554 * W(J) ^ 3
    KA#(J) = KA0#(J) + k1(J) * (1 + (TR#(J) ^ 0.5)) * (0.7 - TR#(J))
    ALPHA#(J) = (1 + KA#(J) * (1 - (TR#(J) ^ 0.5))) ^ 2
    PUREA#(J, J) = ((0.457235 * UGC ^ 2 * TC(J) ^ 2) / PC(J)) *
ALPHA#(J)
    PUREB#(J, J) = (0.077796 * UGC * TC(J)) / PC(J)
Next J
```

```

C# = (1 / Sqr(2)) * Log(Sqr(2) - 1)
T#(1, 1) = 1
T#(2, 2) = 1
T#(1, 2) = Exp(-X1(1, 1) / TEMPS(I))
T#(2, 1) = Exp(-X1(2, 1) / TEMPS(I))
KI#(1, 1) = 0 : KI#(2, 2) = 0 : KI#(1, 2) = X1(3, 1) : KI#(2, 1) = KI#(1,
2)

```

'SOLUTION OF THE PRSV EQUATION OF STATE TO FIND THE CORRECT LIQUID 'AND
VAPOUR PHASE MOLAR VOLUME ROOTS (USING NEWTON-RAPHSON).

'1. LIQUID PHASE.

' CALCULATION OF' EXCESS GIBBS ENERGY USING MODIFIED UNIQUAC.

' PART 1.

```

For J = 1 To TNOC
For K = 1 To TNOC
IS12#(K) = (XORG(I, K) * RA(K)) + IS12#(K - 1)
Next K
F12#(J) = Log(RA(J) / IS12#(TNOC))
F22#(J) = (XORG(I, J) * F12#(J)) + F22#(J - 1)
Next J

```

' PART 2.

```

For J = 1 To TNOC
If (J - 1) = 0 Then
G22#(J - 1) = 0
End If
For K = 1 To TNOC
If (K - 1) = 0 Then
IS2A2#(K - 1) = 0
IS2B2#(K - 1) = 0
End If

IS2A2#(K) = XORG(I, K) * Q(K)
IS2B2#(K) = XORG(I, K) * RA(K)
IS2A2#(K) = IS2A2#(K) + IS2A2#(K - 1)
IS2B2#(K) = IS2B2#(K) + IS2B2#(K - 1)
Next K
G1A2#(J) = Q(J) / RA(J)
G1B2#(J) = (IS2B2#(TNOC) / IS2A2#(TNOC))
G12#(J) = Log(G1A2#(J) * G1B2#(J))
G22#(J) = ((Q(J) * XORG(I, J)) * G12#(J))
G22#(J) = G22#(J) + G22#(J - 1)
Next J

```

G32# = (Z / 2) * G22#(TNOC)

' PART 3.

For J = 1 To TNOC

If (J - 1) = 0 Then

H12#(J - 1) = 0

End If

For K = 1 To TNOC

If (K - 1) = 0 Then

IS32#(K - 1) = 0

End If

For L = 1 To TNOC

If (L - 1) = 0 Then

IS42#(L - 1) = 0

End If

IS42#(L) = XORG(I, L) * QD(L)

IS42#(L) = IS42#(L) + IS42#(L - 1)

Next L

IS32#(K) = (XORG(I, K) * QD(K) * T#(K, J)) / IS42#(TNOC)

IS32#(K) = IS32#(K) + IS32#(K - 1)

Next K

H12#(J) = QD(J) * XORG(I, J) * (Log(IS32#(TNOC)))

H12#(J) = H12#(J) + H12#(J - 1)

Next J

GEXCESS# = F22#(TNOC) + G32# - H12#(TNOC)

'CALCULATION OF THE EXCLUDED VOLUME PARAMETER (bm).

For J = 1 To TNOC

For K = 1 To TNOC

CSVC#(J, K) = (((PUREB#(J, J) - (PUREA#(J, J) / (UGC * TEMPS(I)))) +
(PUREB#(K, K) - (PUREA#(K, K) / (UGC * TEMPS(I)))) / 2) * (1 - (KI#(J,
K) / 100))

Next K

Next J

For J = 1 To TNOC

For K = 1 To TNOC

INTQSUM#(K) = (XORG(I, J) * XORG(I, K) * CSVC#(J, K)) + INTQSUM#(K - 1)

Next K

EXTQSUM#(J) = INTQSUM#(TNOC) + EXTQSUM#(J - 1)

Next J

QORG# = EXTQSUM#(TNOC)

For J = 1 To TNOC

DSUM#(J) = ((XORG(I, J) * PUREA#(J, J)) / (PUREB#(J, J) * UGC *
TEMPS(I))) + DSUM#(J - 1)

Next J

DORG# = DSUM#(TNOC) + (GEXCESS# / C#)

BORG# = QORG# / (1 - DORG#)

'CALCULATION OF' THE ENERGY OF ATTRACTION PARAMETER (am) and compressibility factor

AORG# = UGC * TEMPS(I) * BORG# * DORG#

AORG1 = AORG# * P / (UGC * TEMPS(I)) ^ 2

BORG1 = BORG# * P / (UGC * TEMPS(I))

ZORG# = Z3ROOT(AORG1, BORG1)

VORG# = ZORG# * (UGC * TEMPS(I)) / P

PORG = ((UGC * TEMPS(I)) / (VORG# - BORG#)) - (AORG# / (VORG# ^ 2 + (2 * BORG# * VORG#) - BORG# ^ 2))

'2- VAPOUR-PHASE.

' CALCULATION OF EXCESS GIBBS ENERGY USING MODIFIED UNIQUAC.

' PART 1.

For K = 1 To TNOC

YEXP1(I, K) = (Exp(ANTA(K) - ANTB(K) / (ANTC(K) + TEMPS(I)))) / 750

YEXP1(I, K) = YEXP1(I, K) / P

YEXP1(I, K) = YEXP1(I, K) * XORG(I, K)

Next K

For J = 1 To TNOC

If (J - 1) = 0 Then

F22#(J - 1) = 0

End If

For K = 1 To TNOC

If (K - 1) = 0 Then

IS12#(K - 1) = 0

End If

IS12#(K) = YEXP1(I, K) * RA(K)

IS12#(K) = IS12#(K - 1) + IS12#(K)

Next K

F12#(J) = Log(RA(J) / IS12#(TNOC))

F22#(J) = (YEXP1(I, J) * F12#(J)) + F22#(J - 1)

Next J

' PART 2.

For J = 1 To TNOC

If (J - 1) = 0 Then

G22#(J - 1) = 0

End If

For K = 1 To TNOC

If (K - 1) = 0 Then

IS2A2#(K - 1) = 0

IS2B2#(K - 1) = 0

End If

IS2A2#(K) = YEXP1(I, K) * Q(K)

```

IS2B2#(K) = YEXP1(I, K) * RA(K)
IS2A2#(K) = IS2A2#(K) + IS2A2#(K - 1)
IS2B2#(K) = IS2B2#(K) + IS2B2#(K - 1)
Next K

G1A2#(J) = Q(J) / RA(J)
G1B2#(J) = (IS2B2#(TNOC) / IS2A2#(TNOC))
G12#(J) = Log(G1A2#(J) * G1B2#(J))
G22#(J) = ((Q(J) * YEXP1(I, J)) * G12#(J))
G22#(J) = G22#(J) + G22#(J - 1)
Next J

G32# = (Z / 2) * G22#(TNOC)

' PART 3.

For J = 1 To TNOC
  If (J - 1) = 0 Then
    H12#(J - 1) = 0
  End If
  For K = 1 To TNOC
    If (K - 1) = 0 Then
      IS32#(K - 1) = 0
    End If
    For L = 1 To TNOC
      If (L - 1) = 0 Then
        IS42#(L - 1) = 0
      End If
      IS42#(L) = YEXP1(I, L) * QD(L)
      IS42#(L) = IS42#(L) + IS42#(L - 1)
    Next L
    IS32#(K) = (YEXP1(I, K) * QD(K) * T#(K, J)) / IS42#(TNOC)
    IS32#(K) = IS32#(K) + IS32#(K - 1)
  Next K
  H12#(J) = QD(J) * YEXP1(I, J) * (Log(IS32#(TNOC)))
  H12#(J) = H12#(J) + H12#(J - 1)
Next J
GEXCESS# = F22#(TNOC) + G32# - H12#(TNOC)

'EXCLUDED VOLUME PARAMETER (bm).
For J = 1 To TNOC
  For K = 1 To TNOC
    CSVC#(J, K) = (((PUREB#(J, J) - (PUREA#(J, J) / (UGC * TEMPS(I)))) +
(PUREB#(K, K) - (PUREA#(K, K) / (UGC * TEMPS(I)))))) / 2) * (1 - (KI#(J,
K) / 100))
  Next K
Next J
For J = 1 To TNOC
  For K = 1 To TNOC
    INTQSUM#(K) = (YEXP1(I, J) * YEXP1(I, K) * CSVC#(J, K)) + INTQSUM#(K - 1)
  Next K

```

```

EXTQSUM#(J) = INTQSUM#(TNOC) + EXTQSUM#(J - 1)
Next J
QVAP# = EXTQSUM#(TNOC)

For J = 1 To TNOC
  DSUM#(J) = (YEXP1(1, J) * (PUREA#(J, J) / (PUREB#(J, J) * UGC *
  TEMPS(I)))) + DSUM#(J - 1)
Next J

DVAP# = (DSUM#(TNOC) + (GEXCESS# / C#))
BVAP# = QVAP# / (1 - DVAP#)

'ATTRACTIVE PARAMETER (am) and compressibility factor

AVAP# = UGC * TEMPS(I) * BVAP# * DVAP#
ZVAP# = (P * VVAP#) / (UGC * TEMPS(I))

AVAP1# = AVAP# * P / (UGC * TEMPS(I)) ^ 2
BVAP1# = BVAP# * P / (UGC * TEMPS(I))

ZVAP# = ZVROOT(AVAP1#, BVAP1#)
VVAP# = (ZVAP# * UGC * TEMPS(I)) / P

PVAP = ((UGC * TEMPS(I)) / (VVAP# - BVAP#)) - (AVAP# / (VVAP# ^ 2 + (2 *
BVAP# * VVAP#) - BVAP# ^ 2))

' DETERMINATION OF THE FUGACITY COEFFICIENTS OF EACH COMPONENT IN EACH
PHASE.

'1. LIQUID PHASE.
'CALCULATION OF THE LIQUID PHASE ACTIVITY COEFFICIENTS AFTHIS P & T.
' THE UNIQUAC EXPANSION (CALCULATION OF ACTIVITY COEFFICIENTS FOR EACH
' COMPONENT IN THE LIQUID PHASE).

For COMPONENT = 1 To TNOC
  PHIBASE#(COMPONENT) = RA(COMPONENT) * XORG(I, COMPONENT) +
  PHIBASE#(COMPONENT - 1)
  THETABASE#(COMPONENT) = Q(COMPONENT) * XORG(I, COMPONENT) +
  THETABASE#(COMPONENT - 1)
  MODTHETABASE#(COMPONENT) = QD(COMPONENT) * XORG(I, COMPONENT) +
  MODTHETABASE#(COMPONENT - 1)
Next COMPONENT

For COMPONENT = 1 To TNOC
  PHI#(COMPONENT) = (RA(COMPONENT) * XORG(I, COMPONENT)) / PHIBASE#(TNOC)
  THETA#(COMPONENT) = (Q(COMPONENT) * XORG(I, COMPONENT)) / THETABASE#(TNOC)
  MODTHETA#(COMPONENT) = (QD(COMPONENT) * XORG(I, COMPONENT)) /
  MODTHETABASE(TNOC)
Next COMPONENT

```

```

For COMPONENT = 1 To TNOC
  LI#(COMPONENT) = (Z / 2) * (RA(COMPONENT) - Q(COMPONENT)) -
(RA(COMPONENT) - 1)
Next COMPONENT

For COMPONENT = 1 To TNOC
  PART1# = Log(PHI#(COMPONENT) / XORG(I, COMPONENT))
  PART2# = (Z / 2) * Q(COMPONENT) * Log(THETA#(COMPONENT) /
PHI#(COMPONENT))

For J = 1 To TNOC
  PART3SUM#(J) = XORG(I, J) * LI#(J) + PART3SUM#(J - 1)
  PART4SUM#(J) = MODTHETA#(J) * T#(J, COMPONENT) + PART4SUM#(J - 1)
Next J
PART3# = (PHI#(COMPONENT) / XORG(I, COMPONENT)) * PART3SUM#(TNOC)
PART4# = QD(COMPONENT) * Log(PART4SUM#(TNOC))
For J = 1 To TNOC
  PART5TOP#(J) = MODTHETA#(J) * T#(COMPONENT, J)
  For K = 1 To TNOC
    PART5BASE#(K) = MODTHETA#(K) * T#(K, J) + PART5BASE#(K - 1)
  Next K
  PART5TOT#(J) = (PART5TOP#(J) / PART5BASE#(TNOC)) + PART5TOT#(J - 1)
Next J

PART5# = QD(COMPONENT) * PART5TOT#(TNOC)
LNORGGAMMAP#(COMPONENT) = PART1# + PART2# + LI#(COMPONENT) - PART3# -
PART4# + QD(COMPONENT) - PART5#
Next COMPONENT

For XTRACOMP = 1 To TNOC
TERM1# = -Log((P * (VORG# - BORG#)) / (UGC * TEMPS(I)))
For J = 1 To TNOC
PART2BSUM#(J) = (XORG(I, J) * CSVC#(XTRACOMP, J)) + PART2BSUM#(J - 1)
Next J
PART2B# = (1 / (1 - DORG#)) * (2 * PART2BSUM#(TNOC))
PART2C1#(XTRACOMP) = ((PUREA#(XTRACOMP, XTRACOMP) / (PUREB#(XTRACOMP,
XTRACOMP) * UGC * TEMPS(I))) + (LNORGGAMMAP#(XTRACOMP) / C#))
PART2C# = (QORG# / ((1 - DORG#) ^ 2)) * (1 - PART2C1#(XTRACOMP))
PART2A# = PART2B# - PART2C#
TERM2# = (1 / BORG#) * PART2A# * (((P * VORG#) / (UGC * TEMPS(I))) - 1)
PART3A# = (1 / (2 * Sqr(2))) * (AORG# / (BORG# * UGC * TEMPS(I)))
PART3B# = (((UGC * TEMPS(I) * DORG#) / AORG#) - (1 / BORG#)) * PART2A# +
((UGC * TEMPS(I) * BORG#) / AORG#) * PART2C1#(XTRACOMP))
PART3C# = Log((VORG# + BORG# * (1 - Sqr(2))) / (VORG# + BORG# * (1 +
Sqr(2))))
TERM3# = PART3A# * PART3B# * PART3C#
LNORGFUGACITYCOEFFICIENT#(XTRACOMP) = TERM1# + TERM2# + TERM3#
ORGFUGCOEFF#(XTRACOMP) = Exp(LNORGFUGACITYCOEFFICIENT#(XTRACOMP))
Next XTRACOMP

```

'2- VAPOUR PHASE.

'CALCULATION OF THE LIQUID PHASE ACTIVITY COEFFICIENTS AT THIS P & T.
'THE UNIQUAC EXPANSION (CALCULATION OF ACTIVITY COEFFICIENTS FOR EACH
' COMPONENT IN THE LIQUID PHASE).

For COMPONENT = I To TNOC

PHIBASE#(COMPONENT) = RA(COMPONENT) * YEXP1(I, COMPONENT) +

PHIBASE#(COMPONENT - 1)

THETABASE#(COMPONENT) = Q(COMPONENT) * YEXP1(I, COMPONENT) +

THETABASE#(COMPONENT - 1)

MODTHETABASE#(COMPONENT) = QD(COMPONENT) * YEXP1(I, COMPONENT) +

MODTHETABASE#(COMPONENT - 1)

Next COMPONENT

For COMPONENT = 1 To TNOC

PHI#(COMPONENT) = (RA(COMPONENT) * YEXP1(I, COMPONENT)) / PHIBASE#(TNOC)

THETA#(COMPONENT) = (Q(COMPONENT) * YEXP1(I, COMPONENT)) /

THETABASE#(TNOC)

MODTHETA#(COMPONENT) = (QD(COMPONENT) * YEXP1(I, COMPONENT)) /

MODTHETABASE#(TNOC)

Next COMPONENT

For COMPONENT = 1 To TNOC

LI#(COMPONENT) = (Z / 2) * (RA(COMPONENT) - Q(COMPONENT)) - (RA(COMPONENT)

- 1)

Next COMPONENT

For COMPONENT = 1 To TNOC

PART1# = Log(PHI#(COMPONENT) / YEXP1(I, COMPONENT))

PART2# = (Z / 2) * Q(COMPONENT) * Log(THETA#(COMPONENT) / PHI#(COMPONENT))

For J = 1 To TNOC

PART3SUM#(J) = YEXP1(I, J) * LI#(J) + PART3SUM#(J - 1)

PART4SUM#(J) = MODTHETA#(J) * T#(J, COMPONENT) + PART4SUM#(J - 1)

Next J

PART3# = (PHI#(COMPONENT) / YEXP1(I, COMPONENT)) * PART3SUM#(TNOC)

PART4# = QD(COMPONENT) * Log(PART4SUM#(TNOC))

For J = 1 To TNOC

PART5TOP#(J) = MODTHETA#(J) * T#(COMPONENT, J)

For K = 1 To TNOC

PART5BASE#(K) = MODTHETA#(K) * T#(K, J) + PART5BASE#(K - 1)

Next K

PART5TOT#(J) = (PART5TOP#(J) / PART5BASE#(TNOC)) + PART5TOT#(J - 1)

Next J

PART5# = QD(COMPONENT) * PART5TOT#(TNOC)

LNVAPGAMMAP#(COMPONENT) = PART1# + PART2# + LI#(COMPONENT) - PART3# -

PART4# + QD(COMPONENT) - PART5#

Next COMPONENT

For XTRACOMP = 1 To TNOC

```

TERM1# = -Log((P * (VVAP# - BVAP#)) / (UGC * TEMPS(I)))
For J = 1 To TNOC
PART2BSUM#(J) = (YEXP1(I, J) * CSVC#(XTRACOMP, J)) + PART2BSUM#(J - 1)
Next J
PART2B# = (1 / (1 - DVAP#)) * (2 * PART2BSUM#(TNOC))
PART2C1#(XTRACOMP) = ((PUREA#(XTRACOMP, XTRACOMP) / (PUREB#(XTRACOMP,
XTRACOMP) * UGC * TEMPS(I))) + (LNVAPGAMMAP#(XTRACOMP) / C#))
PART2C# = (QVAP# / (1 - DVAP#) ^ 2) * (1 - PART2C1#(XTRACOMP))
PART2A# = PART2B# - PART2C#
TERM2# = (1 / BVAP#) * PART2A# * (((P * VVAP#) / (UGC * TEMPS(I))) - 1)
PART3A# = (1 / (2 * Sqr(2))) * (AVAP# / (BVAP# * UGC * TEMPS(I)))
PART3B# = (((UGC * TEMPS(I) * DVAP#) / AVAP#) - (1 / BVAP#)) * PART2A# +
((UGC * TEMPS(I) * BVAP#) / AVAP#) * PART2C1#(XTRACOMP))
PART3C# = Log((VVAP# + BVAP# * (1 - Sqr(2))) / (VVAP# + BVAP# * (1 +
Sqr(2))))
TERM3# = PART3A# * PART3B# * PART3C#
LNVAPFUGACITYCOEFFICIENT#(XTRACOMP) = TERM1# + TERM2# + TERM3#
VAPFUGCOEFF#(XTRACOMP) = Exp(LNVAPFUGACITYCOEFFICIENT#(XTRACOMP))
Next XTRACOMP

'CALCULATION OF THE OBJECTIVE FUNCTION.

For COMPONENT = 1 To TNOC
  ORGFUGACITYP#(COMPONENT) = ORGFUGCOEFF#(COMPONENT) * XORG(I, COMPONENT)
  VAPFUGACITYP#(COMPONENT) = VAPFUGCOEFF#(COMPONENT) * YEXP1(I, COMPONENT)
  YORGCAL(I, COMPONENT) = ORGFUGACITYP#(COMPONENT) /
  VAPFUGCOEFF#(COMPONENT)
  SUMYORGCAL(I, COMPONENT) = YORGCAL(I, COMPONENT) + SUMYORGCAL(I,
  (COMPONENT - 1))

  Sheet1.Cells(30 + I, COMPONENT + 30) = ORGFUGCOEFF#(COMPONENT)
  Sheet1.Cells(30 + I, COMPONENT + 33) = VAPFUGCOEFF#(COMPONENT)
Next COMPONENT

For COMPONENT = 1 To (TNOC)
  FF1#(COMPONENT) = Abs(YORGCAL(I, COMPONENT) - YEXP(I, COMPONENT)) +
  FF1#(COMPONENT - 1)
Next COMPONENT
OFVALUE#(I) = FF1#(TNOC) + OFVALUE#(I - 1)
Next I
PRSVUNIQUAC1 = (OFVALUE#(Points) / (Points * TNOC)) * 1
Else
  PRSVUNIQUAC1 = 100000
End If
Sheet1.Cells(9, 9) = PRSVUNIQUAC1
End Function

```

D.1.2 Area Method main program for binary LLE

D.1.2.1 Area Method main program for binary LLE

```
Private Sub AreaMethod_Click()
Dim GMIXING, FAXA, FAXB, N, XA, XB
Dim XA22 As Double: Dim XB22 As Double
Dim start, finish
    start = Timer
    N = 100
    AreaMax = -100000
    'Input the pure component properties for PRSV and UNIQUAC and the
    interaction parameters
    Call INPUTDATA
    ' Opening two "for-next" loops to search the entire composition &
    estimating Gibbs energy at each point
    For XA = 0.001 To 0.99 Step 0.001
        XA22 = XA
        Call PHICALCL(XA, GMIXING)
        FAXA = GMIXING

        For XB = 0.99 To XA Step -0.005
            XB22 = XB
            Call PHICALCL(XB, GMIXING)
            FAXB = GMIXING
        ' Integration of the area under Gibbs free energy curve between XA & XB &
        the string No.
            INTEGRATION = IntegrateSimpson.Simpson(XA22, XB22, 100)

        'Calculating the Maximum Positive Net Area M.P.N.A
            AREA = Abs((FAXA + FAXB) * (XB - XA) / 2) - Abs(INTEGRATION)

            'Searching for the M.P.N.A.
                If AREA >= AreaMax Then
                    AreaMax = AREA
                    XAMax = XA
                    XBMax = XB
                End If
            Next XB
        Next XA
    'Finishing & writing the results to the sheet
        finish = Timer
        Sheet2.Cells(11, 19) = XAMax
        Sheet2.Cells(11, 20) = XBMax
        Sheet2.Cells(11, 18) = AreaMax
        Sheet2.Cells(11, 21) = finish - start
End Sub
```

D.1.2.2 Sub program to calculate roots of PRSV EOS

D.1.2.2.1 The compressibility factor for liquid phase

```
Public Function Z3ROOT(AM, BM)
'On Error Resume Next
' Function to calculate three roots of cubic equation and the result is
the minimum root is for liquid phase

Dim ALFA, Beta, Gamma, PP, QQ, DIS, UU, VV As Double
Dim y1, Y2, Y3, Z1, Z2, Z3, ZC, PPI As Double
Dim PP11, APP1 As Double

ALFA = BM - 1
Beta = AM - 3 * BM ^ 2 - 2 * BM
Gamma = -AM * BM + BM ^ 2 + BM ^ 3

PP = (3 * Beta - ALFA ^ 2) / 3
QQ = (2 * ALFA ^ 3 - 9 * ALFA * Beta + 27 * Gamma) / 27
DIS = (PP / 3) ^ 3 + (QQ / 2) ^ 2

UU = (-QQ / 2 + (Abs(DIS)) ^ 0.5)
UU = WorksheetFunction.Power(UU, 1 / 3)
VV = (-QQ / 2 - (Abs(DIS)) ^ 0.5)
VV = WorksheetFunction.Power(VV, 1 / 3)
If DIS < 0 Then

PP11 = (Abs(PP) / 3) ^ 3
APP1 = -QQ / (2 * (PP11) ^ 0.5)
PPI = Application.Acos(APP1)
y1 = 2 * ((Abs(PP) / 3) ^ 0.5) * Cos(PPI / 3)
Y2 = -2 * ((Abs(PP) / 3) ^ 0.5) * Cos((3.14159265358979 + PPI) / 3)
Y3 = -2 * ((Abs(PP) / 3) ^ 0.5) * Cos((3.14159265358979 - PPI) / 3)

Z1 = (y1 - ALFA / 3)
Z2 = (Y2 - ALFA / 3)
Z3 = (Y3 - ALFA / 3)
ZC = Application.Min(Z1, Z2, Z3)

Z3ROOT = ZC
Else
PPI = 0
y1 = UU + VV
Z1 = (y1 - ALFA / 3)
Z3ROOT = Z1
End If
End Function
```


D.1.2.2.2 The compressibility factor for Vapour Phase

Public Function ZVROOT(AM, BM)

' Function to calculate three roots of cubic equation and the result is the maximum root is selected for vapour phase.

Dim ALFA, Beta, Gamma, PP, QQ, DIS, UU, VV As Double

Dim y1, Y2, Y3, Z1, Z2, Z3, ZC, PPI As Double

Dim PP11, APP1 As Double

ALFA = BM - 1

Beta = AM - 3 * BM ^ 2 - 2 * BM

Gamma = -AM * BM + BM ^ 2 + BM ^ 3

PP = (3 * Beta - ALFA ^ 2) / 3

QQ = (2 * ALFA ^ 3 - 9 * ALFA * Beta + 27 * Gamma) / 27

DIS = (PP / 3) ^ 3 + (QQ / 2) ^ 2

UU = (-QQ / 2 + (Abs(DIS)) ^ 0.5)

UU = WorksheetFunction.Power(UU, 1 / 3)

VV = (-QQ / 2 - (Abs(DIS)) ^ 0.5)

VV = WorksheetFunction.Power(VV, 1 / 3)

If DIS < 0 Then

PP11 = (Abs(PP) / 3) ^ 3

APP1 = -QQ / (2 * (PP11) ^ 0.5)

PPI = Application.Acos(APP1)

y1 = 2 * ((Abs(PP) / 3) ^ 0.5) * Cos(PPI / 3)

Y2 = -2 * ((Abs(PP) / 3) ^ 0.5) * Cos((3.14159265358979 + PPI) / 3)

Y3 = -2 * ((Abs(PP) / 3) ^ 0.5) * Cos((3.14159265358979 - PPI) / 3)

Z1 = (y1 - ALFA / 3)

Z2 = (Y2 - ALFA / 3)

Z3 = (Y3 - ALFA / 3)

ZC = Application.Max(Z1, Z2, Z3)

ZVROOT = ZC

Else

PPI = 0

y1 = UU + VV

Z1 = (y1 - ALFA / 3)

ZVROOT = Z1

End If

End Function

D.1.2.3 Calculation of pure component Gibbs free energy

```
Public Sub PUREGCALC()
```

```
' Calculation of pure component Gibbs free energy at constant T& P.
```

```
Dim LOWPUREMIXG#(10), PUREV#(10, 10), TR#(10), K0#(10), K  
Dim ALPHA#(10), KC#(10), GPURE1#(10, 10), GPURE2#(10, 10), GPURE3A#(10,  
10), GPURE3B#(10, 10)  
Dim DSUM#(10), PUREGSUM(10), GPURE3#(10, 10), GPURE4#(10, 10)
```

```
Dim J, CSVC1#, CSVC2#  
Dim VNEW#, VCOUNT, VOLD#, PART1F1#, PART2F1#, PART3F1#, PART4F1#  
Dim FUNCTION1#, FUNCTION2#, PART1F2#, PART2F2#, PART3F2#  
Dim i, ZPP#, AP#, BP#
```

```
'CALCULATION OF PRSV EOS PURE COMPONENT PARAMETERS Ai AND Bi.
```

```
For J = 1 To TNOC  
  TR#(J) = TEMP / TC(J)  
  K0#(J) = 0.378893 + (1.4897153 * W(J)) - (0.17131848 * W(J) ^ 2) +  
(0.0196554 * W(J) ^ 3)  
  KC#(J) = K0#(J) + (k1(J) * ((1 + Sqr(TR#(J))) * (0.7 - TR#(J))))  
  ALPHA#(J) = (1 + (KC#(J) * (1 - Sqr(TR#(J))))) ^ 2  
  PUREA#(J) = (((0.457235 * UGC ^ 2 * TC(J) ^ 2) / PC(J)) * ALPHA#(J))  
  PUREB#(J) = (0.077796 * UGC * TC(J)) / PC(J)  
Next J
```

```
'CROSS SECOND VIRIAL COEFFICIENT CALCULATION.
```

```
For J = 1 To TNOC  
  For K = 1 To TNOC  
    CSVC1# = PUREB#(J) - (PUREA#(J) / (UGC * TEMP))  
    CSVC2# = PUREB#(K) - (PUREA#(K) / (UGC * TEMP))  
    CSVC#(J, K) = ((CSVC1# + CSVC2#) / 2) * (1 - KX#(J, K))  
  Next K  
Next J
```

```
'CALCULATION OF THE PURE COMPONENT MOLAR VOLUMES AND GIBBS FREE ENERGIES  
(AT FIXED T AND P)
```

```
' FOR EACH ROOT OF THE PRSV EOS. Newton-Raphson method is used
```

```
For J = 1 To 2  
  For K = 1 To TNOC  
    VNEW# = INITIALV#(J)  
    VCOUNT = 0  
    Do  
      VCOUNT = VCOUNT + 1
```

```

VOLD# = VNEW#
PART1F1# = P * (VOLD# ^ 3)
PART2F1# = ((P * PUREB#(K)) - (UGC * TEMP)) * VOLD# ^ 2
PART3F1# = ((3 * P * (PUREB#(K) ^ 2)) + (2 * UGC * TEMP * PUREB#(K)) -
PUREA#(K)) * VOLD#
PART4F1# = ((P * (PUREB#(K) ^ 3)) + (UGC * TEMP * (PUREB#(K) ^ 2)) -
(PUREA#(K) * PUREB#(K)))
FUNCTION1# = PART1F1# + PART2F1# - PART3F1# + PART4F1#
PART1F2# = 3 * P * (VOLD# ^ 2)
PART2F2# = 2 * ((P * PUREB#(K)) - (UGC * TEMP)) * VOLD#
PART3F2# = ((3 * P * (PUREB#(K) ^ 2)) + (2 * UGC * TEMP * PUREB#(K)) -
PUREA#(K))
FUNCTION2# = PART1F2# + PART2F2# - PART3F2#
VNEW# = VOLD# - (FUNCTION1# / FUNCTION2#)
If VCOUNT > 15 Then
GoTo VJUMP1
End If
Loop Until Abs(FUNCTION1#) < 1E-20
VJUMP1:
' OR the pure component molar volue can be estimated by calling the root
finder
AP# = PUREA#(K) * P / (UGC * TEMP) ^ 2
BP# = PUREB#(K) * P / (UGC * TEMP)
ZPP# = Z3ROOT(AP#, BP#)
VOLD# = (ZPP# * UGC * TEMP) / P

      PUREV#(J, K) = VOLD#
      GPURE1#(J, K) = (P * PUREV#(J, K)) / (UGC * TEMP)
      GPURE2#(J, K) = Log(PUREV#(J, K) / (PUREV#(J, K) - PUREB#(K)))
      GPURE3A#(J, K) = (PUREA#(K) / (2 * Sqr(2) * UGC * TEMP *
PUREB#(K)))
      GPURE3B#(J, K) = (PUREV#(J, K) + ((1 - Sqr(2)) * PUREB#(K))) /
(PUREV#(J, K) + ((1 + Sqr(2)) * PUREB#(K)))
      GPURE3#(J, K) = GPURE3A#(J, K) * Log(GPURE3B#(J, K))
      'GPURE4#(J, K) = Log(100000! * (PUREV#(J, K) / (UGC * TEMP)))
      GPURE4#(J, K) = Log((PUREV#(J, K) / (UGC * TEMP)))
      PURECOMP#(J, K) = GPURE1#(J, K) + GPURE2#(J, K) + GPURE3#(J,
K) - GPURE4#(J, K)
      Next K
    Next J

End Sub

```

D.1.2.4 Calculation of Gibbs free energy for the mixture

```
Public Sub PHICALCL(x1, GMIXING)
Dim F12#(10), F22#(10), H12#(10)
Dim IS12#(10), IS2A2#(10), IS2B2#(10), IS32#(10), IS42#(10)
Dim G1A2#(10), G1B2#(10), G12#(10), G22#(10)
Dim T#(10, 10), TR#(10), K0#(10), KC#(10)
'Dim X(10), MIXTV#(10), ALPHA#(10), INTQSUM#(10), EXTQSUM#(10)
Dim MIXTV#(10), ALPHA#(10), INTQSUM#(10), EXTQSUM#(10)
Dim DSUM#(10), GPART1#(10), GPART2#(10), GPART3A#(10)
Dim GPART4#(10, 10), MIXTUREG(10), RADANGLE#(3), GPART3B#(10)
Dim GPART3#(10), QP#, AP#, YEXP, GEXCESS#, Z, L, i, J, K, G32#
Dim D#, b#, VNEW#, VCOUNT, VOLD#
Dim PART1F1#, PART2F1#, PART3F1#, PART4F1#
Dim FUNCTION1#, FUNCTION2#
Dim PART1F2#, PART2F2#, PART3F2#, PUREGMIX, LOWMIXG, LOWG
'Dim GMIXING, APV#
Dim APV#:Dim ZP#, BP#

Call PUREGCALC

'CALCULATION OF EXCESS GIBBS ENERGY USING MODIFIED UNIQUAC.

CX# = (1 / Sqr(2)) * Log(Sqr(2) - 1)

GEXCESS# = 0

For J = 1 To TNOC
  For K = 1 To TNOC
    IS12#(K) = (x(K) * R(K)) + IS12#(K - 1)
  Next K
  F12#(J) = Log(R(J) / IS12#(TNOC))
  F22#(J) = (x(J) * F12#(J)) + F22#(J - 1)
Next J

For J = 1 To TNOC
  For K = 1 To TNOC
    IS2A2#(K) = (x(K) * Q(K)) + IS2A2#(K - 1)
    IS2B2#(K) = (x(K) * R(K)) + IS2B2#(K - 1)
  Next K
  G1A2#(J) = Q(J) / R(J)
  G1B2#(J) = (IS2B2#(TNOC) / IS2A2#(TNOC))
  G12#(J) = Log(G1A2#(J) * G1B2#(J))
  G22#(J) = ((Q(J) * x(J)) * G12#(J)) + G22#(J - 1)
Next J

G32# = (ZPAC / 2) * G22#(TNOC)

For J = 1 To TNOC
  For K = 1 To TNOC
```

```

For L = 1 To TNOC
    IS42#(L) = (x(L) * QD(L)) + IS42#(L - 1)
Next L
T#(K, J) = Exp(-AX#(K, J) / TEMP)
IS32#(K) = ((x(K) * QD(K) * T#(K, J)) / IS42#(TNOC)) + IS32#(K - 1)
Next K
H12#(J) = (QD(J) * x(J) * (Log(IS32#(TNOC)))) + H12#(J - 1)
Next J

GEXCESS# = F22#(TNOC) + G32# - H12#(TNOC)

'CALCULATION OF THE EXCLUDED VOLUME PARAMETER (BM).

For J = 1 To TNOC
    For K = 1 To TNOC
        INTQSUM#(K) = (x(J) * x(K) * CSVC#(J, K)) + INTQSUM#(K - 1)
    Next K
    EXTQSUM#(J) = INTQSUM#(TNOC) + EXTQSUM#(J - 1)
Next J
QP# = EXTQSUM#(TNOC)

For J = 1 To TNOC
    DSUM#(J) = ((x(J) * PUREA#(J)) / (PUREB#(J) * UGC * TEMP)) + DSUM#(J - 1)
Next J

D# = DSUM#(TNOC) + (GEXCESS# / CX#)
b# = QP# / (1 - D#)

'CALCULATION OF THE ENERGY OF ATTRACTION PARAMETER (am).

AP# = (UGC * TEMP * b# * D#)
BP# = b# * P / (UGC * TEMP)

'CALCULATION OF THE MOLAR VOLUMES (AT FIXED T AND P), FOR EACH ROOT OF THE
PRSV EOS.

For J = 1 To 2 Step 1
    VNEW# = INITIALV#(J)
    VCOUNT = 0
    Do
        VCOUNT = VCOUNT + 1
        VOLD# = VNEW#
        PART1F1# = P * VOLD# ^ 3
        PART2F1# = ((P * b#) - (UGC * TEMP)) * VOLD# ^ 2
        PART3F1# = ((3 * P * (b# ^ 2)) + (2 * UGC * TEMP * b#) - AP#) * VOLD#
        PART4F1# = ((P * (b# ^ 3)) + (UGC * TEMP * (b# ^ 2)) - (AP# * b#))
        FUNCTION1# = PART1F1# + PART2F1# - PART3F1# + PART4F1#
        PART1F2# = 3 * P * VOLD# ^ 2
        PART2F2# = 2 * ((P * b#) - (UGC * TEMP)) * VOLD#
        PART3F2# = ((3 * P * (b# ^ 2)) + (2 * UGC * TEMP * b#) - AP#)
        FUNCTION2# = PART1F2# + PART2F2# - PART3F2#
    Loop While FUNCTION1# > 0

```

```

VNEW# = VOLD# - (FUNCTION1# / FUNCTION2#)

If VCOUNT > 15 Then
GoTo VJUMP2
End If

Loop Until Abs(FUNCTION1#) < 1E-20
VJUMP2:
MIXTV#(J) = VOLD#
APV# = AP# * P / (UGC * TEMP) ^ 2
ZP# = Z3ROOT(APV#, BP#)
MIXTV#(J) = (ZP# * UGC * TEMP) / P
VOLML = Log(MIXTV#(J) * 10 ^ (-6))

'CALCULATION OF DIMENSIONLESS MIXTURE GIBBS FREE ENERGY.

GPART1#(J) = (P * MIXTV#(J)) / (UGC * TEMP)
GPART2#(J) = Log(MIXTV#(J) / (MIXTV#(J) - b#))
GPART3A#(J) = (AP# / (2 * Sqr(2) * UGC * TEMP * b#))
GPART3B#(J) = (MIXTV#(J) + ((1 - Sqr(2)) * b#)) / (MIXTV#(J) + ((1 +
Sqr(2)) * b#))
GPART3#(J) = GPART3A#(J) * Log(GPART3B#(J))

For K = 1 To TNOC
GPART4#(J, K) = (x(K) * Log((MIXTV#(J) / (x(K) * UGC * TEMP)))) +
GPART4#(J, K - 1)
Next K
MIXTUREG(J) = GPART1#(J) + GPART2#(J) + GPART3#(J) - GPART4#(J, TNOC)
Next J

PUREGMIX = 0
For i = 1 To TNOC
PUREGMIX = PUREGMIX + PURECOMP#(1, i) * x(i)
Next i

PUREGMIX = PUREGMIX + PUREGINT
LOWMIXG = MIXTUREG(1)
LOWG = MIXTUREG(1) - PUREGMIX

If MIXTUREG(2) < LOWMIXG Then
LOWMIXG = MIXTUREG(2)
LOWG = MIXTUREG(2) - PUREGMIX
End If
GMIXING = LOWG

End Sub

```

D.1.2.5 Integration of Gibbs free energy curve using Simpson's rule

```
Function Simpson(a As Double, b As Double, N As Integer) As Double
    'n should be an even number
    Dim J As Integer, s1 As Double, s2 As Double, h As Single
    h = (b - a) / N
    s1 = 0
    s2 = 0
    For J = 1 To N - 1 Step 2
        s1 = s1 + f(a + J * h)
    Next J
    For J = 2 To N - 2 Step 2
        s2 = s2 + f(a + J * h)
    Next J
    Simpson = h / 3 * (f(a) + 4 * s1 + 2 * s2 + f(b))
End Function
```

'The Function code (f) is the same as PHICALCL

D.1.3 TPI for VLLE binary systems

D.1.3.1 Main program

```
Private Sub CommandButton2_Click()
Dim Z, GMIXINGV, GMIXING
Call INPUTDATA
Dim RESULT

' Gibbs free energy estimation at each grid considering the phase change

x(1) = -((1 / YLIM) / 2)

For Z = 1 To YLIM
    x(1) = x(1) + 1 / YLIM
    Call PHICALCL(x, GMIXING)
    Call PHICALCV(x, GMIXINGV)
    If GMIXINGV > GMIXING Then
        GMIXINGF(Z) = GMIXING
        VOLUME(Z) = VOLML
    Else: GMIXINGF(Z) = GMIXINGV
        VOLUME(Z) = VOLMV
    End If
    ' Writing the results back to the sheet

    Sheet1.Cells(3 + Z, 2) = x(1)
    XXJ(Z) = x(1)
    Sheet1.Cells(3 + Z, 3) = GMIXINGF(Z)
    Sheet1.Cells(3 + Z, 4) = VOLUME(Z)
Next Z

' Calling the Nelder Mead Module to minimize the tau function
' Calculating the starting values

ReDim initParams(1 To 2, 1 To 1)
'initial values for XA & XB optimization

initParams(1, 1) = ZALFA - (1 / XGRID) * 2 ^ 0.5
initParams(2, 1) = 1 - (1 / XGRID) * 2 ^ 0.5 - ZALFA

Dim nelderObj As New Nelder
RESULT = nelderObj.SolveMaximum("fn", initParams)

Sheets("sheet2").Range("G12").Value = RESULT(1, 1)
Sheets("sheet2").Range("H12").Value = RESULT(2, 1)

' calling the Nelder Mead for the second time and with new starting
points
ReDim initParams(1 To 2, 1 To 1)
```



```

initParams(1, 1) = ZALFA - ((1 / XGRID) * 2 ^ 0.5) - XAH / 2
initParams(2, 1) = 1 - (1 / XGRID) * 2 ^ 0.5 - ZALFA

'Dim nelderObj As New Nelder
RESULT = nelderObj.SolveMaximum("fn", initParams)

Sheets("sheet2").Range("I12").Value = RESULT(1, 1)
Sheets("sheet2").Range("J12").Value = RESULT(2, 1)

```

End Sub

D.1.3.2 Sub procedure to calculate pure component Gibbs free energy

```

Public Sub PUREGCALC()

Dim LOWPUREMIXG#(10), PUREV#(10, 10), TR#(10), K0#(10), K
Dim ALPHA#(10), KC#(10), GPURE1#(10, 10), GPURE2#(10, 10), GPURE3A#(10,
10), GPURE3B#(10, 10)
Dim DSUM#(10), PUREGSUM(10), GPURE3#(10, 10), GPURE4#(10, 10)

Dim J, CSVC1#, CSVC2#
Dim VNEW#, VCOUNT, VOLD#, PART1F1#, PART2F1#, PART3F1#, PART4F1#
Dim FUNCTION1#, FUNCTION2#, PART1F2#, PART2F2#, PART3F2#
Dim I, ZPP#, AP#, BP#

'CALCULATION OF PRSV EOS PURE COMPONENT PARAMETERS Ai AND Bi.

For J = 1 To TNOC
    TR#(J) = TEMP / TC(J)
    K0#(J) = 0.378893 + (1.4897153 * W(J)) - (0.17131848 * W(J) ^ 2) +
(0.0196554 * W(J) ^ 3)
    KC#(J) = K0#(J) + (k1(J) * ((1 + Sqr(TR#(J))) * (0.7 - TR#(J))))
    ALPHA#(J) = (1 + (KC#(J) * (1 - Sqr(TR#(J))))) ^ 2
    PUREA#(J) = (((0.457235 * UGC ^ 2 * TC(J) ^ 2) / PC(J)) * ALPHA#(J))
    PUREB#(J) = (0.077796 * UGC * TC(J)) / PC(J)
Next J
'CROSS SECOND VIRIAL COEFFICIENT CALCULATION.
For J = 1 To TNOC
    For K = 1 To TNOC
        CSVC1# = PUREB#(J) - (PUREA#(J) / (UGC * TEMP))
        CSVC2# = PUREB#(K) - (PUREA#(K) / (UGC * TEMP))
        CSVC#(J, K) = ((CSVC1# + CSVC2#) / 2) * (1 - KX#(J, K))
    Next K
Next J

'CALCULATION OF THE PURE COMPONENT MOLAR VOLUMES AND GIBBS FREE ENERGIES
(AT FIXED T AND P)
' FOR EACH ROOT OF THE PRSV EOS.

```

```

For J = 1 To 2
  For K = 1 To TNOC
    VNEW# = INITIALV#(J)
    VCOUNT = 0
    Do
      VCOUNT = VCOUNT + 1
      VOLD# = VNEW#
      PART1F1# = P * (VOLD# ^ 3)
      PART2F1# = ((P * PUREB#(K)) - (UGC * TEMP)) * VOLD# ^ 2
      PART3F1# = ((3 * P * (PUREB#(K) ^ 2)) + (2 * UGC * TEMP * PUREB#(K))
      - PUREA#(K)) * VOLD#
      PART4F1# = ((P * (PUREB#(K) ^ 3)) + (UGC * TEMP * (PUREB#(K) ^ 2)) -
      (PUREA#(K) * PUREB#(K)))
      FUNCTION1# = PART1F1# + PART2F1# - PART3F1# + PART4F1#
      PART1F2# = 3 * P * (VOLD# ^ 2)
      PART2F2# = 2 * ((P * PUREB#(K)) - (UGC * TEMP)) * VOLD#
      PART3F2# = ((3 * P * (PUREB#(K) ^ 2)) + (2 * UGC * TEMP * PUREB#(K))
      - PUREA#(K))
      FUNCTION2# = PART1F2# + PART2F2# - PART3F2#
      VNEW# = VOLD# - (FUNCTION1# / FUNCTION2#)
      If VCOUNT > 15 Then
        GoTo VJUMP1
      End If
      Loop Until Abs(FUNCTION1#) < 1E-20
      VJUMP1:
      ' AP# = PUREA#(K) * P / (UGC * TEMP) ^ 2
      ' BP# = PUREB#(K) * P / (UGC * TEMP)
      ' ZPP# = Z3ROOT(AP#, BP#)
      ' VOLD# = (ZPP# * UGC * TEMP) / P

      PUREV#(J, K) = VOLD#
      GPURE1#(J, K) = (P * PUREV#(J, K)) / (UGC * TEMP)
      GPURE2#(J, K) = Log(PUREV#(J, K) / (PUREV#(J, K) - PUREB#(K)))
      GPURE3A#(J, K) = (PUREA#(K) / (2 * Sqr(2) * UGC * TEMP * PUREB#(K)))
      GPURE3B#(J, K) = (PUREV#(J, K) + ((1 - Sqr(2)) * PUREB#(K))) /
      (PUREV#(J, K) + ((1 + Sqr(2)) * PUREB#(K)))
      GPURE3#(J, K) = GPURE3A#(J, K) * Log(GPURE3B#(J, K))
      ' GPURE4#(J, K) = Log(100000! * (PUREV#(J, K) / (UGC * TEMP)))
      GPURE4#(J, K) = Log((PUREV#(J, K) / (UGC * TEMP)))
      PURECOMP#(J, K) = GPURE1#(J, K) + GPURE2#(J, K) + GPURE3#(J, K) -
      GPURE4#(J, K)
    Next K
  Next J

End Sub

```

D.1.3.3 Tau Objective Function

Public Function fn(x1 As Variant) As Variant

Dim XA(10), XB(10)

'CALCULATION FOR INITIAL VARIABLE VALUES(ALFA1,ALFA2)

XA(1) = ZALFA - x1(1, 1)

XA(2) = 1 - XA(1)

XB(1) = ZALFA + x1(2, 1)

XB(2) = 1 - XB(1)

If XA(1) > 0 And XA(1) < 1 And XB(1) > 0 And XB(1) < 1 Then

'CALCULATION FOR PURE COMPONENT GIBBS ENERGY PART2

Call PHICALCL(XA, GMIXING)

Call PHICALCV(XA, GMIXINGV)

If GMIXINGV > GMIXING Then

FAYXA = GMIXING

Else: FAYXA = GMIXINGV

End If

Call PHICALCL(XB, GMIXING)

Call PHICALCV(XB, GMIXINGV)

If GMIXINGV > GMIXING Then

FAYXB = GMIXING

Else: FAYXB = GMIXINGV

End If

'CALCULATION OF the tangent plane slope intercept and single delta tau increment

fn = 0

TPS = (FAYXB - FAYXA) / (XB(1) - XA(1))

TPINT = FAYXA - (TPS * XA(1))

TPSCT = (1 / XGRID) * (1 + (TPS) ^ 2)

For J = 1 To XGRID

TPV = (TPS * XXJ(J)) + TPINT

If TPV > GMIXINGF(J) Then

fn = fn + TPSCT

End If

Next J

Else:

```

fn = 1000
End If

```

```

Sheet2.Cells(16, 9) = fn

```

```

XAL = ZALFA - x1(1, 1)
XAH = ZALFA + x1(2, 1)

```

```

End Function

```

D.1.3.4 Sub program of Gibbs free energy calculation for vapour phase

```

Public Sub PHICALCV(x, GMIXINGV)
Dim F12#(10), F22#(10), H12#(10)
Dim IS12#(10), IS2A2#(10), IS2B2#(10), IS32#(10), IS42#(10)
Dim G1A2#(10), G1B2#(10), G12#(10), G22#(10)
Dim T#(10, 10), TR#(10), K0#(10), KC#(10)
Dim MIXTV#(10), ALPHA#(10), INTQSUM#(10), EXTQSUM#(10)
Dim DSUM#(10), GPART1#(10), GPART2#(10), GPART3A#(10)
Dim GPART4#(10, 10), MIXTUREG(10), RADANGLE#(3), GPART3B#(10)
Dim GPART3#(10), QP#, AP#, YEXP, GEXCESS#, Z, L, I, J, K, G32#
Dim D#, B#, VNEW#, VCOUNT, VOLD#
Dim PART1F1#, PART2F1#, PART3F1#, PART4F1#
Dim FUNCTION1#, FUNCTION2#
Dim PART1F2#, PART2F2#, PART3F2#, PUREGMIX, LOWMIXG, LOWG
Dim APV#, ZP#, BP#

```

```

Call PUREGCALC

```

```

TPLIM = 0
x(2) = 1 - x(1)

```

```

'CALCULATION OF EXCESS GIBBS ENERGY USING MODIFIED UNIQUAC.

```

```

CX# = (1 / Sqr(2)) * Log(Sqr(2) - 1)
GEXCESS# = 0

```

```

For J = 1 To TNOC
For K = 1 To TNOC
IS12#(K) = (x(K) * R(K)) + IS12#(K - 1)
Next K
F12#(J) = Log(R(J) / IS12#(TNOC))
F22#(J) = (x(J) * F12#(J)) + F22#(J - 1)
Next J

```

```

For J = 1 To TNOC
For K = 1 To TNOC
IS2A2#(K) = (x(K) * Q(K)) + IS2A2#(K - 1)
IS2B2#(K) = (x(K) * R(K)) + IS2B2#(K - 1)

```

```

        Next K
        G1A2#(J) = Q(J) / R(J)
        G1B2#(J) = (IS2B2#(TNOC) / IS2A2#(TNOC))
        G12#(J) = Log(G1A2#(J) * G1B2#(J))
        G22#(J) = ((Q(J) * x(J)) * G12#(J)) + G22#(J - 1)
    Next J

    G32# = (ZPAC / 2) * G22#(TNOC)

    For J = 1 To TNOC
        For K = 1 To TNOC
            For L = 1 To TNOC
                IS42#(L) = (x(L) * QD(L)) + IS42#(L - 1)
            Next L
            T#(K, J) = Exp(-AX#(K, J) / TEMP)
            IS32#(K) = ((x(K) * QD(K) * T#(K, J)) / IS42#(TNOC)) + IS32#(K - 1)
        Next K
        H12#(J) = (QD(J) * x(J) * (Log(IS32#(TNOC)))) + H12#(J - 1)
    Next J

    GEXCESS# = F22#(TNOC) + G32# - H12#(TNOC)
'CALCULATION OF THE EXCLUDED VOLUME PARAMETER (BM).
    For J = 1 To TNOC
        For K = 1 To TNOC
            INTQSUM#(K) = (x(J) * x(K) * CSVC#(J, K)) + INTQSUM#(K - 1)
        Next K
        EXTQSUM#(J) = INTQSUM#(TNOC) + EXTQSUM#(J - 1)
    Next J

    QP# = EXTQSUM#(TNOC)

    For J = 1 To TNOC
        DSUM#(J) = ((x(J) * PUREA#(J)) / (PUREB#(J) * UGC * TEMP)) + DSUM#(J - 1)
    Next J

    D# = DSUM#(TNOC) + (GEXCESS# / CX#)
    B# = QP# / (1 - D#)

'CALCULATION OF THE ENERGY OF ATTRACTION PARAMETER (am).

    AP# = (UGC * TEMP * B# * D#)
    BP# = B# * P / (UGC * TEMP)

    For J = 1 To 2 Step 1
        VNEW# = INITIALV#(J)
        VCOUNT = 0
        Do
            VCOUNT = VCOUNT + 1
            VOLD# = VNEW#
            PART1F1# = P * VOLD# ^ 3
            PART2F1# = ((P * B#) - (UGC * TEMP)) * VOLD# ^ 2

```

```

PART3F1# = ((3 * P * (B# ^ 2)) + (2 * UGC * TEMP * B#) - AP#) * VOLD#
PART4F1# = ((P * (B# ^ 3)) + (UGC * TEMP * (B# ^ 2)) - (AP# * B#))
FUNCTION1# = PART1F1# + PART2F1# - PART3F1# + PART4F1#
PART1F2# = 3 * P * VOLD# ^ 2
PART2F2# = 2 * ((P * B#) - (UGC * TEMP)) * VOLD#
PART3F2# = ((3 * P * (B# ^ 2)) + (2 * UGC * TEMP * B#) - AP#)
FUNCTION2# = PART1F2# + PART2F2# - PART3F2#
VNEW# = VOLD# - (FUNCTION1# / FUNCTION2#)

```

```

If VCOUNT > 15 Then
GoTo VJUMP2
End If

```

```

Loop Until Abs(FUNCTION1#) < 1E-20
VJUMP2:
MIXTV#(J) = VOLD#
APV# = AP# * P / (UGC * TEMP) ^ 2
ZP# = ZVROOT(APV#, BP#)
MIXTV#(J) = (ZP# * UGC * TEMP) / P
VOLMV = Log(MIXTV#(J) * 10 ^ (-6))

```

```

'CALCULATION OF DIMENSIONLESS MIXTURE GIBBS FREE ENERGY.
GPART1#(J) = (P * MIXTV#(J)) / (UGC * TEMP)
GPART2#(J) = Log(MIXTV#(J) / (MIXTV#(J) - B#))
GPART3A#(J) = (AP# / (2 * Sqr(2) * UGC * TEMP * B#))
GPART3B#(J) = (MIXTV#(J) + ((1 - Sqr(2)) * B#)) / (MIXTV#(J) + ((1 +
Sqr(2)) * B#))
GPART3#(J) = GPART3A#(J) * Log(GPART3B#(J))

```

```

For K = 1 To TNOC
GPART4#(J, K) = (x(K) * Log((MIXTV#(J) / (x(K) * UGC * TEMP)))) +
GPART4#(J, K - 1)
Next K
MIXTUREG(J) = GPART1#(J) + GPART2#(J) + GPART3#(J) - GPART4#(J, TNOC)
Next J

```

```

PUREGMIX = 0
For I = 1 To TNOC
PUREGMIX = PUREGMIX + PURECOMP#(1, I) * x(I)
Next I

```

```

PUREGMIX = PUREGMIX + PUREGINT
LOWMIXG = MIXTUREG(1)
LOWG = MIXTUREG(1) - PUREGMIX

```

```

If MIXTUREG(2) < LOWMIXG Then
LOWMIXG = MIXTUREG(2)
LOWG = MIXTUREG(2) - PUREGMIX
End If
GMIXINGV = LOWG

```

```

End Sub

' Sub program input data

Public Sub INPUTDATA()

Dim I As Integer: J As Integer

'Input #1, TNOC, NA, LINES, MAXITRS, Z
'TEMPS      is the system temperature
'PRESSURE   is the pressure for the system
'TNOC       is number of components in the system
'POINTS     is the number of the data sets
'MAXITRS    is the maximum iteration used in the simplex or optimisation
function
'Z          is the average coordination number usually equals 10 in
UNIQUAC activity equation

'TEMPS = Sheet1.Cells(3, 2).Value
TEMP = Sheet2.Cells(4, 4).Value
P = Sheet2.Cells(4, 5).Value
TNOC = Sheet2.Cells(4, 6).Value
NA = Sheet2.Cells(4, 7).Value
Points = Sheet2.Cells(4, 8).Value
MAXITRS = Sheet2.Cells(4, 9).Value
ZPAC = Sheet2.Cells(4, 10).Value
YLIM = Sheet2.Cells(4, 25).Value
ZLIM = Sheet2.Cells(4, 26).Value

XGRID = Sheet2.Cells(4, 31).Value
ZALFA = Sheet2.Cells(4, 32).Value

'RA      is volume parameter for species i UNIQUAC
'Q       is surface area parameter for species i UNIQUAC
'QD      is surface area parameter for species i UNIQUAC for alcohols and
water

For J = 1 To TNOC
    R(J) = Sheet2.Cells(3 + J, 12).Value
    Q(J) = Sheet2.Cells(3 + J, 13).Value
    QD(J) = Sheet2.Cells(3 + J, 14).Value

    'TC      is critical temperature for species i in PRSV equation of
state
'PC       is critical pressure for species i in PRSV equation of state
'W        is acentric factor in PRSV equation of state
'K1       is kappa value for species i in PRSV equation of state

```

```

TC(J) = Sheet2.Cells(3 + J, 16).Value
PC(J) = Sheet2.Cells(3 + J, 17).Value
W(J) = Sheet2.Cells(3 + J, 18).Value
k1(J) = Sheet2.Cells(3 + J, 19).Value

ANTA(J) = Sheet2.Cells(3 + J, 21).Value
ANTB(J) = Sheet2.Cells(3 + J, 22).Value
ANTC(J) = Sheet1.Cells(3 + J, 23).Value
Next J

AX#(1, 2) = Sheet2.Cells(9, 5).Value
AX#(2, 1) = Sheet2.Cells(10, 5).Value
KX#(1, 2) = Sheet2.Cells(11, 5).Value
KX#(2, 1) = KX#(1, 2)

'AX      is the energy binary parameter used in UNIQUAC
AX11=AX22=AX33=0, AND THE
'      RESULTS : U12,U21, U11=U22=1
'KX      is interaction parameter between unlike molecules Kij=Kji ,
Kii=Kjj=0

For I = 1 To TNOC
  For J = 1 To TNOC
    If I = J Then
      AX#(I, J) = 0
      KX#(I, J) = 0
    End If

    Next J
  Next I

End sub

```


D.2 Ternary systems

D.2.1 VLLE Flash calculation main program

```
Private Sub VLLEFLASHTERNARY_Click()
    Dim result As Variant
    Dim i, STIME, FTIME, ALF1(20), ALF2(20), K, J, ZFSUM(10), COUNTER

    STIME = Timer!
    Call INPUTDATA

    ' CALCULATION FOR FEED COMPOSITION Zi
    For i = 1 To Points
        For K = 1 To TNOC
            ZFSUM(K) = XORG(i, K) + XAQ(i, K) + YEXP(i, K)
        Next K
        For J = 1 To TNOC
            ZF(i, J) = ZFSUM(J) / 3
            Sheet3.Cells(3 + i, J + 3) = ZF(i, J)
        Next J

        'CALCULATION FOR ALFA AND BETA Lorg/F = alfa AND Laq/F = beta

        ALF1(i) = (ZF(i, 1) - YEXP(i, 1)) * (XAQ(i, 2) - YEXP(i, 2)) + (YEXP(i,
2) - ZF(i, 2)) * (XAQ(i, 1) - YEXP(i, 1))
        ALF2(i) = (XORG(i, 1) - YEXP(i, 1)) * (XAQ(i, 2) - YEXP(i, 2)) -
(XORG(i, 2) - YEXP(i, 2)) * (XAQ(i, 1) - YEXP(i, 1))
        ALF(i) = ALF1(i) / ALF2(i)
        BTA(i) = (ZF(i, 3) - YEXP(i, 3) - ALF(i) * (XORG(i, 3) - YEXP(i, 3)))
/ (XAQ(i, 3) - YEXP(i, 3))

        Sheet2.Cells(2 + i, 5) = ALF(i)
        Sheet2.Cells(2 + i, 6) = BTA(i)

    Next i

    ' Part 1 UNIQUAC and PRSV parameters

    ReDim initParams(1 To 9, 1 To 1)
    For i = 1 To 9
        initParams(i, 1) = Sheet1.Cells(8 + i, 5).Value
    Next i

    Dim nelderObj As New Nelder
    result = nelderObj.SolveMaximum("PRSVUNIQUAC1", initParams)

    For i = 1 To 9
        Sheet1.Cells(8 + i, 7) = result(i, 1)
    Next i

    Call WRITERESULTS
```

```

'Part 2 Temperature estimation

    For II = 1 To Points

        ReDim initParams(1 To 1, 1 To 1)
            initParams(1, 1) = TEMPS(II)

        ' Dim nelderObj As New Nelder
            result = nelderObj.SolveMaximum("PRSVUNIQUAC4", initParams)
        '

        Sheet2.Cells(2 + II, 14) = result(1, 1)
    Next II
' Part 3 Pressure estimation

    Call WRITERESULTS

ReDim initParams(1 To 1, 1 To 1)
initParams(1, 1) = Sheet1.Cells(4, 5)

' Dim nelderObj As New Nelder
result = nelderObj.SolveMaximum("PRSVUNIQUAC5", initParams)

    Sheet1.Cells(4, 3) = result(1, 1)

    Call WRITERESULTS

'Part 4 Using Rachford Rice equation for alfa and beta estimation for
each point

    For II = 1 To Points

        ReDim initParams(1 To 2, 1 To 1)
            initParams(1, 1) = ALF(II)
            initParams(2, 1) = BTA(II)

        result = nelderObj.SolveMaximum("PRZERO", initParams)
        Sheet2.Cells(2 + II, 8) = ALF(II)
        Sheet2.Cells(2 + II, 9) = BTA(II)

    Next II

    Call WRITERESULTS

    FTIME = Timer!
    Sheet1.Cells(24, 3) = FTIME - STIME

End Sub

```

D.2.2 VLE Tangent Plane Intersection TPI

D.2.2.1 The main program

Option Explicit

```
Private Sub CommandButton1_Click()
Dim i, result, MINVAL, GLOOP, start, finish
Dim PHIZ, PHIX, HZ(10), HX(10), HZX(10), HZXO(10), HZXA(10), X30, X10, X20
Dim GMIXING, J, kT(10), XXORG(10), SUMXXORG(10), SUMkT(10), STPD(10),
XXAQ(10)
Dim SUMXXAQ(10), SUMYYVAP(10), YYVAP(10), HZXV(10)

start = Timer

Call INPUTDATA: Call PHICALCL: Call PHICALCV: Call WRITING: Call INITIALVAL

step1:
GLOOP = 0

Do
GLOOP = GLOOP + 1
ReDim initParams(1 To 6, 1 To 1)

initParams(1, 1) = Z1: initParams(2, 1) = Z2: initParams(3, 1) = Z3
initParams(4, 1) = ANG1: initParams(5, 1) = ANG2: initParams(6, 1) = ANG3

Dim nelderObj As New Nelder
    result = nelderObj.SolveMaximum("AREACALC", initParams)

    For i = 1 To 6
    Sheet2.Cells(8 + i, 12) = result(i, 1)
    Next i

MINVAL = OFVALUE#
If GLOOP > 1 Then
GoTo GJUMP
End If
MINVAL = OFVALUE#

Loop Until OFVALUE# < 0.0000001

Sheet2.Cells(18, 9) = OFVALUE#
Sheet2.Cells(9, 17) = x1: Sheet2.Cells(10, 17) = Y1
Sheet2.Cells(11, 17) = X2: Sheet2.Cells(12, 17) = Y2
Sheet2.Cells(13, 17) = X3: Sheet2.Cells(14, 17) = Y3
GJUMP:
finish = Timer
Sheet2.Cells(9, 15) = (finish - start)
Sheet2.Cells(18, 9) = OFVALUE#
```

Sheet2.Cells(9, 17) = x1: Sheet2.Cells(10, 17) = Y1
 Sheet2.Cells(11, 17) = X2: Sheet2.Cells(12, 17) = Y2
 Sheet2.Cells(13, 17) = X3: Sheet2.Cells(14, 17) = Y3

End Sub

D.2.2.2 Liquid phase fugacity coefficient

```
Public Sub PHICALCL()
  Dim F12#(10), F22#(10), H12#(10)
  Dim IS12#(10), IS2A2#(10), IS2B2#(10), IS32#(10), IS42#(10)
  Dim G1A2#(10), G1B2#(10), G12#(10), G22#(10)
  Dim T#(10, 10), TR#(10), K0#(10), KC#(10)
  Dim x(10), MIXTV#(10), ALPHA#(10), INTQSUM#(10), EXTQSUM#(10)
  Dim DSUM#(10), GPART1#(10), GPART2#(10), GPART3A#(10)
  Dim GPART4#(10, 10), MIXTUREG(10), RADANGLE#(3), GPART3B#(10)
  Dim GPART3#(10), QP#, AP#, AP1#, YEXP, GEXCESS#, Z, L, i, J, K, G32#
  Dim D#, B#, VNEW#, VCOUNT, VOLD#
  Dim PART1F1#, PART2F1#, PART3F1#, PART4F1#
  Dim FUNCTION1#, FUNCTION2#
  Dim PART1F2#, PART2F2#, PART3F2#, PUREGMIX, LOWMIXG, LOWG
  Dim GMIXING : Dim ZP#, BP#, ZP1#

  Call PUREGCALC

  TPLIM = 0

  ' (X1-X2)PLANE REPRESENTED BY RIGHT ANGLE TRIANGLE IS DIVIDED INTO A
  GRID SIZE AND VALUES OF PHI IS CALCULATED AT THE CENTRE OF EACH GRID

  MINAREA# = ((1 / ZLIM) * (1 / YLIM) * 3)
  x(2) = -((1 / YLIM) / 2)

  For YEXP = 1 To YLIM
    x(2) = x(2) + (1 / YLIM)
    x(1) = -((1 / ZLIM) / 2)

    For Z = 1 To ZLIM
      x(1) = x(1) + (1 / ZLIM)
      x(3) = 1 - (x(1) + x(2))

      If (x(1) + x(2)) > 1 Then
        GoTo NEXTSEARCH
      ElseIf x(3) = 0 Then
        GoTo NEXTSEARCH
      ElseIf (x(1) + x(2)) > (1 - (1 / ZLIM)) And x(3) < (1 / ZLIM)
        Then GoTo NEXTSEARCH
      End If
    Next Z
  Next YEXP

  'CALCULATION OF EXCESS GIBBS ENERGY USING MODIFIED UNIQUAC.
```

```

CX# = (1 / Sqr(2)) * Log(Sqr(2) - 1)
GEXCESS# = 0

For J = 1 To TNOC
  For K = 1 To TNOC
    IS12#(K) = (x(K) * R(K)) + IS12#(K - 1)
  Next K
  F12#(J) = Log(R(J) / IS12#(TNOC))
  F22#(J) = (x(J) * F12#(J)) + F22#(J - 1)
Next J

For J = 1 To TNOC
  For K = 1 To TNOC
    IS2A2#(K) = (x(K) * Q(K)) + IS2A2#(K - 1)
    IS2B2#(K) = (x(K) * R(K)) + IS2B2#(K - 1)
  Next K
  G1A2#(J) = Q(J) / R(J)
  G1B2#(J) = (IS2B2#(TNOC) / IS2A2#(TNOC))
  G12#(J) = Log(G1A2#(J) * G1B2#(J))
  G22#(J) = ((Q(J) * x(J)) * G12#(J)) + G22#(J - 1)
Next J

G32# = (ZPAC / 2) * G22#(TNOC)

For J = 1 To TNOC
  For K = 1 To TNOC
    For L = 1 To TNOC
      IS42#(L) = (x(L) * QD(L)) + IS42#(L - 1)
    Next L
    T#(K, J) = Exp(-AX#(K, J) / TEMP)
    IS32#(K) = ((x(K) * QD(K) * T#(K, J)) / IS42#(TNOC)) + IS32#(K - 1)
  Next K
  H12#(J) = (QD(J) * x(J) * (Log(IS32#(TNOC)))) + H12#(J - 1)
Next J

GEXCESS# = F22#(TNOC) + G32# - H12#(TNOC)

'CALCULATION OF THE EXCLUDED VOLUME PARAMETER (BM).
For J = 1 To TNOC
  For K = 1 To TNOC
    INTQSUM#(K) = (x(J) * x(K) * CSVC#(J, K)) + INTQSUM#(K - 1)
  Next K
  EXTQSUM#(J) = INTQSUM#(TNOC) + EXTQSUM#(J - 1)
Next J
QP# = EXTQSUM#(TNOC)

For J = 1 To TNOC
  DSUM#(J) = ((x(J) * PUREA#(J)) / (PUREB#(J) * UGC * TEMP)) + DSUM#(J - 1)
Next J

```

```

D# = DSUM#(TNOC) + (GEXCESS# / CX#)
B# = QP# / (1 - D#)

```

'CALCULATION OF THE ENERGY OF ATTRACTION PARAMETER (am).

```

AP# = (UGC * TEMP * B# * D#)
' MY ADDING FOR CALCULATION OF Z ROOT
AP1# = AP# * P / (UGC * TEMP) ^ 2
BP# = B# * P / (UGC * TEMP)

```

For J = 1 To 2 Step 1

```

VNEW# = INITIALV#(J)
VCOUNT = 0
Do
VCOUNT = VCOUNT + 1
VOLD# = VNEW#
PART1F1# = P * VOLD# ^ 3
PART2F1# = ((P * B#) - (UGC * TEMP)) * VOLD# ^ 2
PART3F1# = ((3 * P * (B# ^ 2)) + (2 * UGC * TEMP * B#) - AP#) * VOLD#
PART4F1# = ((P * (B# ^ 3)) + (UGC * TEMP * (B# ^ 2)) - (AP# * B#))
FUNCTION1# = PART1F1# + PART2F1# - PART3F1# + PART4F1#
PART1F2# = 3 * P * VOLD# ^ 2
PART2F2# = 2 * ((P * B#) - (UGC * TEMP)) * VOLD#
PART3F2# = ((3 * P * (B# ^ 2)) + (2 * UGC * TEMP * B#) - AP#)
FUNCTION2# = PART1F2# + PART2F2# - PART3F2#
VNEW# = VOLD# - (FUNCTION1# / FUNCTION2#)

If VCOUNT > 15 Then
GoTo VJUMP2
End If

```

Loop Until Abs(FUNCTION1#) < 1E-20

VJUMP2:

MIXTV#(J) = VOLD#

'COMPARASION OF THE VALUES OF Z ROOT USING BOTH METHODS

```

ZP# = (P * VOLD#) / (UGC * TEMP)
ZP1# = Z3ROOT(AP1#, BP#)

```

'CALCULATION OF DIMENSIONLESS MIXTURE GIBBS FREE ENERGY.

```

GPART1#(J) = (P * MIXTV#(J)) / (UGC * TEMP)
GPART2#(J) = Log(MIXTV#(J) / (MIXTV#(J) - B#))
GPART3A#(J) = (AP# / (2 * Sqr(2) * UGC * TEMP * B#))
GPART3B#(J) = (MIXTV#(J) + ((1 - Sqr(2)) * B#)) / (MIXTV#(J) + ((1 + Sqr(2)) * B#))
GPART3#(J) = GPART3A#(J) * Log(GPART3B#(J))

```

For K = 1 To TNOC

```

'GPART4#(J, K) = (x(K) * Log(100000! * (MIXTV#(J) / (x(K) * UGC * TEMP))))
+ GPART4#(J, K - 1)
GPART4#(J, K) = (x(K) * Log((MIXTV#(J) / (x(K) * UGC * TEMP)))) +
GPART4#(J, K - 1)
Next K
MIXTUREG(J) = GPART1#(J) + GPART2#(J) + GPART3#(J) - GPART4#(J, TNOC)
Next J

PUREGMIX = 0

For i = 1 To TNOC
    PUREGMIX = PUREGMIX + x(i) * PURECOMPG#(1, i)
Next i
LOWG = MIXTUREG(1) - PUREGMIX
GMIXING = LOWG

TPLIM = TPLIM + 1
GMIX(1, TPLIM) = x(1)
    GMIX(2, TPLIM) = x(2)
    GMIX(3, TPLIM) = GMIXING
    GMIXINGL(Z, YEXP) = GMIXING
Next Z
NEXTSEARCH:
Next YEXP
    'Sheet1.Cells(4, 7) = TPLIM
End Sub

```

D.2.2.3 Estimation of Angles and length of the Arms of the search from initial values

```

Public Sub INITALVAL()

    Dim M11, M21, M31, RANG1, RANG2, RANG3

    M11 = (Y11 - INITX(2)) / (X11 - INITX(1))
    RANG1 = Atn(M11)
    If M11 < 0 Then
        ANG1 = (57.2957732099 * RANG1)
    ElseIf M11 > 0 Then
        ANG1 = (57.2957732099 * RANG1) + 180
    End If
    Z1 = (Sqr(1 + M11 ^ 2) * Abs(X11 - INITX(1))) * 1000
    M21 = (Y21 - INITX(2)) / (X21 - INITX(1))
    RANG2 = Atn(M21)

    If M21 < 0 Then
        ANG2 = (57.2957732099 * RANG2) + 180
    ElseIf M21 > 0 Then
        ANG2 = (57.2957732099 * RANG2)
    End If

```

```

Z2 = (Sqr(1 + M21 ^ 2) * Abs(X21 - INITX(1))) * 1000
M31 = (Y31 - INITX(2)) / (X31 - INITX(1))
RANG3 = Atn(M31)
If M31 < 0 Then
    ANG3 = (57.2957732099 * RANG3) + 360
ElseIf M31 > 0 Then
    ANG3 = (57.2957732099 * RANG3)
End If
Z3 = (Sqr(1 + M31 ^ 2) * Abs(X31 - INITX(1))) * 1000

Sheet2.Cells(9, 11) = Z1: Sheet2.Cells(10, 11) = Z2
Sheet2.Cells(11, 11) = Z3: Sheet2.Cells(12, 11) = ANG1
Sheet2.Cells(13, 11) = ANG2: Sheet2.Cells(14, 11) = ANG3

End Sub

```

D.2.2.4 Calculation of the Area of intersection of the tangent plane with Gibbs energy surface

```

Public Function AREACALC(X9 As Variant) As Variant
    Dim F12#(10), F22#(10), H12#(10)
    Dim IS12#(10), IS2A2#(10), IS2B2#(10), IS32#(10), IS42#(10)
    Dim G1A2#(10), G1B2#(10), G12#(10), G22#(10)
    Dim T#(10, 10), TR#(10), K0#(10)
    Dim MIXIV#(10), ALPHA#(10), INTQSUM#(10), EXTQSUM#(10)
    Dim DSUM#(10), GPART1#(10), GPART2#(10), GPART3A#(10), GPRT3B#(10)
    Dim GPART3#(10)
    Dim GPART4#(10, 10), MIXTUREG(10), x(10), RADANGLE#(3), GVAL(3)

    Dim OPPOSITE, ADJACENT
    Dim XLP, XHP, XMP, YLP, YHP, YMP
    Dim X1LIM1, X1LIM2
    Dim G32#, QP#, AP#, B#, D#

    Dim VNEW#, VCOUNT, VOLD#
    Dim PART1F1#, PART2F1#, PART3F1#, PART4F1#
    Dim FUNCTION1#, FUNCTION2#, PART1F2#, PART2F2#, PART3F2#
    Dim PUREGMIX, LOWMIXG, LOWG, GMIXING
    Dim GCOUNT, i, J, K, L
    Dim GEXCESS#, MIXTV#(10), GPART3B#(10)
    Dim NUM, DENOM1, SLOPE1, SLOPE2, Intercept
    Dim TPAREA#, GFLAG, LFLAG, XTRAREA#
    Dim counter, TPVALUE
    Dim M11, M21, M31
    Dim RANG1, RANG2, RANG3
    'Dim X1, Y1, X2, Y2, X3, Y3
    Dim MIN1FLAG, X10, X20
    Dim AAAA, GMIXINGLA, GMIXINGVA, ENDCOUNT

```


Dim SLOPE22, Intercept1, Intercept2, Intercept3, OB

'DETERMINATION OF THE CORNERS OF THE 3-PHASE REGION FROM ALL THE INDEPENDENT VARIABLES.

A#(1) = X9(1, 1):A#(2) = X9(2, 1): A#(3) = X9(3, 1)
ANG1 = X9(4, 1):ANG2 = X9(5, 1): ANG3 = X9(6, 1)

If ANG1 > ANG2 And ANG3 > ANG1 And ANG1 > 180 And ANG1 < 360 And ANG2 > 0
And ANG2 < 180 _
And ANG3 > 0 And ANG3 < 330 And A#(1) > 0 And A#(1) < 560 And A#(2) > 0
And _
A#(2) < 400 And A#(3) > 0 And A#(3) < 200 Then

RADANGLE#(1) = 0.01745329444 * ANG1
RADANGLE#(2) = 0.01745329444 * ANG2
RADANGLE#(3) = 0.01745329444 * ANG3

If ANG1 = 0 Or ANG1 = 360 Then
x1 = INITX(1) + (A#(1) / 1000)
Y1 = INITX(2)
ElseIf ANG1 = 90 Then
x1 = INITX(1)
Y1 = INITX(2) + (A#(1) / 1000)
ElseIf ANG1 = 180 Then
x1 = INITX(1) - (A#(1) / 1000)
Y1 = INITX(2)
ElseIf ANG1 = 270 Then
x1 = INITX(1)
Y1 = INITX(2) - (A#(1) / 1000)

Else
OPPOSITE = (A#(1) / 1000) * Sin(RADANGLE#(1))
ADJACENT = (A#(1) / 1000) * Cos(RADANGLE#(1))
x1 = INITX(1) + ADJACENT
Y1 = INITX(2) + OPPOSITE

End If

If ANG2 = 0 Or ANG2 = 360 Then
X2 = INITX(1) + (A#(2) / 1000)
Y2 = INITX(2)
ElseIf ANG2 = 90 Then
X2 = INITX(1)
Y2 = INITX(2) + (A#(2) / 1000)
ElseIf ANG2 = 180 Then
X2 = INITX(1) - (A#(2) / 1000)
Y2 = INITX(2)
ElseIf ANG2 = 270 Then
X2 = INITX(1)
Y2 = INITX(2) - (A#(2) / 1000)

```

Else
  OPPOSITE = (A#(2) / 1000) * Sin(RADANGLE#(2))
  ADJACENT = (A#(2) / 1000) * Cos(RADANGLE#(2))
  X2 = INITX(1) - ADJACENT
  Y2 = INITX(2) - OPPOSITE
End If

```

```

If ANG3 = 0 Or ANG3 = 360 Then
  X3 = INITX(1) + (A#(3) / 1000)
  Y3 = INITX(2)
ElseIf ANG3 = 90 Then
  X3 = INITX(1)
  Y3 = INITX(2) + (A#(3) / 1000)
ElseIf ANG3 = 180 Then
  X3 = INITX(1) - (A#(3) / 1000)
  Y3 = INITX(2)
ElseIf ANG3 = 270 Then
  X3 = INITX(1)
  Y3 = INITX(2) - (A#(3) / 1000)
Else
  OPPOSITE = (A#(3) / 1000) * Sin(RADANGLE#(3))
  ADJACENT = (A#(3) / 1000) * Cos(RADANGLE#(3))
  X3 = INITX(1) - ADJACENT
  Y3 = INITX(2) - OPPOSITE
End If

```

```

If x1 > 0 And Y1 > 0 And (x1 + Y1) < 0.9999 And X2 > 0 And Y2 > 0 And
(X2 + Y2) < 0.9999 And X3 > 0 And Y3 > 0 And (X3 + Y3) < 0.9999 Then

```

```

' If ANG1 > 0 And ANG1 < 360 And ANG2 > 0 And ANG2 < 360 And ANG3 >
0 And ANG3 < 360 Then

```

```

'DETERMINATION OF THE LOWEST, MID AND HIGHEST X COMPOSITIONS
OFFHE 'CURRENTIHREE PHASE TRIANGLE.

```

```

XLP = x1:XMP = x1:XHP = x1
YLP = Y1: YMP = Y1:YHP = Y1

```

```

If X2 < XLP Then
  XLP = X2:YLP = Y2: XMP = X2: YMP = Y2
End If

```

```

If X2 >= XHP Then
  XHP = X2
  YHP = Y2
End If

```

```

If X3 < XLP Then

```

```

XLP = X3
YLP = Y3

ElseIf X3 >= XHP Then
    XMP = XHP:YMP = YHP: XHP = X3:YHP = Y3
Else
    XMP = X3:YMP = Y3
End If

'CALCULATION OF THE (MIXING VALUES Pa VERTICES OF' 3-PHASE
'TRIANGLE AND
'SUBSEQUENT DETERMINATION OF TANGENT PLANE SLOPES AND
INTERCEPT.

For GCOUNT = 1 To 3
    If GCOUNT = 1 Then x(1) = XLP: x(2) = YLP
    If GCOUNT = 2 Then x(1) = XMP: x(2) = YMP
    If GCOUNT = 3 Then x(1) = XHP: x(2) = YHP

    x(3) = 1 - (x(1) + x(2))

    'CALCULATION OF EXCESS GIBBS ENERGY USING MODIFIED
UNIQUAC.

    X10 = x(1)
    X20 = x(2)

    If GCOUNT = 2 Then
        Call PHICALCVA(X10, X20, GMIXING)
        GVAL(GCOUNT) = GMIXING
    Else
        Call PHICALCA(X10, X20, GMIXING)

        GVAL(GCOUNT) = GMIXING
    End If

Next GCOUNT

NUM = ((GVAL(1) - GVAL(3)) * (YMP - YHP)) - ((GVAL(2) - GVAL(3)) *
(YLP - YHP))
DENOM1 = ((XLP - XHP) * (YMP - YHP)) + ((XHP - XMP) * (YLP - YHP))
SLOPE1 = NUM / DENOM1
SLOPE2 = ((GVAL(2) - GVAL(3)) + (SLOPE1 * (XHP - XMP))) / (YMP - YHP)
Intercept = GVAL(3) - (SLOPE1 * XHP) - (SLOPE2 * YHP)

'DETERMINATION OF TOTAL TANGENT PLANE AREA WHEN TP > PHI.
'IE. SOLUTION AT MIN TP AREA ENCLOSED BY CURVE OR CURVES.

TPAREA# = 0
TPCOUNT1 = 0

```

```

        TPCOUNT2 = TPCOUNT2 + 1
        GFLAG = 0
        LFLAG = 0
        XTRAREA# = ((1 / YLIM) * (1 / ZLIM)) * (Sqr(1 + SLOPE1 ^ 2) *
Sqr(1 + SLOPE2 ^ 2))

        'TPLIM = Sheet1.Cells(4, 7).Value

        For counter = 1 To TPLIM
            TPCOUNT1 = TPCOUNT1 + 1
            TPVALUE = (SLOPE1 * GMIX(1, counter)) + (SLOPE2 * GMIX(2,
counter)) + Intercept
            If TPVALUE > GMIX(3, counter) Then
                TPAREA# = TPAREA# + XTRAREA#
            End If
        Next counter

        AREACALC = TPAREA#

        Sheet3.Cells(TPCOUNT2 + 11, 1) = TPCOUNT2
        Sheet3.Cells(TPCOUNT2 + 11, 2) = AREACALC

        OFVALUE# = TPAREA#
        AREACALC = TPAREA#

        'OB = Abs(X1 - X1E) + Abs(Y1 - Y1E) + Abs(X2 - X2E) + Abs(Y2 - Y2E) +
Abs(X3 - X3E) + Abs(Y3 - Y3E)
        ' AREACALC = TPAREA# + OB
        Else
            AREACALC = 10000

        End If
        Else
            AREACALC = 10000
        End If
    End Function

```

D.2.2.5 Writing the results to the spread Sheet and storing them

```
Public Sub WRITING()  
Dim GMIXINGF, YEXP, Z, GMIXINFL  
  
Sheets("Sheet5").Range("I4:JC500").ClearContents  
TPLIM = 0  
MINAREA# = ((1 / ZLIM) * (1 / YLIM) * 3)  
x(2) = -((1 / YLIM) / 2)  
For YEXP = 1 To YLIM  
  
x(2) = x(2) + (1 / YLIM)  
x(1) = -((1 / ZLIM) / 2)  
  
For Z = 1 To ZLIM  
x(1) = x(1) + (1 / ZLIM)  
x(3) = 1 - (x(1) + x(2))  
  
If (x(1) + x(2)) > 1 Then  
GoTo NEXTSEARCH  
ElseIf x(3) = 0 Then  
GoTo NEXTSEARCH  
ElseIf (x(1) + x(2)) > (1 - (1 / ZLIM)) And x(3) < (1 /  
ZLIM) Then  
GoTo NEXTSEARCH  
End If  
  
Sheet5.Cells(4 + Z, 9) = x(1)  
  
If GMIXINGV(Z, YEXP) > GMIXINGL(Z, YEXP) Then  
GMIXINGF = GMIXINGL(Z, YEXP)  
Else  
GMIXINGF = GMIXINGV(Z, YEXP)  
End If  
  
Sheet5.Cells(4, 9 + YEXP) = x(2)  
Sheet5.Cells(4 + Z, 9 + YEXP) = GMIXINGF  
  
TPLIM = TPLIM + 1  
GMIX(1, TPLIM) = x(1)  
GMIX(2, TPLIM) = x(2)  
GMIX(3, TPLIM) = GMIXINGF  
Sheet1.Cells(3 + TPLIM, 3) = x(1)  
Sheet1.Cells(3 + TPLIM, 4) = x(2)  
Sheet1.Cells(3 + TPLIM, 5) = GMIXINGF  
  
Next Z  
NEXTSEARCH:  
Next YEXP  
End Sub
```

D.2.3 VLE Tangent Plane Distance Function TPDF

D.2.3.1 TPDF Main program

```
Private Sub CommandButton3_Click()
    Dim i, result, MINVAL, GLOOP, start, finish

    TPCOUNT3 = -1: TPCOUNT4 = -1: TPCOUNT5 = -1

    Sheets("Sheet3").Range("B10:L1000").ClearContents

    start = Timer

    'TEST FOR ORGANIC PHASE
    ReDim initParams(1 To 2, 1 To 1)
        initParams(1, 1) = Sheet2.Cells(9, 13)
        initParams(2, 1) = Sheet2.Cells(10, 13)

        Dim nelderObj As New Nelder
        result = nelderObj.SolveMaximum("TESTORG", initParams)

        For i = 1 To 2
            Sheet2.Cells(8 + i, 14) = result(i, 1)
        Next i
    ' TEST FOR AQUEOUS PHASE

    ReDim initParams(1 To 2, 1 To 1)
        initParams(1, 1) = Sheet2.Cells(11, 13)
        initParams(2, 1) = Sheet2.Cells(12, 13)

        ' Dim nelderObj As New Nelder
        result = nelderObj.SolveMaximum("TESTAQ", initParams)

        For i = 1 To 2
            Sheet2.Cells(10 + i, 14) = result(i, 1)
        Next i
    ' TEST FOR VAPOUR PHASE

    ReDim initParams(1 To 2, 1 To 1)
        initParams(1, 1) = Sheet2.Cells(13, 13)
        initParams(2, 1) = Sheet2.Cells(14, 13)

        'Dim nelderObj As New Nelder
        result = nelderObj.SolveMaximum("TESTVAP", initParams)

        For i = 1 To 2
            Sheet2.Cells(12 + i, 14) = result(i, 1)
        Next i
    finish = Timer
    Sheet2.Cells(9, 15) = (finish - start)

End Sub
```

D.2.3.2 Search in Organic Phase

```
Public Function TESTORG(X8 As Variant) As Variant
Dim i, result, MINVAL, GLOOP, start, finish
  Dim PHIZ, PHIX, HZ(10), HX(10), HZX(10), HZXO(10), HZXA(10), X30, X10,
X20
  Dim GMIXING, J, kT(10), XXORG(10), SUMXXORG(10), SUMkT(10), STPD(10),
XXAQ(10)
  Dim SUMXXAQ(10), SUMYYVAP(10), YYVAP(10), HZXV(10)

  XORG(1, 1) = X8(1, 1): XORG(1, 2) = X8(2, 1): _
  XORG(1, 3) = 1 - 1.00001 * (XORG(1, 1) + XORG(1, 2))

  If X8(1, 1) > 0 And X8(2, 1) > 0 And (X8(1, 1) + X8(2, 1)) < 1 Then

    Call INPUTDATA

    XZ(1, 1) = INITX(1): XZ(1, 2) = INITX(2):
    XZ(1, 3) = 1 - (XZ(1, 1) + XZ(1, 2))
    Call PHIXZ

    HZ(1) = Log(XZ(1, 1)) + Log(FZCOF(1))
    HZ(2) = Log(XZ(1, 2)) + Log(FZCOF(2))
    HZ(3) = Log(XZ(1, 3)) + Log(FZCOF(3))

    ' ORGANIC PHASE TPD FUNCTION TEST

    Call PHIXORG
    HX(1) = Log(XORG(1, 1)) + Log(FORGCOF(1))
    HX(2) = Log(XORG(1, 2)) + Log(FORGCOF(2))
    HX(3) = Log(XORG(1, 3)) + Log(FORGCOF(3))

    ' NEW ADDING Yi AND SUM OF Yi
    For J = 1 To TNOC
      kT(J) = HX(J) - HZ(J)
      kT(J) = kT(J) / (UGC * TEMP)
      SUMkT(J) = kT(J) + SUMkT(J - 1)
    Next J

    For J = 1 To TNOC
      XXORG(J) = Exp(-kT(J)) * XORG(1, J)
      SUMXXORG(J) = XXORG(J) + SUMXXORG(J - 1)
    Next J

    For J = 1 To TNOC
      XORG(1, J) = XXORG(J) / SUMXXORG(TNOC)
    Next J

    For J = 1 To TNOC
      HZXO(J) = XORG(1, J) * (HX(J) - HZ(J))
```

```

Next J

For J = 1 To TNOC
HZXO(J) = XORG(1, J) * (HX(J) - HZ(J)) + HZXO(J - 1)
Next J

TESTORG = HZXO(TNOC)

TPCOUNT3 = 1 + TPCOUNT3
Sheet3.Cells(10 + TPCOUNT3, 1) = TPCOUNT3
Sheet3.Cells(10 + TPCOUNT3, 3) = TESTORG
Sheet3.Cells(10 + TPCOUNT3, 7) = XORG(1, 1)
Sheet3.Cells(10 + TPCOUNT3, 8) = XORG(1, 2)

Else
TESTORG = 100

End If

Sheet2.Cells(18, 10) = TESTORG
Sheet2.Cells(19, 10) = SUMXXORG(TNOC)
End Function

```

D.2.3.3 Sub program calculation of organic phase fugacity coefficients

```

Public Sub PHIXORG()

Dim PHIBASE#(10), THETABASE#(10), MODTHETABASE#(10), PHI#(10), THETA#(10)
Dim MODTHETA#(10), LI#(10), PART3SUM#(10), PART4SUM#(10)
Dim PART5TOP#(10), PART5BASE#(10), PART5TOT#(10), T#(10, 10)
Dim LNVAPGAMMAP#(10), LNORGGAMMAP#(10), LNAQGAMMAP#(10), VAPFUGCOEFF#(10)
Dim LNAQFUGACITYCOEFFICIENT#(10), LNORGFUGACITYCOEFFICIENT#(10),
LNVAPFUGACITYCOEFFICIENT#(10)
Dim ORGFUGCOEFF#(10), ORGFUGACITYP#(10), AQFUGCOEFF#(10), AQFUGACITYP#(10)
Dim FF1#(10), KI#(10, 10), INTQSUM#(10), EXTQSUM#(10), DSUM#(10)
Dim F12#(50), F22#(50), H12#(50), FF3#(10)
Dim IS12#(50), IS2A2#(50), IS2B2#(50), IS32#(50), IS42#(50)
Dim G1A2#(50), G1B2#(50), G12#(50), G22#(50), VAPFUGACITYP#(10)
Dim CSVC#(10, 10), PUREA#(10, 10), PUREB#(10, 10), PART2C1#(10),
PART2BSUM#(10)
Dim TR#(10), KA0#(10), KA#(10), ALPHA#(10), FF4#(10)

Dim G32#, GEXCESS#, QORG#, DORG#, BORG#, AORG#
Dim QAQ#, DAQ#, BAQ#, AAQ#, VAQ#, PAQ#, ZAQ#
Dim VNEW#, VOLD#, VORG#, ZORG#, PORG#
Dim QVAP#, AVAP#, BVAP#, DVAP#, VVAP#, ZVAP#, PVAP#
Dim PART1F1#, PART2F1#, PART3F1#, PART4F1#
Dim PART1F2#, PART2F2#, PART3F2#, FUNCTION1#, FUNCTION2#
Dim J, K, i, L, COMPONENT, XTRACOMP

```



```

Dim PART1#, PART2#, PART3#, PART4#, PART5#
Dim TERM1#, TERM2#, TERM3#, PART3A#, PART3B#, PART3C#
Dim PART2A#, PART2B#, PART2C#, PRESS#, PRESS1#, PRESS2#
Dim OFVALUE#(100), FF11(20), SUMXORGCAL(20, 10), SUMXAQCAL(20, 10)
Dim SUMYORGCAL(20, 10), SUMYAQCAL(20, 10), FF2(20)
Dim AVAP1#, BVAP1#, TEMPS(10), C#, RA(10), Z

```

```
Call INPUTDATA
```

```
Z = 10
```

```
For i = 1 To 1
```

```

TEMPS(i) = TEMP
For J = 1 To TNOC
RA(J) = R(J)
Next J

```

```
'PHYSICAL CONSTANTS AND FIXED PARAMETERS.
```

```

For J = 1 To TNOC
TR#(J) = TEMPS(i) / TC(J)
KA0#(J) = 0.378893 + 1.4897153 * W(J) - 0.17131848 * W(J) ^ 2 +
0.0196554 * W(J) ^ 3
KA#(J) = KA0#(J) + k1(J) * (1 + (TR#(J) ^ 0.5)) * (0.7 - TR#(J))
ALPHA#(J) = (1 + KA#(J) * (1 - (TR#(J) ^ 0.5))) ^ 2
PUREA#(J, J) = ((0.457235 * UGC ^ 2 * TC(J) ^ 2) / PC(J)) *
ALPHA#(J)
PUREB#(J, J) = (0.077796 * UGC * TC(J)) / PC(J)
Next J

```

```

AX(1, 2) = Sheet2.Cells(9, 5): AX(2, 1) = Sheet2.Cells(10, 5)
AX(2, 3) = Sheet2.Cells(11, 5): AX(3, 2) = Sheet2.Cells(12, 5)
AX(3, 1) = Sheet2.Cells(13, 5): AX(1, 3) = Sheet2.Cells(14, 5)

```

```

C# = (1 / Sqr(2)) * Log(Sqr(2) - 1)
T#(1, 1) = 1: T#(2, 2) = 1: T#(3, 3) = 1

```

```

T#(1, 2) = Exp(-AX(1, 2) / TEMPS(i)): T#(2, 1) = Exp(-AX(2, 1) /
TEMPS(i))
T#(2, 3) = Exp(-AX(2, 3) / TEMPS(i)): T#(3, 2) = Exp(-AX(3, 2) /
TEMPS(i))
T#(3, 1) = Exp(-AX(3, 1) / TEMPS(i)): T#(1, 3) = Exp(-AX(1, 3) /
TEMPS(i))

```

```
KI#(1, 1) = 0: KI#(2, 2) = 0: KI#(3, 3) = 0
```

```
KI#(1, 2) = Sheet2.Cells(15, 5).Value
```

```

KI#(2, 3) = Sheet2.Cells(16, 5).Value
KI#(1, 3) = Sheet2.Cells(17, 5).Value

KI#(2, 1) = KI#(1, 2): KI#(3, 2) = KI#(2, 3): KI#(3, 1) = KI#(1, 3)

```

'SOLUTION OF THE PRSV EQUATION OF STATE TO FIND THE CORRECT LIQUID
'AND VAPOUR PHASE MOLAR VOLUME ROOTS (USING NEWTON-RAPHSON).

'1. ORGANIC PHASE.

' CALCULATION OF' EXCESS GIBBS ENERGY USING MODIFIED UNIQUAC.

```

For J = 1 To TNOC
  For K = 1 To TNOC
    IS12#(K) = (XORG(i, K) * RA(K)) + IS12#(K - 1)
  Next K
  F12#(J) = Log(RA(J) / IS12#(TNOC))
  F22#(J) = (XORG(i, J) * F12#(J)) + F22#(J - 1)
Next J

```

' PART 2.

```

For J = 1 To TNOC
  If (J - 1) = 0 Then
    G22#(J - 1) = 0
  End If
  For K = 1 To TNOC
    If (K - 1) = 0 Then
      IS2A2#(K - 1) = 0
      IS2B2#(K - 1) = 0
    End If

    IS2A2#(K) = XORG(i, K) * Q(K)
    IS2B2#(K) = XORG(i, K) * RA(K)
    IS2A2#(K) = IS2A2#(K) + IS2A2#(K - 1)
    IS2B2#(K) = IS2B2#(K) + IS2B2#(K - 1)
  Next K
  G1A2#(J) = Q(J) / RA(J)
  G1B2#(J) = (IS2B2#(TNOC) / IS2A2#(TNOC))
  G12#(J) = Log(G1A2#(J) * G1B2#(J))
  G22#(J) = ((Q(J) * XORG(i, J)) * G12#(J))

  G22#(J) = G22#(J) + G22#(J - 1)
Next J

G32# = (Z / 2) * G22#(TNOC)

```

' PART 3.

```
For J = 1 To TNOC
  If (J - 1) = 0 Then
    H12#(J - 1) = 0
  End If
  For K = 1 To TNOC
    If (K - 1) = 0 Then
      IS32#(K - 1) = 0
    End If
    For L = 1 To TNOC
      If (L - 1) = 0 Then
        IS42#(L - 1) = 0
      End If

      IS42#(L) = XORG(i, L) * QD(L)
      IS42#(L) = IS42#(L) + IS42#(L - 1)
    Next L
    IS32#(K) = (XORG(i, K) * QD(K) * T#(K, J)) / IS42#(TNOC)
    IS32#(K) = IS32#(K) + IS32#(K - 1)
  Next K
  H12#(J) = QD(J) * XORG(i, J) * (Log(IS32#(TNOC)))
  H12#(J) = H12#(J) + H12#(J - 1)
Next J
GEXCESS# = F22#(TNOC) + G32# - H12#(TNOC)
```

'CALCULATION OF THE EXCLUDED VOLUME PARAMETER (bm).

```
For J = 1 To TNOC
  For K = 1 To TNOC
    CSVC#(J, K) = (((PUREB#(J, J) - (PUREA#(J, J) / (UGC *
TEMPS(i)))) + _
    (PUREB#(K, K) - (PUREA#(K, K) / (UGC * TEMPS(i)))))) / 2) * (1
- (KI#(J, K) / 1))
    'CSVC#(J, K) = (((PUREB#(J, J) - (PUREA#(J, J) / (UGC *
TEMPS(I)))) + (PUREB#(K, K) - (PUREA#(K, K) / (UGC * TEMPS(I)))))) / 2) *
(1 - (KI#(J, K) / 1))
  Next K
Next J
```

```
For J = 1 To TNOC
  For K = 1 To TNOC
    INTQSUM#(K) = (XORG(i, J) * XORG(i, K) * CSVC#(J, K)) +
INTQSUM#(K - 1)
  Next K
  EXTQSUM#(J) = INTQSUM#(TNOC) + EXTQSUM#(J - 1)
Next J
```

```
QORG# = EXTQSUM#(TNOC)
For J = 1 To TNOC
```

```

        DSUM#(J) = ((XORG(i, J) * PUREA#(J, J)) / (PUREB#(J, J) * UGC *
TEMPS(i))) + DSUM#(J - 1)
    Next J
    DORG# = DSUM#(TNOC) + (GEXCESS# / C#)
    BORG# = QORG# / (1 - DORG#)

'CALCULATION OF' THE ENERGY OF ATTRACTION PARAMETER (am).

AORG# = UGC * TEMPS(i) * BORG# * DORG#
VNEW# = 0.00005
Do
VOLD# = VNEW#
PART1F1# = P * (VOLD# ^ 3)
PART2F1# = ((P * BORG#) - (UGC * TEMPS(i))) * (VOLD# ^ 2)
PART3F1# = ((3 * P * (BORG# ^ 2)) + (2 * UGC * TEMPS(i) * BORG#) -
AORG#) * VOLD#
PART4F1# = ((P * (BORG# ^ 3)) + (UGC * TEMPS(i) * (BORG# ^ 2)) -
(AORG# * BORG#))
FUNCTION1# = PART1F1# + PART2F1# - PART3F1# + PART4F1#
PART1F2# = 3 * P * (VOLD# ^ 2)
PART2F2# = 2 * ((P * BORG#) - (UGC * TEMPS(i))) * VOLD#
PART3F2# = ((3 * P * (BORG# ^ 2)) + (2 * UGC * TEMPS(i) * BORG#) -
AORG#)
FUNCTION2# = PART1F2# + PART2F2# - PART3F2#
VNEW# = VOLD# - (FUNCTION1# / FUNCTION2#)
Loop Until Abs(FUNCTION1#) < 0.00001
VORG# = VOLD#
ZORG# = (P * VORG#) / (UGC * TEMPS(i))
PORG = ((UGC * TEMPS(i)) / (VORG# - BORG#)) - (AORG# / (VORG# ^ 2 + (2
* BORG# * VORG#) - BORG# ^ 2))

' DETERMINATION OF THE FUGACITY COEFFICIENTS OF EACH COMPONENT IN EACH
PHASE.

'1. ORGANIC PHASE.
'CALCULATION OF THE LIQUID PHASE ACTIVITY COEFFICIENTS AFTHIS P & T.
' THE UNIQUAC EXPANSION (CALCULATION OF ACTIVITY COEFFICIENTS FOR EACH
' COMPONENT IN THE LIQUID PHASE).

For COMPONENT = 1 To TNOC
    PHIBASE#(COMPONENT) = RA(COMPONENT) * XORG(i, COMPONENT) +
PHIBASE#(COMPONENT - 1)
    THETABASE#(COMPONENT) = Q(COMPONENT) * XORG(i, COMPONENT) +
THETABASE#(COMPONENT - 1)
    MODTHETABASE#(COMPONENT) = QD(COMPONENT) * XORG(i, COMPONENT) +
MODTHETABASE#(COMPONENT - 1)
Next COMPONENT

```

```

For COMPONENT = 1 To TNOC
    PHI#(COMPONENT) = (RA(COMPONENT) * XORG(i, COMPONENT)) /
PHIBASE#(TNOC)
    THETA#(COMPONENT) = (Q(COMPONENT) * XORG(i, COMPONENT)) /
THETABASE#(TNOC)
    MODTHETA#(COMPONENT) = (QD(COMPONENT) * XORG(i, COMPONENT)) /
MODTHETABASE(TNOC)
Next COMPONENT

For COMPONENT = 1 To TNOC
    LI#(COMPONENT) = (Z / 2) * (RA(COMPONENT) - Q(COMPONENT)) -
(RA(COMPONENT) - 1)
Next COMPONENT

For COMPONENT = 1 To TNOC
    PART1# = Log(PHI#(COMPONENT) / XORG(i, COMPONENT))
    PART2# = (Z / 2) * Q(COMPONENT) * Log(THETA#(COMPONENT) /
PHI#(COMPONENT))

    For J = 1 To TNOC
        PART3SUM#(J) = XORG(i, J) * LI#(J) + PART3SUM#(J - 1)
        PART4SUM#(J) = MODTHETA#(J) * T#(J, COMPONENT) +
PART4SUM#(J - 1)
    Next J
    PART3# = (PHI#(COMPONENT) / XORG(i, COMPONENT)) *
PART3SUM#(TNOC)
    PART4# = QD(COMPONENT) * Log(PART4SUM#(TNOC))
    For J = 1 To TNOC
        PART5TOP#(J) = MODTHETA#(J) * T#(COMPONENT, J)
        For K = 1 To TNOC
            PART5BASE#(K) = MODTHETA#(K) * T#(K, J) +
PART5BASE#(K - 1)
        Next K
        PART5TOT#(J) = (PART5TOP#(J) / PART5BASE#(TNOC)) +
PART5TOT#(J - 1)
    Next J

    PART5# = QD(COMPONENT) * PART5TOT#(TNOC)
    LNORGGAMMAP#(COMPONENT) = PART1# + PART2# + LI#(COMPONENT) -
PART3# - PART4# + QD(COMPONENT) - PART5#
Next COMPONENT

For XTRACOMP = 1 To TNOC
    TERM1# = -Log((P * (VORG# - BORG#)) / (UGC * TEMPS(i)))
    For J = 1 To TNOC
        PART2BSUM#(J) = (XORG(i, J) * CSV#(XTRACOMP, J)) +
PART2BSUM#(J - 1)
    Next J
    PART2B# = (1 / (1 - DORG#)) * (2 * PART2BSUM#(TNOC))

```

```

PART2C1#(XTRACOMP) = ((PUREA#(XTRACOMP, XTRACOMP) /
(PUREB#(XTRACOMP, XTRACOMP) * UGC * TEMPS(i))) + (LNORGGAMMAP#(XTRACOMP) /
C#))
PART2C# = (QORG# / ((1 - DORG#) ^ 2)) * (1 -
PART2C1#(XTRACOMP))
PART2A# = PART2B# - PART2C#
TERM2# = (1 / BORG#) * PART2A# * (((P * VORG#) / (UGC *
TEMPS(i))) - 1)

PART3A# = (1 / (2 * Sqr(2))) * (AORG# / (BORG# * UGC *
TEMPS(i)))
PART3B# = (((UGC * TEMPS(i) * DORG#) / AORG#) - (1 / BORG#))
* PART2A# + ((UGC * TEMPS(i) * BORG#) / AORG#) * PART2C1(XTRACOMP))
PART3C# = Log((VORG# + BORG# * (1 - Sqr(2))) / (VORG# + BORG#
* (1 + Sqr(2))))
TERM3# = PART3A# * PART3B# * PART3C#
LNORGFUGACITYCOEFFICIENT#(XTRACOMP) = TERM1# + TERM2# + TERM3#
ORGFUGCOEFF#(XTRACOMP) =
Exp(LNORGFUGACITYCOEFFICIENT#(XTRACOMP))
FORGCOF(XTRACOMP) = ORGFUGCOEFF#(XTRACOMP)
Next XTRACOMP

```

```

Next i

```

```

End Sub

```

D.2.4 Initial generator

D.2.4.1 Main program

```
Private Sub InitialGenerator_Click()

Dim PHIBASE#(10), THETABASE#(10), MODTHETABASE#(10), PHI#(10), THETA#(10)
Dim MODTHETA#(10), LI#(10), PART3SUM#(10), PART4SUM#(10)
Dim PART5TOP#(10), PART5BASE#(10), PART5TOT#(10), T#(10, 10)
Dim LNVAPGAMMAP#(10), LNORGGAMMAP#(10), LNAQGAMMAP#(10), VAPFUGCOEFF#(10)
Dim LNAQFUGACITYCOEFFICIENT#(10), LNORGFUGACITYCOEFFICIENT#(10),
LNVAPFUGACITYCOEFFICIENT#(10)
Dim ORGFUGCOEFF#(10), ORGFUGACITYP#(10), AQFUGCOEFF#(10), AQFUGACITYP#(10)
Dim FF1#(10), INTQSUM#(10), EXTQSUM#(10), DSUM#(10)
Dim F12#(50), F22#(50), H12#(50), FF3#(10)
Dim IS12#(50), IS2A2#(50), IS2B2#(50), IS32#(50), IS42#(50)
Dim G1A2#(50), G1B2#(50), G12#(50), G22#(50), VAPFUGACITYP#(10)
Dim CSVC#(10, 10), PUREA#(10, 10), PUREB#(10, 10), PART2C1#(10),
PART2BSUM#(10)
Dim TR#(10), KA0#(10), KA#(10), ALPHA#(10), FF4#(10), C#
Dim PART1#, PART2#, PART3#, PART4#, PART5#, AQGAMMAP(10), ORGGAMMAP(10),
ORGACTIVITYP(10)

Dim i, PSTD(10), TOTP, COMPONENT, J, K, SMYCAL(10), SMXORG(10), result
Dim KORGD(10), KAQD(10), SMXAQ(10), start, finish

start = Timer

Sheets("Sheet4").Range("A2:B8000").ClearContents
Sheets("Sheet4").Range("T3:AH1000").ClearContents

TPCOUNT7 = 0: TPCOUNT6 = 0

Call INPUTDATA: Call UNIQUAC1: Call PRSVPHI

For J = 1 To TNOC
KORG(J) = KORGN(J)
KAQ(J) = KAQN(J)
Next J

step1:

ReDim initParams(1 To 2, 1 To 1)
For J = 1 To 2
initParams(J, 1) = Sheet3.Cells(2 + J, 10).Value
Next J
Dim nelderObj As New Nelder
result = nelderObj.SolveMaximum("ABTA", initParams)
For J = 1 To 2
Sheet3.Cells(2 + J, 12) = result(J, 1)
Next J
```

```

ALF(1) = result(1, 1): BTA(1) = result(2, 1)

Call PRSVPHI

For J = 1 To TNOC
KAQD(J) = Abs(KAQ(J) - KAQN(J)) + KAQD(J - 1)
KORGD(J) = Abs(KORG(J) - KORGN(J)) + KORGD(J - 1)
Next J
If KAQD(1) > 0.0001 And KORGD(1) > 0.001 And KAQD(2) > 0.0001 And KORGD(2)
> _
    0.0001 And KAQD(3) > 0.0001 And KORGD(3) > 0.0001 Then

TPCOUNT7 = 1 + TPCOUNT7

Sheet4.Cells(2 + TPCOUNT7, 20) = KAQD(1): Sheet4.Cells(2 + TPCOUNT7, 24) =
KORGD(1)
Sheet4.Cells(2 + TPCOUNT7, 21) = KAQD(2): Sheet4.Cells(2 + TPCOUNT7, 25) =
KORGD(2)
Sheet4.Cells(2 + TPCOUNT7, 22) = KAQD(3): Sheet4.Cells(2 + TPCOUNT7, 26) =
KORGD(3)
Sheet4.Cells(2 + TPCOUNT7, 28) = KAQN(1): Sheet4.Cells(2 + TPCOUNT7, 32) =
KORGN(1)
Sheet4.Cells(2 + TPCOUNT7, 29) = KAQN(2): Sheet4.Cells(2 + TPCOUNT7, 33) =
KORGN(2)
Sheet4.Cells(2 + TPCOUNT7, 30) = KAQN(3): Sheet4.Cells(2 + TPCOUNT7, 34) =
KORGN(3)

For J = 1 To TNOC
KAQ(J) = KAQN(J)
KORG(J) = KORGN(J)
Next J
GoTo step1
Else
GoTo STEP2

End If
STEP2:
For J = 1 To TNOC
Sheet3.Cells(3 + J, 3) = KAQ(J): Sheet3.Cells(3 + J, 5) = KORG(J)
Sheet3.Cells(7 + J, 15) = XORG(1, J): Sheet3.Cells(7 + J, 16) = XAQ(1, J)
Sheet3.Cells(7 + J, 17) = YCAL(1, J)
Next J

Sheet2.Cells(9, 10) = XORG(1, 1): Sheet2.Cells(10, 10) = XORG(1, 2)
Sheet2.Cells(11, 10) = XAQ(1, 1): Sheet2.Cells(12, 10) = XAQ(1, 2)
Sheet2.Cells(13, 10) = YCAL(1, 1): Sheet2.Cells(14, 10) = YCAL(1, 2)

    finish = Timer
        Sheet2.Cells(9, 15) = (finish - start)
End Sub

```


D.2.4.2 The organic and aqueous ratio

Public Function ABTA(x1 As Variant) As Variant

```
Dim J, i, PARTBB(10, 10): ZF(10, 10), XORGAL(10, 10), XAQCAL(10, 10)
Dim SUMXORG(10, 10), SUMXAQ(10, 10), SUMYCAL(10, 10), FF1#(10)

i = 1

ALF(1) = x1(1, 1): BTA(1) = x1(2, 1)

If ALF(1) > 0 And ALF(1) < 1 And BTA(1) < 1 And BTA(1) > 0 Then

For J = 1 To (TNOC - 1)
    ZF(1, J) = INITX(J)
Next J

ZF(1, 3) = 1 - (INITX(1) + INITX(2))

For J = 1 To TNOC
    PARTBB(i, J) = KORG(J) * KAQ(J) + ALF(i) * KAQ(J) * (1 - KORG(J))
+ BTA(i) * KORG(J) * (1 - KAQ(J))
    XORG(i, J) = (ZF(i, J) * KAQ(J)) / PARTBB(i, J)
    XAQ(i, J) = (ZF(i, J) * KORG(J)) / PARTBB(i, J)
    YCAL(i, J) = (ZF(i, J) * KORG(J) * KAQ(J)) / PARTBB(i, J)

    SUMXORG(i, J) = XORG(i, J) + SUMXORG(i, J - 1)
    SUMXAQ(i, J) = XAQ(i, J) + SUMXAQ(i, J - 1)
    SUMYCAL(i, J) = YCAL(i, J) + SUMYCAL(i, J - 1)
Next J
For J = 1 To TNOC
    XORG(i, J) = XORG(i, J) / SUMXORG(i, TNOC)
    XAQ(i, J) = XAQ(i, J) / SUMXAQ(i, TNOC)
    YCAL(i, J) = YCAL(i, J) / SUMYCAL(i, TNOC)
Next J

FF1#(i) = Abs(SUMYCAL(i, TNOC) - 1) + Abs(SUMXORG(i, TNOC) - 1) +
Abs(SUMYCAL(i, TNOC) - 1) + Abs(SUMXAQ(i, TNOC) - 1)

ABTA = FF1#(i)

TPCOUNT6 = 1 + TPCOUNT6
Sheet4.Cells(1 + TPCOUNT6, 1) = TPCOUNT6: Sheet4.Cells(1 + TPCOUNT6,
2) = ABTA

Else
ABTA = 100
End If
End Function
```

D.2.5 Nelder Mead Simplex

D.2.5.1 Declaration and sub procedures

```
Private maxIterations_ As Single
Private objectMode_ As Boolean
Private callbackObject_ As Object
Public Tolerance_ As Double 'determines when to converge
Private FunctionName_ As String

Public Sub AssignObject(callbackObject As Object)
    objectMode_ = True
    Set callbackObject_ = callbackObject
End Sub
Private Function RunFunction(FunctionName As String, x As Variant) As
Double
    If objectMode_ = False Then
        RunFunction = Application.Run(FunctionName, x)
    Else
        RunFunction = CallByName(callbackObject_, FunctionName, VbMethod, x)
    End If
End Function
```

D.2.5.2 Main minimisation function

```
Public Function SolveMaximum(FunctionName As String, x0 As Variant) As
Variant
' Sheets("sheet3").Range("A1:Z1000").Value = ""
    FunctionName_ = FunctionName
    initialSimplex = GetInitialSimplex(x0)
    N = UBound(x0, 1)

    simplexMat = initialSimplex

    Dim counter As Single
    ReDim TempVec(1 To N, 1 To 1)
    counter = 2
    For iter = 1 To maxIterations_

        'check for convergence
        ReDim tmpMat(1 To N, 1 To 1)
        For i = 2 To N + 1 'looping over points
            For J = 2 To N + 1 'looping over coordinates of a point
                tmpMat(i - 1, 1) = tmpMat(i - 1, 1) + Abs(simplexMat(i, J) -
simplexMat(1, J))
            Next J
        Next i
        SortMatrix tmpMat, 1
        DENOM = 0
        For i = 1 To N
            DENOM = DENOM + Abs(simplexMat(1, i + 1))
        Next i
```

```

If DENOM < 1 Then
    DENOM = 1
End If
simplexSize = tmpMat(N, 1) / DENOM

If simplexSize < Tolerance_ Then
    For i = 1 To N
        TempVec(i, 1) = simplexMat(1, i + 1)
    Next i
    SolveMaximum = TempVec
    Exit Function
End If

'best point of simplexMat is the first row and worst is the last row
'so lets reflect the worst point to go farthest away from it

'calculate centroid of the point excluding the worst point
ReDim CENTROID(1 To N, 1 To 1)
For i = 2 To N + 1 'columns
    tmpsum = 0
    For J = 1 To N 'rows
        tmpsum = tmpsum + simplexMat(J, i)
    Next J
    CENTROID(i - 1, 1) = tmpsum / N
Next i

ReDim reflectedVec(1 To N, 1 To 1)
ReDim expandedVec(1 To N, 1 To 1)
ReDim contractedVec(1 To N, 1 To 1)
ReDim paramsBest(1 To N, 1 To 1)
ReDim paramsWorst(1 To N, 1 To 1)
For i = 1 To N
    reflectedVec(i, 1) = 2 * CENTROID(i, 1) - simplexMat(N + 1, i + 1)
    paramsWorst(i, 1) = simplexMat(N + 1, i + 1)
    paramsBest(i, 1) = simplexMat(1, i + 1)
Next i
acceptedVec = reflectedVec
FvalReflected = RunFunction(FunctionName_, reflectedVec)
Fval2ndWorst = simplexMat(N, 1)
FvalBest = simplexMat(1, 1)
FvalWorst = simplexMat(N + 1, 1)

If FvalReflected < Fval2ndWorst Then
    'we are doing good in moving towards this direction
    'let us see if this new point outperforms our best point
    If FvalReflected < FvalBest Then
        'let us go more and expand in this direction
        For i = 1 To N
            expandedVec(i, 1) = 2 * reflectedVec(i, 1) - CENTROID(i, 1)
        Next i
        FvalExpanded = RunFunction(FunctionName_, expandedVec)
    End If
End If

```

```

        If FvalExpanded < FvalBest Then
            acceptedVec = expandedVec
        End If
    End If

Else

    If FvalReflected < FvalWorst Then
        TempVec = reflectedVec
    Else
        TempVec = paramsworst
    End If
    For i = 1 To N
        contractedVec(i, 1) = 0.5 * TempVec(i, 1) + 0.5 * CENTROID(i, 1)
    Next i
    FvalContracted = RunFunction(FunctionName_, contractedVec)
    If FvalContracted < Fval2ndWorst Then
        acceptedVec = contractedVec
    Else
        'shrink all coordinates
        For i = 2 To N
            For J = 2 To N + 1
                simplexMat(i, J) = (paramsBest(J - 1, 1) + simplexMat(i, J)) / 2
                TempVec(J - 1, 1) = simplexMat(i, J)
            Next J
            simplexMat(i, 1) = RunFunction(FunctionName_, TempVec)
        Next i
        For i = 1 To N
            TempVec(i, 1) = (simplexMat(1, i + 1) + simplexMat(N + 1, i + 1)) / 2
        Next i
        acceptedVec = TempVec
    End If

End If

'replace worst parameters with new choice
For i = 1 To N
    simplexMat(N + 1, i + 1) = acceptedVec(i, 1)
Next i
simplexMat(N + 1, 1) = RunFunction(FunctionName_, acceptedVec)

'ShowMatrix "sheet3", counter, 1, simplexMat
'tmpstr = "A" & counter - 1
'Sheets("sheet3").Range(tmpstr).Value = "iter=" & iter & " simplex
size=" & simplexSize
'counter = counter + 5

SortMatrix simplexMat, 1
Sheet2.Cells(9, 16) = iter
Next iter

```

```

    MsgBox "iterations did not converge"
End Function
'returns initial matrix with simplex coordinates

```

D.2.5.3 Getting the initial ,storing and sorting the Matrix

```

Private Function GetInitialSimplex(paramVec As Variant) As Variant
    N = UBound(paramVec, 1)
    'first column of this structure will have function values
    'rest of columns will have coordinates
    ReDim outMat(1 To N + 1, 1 To N + 1)
    'set first vector simply to initial params
    outMat(1, 1) = RunFunction(FunctionName_, paramVec)
    For i = 2 To N + 1
        outMat(1, i) = paramVec(i - 1, 1)
    Next i

    'calc scaling factor by taking highest value of input param
    ReDim sortedVec(1 To N, 1 To 1)
    For i = 1 To N
        sortedVec(i, 1) = Abs(paramVec(i, 1))
    Next i
    SortMatrix sortedVec, 1
    scalingfactor = sortedVec(N, 1)
    If scalingfactor < 1 Then
        scalingfactor = 1
    End If

    'set the remaining vectors to unit vectors
    For i = 2 To N + 1 'loop over each row
        For J = 2 To N + 1 'loop over cells in a row
            outMat(i, J) = paramVec(J - 1, 1)
        Next J
        outMat(i, i) = outMat(i, i) + scalingfactor
        ReDim tmpParam(1 To N, 1 To 1)
        For J = 2 To N + 1
            tmpParam(J - 1, 1) = outMat(i, J)
        Next J
        outMat(i, 1) = RunFunction(FunctionName_, tmpParam)
    Next i

    SortMatrix outMat, 1
    GetInitialSimplex = outMat
End Function

Private Sub Class_Initialize()
    maxIterations_ = 100000
    Tolerance_ = 0.0001
    objectMode_ = False
End Sub

```

```
'Sorts a given matrix in ascending order and up to a
' a number os columns specified by cols
```

```
Private Sub SortMatrix(ByRef inMatrix As Variant, cols As Single)
```

```
    Dim i As Single, J As Single
    Dim TempRecord As Variant
```

```
    For i = LBound(inMatrix, 1) To UBound(inMatrix, 1) - 1
        For J = i + 1 To UBound(inMatrix, 1)
```

```
            Dim CompareFlag As Boolean
            CompareFlag = False
```

```
            Dim K As Single
```

```
            For K = 1 To cols
```

```
                If inMatrix(i, K) > inMatrix(J, K) Then
```

```
                    Dim k1 As Single
```

```
                    If K > 1 Then
```

```
                        'all columns to the left of the k column of ith row
                        'should be equal or more than corresponding
                        'columns of jth row to allow swap
```

```
                        Dim tmpflag As Boolean
```

```
                        tmpflag = False
```

```
                        For k1 = 1 To K - 1
```

```
                            If inMatrix(i, k1) < inMatrix(J, k1) Then
```

```
                                tmpflag = True
```

```
                            End If
```

```
                        Next k1
```

```
                        If tmpflag = False Then
```

```
                            CompareFlag = True
```

```
                        End If
```

```
                    Else
```

```
                        'the first column of ith row is more than first
                        'col of jth row =>allow swap
```

```
                        CompareFlag = True
```

```
                    End If
```

```
                End If
```

```
            Next K
```

```
        If CompareFlag = True Then
```

```
            TempRecord = GetMatrixRowAsColumn(inMatrix, J)
```

```
            SetMatrixRow inMatrix, J, GetMatrixRowAsColumn(inMatrix, i)
```

```
            SetMatrixRow inMatrix, i, TempRecord
```

```
        End If
```

```
    Next J
```

```
Next i
```

```
End Sub
```

```
Private Function GetMatrixRowAsColumn(ByVal x As Variant, row As Single)
As Variant
```

```

Dim TempMat As Variant
ReDim TempMat(1 To UBound(x, 2), 1 To 1)
Dim i As Single
For i = 1 To UBound(x, 2)
    TempMat(i, 1) = x(row, i)
Next i
GetMatrixRowAsColumn = TempMat
End Function

```

```

Private Sub SetMatrixRow(ByRef x As Variant, J As Single, ByVal y As
Variant)
    Dim i As Single
    For i = 1 To UBound(x, 2)
        x(J, i) = y(i, 1)
    Next i
End Sub

```

E. Computer programs on a Compact Disc

A Compact Disc is attached to this thesis containing a list of computer programs in Vba excel for the methods and systems relevant to this work.